Dedicated to my family and Sarah

Abstract

Chapter 1; A literature review of chemotherapeutic agents, bioreductive prodrugs and polycyclic diazoles, along with the aims and objects of the thesis is presented.

Chapter 2; A review of "oxidative" homolytic aromatic substitutions carried out in the presence of the "reductant" Bu_3SnH is presented. This is followed by the first report of one-pot double intramolecular homolytic aromatic substitutions of alkyl radicals onto heteroarenes. Bu_3SnH / ACCN (1,1'-azobis(cyclohexanecarbonitrile)) mediated double six-membered radical cyclizations using phenylselenides proceeded in excellent yield to give dipyrido ring-fused imidazo[5,4-*f*]benzimidazole and imidazo[4,5-*f*]benzimidazole. Optimized yields of 5 and 7-membered radical cyclizations were obtained through ring activation with camphorsulfonic acid or acetic anhydride. Annulated imidazobenzimidazoles were converted into iminoquinone and quinone derivatives for anti-cancer studies.

Chapter 3; A review of oxidative cyclizations of *ortho*-substituted *tertiary*-anilines is presented. A mechanism for oxidative cyclizations of *o*-*tert*-amino acetanilides to give alicyclic ring-fused diazoles is proposed using the hydrogen-bonded amine-*N*-oxide intermediate (X-ray crystal structure provided). Oxone® in formic acid is shown to give high yields of annulated benzimidazoles, as well as [1,4]oxazino ring-fused, and unsymmetrical pentacyclic imidazo[5,4-*f*]benzimidazoles. Imidazo[5,4-*f*]benzimidazoles were converted into quinones, and an X-ray crystal structure of [1,4]oxazino[4,3-*a*][1,4]oxazino[4',3':1,2]imidazo[5,4-*f*]benzimidazoliumquinone di(trifluoroacetate) obtained.

Chapter 4; Cytotoxicity towards two human cancer cell lines known to over-express NAD(P)H:quinone oxidoreductase 1 (NQO1), as well as a human normal fibroblast cell line is presented. Increasing the alicyclic ring size or the degree of ring fusion, resulted in decreased cytotoxicity, while the [1,4]-oxazino ring increased toxicity. Mitomycin C (MMC) showed higher cytotoxicity than the synthesized compounds, and computational docking of MMC into the active site of NQO1 revealed it to be a better substrate for NQO1 than the synthesized compounds. Cytotoxicity testing performed at the US National Cancer Institute using 60 human cancer cell lines showed an iminoquinone to be particularly potent, with a good correlation to NQO1.

Chapter 5; All experimental detail is described for Chapter 2, 3 and 4.

Acknowledgements

I gratefully acknowledge my supervisor, Dr. Fawaz Aldabbagh, for his hard work, help and guidance, which he afforded me over the course of my PhD.

I would like to thank fellow group member Sarah Bonham, who carried out all MTT assay cytotoxicity studies in this thesis.

I wish to acknowledge Dr. Michael Carty (Department of Biochemistry, NUI Galway) for allowing the use of tissue culture facilities, and for his expertise and advice.

I wish to acknowledge the Development Therapeutics Program at the US National Cancer Institute, for carrying out the growth inhibition studies.

I acknowledge the substantial contribution of Dr. Patricia Saenz-Méndez (Computational Chemistry and Biology Group, Facultad de Química, UdelaR, Uruguay), who carried out all computational docking studies.

I wish to acknowledge Prof. Patrick McArdle (Inorganic section, School of Chemistry, NUI Galway), who obtained all the crystal structures.

I gratefully acknowledge the generous financial support of the Irish Research Council for Science, Engineering and Technology, under the Embark Initiative, which enabled this research to be carried out.

I wish to thank all the staff and postgraduates at the School of Chemistry, NUI Galway, for their support throughout my PhD. In particular, I would like to thank the Aldabbagh Research Group members, both past and present, for their advice, in-depth discussions, humor, and invaluable friendships.

I am hugely grateful for the love and support of my parents Martin and Carmel, and for the friendship and encouragement of all of my brothers.

I wish to convey my deepest gratitude to my best friend in the world, and my loving partner Sarah Bonham. You are my rock. May our paths never part.

I also wish to thank all the Bonham family for the very warm welcome extended to me and for their unconditional support of us both.

Abbreviations

Ac	acetyl
ACCN	1,1′-azobis(cyclohexanecarbonitrile)
Ac_2O	acetic anhydride
AcOH	acetic acid
AIBN	2,2′-azobis(isobutyronitrile)
APBI	acetamido pyrrolo[1,2-*a*]benzimidazolequinone
ATR	universal attenuated total reflectance
Bn	benzyl
Boc	*tert*-butoxycarbonyl
Bu	butyl
$Bu_3Sn^{\bullet}$	tributyltin radical
Bu_3SnH	tributyltin hydride
c.	concentrated
°C	degrees celsius
CCDC	Cambridge Crystallographic Data Centre
Calcd	calculated
CNS	central nervous system
CSA	camphorsulfonic acid
DCM	dichloromethane
DEPT	distortionless enhancement by polarization transfer
DLP	dilauroyl peroxide
DMF	*N,N*-dimethyl formamide
DMSO	dimethyl sulfoxide
DNA	deoxyribonucleic acid
DTP	development therapeutics program
ESI	electrospray ionization
Et	ethyl
Et_3B	triethylborane
Et_3N	triethylamine
Et_2O	diethyl ether
EtOAc	ethyl acetate

EtOH	ethanol
Eq.	equivalents
EWG	electron withdrawing group
FA	Fanconi anaemia
FAD	flavin adenine dinucleotide
FBS	fetal bovine serum
FT-IR	fourier transform infrared
GI_{50}	growth inhibition: concentration required to inhibit cell growth by 50%
h	hours
HCR	hypoxic cytotoxicity ratio
HMQC	heteronuclear multiple quantum coherence
$HOO^{\bullet}$	hydroperoxy radical
HPLC	high performance liquid chromatography
HRMS	high resolution mass spectra
Hz	hertz
IC_{50}	inhibition concentration: concentration required to inhibit cell population by 50%
I.E.	interaction energy
i-Pr	*iso*-propyl
IR	infrared
IUPAC	International Union of Pure and Applied Chemistry
LC_{50}	lethal concentration: concentration required to kill 50% of cells
LUMO	lowest unoccupied molecular orbital
m-	*meta*-
M	molar
mCPBA	*meta*-chloroperoxybenzoic acid
MD	molecular dynamics
Me	methyl
MEM	minimum essential media
MeOH	methanol
$(Me_3Si)_3SiH$	tris(trimethylsilyl)silane
$MeSO_3H$	methanesulfonic acid

MHz	megahertz
min	minutes
MMC	mitomycin C
μM	micromolar
mM	millimolar
MOE	Molecular Operating Environment
mp	melting point
MTT	3-(4,5-dimethylthiazol-2-yl)-2,5-diphenyltetrazolium bromide
NADH	nicotinamide adenine dinucleotide
NADPH	nicotinamide adenine dinucleotide phosphate
NCI	National Cancer Institute
NMR	nuclear magnetic resonance
NQO1	NAD(P)H:quinone oxidoreductase 1
o-	*ortho*-
$O_2^{\bullet-}$	superoxide radical anion
PBI	pyrrolo[1,2-*a*]benzimidazolequinone
PDB	Protein Data Bank
Pet. ether	petroleum ether
Ph	phenyl
PhH	benzene
PhMe	toluene
ppm	parts per million
psi	per square inch
RNA	ribonucleic acid
rt	room temperature
SET	single electron transfer
SOMO	singly occupied molecular orbital
SO_2Ph	phenylsulfonyl
SPh	phenylsulfanyl
$S_{RN}1$	unimolecular radical nucleophilic substitution
t-	*tertiary*-
tert-	*tertiary*-
TFA	trifluoroacetic acid
TGI	total growth inhibition

THF	tetrahydrofuran
TLC	thin layer chromatography
1°	primary
2°	secondary
3°	tertiar

Chapter 1

1 General Introduction

1.1 Introduction

Chemotherapeutic agents are cytotoxic compounds used in chemotherapy to preferentially kill cancer cells. Most chemotherapeutic agents kill cells by disrupting the processes of DNA replication or by interacting directly with DNA.

Some of the main chemotherapeutic agents in use today are (Figure 1.1):

Platinum co-ordination complexes (e.g. cisplatin)

Taxanes (e.g. paclitaxel)

Antimetabolites (e.g. fluorouracil, capecitabine)

Alkylating agents (e.g. cyclophosphamide)

Anti-tumor antibiotics (e.g. mitomycin C (MMC)(also an alkylating agent))

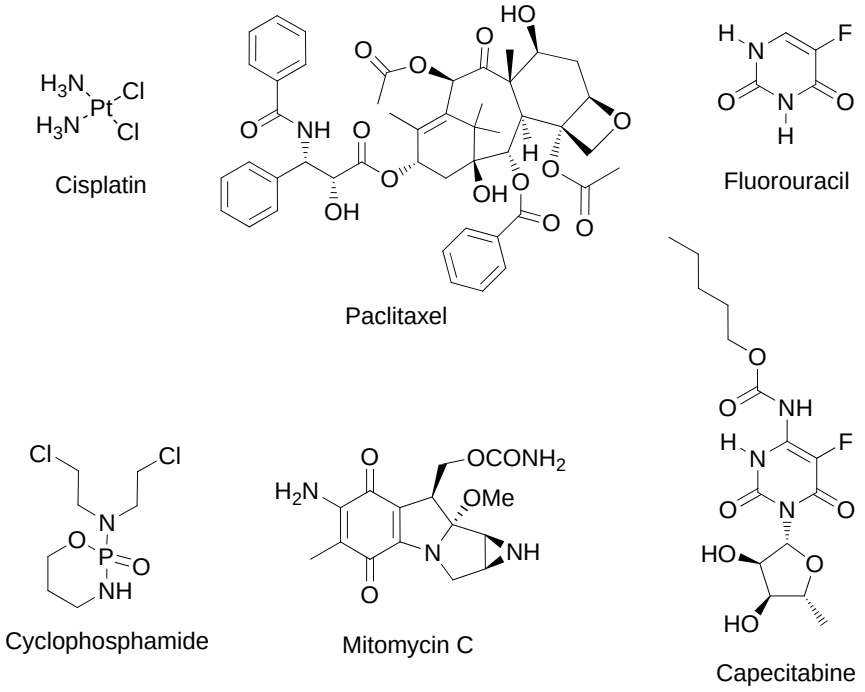

Figure 1.1; Some chemotherapeutic agents in use today.

The clinical use of many of these chemotherapeutic agents is impeded by a lack of selective toxicity towards tumor cells, causing severe side effects for the patient. One strategy of improving selective toxicity has been to develop prodrugs. The term prodrug refers to a pharmacologically inactive compound that is converted to an active drug by a metabolic biotransformation. The design of prodrugs can be useful in overcoming problems associated with solubility, absorption and distribution, instability, toxicity and site specificity. This strategy has the potential to produce

tumor-selective toxicity if activation of the prodrug is primarily a property of tumor cells.[1]

As a pyrimidine antimetabolite, the above mentioned fluorouracil is metabolized and incorporated into DNA and RNA where it inhibits DNA replication, ultimately leading to apoptosis (programmed cell death). A prodrug analogue called capecitabine (Figure 1.1) has been developed which is converted to fluorouracil in the body by the enzyme thymidine phosphorylase.[2] This enzyme is present in higher levels in tumor tissue than in normal tissue, making the drug more toxic to tumor cells. Capecitabine is in phase III and IV trials for the treatment of breast, colorectal, pancreatic, gastric, oesophageal, hepatocellular, biliary tract, and head and neck cancers. It is recommended to be used in combination with other drugs such as the taxane docetaxel.[2]

Cyclophosphamide is a prodrug which undergoes oxidative activation by cytochrome P450 oxidases to ultimately release a powerful DNA alkylating nitrogen mustard that causes DNA crosslinks, usually at the guanine *N*-7 position (Scheme 1.1).[1, 3] DNA crosslinks inhibit replication and leads to apoptosis.

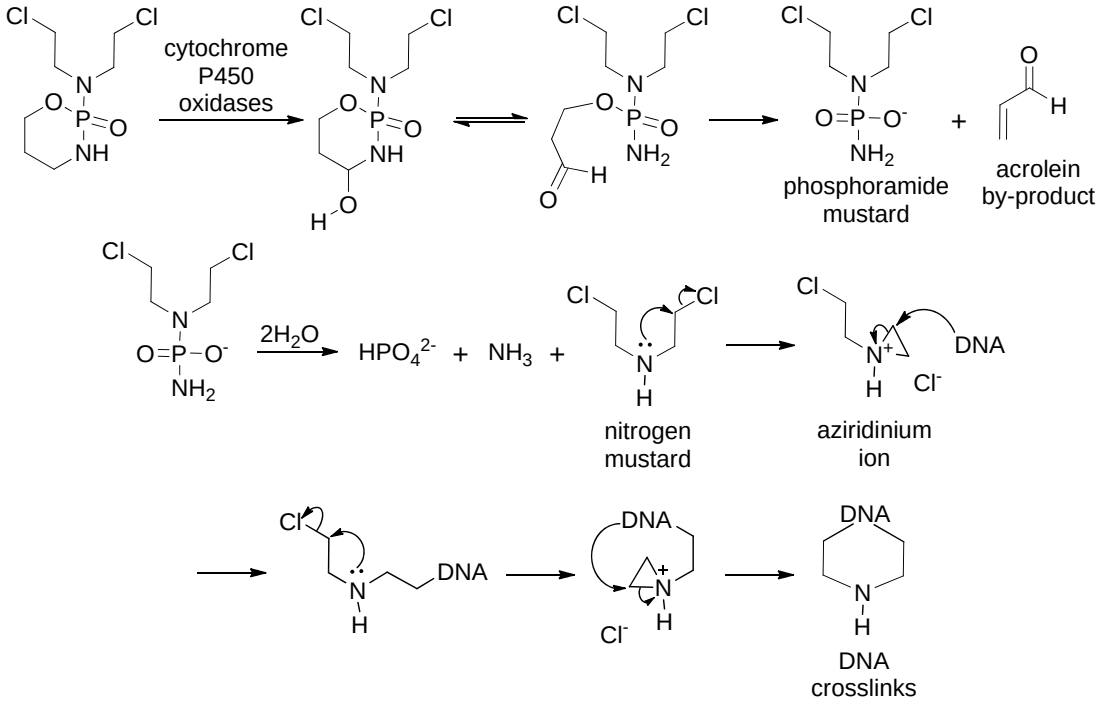

Scheme 1.1; Mechanism of action for cyclophosphamide.

1.2 Bioreductive prodrugs

There has been huge interest in the development of bioreductive prodrugs which possess tumor selective toxicity. Many cancers over-express reductive enzymes such as NQO1 (NAD(P)H:quinone oxidoreductase 1),[4] making bioreductive activation more efficient in the cancer cells, giving rise to tumor selective toxicity.

Bioreduction via single electron reducing enzymes, such as cytochrome P450 reductase, can be reversed in the presence of oxygen. Many solid tumors contain poorly oxygenated (hypoxic) regions due to disorganized cell and vascular growth. Solid tumors possessing hypoxic regions tend to be difficult to treat and are associated with metastasis (spreading of cancer to other locations). A goal of scientists has been to develop compounds which can be reduced by these reductive enzymes to cytotoxic species, but which can be re-oxidized to the non-toxic form in normal well oxygenated tissue. In this way, selective toxicity towards hypoxic tumors can be achieved.[5] Most bioreductive anti-cancer agents can be classified into three main groups; *N*-oxides, nitroaromatics and quinones.

1.2.1 *N*-oxides

Tirapazamine is a well known aromatic *N*-oxide bioreductive prodrug which is currently in clinical trials, and is expected to be the first bioreductive prodrug of its kind to be registered for clinical use.[5-6] It undergoes single electron reduction, primarily by cytochrome P450, to form a free radical.[5] In normal oxygenated tissue this process is reversed with the formation of a superoxide radical anion ($O_2^{\bullet -}$) (Scheme 1.2).

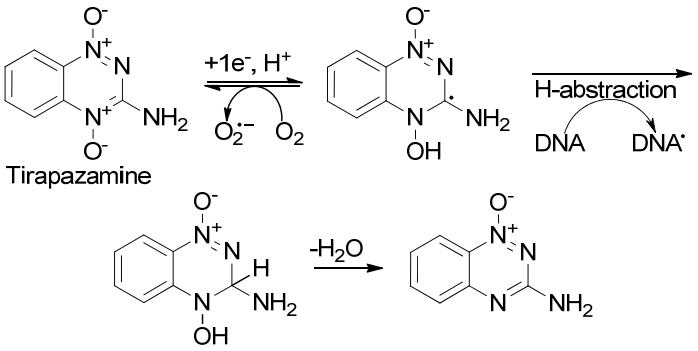

Scheme 1.2; Mechanism of action of tirapazamine.

In hypoxic regions the radical can abstract a hydrogen atom from DNA, ultimately leading to DNA cleavage. As a result, tirapazamine has a hypoxic cytotoxicity ratio (HCR; ratio of toxicity under hypoxic conditions to toxicity under normal aerobic conditions) of as high as 300 in *in vitro* studies.[5-6] Reduction of tirapazamine by the 2-electron reducing enzyme NQO1 leads to an inactive species. Clinical trials have shown tirapazamine to be effective when used in combination with cisplatin and radiotherapy.[7-8]

1.2.2 Nitroaromatics

Nitroaromatic compounds are reduced in a stepwise addition of up to six electrons, catalyzed by various one-electron reductases. The radical anion intermediate derived from the first reduction step is readily re-oxidized in the presence of oxygen, resulting in hypoxia selectivity.[7, 9]

The first bioreductive nitroaromatic anti-cancer agent to show significant hypoxia selectivity was the aziridine containing 2-nitroimidazole RSU1069 (Figure 1.2) which had a HCR of up to 100.[7] However marked gastrointestinal toxicity prevented further clinical development. As a result, the less toxic prodrug RB 6145 was developed in which the aziridine was replaced by a mustard group. RB 6145 produced excellent selectivity towards hypoxia, but in preclinical trials it was shown to possess retina toxicity, which prevented further development.[7, 9]

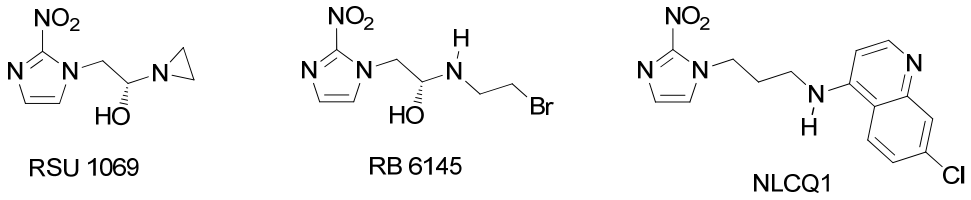

Figure 1.2; 2-Nitroimidazole drug candidates.

NLCQ1 is a nitroaromatic bioreductive anti-cancer agent (Figure 1.2) which is bioactivated by the one-electron reductases P450R and cytochrome b_5 reductase, and is a poor substrate for the two electron reducing enzyme NQO1. It is a weak DNA-intercalator (binds to DNA by inserting between the base pairs, disrupting DNA replication) and has a HCR of up to 40. It compares favorably to other bioreductive anti-cancer agents and is entering clinical trials.[9]

1.2.3 Quinones

Quinone anti-cancer agents were among the first bioreductive prodrugs to be studied. They undergo reversible single electron reduction by cytochrome c (P450) reductase (cP450R) or irreversible two electron reduction by NQO1 (Scheme 1.3).[4, 10-12]

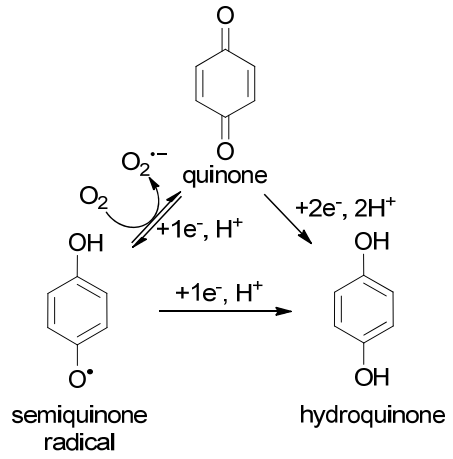

Scheme 1.3; Reversible and irreversible quinone bioreduction.

Since hypoxia selective drugs only target the hypoxic regions of tumors, they must be used in conjunction with other drugs or therapies which are toxic to the aerobic regions of tumors. It has been established that NQO1 is over expressed in many tumor cells.[4, 11-12] Therefore quinone-based bioreductive anti-cancer agents can achieve tumor selective toxicity in both hypoxic tumor cells (through single electron reduction) and in oxygenated tumor cells (through two electron reduction by elevated levels of NQO1). As a result, quinone-based bioreductive drugs can be used as single-agent therapies without the need for other drugs.[11]

1.2.3.1 Mitomycin C and indolequinone alternatives

Mitomycin C (MMC) is the best known bioreductive quinone prodrug and has been in clinical use for over three decades. Reductive activation to the electron rich hydroquinone species facilitates the loss of a methoxy leaving group to form a more stable aromatic indole molecule (Scheme 1.4). The electron releasing nature of the indole hydroquinone now results in ring-opening of the aziridine with the formation of a reactive methide species, which is susceptible to nucleophilic attack by DNA bases. The carbamate group can also be lost with the resultant cation being stabilized by the indole nitrogen lone pair to create another electrophilic site, which can be

attacked by another DNA nucleophile. The end result is a guanine-guanine DNA crosslink which cannot be repaired and results in cell death.[1, 12-13] Clinical use of MMC is restricted due to cumulative and unpredictable toxicity. The most severe side effects are related to bone marrow toxicity causing anemia, bruising, nose bleeds and low immunity.[4]

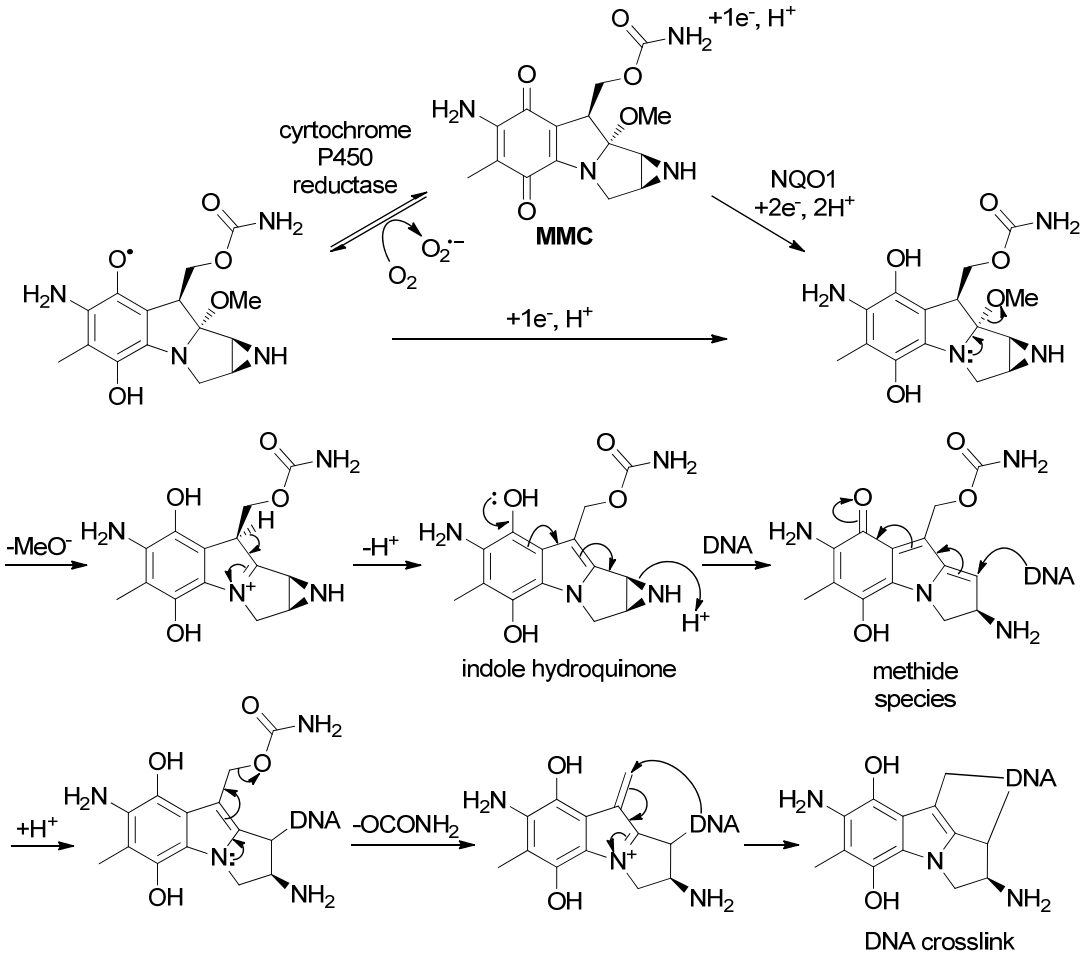

Scheme 1.4; Mechanism of action of **MMC**.

The mode of action of MMC is well studied and numerous analogues with a similar mode of action have been synthesized. Moody and co-workers have published extensively on the synthesis of a range of indolequinones, most notably the cyclopropamitosenes which have a cyclopropane ring in place of the aziridine (Figure 1.3).[12, 14-16]

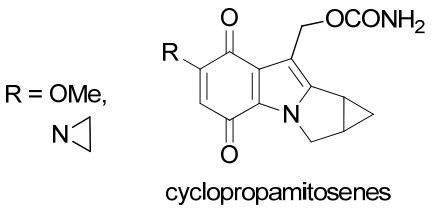

Figure 1.3; Cyclopropamitosenes.

Initial efforts focused on hypoxia selectivity, as it was hoped that following single electron reduction, the cyclopropane ring would open via a radical route to give a carbon centered radical which could undergo hydrogen abstraction from DNA, ultimately leading to DNA cleavage. Later studies focused on structural requirements of NQO1 substrates. Analogues bearing an aziridine substituent at R were most potent but non-aziridine cyclopropamitosenes were more selective towards hypoxia. Many pyrrolo[1,2-*a*]indolequinones and 1,2-disubstituted indolequinones were synthesized, but were found to be less active. Using cyclic voltammetry, the reductive potentials of many analogues were measured to determine if ease of reduction influenced rate of metabolism by NQO1. Whilst it was a factor, there was no overall correlation.[12]

The indolequinone structure has been used as a trigger to release known cytotoxins with targeted drug delivery, minimizing the undesirable side effects while retaining desirable therapeutic activities. Borch and co-workers synthesized indolequinones substituted at the 2- and 3-positions with phosphoramide mustards (Figure 1.4).[17-18]

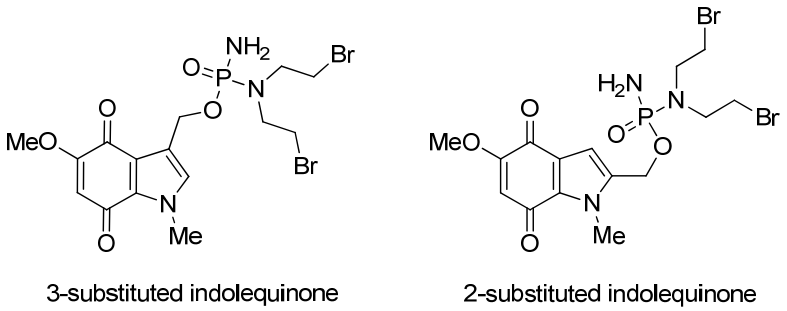

Figure 1.4; Indolequinone phosphoramidate prodrugs.

Following reduction of the quinone moiety, the molecules were shown to rapidly release the phosphoramidate anion. The molecules were broadly active, with some selectivity towards melanoma, renal and central nervous system (CNS) cell lines. The 3-substituted analogues were shown to be potent NQO1 inhibitors while the 2-

substituted analogues were shown to be excellent NQO1 substrates. However no direct correlation between *in vitro* activity and NQO1 activity was observed.[17-18]

1.2.3.2 Benzimidazolequinones

Skibo and co-workers reported the synthesis of a number of pyrrolo[1,2-*a*]benzimidazolequinones (PBIs) which possess an aziridine substituent at the 6-position (Figure 1.5).

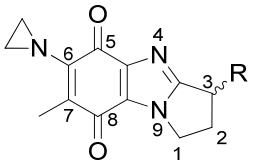

PBI

R = OAc, $OCONH_2$, $NHCOCH_3$, NH_2, $NHCONH_2$

Figure 1.5; Quinones reported by the Skibo group.

These were found to be cytotoxic towards a range of cancer cell lines through testing at the US National Cancer Institute (NCI) under the Development Therapeutics Program 60-Human Cancer Cell line Screen (DTP NCI-60).[19-21] The NCI-60 is a cytotoxicity screening program whereby anti-cancer compounds are evaluated against 60 different human tumor cell lines (discussed in detail in Chapter 4). The electron deficient nature of the quinone system means that the aziridine ring is deactivated but becomes activated upon reduction by NQO1 to the electron rich hydroquinone. A substituent at the 3-position on the pyrrolo[1,2-*a*] fused ring which is capable of hydrogen bonding contributes considerably to the potency. It is also suggested that the substituent at the 3-position can increase cytotoxicity by improving the ability of the molecule to pass through cellular membranes.[20-21] Hydrogen bonding holds the molecule in the correct position in the major groove of DNA, resulting in nucleophilic attack of the aziridine ring by the DNA phosphate backbone or by DNA bases leading to DNA damage and cell death.[19, 21]

Aldabbagh and co-workers reported the synthesis of a series of alicyclic ring-fused [1,2-*a*]benzimidazolequinones **1** and **2** with and without an additional fused cyclopropane ring (Figure 1.6). These compounds were found to be

electrochemically easier to reduce than the cyclopropamitosenes and were significantly more cytotoxic than indolequinone analogues.[22-25]

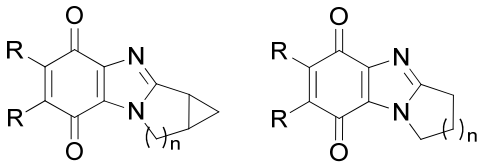

1a; R = H, n = 1
1b; R = H, n = 2
1c; R = Me, n = 1

2a; R = H, n = 2
2b; R = Me, n = 1
2c; R = Me, n = 2
2d; R = Me, n = 3

Figure 1.6; Diazole analogues of cyclopropamitosenes reported by the Aldabbagh group.

The presence of the fused cyclopropane ring was not necessary for activity, with analogue **2a** being most toxic and having the highest activity under hypoxic conditions. Toxicity towards normal human cells (GM00637) was in the nanomolar range (10^{-9} M), while the presence of methyl substituents reduced toxicity.

Later alicyclic ring-fused [1,2-*a*]benzimidazolequinones **3a-c** and aziridine substituted analogues **4a-c** were reported. The cytotoxicity was evaluated towards the normal human skin fibroblast cell line (GM00637). Increasing the size of the alicyclic ring to six or seven membered was found to decrease potency (Figure 1.7).[26-27]

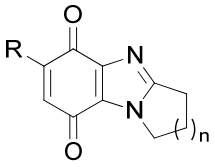

3a; R = OMe, n = 1
3b; R = OMe, n = 2
3c; R = OMe, n = 3
4a; R = N  , n = 1
4b; R = N  , n = 2
4c; R = N , n = 3

Figure 1.7; Methoxy substituted **3a-c** and aziridine analogues **4a-c** alicyclic ring fused [1,2-*a*]benzimidazolequinones.

The role of the aziridine was investigated by comparing the response of a Fanconi anemia (FA) cell line (PD20i) to compounds **3a** and **4a**. FA is a rare human genetic disease, leading to a high incidence of cancer in early adulthood. FA cells possess a number of mutated proteins and lack a protein known as FANCD2, which leads to hypersensitive toxicity to DNA-cross-linking agents, including MMC.[28] The response of FA cells to 6-aziridinylbenzimidazolequinone **4a** was found to be similar

to that of MMC, with cytotoxicity in the nanomolar range (10^{-9} M). In contrast 6-methoxybenzimidazolequinone **3a** was found to possess negligible toxicity at the same concentrations, implicating the aziridinyl group in the hypersensitivity of FA cells lacking FANCD2. An isogenic FA cell line (PD20:RV) expressing wild-type FANCD2 protein from an inserted transgene was treated with **3a** and **4a**, and resulted in the toxicity of **4a** being significantly reduced, implicating the FANC complex in cellular response to **4a**.[27]

Non-fused aziridine containing benzimidazolequinone **5** was found to induce a similar hypersensitive response by the Fanconi anaemia cell line PD20i at concentrations in the nanomolar range. The 4,7-dimethoxybenzimidazole compound **6** induced a similar cellular response to that of benzimidazolequinone **5**, at the same compound concentrations, suggesting that the quinone moiety was not required to induce such a hypersensitive response.[27-28]

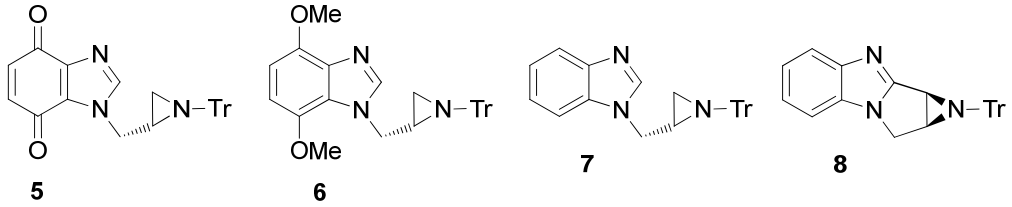

Figure 1.8; Non-fused and fused aziridinyl containing benzimidazoles reported by the Aldabbagh group.

The non-fused aziridine containing compound **7** and the [1,2-*a*]-fused analogue **8** have recently been reported by Aldabbagh and co-workers.[29] The toxicity of **7** and **8** was evaluated towards human normal fibroblast cell line (GM00637) and two breast cancer cell lines (MCF-7, HCC1937) in order to assess the impact of ring fusion on toxicity. The fused compound **8** was found to be less toxic to all cell lines compared to the non-fused compound **7**.[29]

Garuti *et al* reported the synthesis of 2-(pyridinyl)benzimidazolequinones and showed that the location of the *N*-heteroatom in the pyridine ring had a considerable impact on the activity (Figure 1.9).[30]

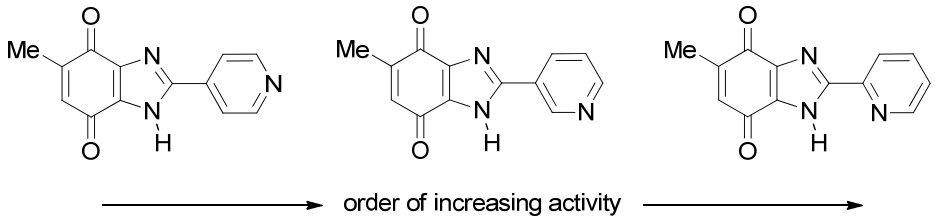

Figure 1.9; Influence of position of *N*-heteroatom in 2-(pyridinyl)benzimidazolequinones.

Shifting the nitrogen from the 4-position to the 3- and 2-positions resulted in a progressive increase of anti-proliferation activity towards human erythroleukemia and colon carcinoma cell lines.

Moriarty and Aldabbagh reported the synthesis of benzimidazolequinones containing fused and non-fused aryl, pyridinyl and naphthyl rings **9-12**. Fused compounds **9**, **10** were 10-30 times less toxic than non-fused **11**, **12**, but showed greater selectivity towards prostate and cervical cancer cell lines (Figure 1.10).[31]

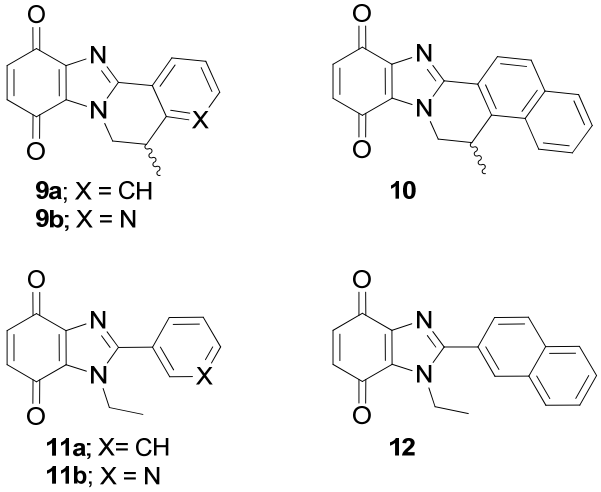

Figure 1.10; Aromatic fused and non-fused substituted benzimidazolequinones.

1.2.3.3 Imidazo[4,5-*f*]benzimidazolequinones and polycyclic diazole containing systems

As part of studies related to the PBIs (Figure 1.5), Skibo and co-workers synthesized 6-acetamido pyrrolo[1,2-*a*]benzimidazolequinones (APBIs, Figure 1.11) which showed a strong inverse correlation to NQO1 when tested in the NCI-60 cell screen. Therefore reduction of the APBIs by NQO1 leads to inactivation. It was thought that the unreduced APBIs intercalate DNA and inhibit the first step of topoisomerase II-mediated relaxation of supercoiled DNA.[21, 32-33] Topoisomerase II is an enzyme which is involved in DNA coiling and uncoiling, and is important in DNA replication processes.

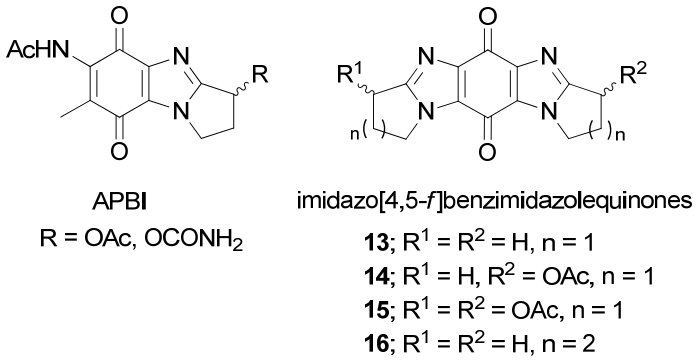

Figure 1.11; APBIs and imidazo[4,5-*f*]benzimidazolequinones.

In efforts to prepare APBI analogues which would not be inactivated by NQO1 reduction, a small number of dipyrroloimidazo[4,5-*f*]benzimidazolequinones were prepared (Figure 1.11). It was hoped that the increased steric bulk about the quinone moiety would limit NQO1 reduction, thus leading to potent topoisomerase II inhibitors.[34]

From experiments carried out with rat liver NQO1, imidazo[4,5-*f*]benzimidazolequinones **13** and **14** were found to be excellent substrates for NQO1 while the two diastereomeric forms of **15** were found not to be NQO1 substrates. Relaxation assays were carried out with recombinant human topoisomerase II and showed that compounds **13-15** were topoisomerase II inhibitors. However toxicity results from the NCI-60 screen for compounds **13** and **15** were unpredictable and difficult to explain.

The two diastereomers of **15** were separated and tested separately. Both were expected to be active since they were topoisomerase II inhibitors, but were not NQO1 substrates. The *cis* diastereomer showed potent non-selective toxicity towards all cell lines while the *trans* diastereomer was completely inactive on all cell lines. Compound **13** was expected to have low toxicity, since topoisomerase II inhibition would be impeded by NQO1 reduction. However it was shown to have variable and selective toxicity with a high specificity towards melanoma cell lines.[34] Molecular modeling of dipyridoimidazo[4,5-*f*]benzimidazolequinone **16** into human NQO1 showed **16** to be an excellent substrate.[35]

Many large polycyclic heteroaromatic quinones have been reported to possess anti-cancer properties.[36] It is thought that such molecules can intercalate DNA causing enzymatic blockade and reading errors during replication processes.[10, 33, 37-40]

The Suh group reported the synthesis of a number of fused and non-fused substituted imidazoquinolinedione heterocycles (Figure 1.12).[38-39] These were found to have higher *in vitro* activity than cisplatin on a range of cancer cell lines, but had 3-30 times lower activity than the clinically used doxorubicin, a DNA intercalator and topoisomerase II inhibitor (Figure 1.12).[41] The [1,4]oxazino fused imidazo[4,5-*g*]quinolinedione **17b** was the most potent analogue, but most were active against various human tumor cell lines including lung (A 549), ovarian (SK-OV-3), melanoma (SK-MEL-2), brain (XF 498) and colon (HCT15) cancer. The mechanism of cytotoxicity was thought to be reduction by NQO1 and topoisomerase II inhibition via DNA intercalation.[38]

The group later reported the synthesis of imidazo[4,5-*g*]phthalazine-5,8-diones **18** with various hydrophobic substituents at the *N*-1 position (Figure 1.12). The methyl, isopropyl and phenyl analogues were found to be 2-400 times more active than doxorubicin on ovarian, melanoma, CNS and colon cancer cell lines.[42]

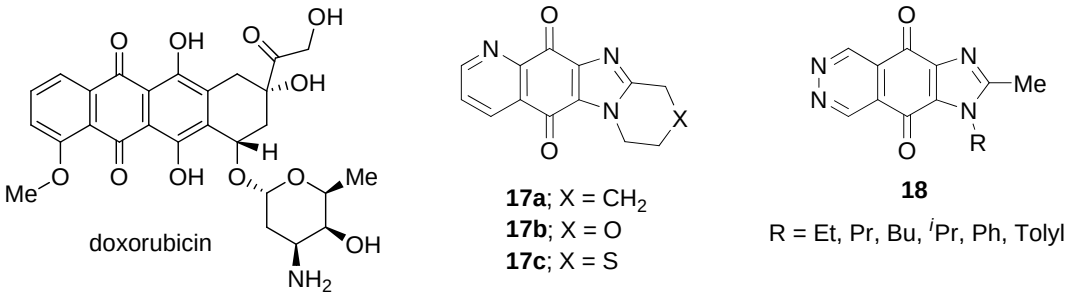

Figure 1.12; Intercalating heterocyclic quinones.

In 1991 Ireland and co-workers isolated the pyrroloindole iminoquinone Wakayin from ascidian *Clavelina* (Figure 1.13). It exhibited *in vitro* cytotoxicity against a human colon tumor cell line, inhibition of topoisomerase II and antimicrobial activity against *Bacillus subtilis*.[43]

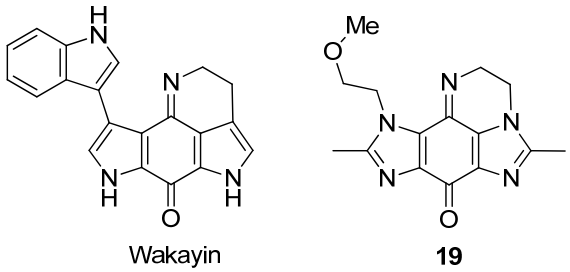

Figure 1.13; Natural product Wakayin and synthetic analogue.

N-Substituted di-imidazole analogues were reported by Skibo and co-workers which showed varying cytotoxicity. Compound **19** showed a high degree of selectivity towards renal cancer cell lines. However its NCI-60 cytotoxicity profile showed that it had a different mode of action to that of Wakayin. A good correlation was obtained to the molecular target Flt-1, a receptor for vascular endothelial growth factor.[44]

1.3 Thesis aims and objectives

The aim of this thesis is to synthesize a novel series of polycyclic quinones based on the imidazo[5,4-*f*]benzimidazole substructure (Figure 1.14). This versatile substructure has a number of sites available for functionalization which gives rise to a huge number of possible analogues.

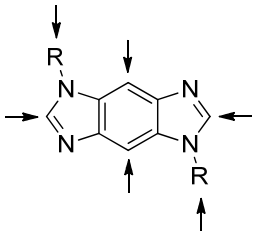

Imidazo[5,4-*f*]benzimidazole

(arrows indicate the functionalizable positions)

Figure 1.14; Imidazo[5,4-*f*]benzimidazole substructure.

In keeping with the ongoing research efforts of the Aldabbagh group, the aim is that the series of imidazo[5,4-*f*]benzimidazolequinones will have representatives which possess differing key structural features including, but not limited to, isomeric [4,5-*f*] form, ring size, ring fusion and incorporation of heteroatoms into aliphatic rings. The series will be biologically evaluated by testing on a number of different cancer cell lines by the Aldabbagh group and independently using the NCI-60 screening program. Computational calculations will be used to further assess the series and account for the observed biological activities.

The objectives of this thesis are to develop general synthetic methodologies for the preparation of the novel series of imidazo[5,4-*f*]benzimidazolequinones so as analogues not prepared in this thesis can be easily prepared in the future. Further investigation will be carried out to shed more light on the varied and unpredictable biological activity displayed by the isomeric imidazo[4,5-*f*]benzimidazolequinones previously reported.[34] Using the results of all biological evaluations the anti-cancer activity of this previously unknown series of imidazo[5,4-*f*]benzimidazolequinones will be determined and all findings will be reported in the literature.

Chapter 2

2 Synthesis of Alicyclic Ring-Fused Imidazobenzimidazolequinone Anti-Cancer Agents using Bu_3SnH / Azo-Initiator Mediated Homolytic Aromatic Substitutions

2.1 Introduction

2.1.1 Bu_3SnH / azo-initiator mediated oxidative homolytic aromatic substitution

2.1.1.1 Overview

Like other aromatic substitution processes, homolytic aromatic substitution is an addition-elimination process. The attacking radical ($R^{\bullet}$, Scheme 2.1) adds to the aromatic π-system to give a σ-complex with the radical now delocalized around the π-system (hence, is now a more stable π-radical). This step has a high activation energy and represents the rate determining step, since aromaticity must be broken. Elimination of a leaving group allows aromaticity to be regained (Scheme 2.1).[45-46] When the leaving group (L, Scheme 2.1) is not a hydrogen atom, the process is often referred to as a radical *ipso*-substitution. Literature examples of radical *ipso*-substitutions involve displacement of a good radical leaving group such as a phenylsulfide,[47-50] phenylsulfoxide,[48-49] sulfones,[47-51] sulfonates,[52-54] or phosphinates.[55-56]

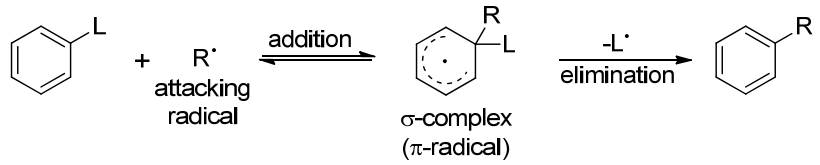

Scheme 2.1; Homolytic aromatic substitution.

Aromatic radical *ipso*-substitution can be advantageous since it is regioselective and often high yielding. However, the requirement of a suitable radical leaving group makes the technique somewhat limited and the synthetic steps required to incorporate the leaving group decrease the overall efficiency. Homolytic aromatic substitution can be carried out in high yield and with good regioselectivity without the requirement of a leaving group (i.e. L = H, Scheme 2.1). However, the hydrogen atom is a poor leaving group, and must be removed by an oxidant. Hence, this type of radical substitution is often referred to as oxidative homolytic aromatic substitution.

Although the attacking radical can be generated in a number of different ways (photolysis[57], electrolysis[58], redox reactions[59]), the majority use an azo-initiator such as AIBN (2,2'-azobisisobutyronitrile) or ACCN (1,1'-azobiscyclohexanecarbonitrile) (Scheme 2.2) and a mediator such as tributyltin hydride (Bu_3SnH) or a related group 14 hydride.[45]

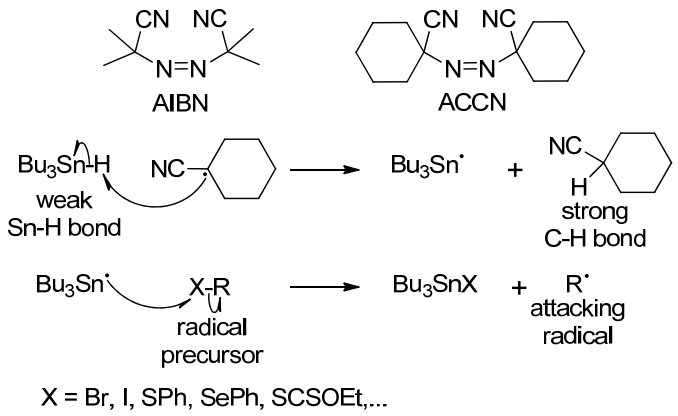

Scheme 2.2; Formation of $R^{\bullet}$ by Bu_3SnH and ACCN.

Thermal decomposition of azo-initiators results in the release of nitrogen gas with the formation of two tertiary initiating radicals. The initiating radicals efficiently abstract hydrogen from Bu_3SnH, forming a strong C-H bond in place of the weak Sn-H bond (Scheme 2.2). The resultant tributyltin radical ($Bu_3Sn^{\bullet}$) can abstract most common radical leaving groups such as halides, phenylsulfides, phenylselenides and xanthates, to form the attacking radical ($R^{\bullet}$). This process is thermodynamically favored since a strong Sn-X bond is formed in place of a weaker C-X bond in the radical precursor (Scheme 2.2).

However, the presence of Bu_3SnH in the reaction mixture can result in the reduction of carbon centered radicals, which competes with aromatic substitution.[60-61] This can be overcome by keeping the Bu_3SnH concentration low (by slow addition) or by the use of an alternative mediator such as tris(trimethylsilyl)silane ($(Me_3Si)_3SiH$) which has a lower reaction rate with carbon centered radicals (by ~1 order of magnitude less).[62]

The stability of carbon centered radicals (determined through bond dissociation energies) follows the order:[63-66]

$$3^{\circ\bullet} > 2^{\circ\bullet} > 1^{\circ\bullet} > Me^{\bullet} > vinyl^{\bullet} > Ph^{\bullet}$$

$$\rightarrow \text{decreasing order of stability} \rightarrow$$

As expected, the low stability of phenyl radicals gives rise to a significantly higher rate of radical substitution onto benzene than primary alkyl radicals.[67-69] However polar effects have a far greater influence on the reactivity of alkyl radicals than on aryl radicals. The SOMO (singly occupied molecular orbital) of alkyl radicals are relatively high in energy, giving them nucleophilic character.[68] Therefore the rate of nucleophilic alkyl radical substitution onto arenes increases as the arene is made more electron-deficient by electron-withdrawing groups.[70] By making the arene more electron-deficient, its π^* LUMO (lowest unoccupied molecular orbital) is lowered, allowing greater interaction with the relatively high energy SOMO of the nucleophilic alkyl radical.[66, 68] When the arene is an electron-deficient heteroarene, substitutions with nucleophilic alkyl radicals occur with a higher rate than with aryl radicals.[68] This is due to the fact that aryl radicals have very little polar character[70] and adding substituents onto the ring of aryl radicals has little impact on the polarity of the radical. Aryl radicals are considered to reside in orbitals which are perpendicular to the π-cloud, and thus have little interaction with the π-cloud.[71] Rates of nucleophilic alkyl radical substitutions onto heteroarenes have been increased further by making the heteroarene more electron-deficient through protonation of the basic nitrogens.[25, 61, 64, 68]

Although the stability of alkyl radicals increases when going from primary to tertiary, the nucleophilic character also increases, making tertiary radicals the most nucleophilic alkyl radicals.[61] This makes tertiary alkyl radicals more reactive towards homolytic aromatic substitution than secondary alkyl radicals which in turn are more reactive than primary.[61, 64] However, the relative rates of reduction of alkyl radicals by Bu_3SnH follows the order of stability. Thus, primary alkyl radicals, being less stable than secondary or tertiary, are reduced quickest followed by secondary, with tertiary being reduced slowest.[60] Therefore, homolytic aromatic substitution by primary alkyl radicals is more challenging than their secondary or tertiary counterparts.

Intramolecular homolytic aromatic substitutions have received considerably more interest than intermolecular substitutions. With intramolecular radical substitutions, the arene is held closer to the attacking radical, leading to increased rates of substitution, increased regioselectivity and decreased rates of radical reduction.

2.1.1.2 Oxidative homolytic aromatic substitutions of (hetero)aryl radicals

2.1.1.2.1 Intermolecular substitutions onto (hetero)arenes

In order to allow intermolecular substitution of aryl radicals to out-compete reduction by Bu_3SnH, the arene must be used in high concentration or used as solvent, with the concentration of Bu_3SnH kept low by slow addition. Martinez-Barrasa and co-workers synthesized a range of biaryls in 41-85% yield through AIBN / Bu_3SnH (or $(Me_3Si)_3SiH$) mediated substitutions of aryl and heteroaryl radicals onto arene solvents.[71]

McLoughlin *et al* generated imidazol-2 and 5-yl radicals from the respective bromides using 5 and 1.5 equivalents of AIBN and Bu_3SnH respectively. The σ-imidazolyl radicals underwent addition onto a range of arenes and heteroarene solvents to give a more stable π-cyclohexadienyl radical, which upon oxidative rearomatization gave moderate yields of substituted products. The protocol is outlined in Scheme 2.3 using benzene as solvent.

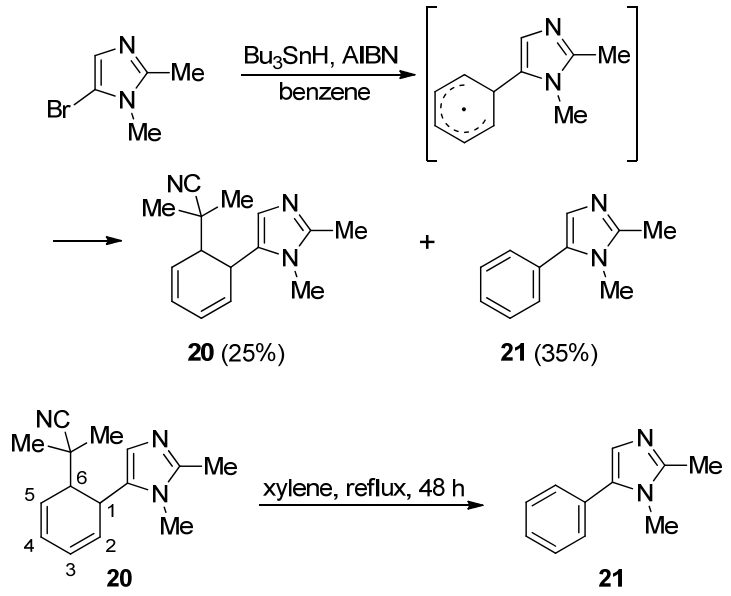

Scheme 2.3; Homolytic aromatic substitution of imidazol-5-yl radical onto benzene.

Large amounts of AIBN initiator were used, as it was proposed that AIBN fulfilled a dual role in the non-chain reaction, providing continual initiation, as well as facilitating the required hydrogen abstraction in the oxidative rearomatization step. In the case of the substitution of the imidazol-5-yl radical onto benzene, significant

trapping of the intermediate σ-complex by the initiating 2-cyanoprop-2-yl radical occurred, resulting in the stable 2,4-cyclohexadiene **20**. Diene **20** could be quantitatively rearomatized to give the substituted aromatic product **21** by refluxing at higher temperatures in xylene (Scheme 2.3).[72]

2.1.1.2.2 Intramolecular substitutions onto (hetero)arenes

Bu_3SnH / AIBN mediated intramolecular cyclizations of the indol-2-yl radical onto phenyl substituents have been reported by Fiumana and Jones (Scheme 2.4).[73] The less strained 6-membered cyclization proceeded in the highest yield of 65%, followed by the 7-membered cyclization in 37% yield, with the most strained 5-membered cyclization occurring in the lowest yield of 25%. In all cases some of the radical reduction product **23** was obtained. The attempted 8-membered cyclization resulted in [1,5]-hydrogen abstraction with the resultant secondary alkyl radical cyclizing back onto the indole-2 position to give a 5-membered ring bearing a benzyl group **24**.[73]

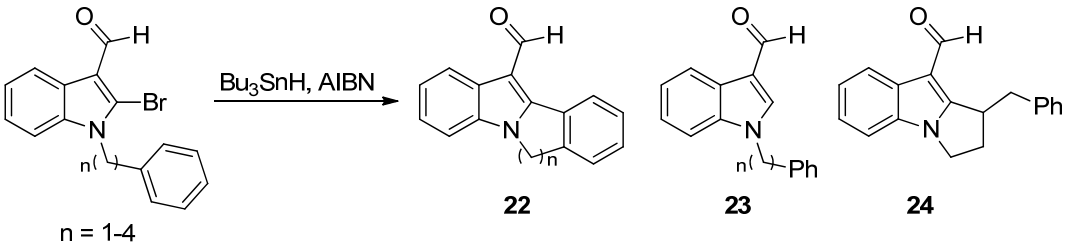

n	**22** (%)	**23** (%)	**24** (%)
1	25	55	-
2	65	25	-
3	37	32	-
4	0	27	48

Scheme 2.4; Heteroaryl radical cyclizations to arenes.

Harrowven *et al* reported that intramolecular cyclizations of aryl radicals to arenes[74-75] and heteroarenes[76-77] proceeded with greater efficiency when aryl iodide radical precursors were used rather than aryl bromides, with only catalytic amounts of AIBN and ~1.5-2.5 equivalents of Bu_3SnH being required (Scheme 2.5). The introduction of both electron withdrawing groups and electron donating groups had little effect on the yields of cyclized products.[74] The protocol allowed for the selective homolysis of

the carbon iodine bond, while leaving chlorine and bromine substituents unchanged.[75]

The efficiency of the process meant that double 6-membered radical cyclizations could be carried out to give [5]helicenes and [7]helicenes in high yield (Scheme 2.6).[75]

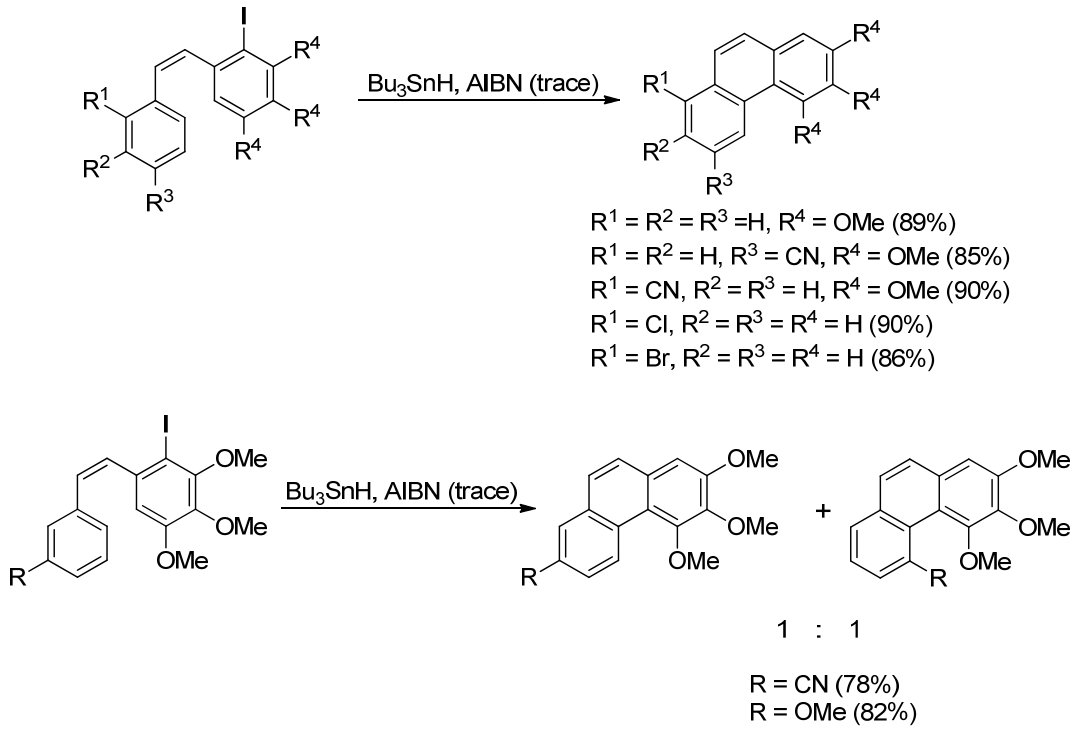

Scheme 2.5; Six-membered aryl radical cyclizations onto arenes linked by vinyl tethers.

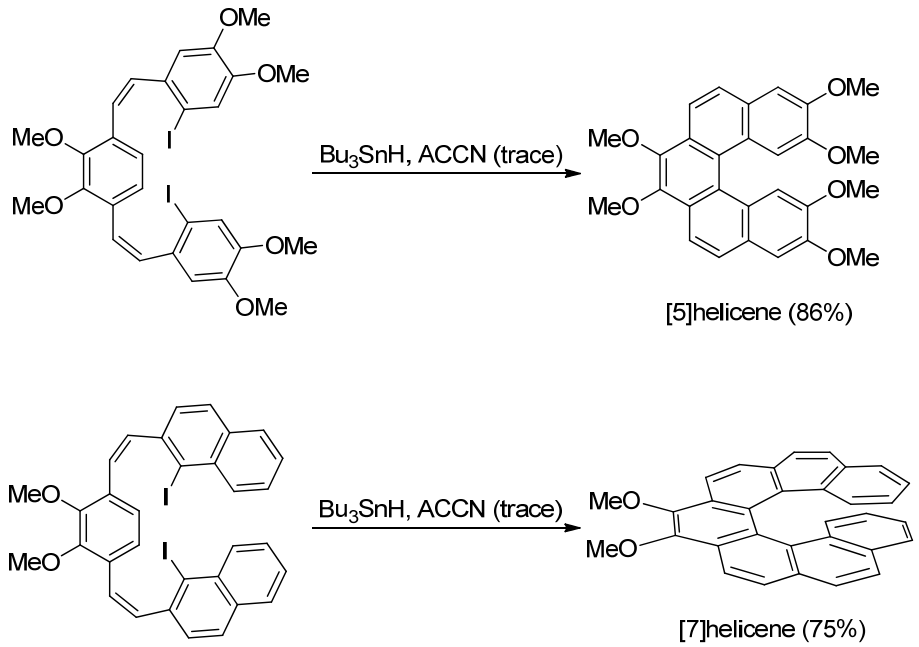

Scheme 2.6; Double aryl radical cyclizations onto arenes to give [5]helicenes and [7]helicenes.

The mechanism proposed by Harrowven *et al* (Scheme 2.7)[76] was similar to the pseudo-$S_{RN}1$ mechanism which had been proposed previously by Bowman *et al*.[78] The aryl radical, formed from the reaction of the starting material with AIBN / Bu_3SnH, cyclizes onto the adjacent heteroarene forming a σ-complex (Scheme 2.7).

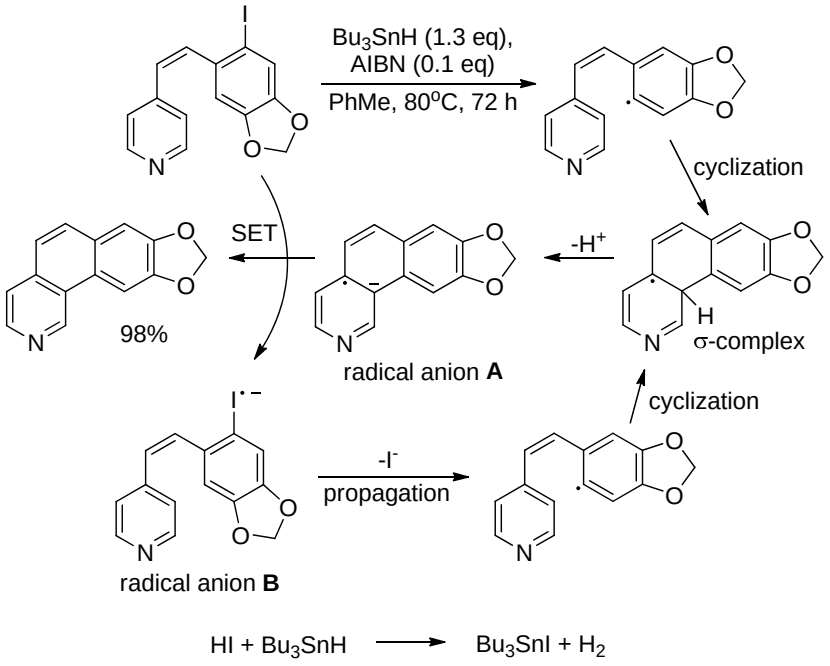

Scheme 2.7; Proposed pseudo-$S_{RN}1$ mechanism.

Loss of a proton gives the radical anion **A**, which undergoes single electron transfer (SET) to the starting material, giving the substituted product and the radical anion **B**. Loss of iodide from radical anion **B** generates another aryl radical which completes the chain mechanism. It is presumed that the hydrogen iodide formed reacts ionically with Bu_3SnH to give Bu_3SnI and hydrogen gas. It was proposed that cyclizations of aryl bromides did not proceed by a chain mechanism because SET to aryl bromides is less efficient than to aryl iodides, thus significantly more initiator was required for cyclization of aryl bromides.[76] Using these conditions all attempts to effect cyclization reactions leading to 5-membered rings failed, yielding only the reduction products.[76-77]

Clyne and Aldabbagh cyclized imidazol-2[57] and 5-yl[79] radicals onto arenes using both Bu_3SnH / AIBN and photochemical mediation of the corresponding bromides or iodides. The greatest yields of cyclized products were achieved for 6-

membered annulation reactions, with 7-membered next and 5-membered being most difficult to achieve (Scheme 2.8 & 2.9).

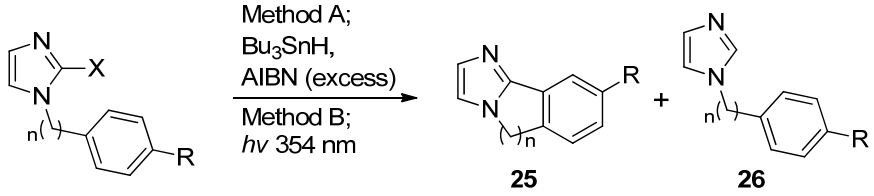

X	R	Method	n = 1		n = 2		n = 3	
			25 (%)	**26** (%)	**25** (%)	**26** (%)	**25** (%)	**26** (%)
Br	H	A	0	45	35	26	0	65
Br	F	A	-	-	32	19	-	-
Br	Cl	A	-	-	20	31	-	-
I	H	B	0	45	70	0	48	0
I	Cl	B	-	-	66	0	-	-
I	CF_3	A	-	-	21	51	-	-
I	NO_2	A	-	-	32	0	-	-
I	CF_3	B	-	-	53	0	-	-

Scheme 2.8; Imidazol-2-yl radical cyclizations onto arenes.

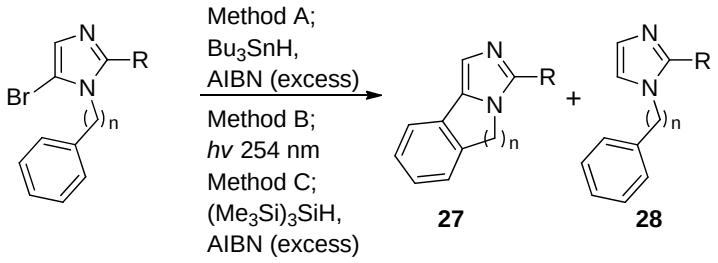

R	Method	n = 1		n = 2		n = 3	
		27 (%)	**28** (%)	**27** (%)	**28** (%)	**27** (%)	**28** (%)
H	A	-	-	64	3	0	69
Ph	A	-	-	59	8	20	46
H	B	-	-	0	0	-	-
Ph	B	8	0	67	0	34	0
H	C	0	63	-	-	-	-
Ph	C	22	27	-	-	-	-

Scheme 2.9; Imidazol-5-yl radical cyclization onto arenes.

Curran and Keller reported the homolytic aromatic substitution of aryl radicals under mild conditions in the presence of low levels of oxygen without the need for an initiator (Scheme 2.10).[80] A vinyl radical cyclization was also reported, along with intermolecular aryl radical substitutions onto benzene. $(Me_3Si)_3SiH$ was used as the mediator since Bu_3SnH was deemed not to be effective under such conditions. Pyridine was added to neutralize the HI formed, and a catalytic amount of iodine was added to aid initiation.[80]

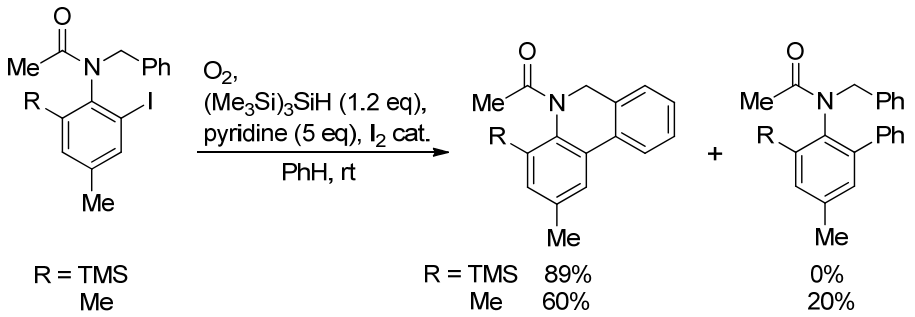

Scheme 2.10; O_2-facilitated intramolecular homolytic aromatic substitution.

A chain mechanism was proposed, whereby following initiation, iodine is abstracted from the aryl iodide to generate an aryl radical, which adds to the arene to give an intermediate π-radical (Scheme 2.11). The abstraction of hydrogen from the π-radical by molecular oxygen re-generates aromaticity, giving the hydroperoxy radical ($HOO^{\bullet}$) which abstracts hydrogen from $(Me_3Si)_3SiH$ to propagate the chain. It was proposed that in cases where the radical generation and addition to the aromatic system are fast enough, oxygen is likely to promote the target reaction by providing a rapid and productive path for rearomatization.[80]

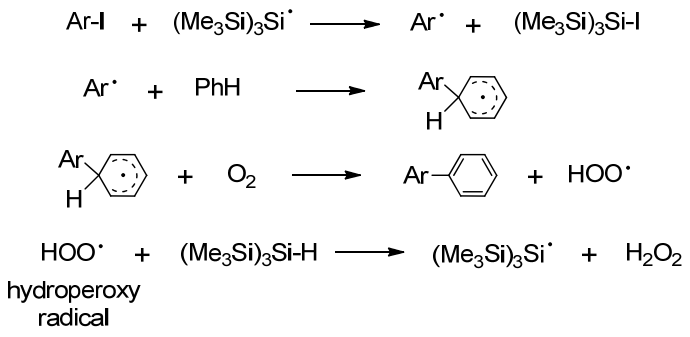

Scheme 2.11; Mechanism of O_2-facilitated homolytic aromatic substitution.

2.1.1.3 Oxidative homolytic aromatic substitutions of alkyl radicals

2.1.1.3.1 Intermolecular substitutions onto activated heteroarenes

Minisci *et al* showed that Bu_3SnH / AIBN mediated intermolecular homolytic aromatic substitution of alkyl radicals onto basic heteroarenes was possible if the heteroarene was activated by protonation (Scheme 2.12).[61]

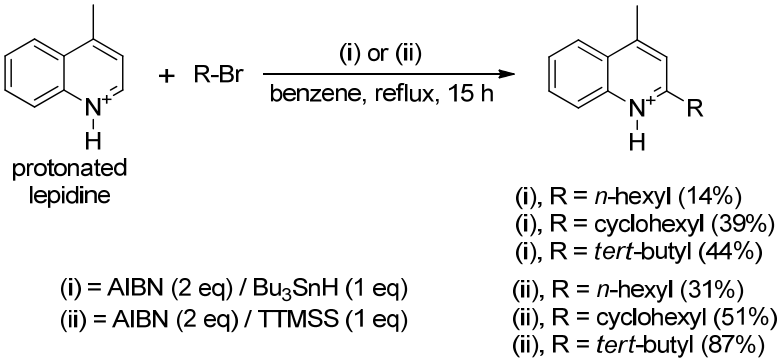

Scheme 2.12; Intermolecular alkyl radical substitutions onto protonated lepidine.

Nucleophilic primary, secondary and tertiary alkyl radicals substituted selectively onto the most electrophilic 2-position of protonated lepidine, with the most nucleophilic tertiary alkyl radicals giving highest yields. Use of Bu_3SnH / AIBN as the radical mediating system gave moderate yields of substituted products, which were improved by using the weaker reductant $(Me_3Si)_3SiH$ (Scheme 2.12). Stoichiometric amounts of AIBN were used as the source of initiating radicals and of hydrogen abstracting species to regenerate aromaticity. However, the best results were obtained when peroxy initiators such as di-*tert*-butyl peroxyoxalate were used with phenylsilanes as mediators.[61] Other intermolecular oxidative homolytic aromatic substitutions carried out in the absence of group 14 hydrides have been reported to be facile.[81]

2.1.1.3.2 Intramolecular substitutions onto (hetero)arenes

Beckwith and Storey reported a radical translocation route to oxindoles **29**. Treatment of bromoanilide precursors with Bu_3SnH / AIBN gave an aryl radical. A 1,5-hydrogen abstraction occurred, giving a stabilized tertiary alkyl radical, which cyclized back onto aromatic ring to give oxindoles (Scheme 2.13).[82]

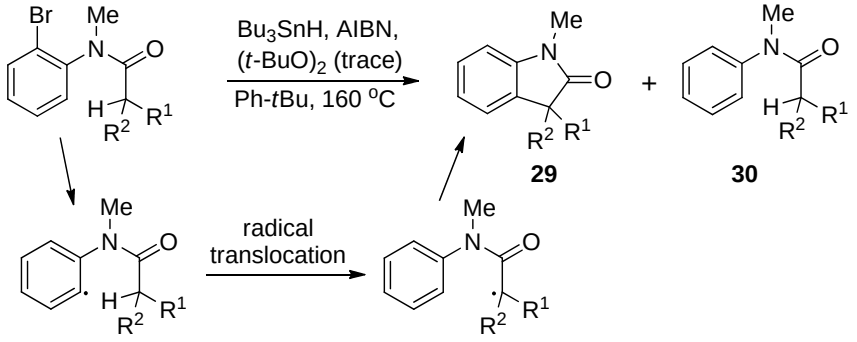

R^1	R^2	**29** (%)	**30** (%)
Me	Me	70	10
Me	H	51	38
H	H	47	44
cyclopropyl		81	1
cyclobutyl		62	25
cyclopentyl		87	13
cyclohexyl		85	0

Scheme 2.13; Aryl radical translocation and homolytic aromatic substitution to give oxindoles.

Highest yields of oxindoles were achieved when the reaction was performed in *tert*-butylbenzene at 160 °C, with catalytic amounts of di-*tert*-butyl peroxide added in portions. The yields of oxindoles **29** progressively increased as the cyclizing alkyl radical was change from being primary to secondary to tertiary, with the reduction products **30** progressively decreasing. Cyclizations of cycloalkyl radicals also proceeded in high yield with little reduction.

Storey and Ladwa cyclized various cycloalkyl radicals using 1.5 and 2 equivalents of Bu_3SnH and AIBN, respectively, to give spiro-cyclic 5-azaoxindoles **31** in 55-71% yield (Scheme 2.14).[83] In this case the halogen was situated α to the amide, hence eliminating the radical translocation step. Although the cyclopropyl radical has been shown to have similar reactivity to that of vinyl radicals, the lower rate of cyclization was attributed to it having the lowest nucleophilicity and thus being least attracted to the electron deficient pyridine ring. Cyclization of primary

alkyl radicals did not occur and cyclizations of secondary radicals gave yields of less than 8%.[83]

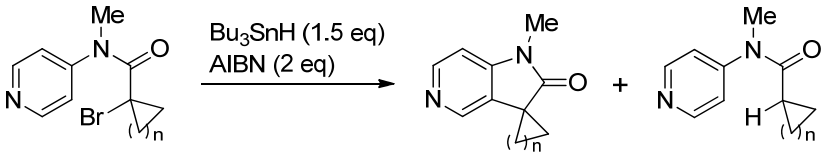

31 **32**

n	**31** (%)	**32** (%)
1	55	21
2	73	11
3	76	12
4	71	10

Scheme 2.14; Synthesis of spiro-cyclic 5-azaoxindoles.

Pavé *et al* used homolytic aromatic substitution of primary alkyl radicals as the key step in the stereocontrolled synthesis of a lead intermediate 3-aminochromans **33** (Scheme 2.15).[84]

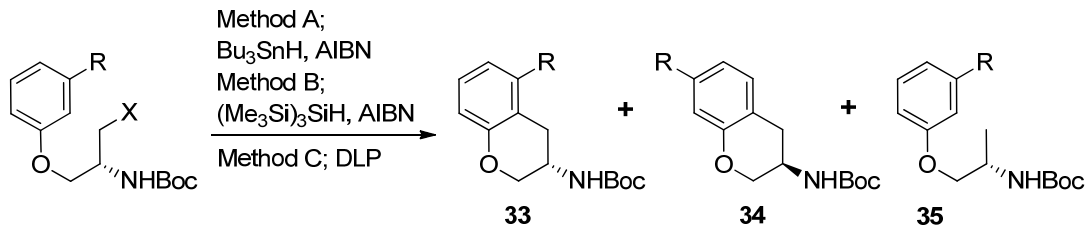

33 **34** **35**

R	X	Method	**33** (%)	**34** (%)	**35** (%)
$COCH_3$	I	A	31	16	34
$COCH_3$	I	B	36	18	12
$COCH_3$	SCSOEt	C	69	20	<5
CO_2CH_3	SCSOEt	C	56	17	<5

Scheme 2.15; Primary alkyl radical cyclizations onto arenes.

Using Bu_3SnH or $(Me_3Si)_3SiH$ with AIBN gave low yields of the desired cyclized compound **33**, with selectivity also being an issue. The yield of the desired compound **33** was improved by using the xanthate / dilauroyl peroxide (DLP) method developed by Zard and co-workers.[85-86]

Osornio *et al* cyclized primary alkyl radicals onto quinolones and isoquinolones using Bu_3SnH / AIBN as the radical mediating system.[87] Cyclizations onto quinolones proceeded in high yield via an oxidative non-chain mechanism

requiring excess azo-initiator. Incomplete consumption of starting materials was observed when catalytic amounts of AIBN were used, leading to the conjecture that this reagent also functioned as the oxidant in the rearomatization step. Cyclization of propyl radicals resulted in the expected substitution at the most electron deficient C-2 position and the unexpected substitution at C-8 as the minor product (Scheme 2.16). Although the C-2 was the most electrophilic and hence, most activated position, cyclization at C-8 was possible as it gave rise to an unstrained 6-membered ring.[87]

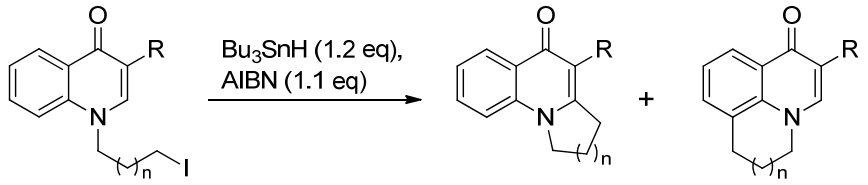

36 **37**

n	R	**36** (%)	**37** (%)
1	CO_2Et	60	24
1	CN	65	22
2	CO_2Et	90	0

Scheme 2.16; Primary alkyl radical cyclizations onto quinolones.

The analogous cyclizations onto isoquinolones only proceeded via a reductive chain mechanism, even with excess AIBN, with 5-exo-trig cyclizations being most efficient, as expected from Baldwin's rules (Scheme 2.17).[87]

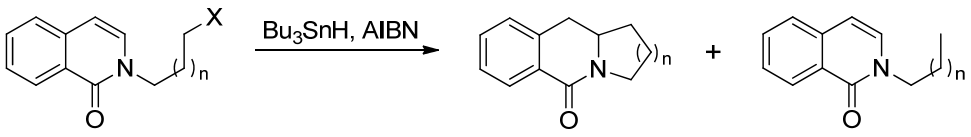

38 **39**

n	X	**38** (%)	**39** (%)
1	Br	88	7
1	I	77	16
2	I	51	36

Scheme 2.17; Primary alkyl radical cyclizations onto isoquinolone.

Aldabbagh *et al* carried out Bu_3SnH / AIBN mediated oxidative primary alkyl radical substitutions onto imidazole-4 and 5-carbaldehyde.[88-89] Cyclization onto imidazole-4-carbaldehyde occurred selectively at the most electrophilic C-5 position (Scheme 2.18). The 6-membered cyclization gave the highest yield with no reduction. The 5-

membered cyclization proceeded in higher yield than the 7-membered, with small amounts of reduction obtained in both cases.

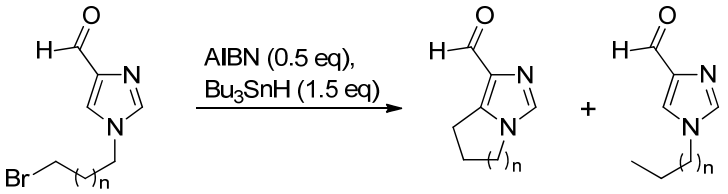

N-alkyl-imidazole-4-carbaldehyde **40** **41**

n	**40** (%)	**41** (%)
1	42	10
2	49	0
3	14	8

Scheme 2.18; Primary alkyl radical cyclizations onto imidazole-4-carbaldehydes.

Cyclizations onto imidazole-5-carbaldehyde showed a marked difference between the 5 and 6-membered cyclizations. The 5-membered cyclization gave only reduced product, while the 6- membered gave only cyclized with no reduction (Scheme 2.19).

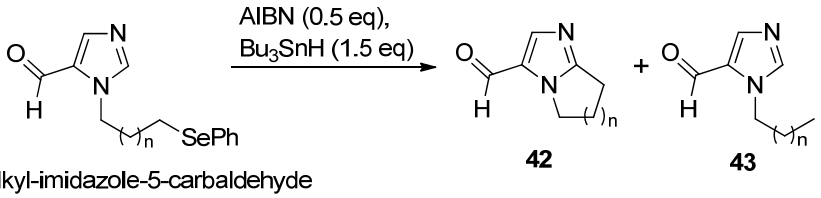

N-alkyl-imidazole-5-carbaldehyde **42** **43**

n	**42** (%)	**43** (%)
1	0	73
2	53	0

Scheme 2.19; Primary alkyl radical cyclizations onto imidazole-5-carbaldehydes.

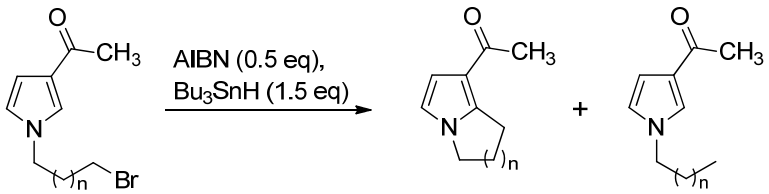

N-alkyl-3-substituted pyrroles **44** **45**

n	**44** (%)	**45** (%)
1	46	11
2	45	0
3	54	18

Scheme 2.20; Primary alkyl radical cyclizations onto 3-substituted pyrroles.

Regioselective radical cyclizations onto the most electrophilic C-2 position of *N*-alkyl-3-substituted pyrroles were also reported, giving moderate yields of cyclized products, with reduced products only reported for the 5- and 7-membered cyclizations (Scheme 2.20).[88-89]

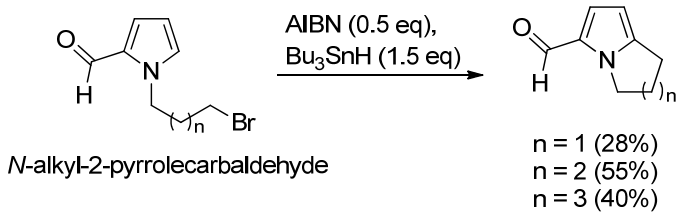

Scheme 2.21; Primary alkyl radical cyclizations onto 2-pyrrolecaraldehehyde.

Cyclizations onto 2-pyrrolecarbaldehyde proceeded without the formation of reduced products. The relatively low yields obtained were due to the common problem of separating tributyltin residues from the products (Scheme 2.21).[88-89]

Bowman and co-workers reported the synthesis of [1,2-*b*]-fused pyrazoles via primary alkyl radical cyclizations onto the pyrazole C-5 position (Scheme 2.22).[90-91] A radical stabilizing group at the C-4 position was essential to facilitate cyclization, with a phenyl substituent giving rise to the best yields of cyclized products. The 6-membered cyclizations proceeded with the highest yields, with little difference between 5- and 7-membered cyclizations. Use of triethylborane (Et_3B) as initiator with $(Me_3Si)_3SiH$ as mediator improved the 6-membered cyclization onto pyrazole-4-ethylester, but did not improve the analogous 5- or 7-membered cyclizations. No explanation was given for the formation of the unexpected alkene by-product **48**, which was obtained when the rate of cyclization was slow.[90-91]

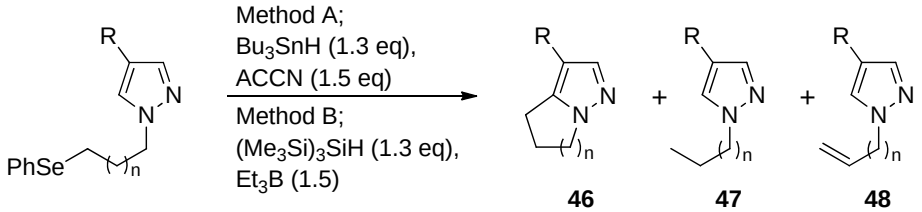

Method	R	n = 1			n = 2			n = 3		
		46 (%)	**47**(%)	**48** (%)	**46**(%)	**47** (%)	**48** (%)	**46** (%)	**47** (%)	**48** (%)
A	Ph	38	17	0	63	0	0	37	48	0
A	CO_2Et	0	38	11	0	0	67	0	0	41
B	CO_2Et	0	73	0	36	0	0	0	62	0

Scheme 2.22; Primary alkyl radical cyclizations onto pyrazoles.

Aldabbagh and co-workers used Bu_3SnH / ACCN mediated homolytic aromatic substitution as the key step in the synthesis of [1,2-*a*]-fused tricyclic bioreductive benzimidazolequinones.[25] Good yields were obtained when the heteroarene was activated through protonation by camphorsulfonic acid (CSA), with excess initiator used to aid in the rearomatization step (Scheme 2.23).

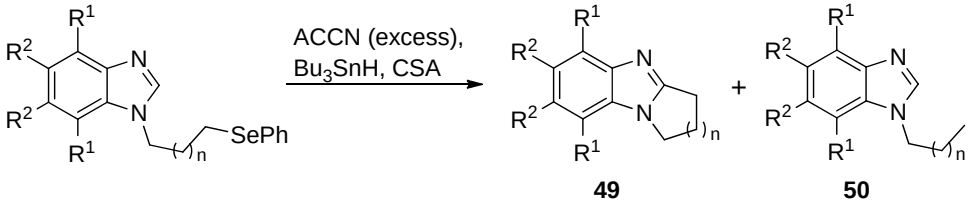

n	R^1	R^2	**49** (%)	**50** (%)
1	Me	H	32	54
2	Me	H	69	0
3	Me	H	63	21
2	H	OMe	70	0

Scheme 2.23; Primary alkyl radical cyclization onto activated benzimidazoles.

The efficiency of cyclizations followed the trends seen by others where 6-membered cyclizations were most efficient, with 7-membered next and 5-membered cyclization giving a considerable amount of reduction. The yields of 6- and 7-membered cyclizations reported here are better than those reported earlier by Aldabbagh *et al* for the analogous radical *ipso*-substitutions at the benzimidazole C-2 positions, proving that a radical leaving group at the C-2 position is not necessary to obtain good yields of cyclization products.[47, 50]

2.1.2 Aims and objectives

- To develop a protocol for the first double radical cyclizations of primary alkyl radicals onto heteroarenes; that is double homolytic aromatic substitutions onto imidazobenzimidazole.
- To explore the scope of the protocol by carrying out annulation reactions leading to 5-, 6- and 7-membered rings.
- To further functionalize imidazo[4,5-*f*]benzimidazoles and imidazo[5,4-*f*]benzimidazoles to give biologically active quinones, which will be evaluated as anti-cancer agents (see Chapter 4).

2.1.3 Synthetic strategy

It was envisaged that by alkylating imidazo[5,4-*f*(4,5-*f*)]benzimidazole **51** with alkyl chains bearing a phenylselenide group, two isomers would be obtained. Following separation of the isomers, a Bu_3SnH / ACCN mediated double homolytic aromatic substitution reaction would represent the key step in the synthesis, and would result in pentacyclic heteroaromatic systems. Nitration and functional group interconversion of the pentacyclic systems would ultimately give the desired dialicyclic ring-fused imidazobenzimidazolequinones (Scheme 2.24). This would represent the first viable synthesis of alicyclic ring-fused imidazo[5,4-*f*]benzimidazoles, which would also give the isomeric imidazo[4,5-*f*]benzimidazole system.

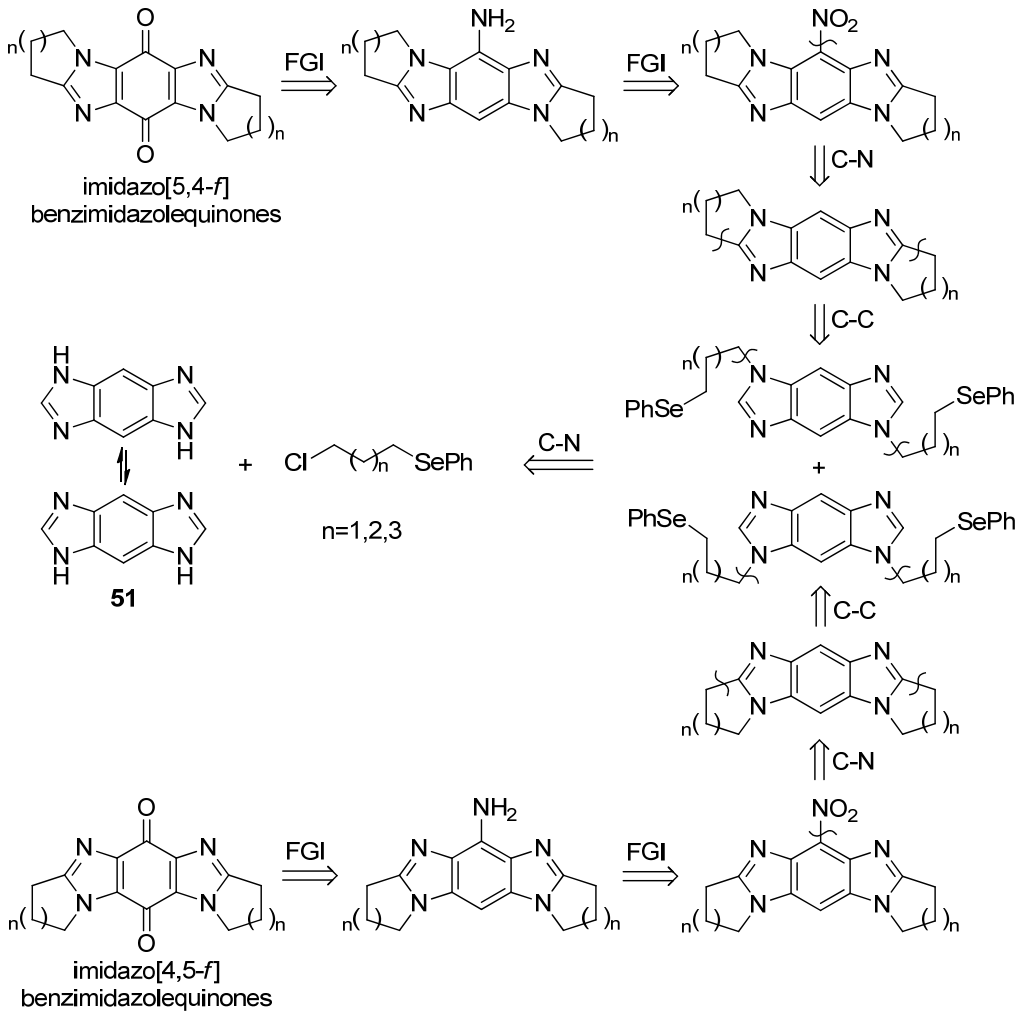

Scheme 2.24; Retrosynthetic analysis of the target imidazobenzimidazolequinone molecules.

2.2 Results and discussion

2.2.1 Preparation of radical precursors and *N*-alkylimidazobenzimidazoles

Compound **51** was prepared by the Philips condensation reaction between 1,2,4,5-benzenetetraamine tetrahydrochloride and concentrated formic acid with a small amount of hydrochloric acid added, giving a near quantitative yield (Scheme 2.25).[92-93]

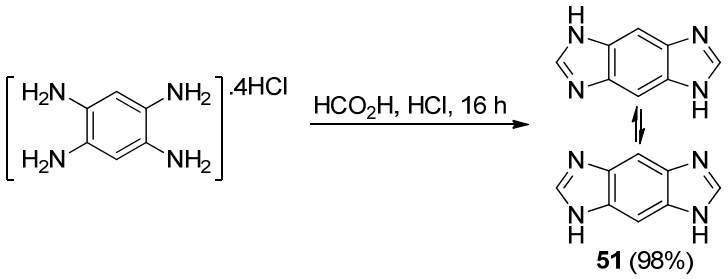

Scheme 2.25; Synthesis of imidazo[5,4-*f*(4,5-*f*)]benzimidazole **51**.

The phenylselenide group is efficiently abstracted by alkyltin radicals with a rate close to that of bromine.[94] Because of this and their ease of preparation, phenylselenides are versatile and well established as alkyl radical precursors. The corresponding bromides and iodides are susceptible to nucleophilic substitution by amines and heteroaromatic bases. Phenylselenides are far less susceptible to nucleophilic attack by such bases.[47, 50, 95-97] They are often more stable towards isolation, purification and long-term storage than their halogen counterparts. Phenylseleno esters[98-99] and imidoyl phenylselenides[100] have also been used as acyl and imidoyl radical precursors, respectively.

ω-Chloroalkyl phenylselenides **52a-c** were synthesized according to the procedure developed by Aldabbagh and Bowman.[47, 50, 101] However, it was found that the reaction was complete 2 hours after addition of 1-chloro-*ω*-iodoalkanes, and that carrying the reaction out at the lower temperature of -10 ^{o}C eliminated the formation of di-substituted by-products. Therefore upon workup, the purity of the products was such that no chromatography was needed and yields were excellent (Scheme 2.26).

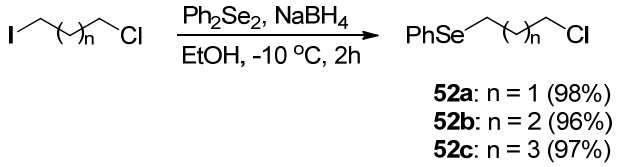

Scheme 2.26; Synthesis of ω-chloroalkyl phenylselenides.

In the literature ω-chloroalkyl phenylselenides were converted to the corresponding iodoalkyl phenylselenides prior to reaction with *N*-heterocycles.[25, 47, 50, 102] It was found that ω-chloroalkyl phenylselenides **52a-c** could be used to react with imidazobenzimidazole **51** without prior conversion to iodides. In fact, the chlorides were superior alkylating agents, as unwanted excessive alkylation did not occur. The slower rate of substitution (due to lower reactivity than the iodides) could be compensated for by increasing the temperature to 120 °C. However, the reaction proceeded to completion at 80 °C overnight. The mixture of 1,5 and 1,7-isomers produced, were readily separated by chromatography yielding the radical precursors **53a-c** and **54a-c** in excellent overall yields (Scheme 2.27).

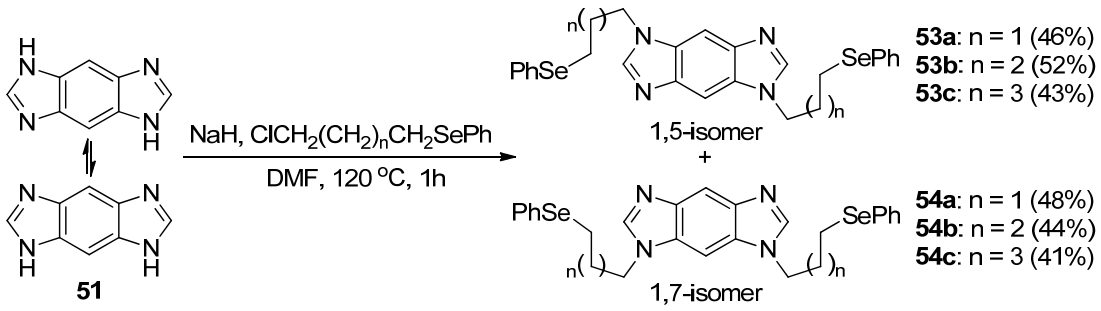

Scheme 2.27; Synthesis of radical precursors.

Using 1.1 equivalents of sodium hydride and 1-chlorobutane, effective mono-alkylation of **51** was achieved, giving compound **57** in 59% yield and a combined yield of 23% of dialkylated imidazo[5,4-*f*]benzimidazole **55** and imidazo[4,5-*f*]benzimidazole **56** (Scheme 2.28). Attempts at varying the equivalents, reaction times and temperature failed to increase the yield of 1-butyl-5(7)*H*-imidazo[5,4-*f*(4,5-*f*)]benzimidazole **57**.

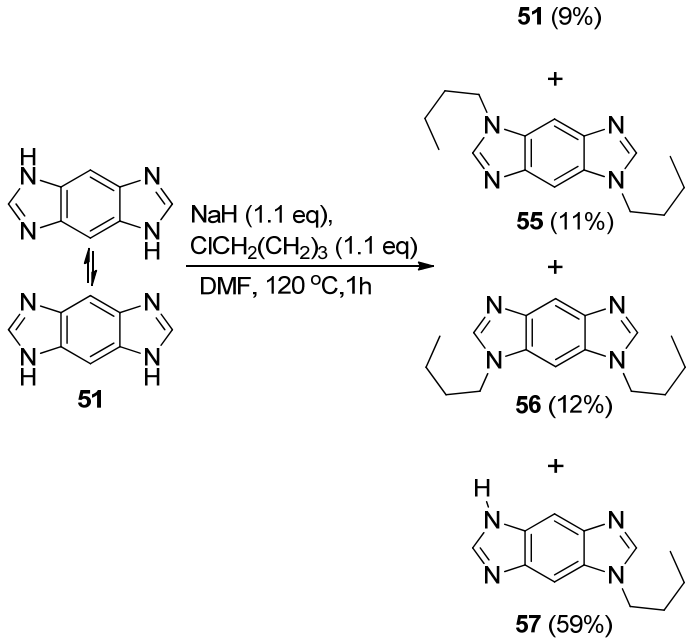

Scheme 2.28; Synthesis of 1-butyl-5(7)*H*-imidazo[5,4-*f*(4,5-*f*)]benzimidazole **57**.

The imidazobenzimidazole **57** was alkylated with 4-chlorobutyl phenylselenide under the conditions of Scheme 2.27, yielding the phenylselenide radical precursors **58** (43%) and **59** (40%), each bearing only one radical precursor group (Scheme 2.29).

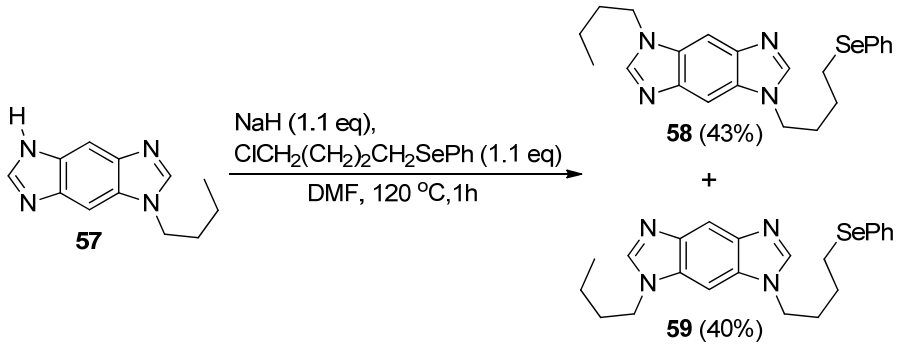

Scheme 2.29; Synthesis of 1-butyl-5-(4-(phenylselano)butyl)imidazo[5,4-*f*]benzimidazole **58** and 1-butyl-7-(4-(phenylselano)butyl)imidazo[4,5-*f*]benzimidazole **59**.

Although 1,5- and 1,7-dibutyl imidazobenzimidazoles **55** and **56** had been inadvertently prepared earlier (Scheme 2.28), a higher yielding synthesis was required. Therefore compounds **55** and **56** were prepared by alkylation of **51** using 2.1 equivalents of sodium hydride and 1-chlorobutane (Scheme 2.30). Compound **55** was later converted to a biologically active quinone compound and was included in anti-cancer studies.

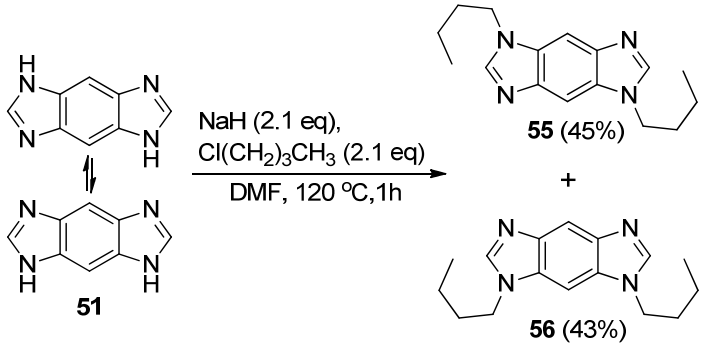

Scheme 2.30; Synthesis of 1,5-dibutylimidazo[5,4-*f*]benzimidazole **55** and 1,7-dibutylimidazo[4,5-*f*]benzimidazole **56**.

2.2.2 One-pot double homolytic aromatic substitutions

The separated radical precursors 1,5-di(*ω*-(phenylselano)alkyl)imidazo[5,4-*f*]benzimidazoles **53a-c** and 1,7-di(*ω*-(phenylselano)alkyl)imidazo[4,5-*f*]benzimidazoles **54a-c** were subjected to Bu_3SnH / ACCN mediated homolytic aromatic substitution. The conditions for the one-pot double radical substitution protocol were optimized using the 6-membered cyclization of dibutyl phenylselenide **53b**. Initially the conditions of Lynch *et al* were used, where Bu_3SnH (2.5 equivalents per cyclization) and ACCN (4 equivalents per cyclization) in toluene (0.06 M) were slowly added via a syringe pump to a refluxing solution of **53b** (1 equivalents) and camphorsulfonic acid (1 equivalents per cyclization) in toluene under an atmosphere of N_2.[25] After 1, 5 and 9 hours, a further 0.5 equivalents of ACCN in toluene (0.06 M) was added (Scheme 2.31). After workup and purification by chromatography, 60% of desired product **60b** was obtained.

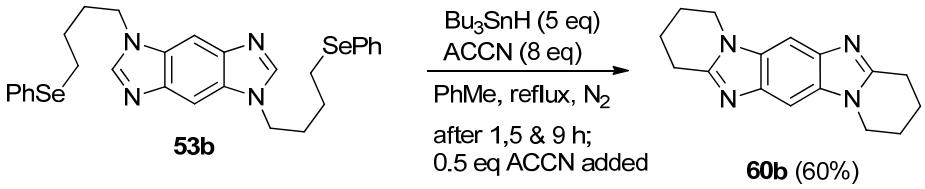

Scheme 2.31; Initial conditions used for double alkyl radical cyclizations.

Although no reduced products were observed, a number of unidentified products were obtained. Since no radical reduction was observed, the reaction was repeated without activation by CSA, which led to a cleaner product mixture, but significant

amounts of unidentified products still remained. After prolonged periods of storage in solution in the open air, mixtures of these unidentified products changed into the desired aromatic product. Therefore it was assumed that the complex mixtures were non-aromatic products obtained as a result of trapping of the π-radical intermediates formed after cyclization.[72, 103] Investigations showed that heating the reaction mixture in the open air for 48 hours after completion of syringe pump addition of Bu_3SnH / ACCN aided rearomatization to some extent. McLoughlin *et al* showed that dienes, derived from the trapping of π-radical intermediates by 2-cyanoisopropyl radicals, could be quantitatively rearomatized by heating at reflux in xylene.[72] It was found that carrying out the reaction in the absence of an inert environment (*i.e.* without excluding air) led to a significant increase in the desired aromatic substitution product. Some non-aromatic products were still obtained, but it was found that exposure to direct sunlight or irradiation at 350 nm for 3 hours facilitated total rearomatization.

Optimized yields were obtained using five equivalents of Bu_3SnH and ACCN (or 2.5 equivalents per phenylselenide moiety) (Scheme 2.32). When less than four equivalents of Bu_3SnH were used, starting material was observed in the crude product mixture. Using these conditions, dipyrido ring fused imidazo[5,4-*f*]benzimidazole **60b** was obtained in the excellent yield of 90% (Table 1, Entry 4). Compound **60b** was previously reported by Baxter *et al*, but with a yield of less than 1%.[104] The less favorable 5- and 7-membered cyclizations gave significant amounts of reduced products (Entry 1 & 5). Thus ring-activation by CSA (2.1 equivalents) was deemed necessary (method 2). Although the acid improved the double 7-membered nucleophilic alkyl radical cyclizations to give **60c** in 54% yield (entry 6), it led to an intractable mixture for the attempted 5-membered analogue (entry 2). Replacing CSA with acetic anhydride (2.1 equivalents, method 3) facilitated the 5-membered cyclization to give the improved, but modest yield of **60a** (47%) (entry 3).

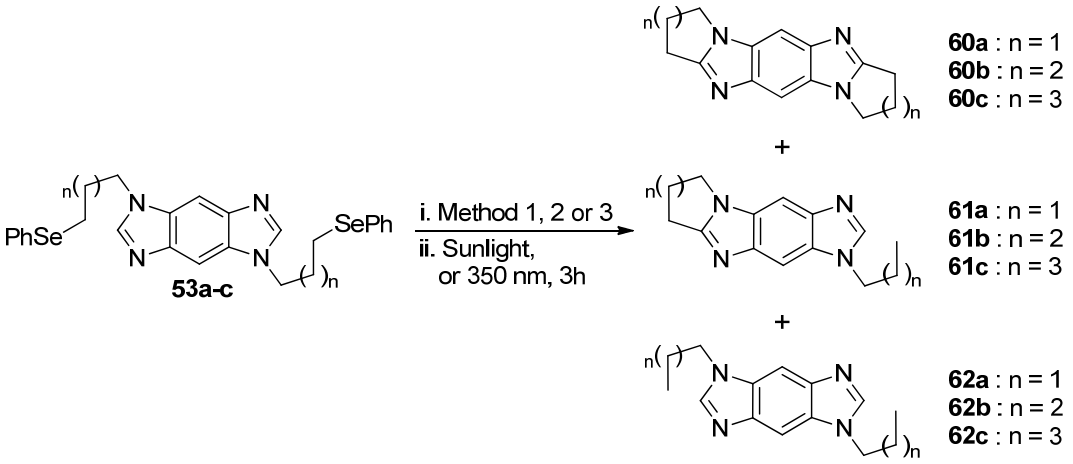

Scheme 2.32; One-pot double primary radical cyclizations onto imidazo[5,4-*f*]benzimidazoles.

i. Method 1: Bu_3SnH (5 equiv, 0.06 M), ACCN (5 equiv.), toluene, syringe pump addition (2.2 mL/h), reflux, air; **Method 2:** Method 1 & CSA (2.1 equiv.); **Method 3:** Method 1 & Ac_2O (2.1 equiv.);
ii. Sunlight, 15-20 °C or 350 nm, Rayonet reactor, rt.

Table 1; One-pot double primary radical cyclizations onto imidazo[5,4-*f*]benzimidazoles.

Entry	Precursors	Method	Products (%)[a]					
1	**53a**	1	**60a**	(32)	**61a**	(31)	**62a**	(10)
2	**53a**	2	-[b]		-[b]		-[b]	
3	**53a**	3	**60a**	(47)	**61a**	(30)	**62a**	(0)
4	**53b**	1	**60b**	(90)	**61b**	(0)	**62b**	(0)
5	**53c**	1	**60c**	(29)	**61c**	(32)	**62c**	(8)
6	**53c**	2	**60c**	(54)	**61c**	(13)	**62c**	(0)
7	**53c**	3	**60c**	(34)	**61c**	(31)	**62c**	(0)

[a] Isolated yields; [b] Intractable mixture.

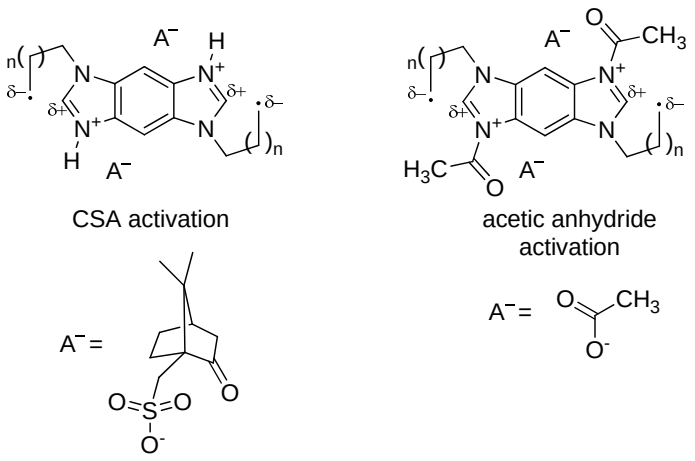

Scheme 2.33; Quaternization of *N*-3&7 of imidazo[5,4-*f*]benzimidazoles.

The yields of cyclization products obtained compare very favorably to yields of alkyl radical cyclizations carried out in the past.[25, 47-50, 83, 90-91] The results are all the more impressive, when it is taken into consideration that double cyclizations are carried out.

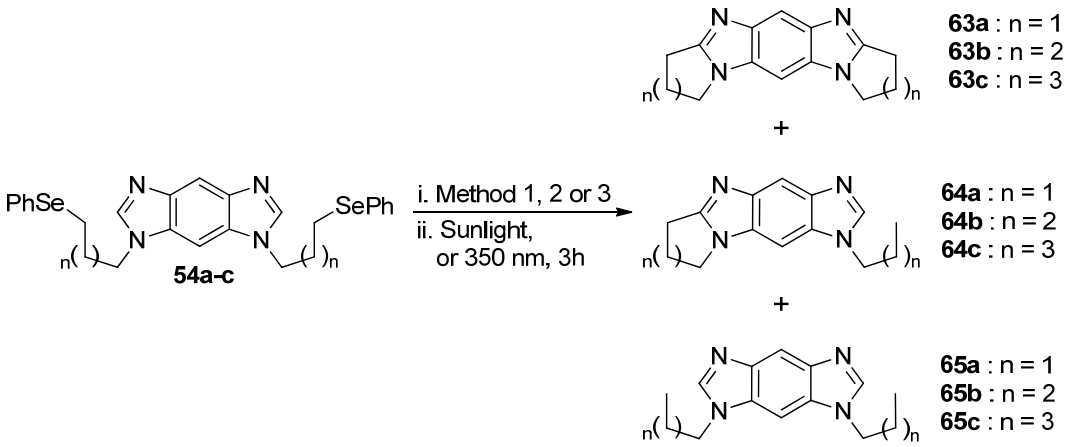

Scheme 2.34; One-pot double primary radical cyclizations onto imidazo[4,5-*f*]benzimidazoles.

Table 2; One-pot double primary radical cyclizations onto imidazo[4,5-*f*]benzimidazoles.

Entry	Precursors	Method	Products (%)[a]					
1	**54a**	3	**63a**	(48)	**64a**	(27)	**65a**	(0)
2	**54b**	1	**63b**	(81)	**64b**	(0)	**65b**	(0)
3	**54c**	2	**63c**	(48)	**64c**	(16)	**65c**	(0)

[a] Isolated yields.

The optimized reaction conditions in Table 1 were applied to cyclizations onto imidazo[4,5-*f*]benzimidazole (Scheme 2.34, Table 2). The double 6-membered cyclization proceeded in excellent yield without activation giving **63b** in 81% yield (entry 2). Compound **63b** has previously been reported by Meth-Cohn and Suschitzky using an alternative lower yielding procedure which is discussed in Chapter 3.[105] Acetic anhydride and CSA quaternization of the 3,5-*N* basic sites of imidazo[4,5-*f*]benzimidazole allowed respective 5- and 7-membered radical cyclizations to occur, with reduction minimized (entries 1 and 3).

Schulz and Skibo have previously reported the synthesis of **63a** as part of the synthesis of imidazo[4,5-*f*]benzimidazolequinone **13** (Chapter 1), but with a yield of 10%, even the modest yield of 48% reported here is a significant improvement.[34]

The radical cyclizations reported in Table 1 & 2 were carried out using apparatus which was open to the air. However, water was excluded by initially flushing the system with N_2 gas with a drying tube placed on top of the condenser. Later, the Bu_3SnH / ACCN mediated radical cyclization of precursor **58** was carried out without initially flushing with N_2 and without a drying tube, resulting in the formation of alkene **66** in a yield of 68% (Scheme 2.35, path A). Allin *et al* reported similar alkene by-products, but gave no explanation for their formation.[90-91] Carrying out the reaction under an atmosphere of N_2 until half of the volume of Bu_3SnH and ACCN in the syringe pump had been added, and opening the system to the air for the remainder of the reaction, resulted in the formation of the desired annulated product **61b** in an excellent yield of 87% (Scheme 2.35, path B).

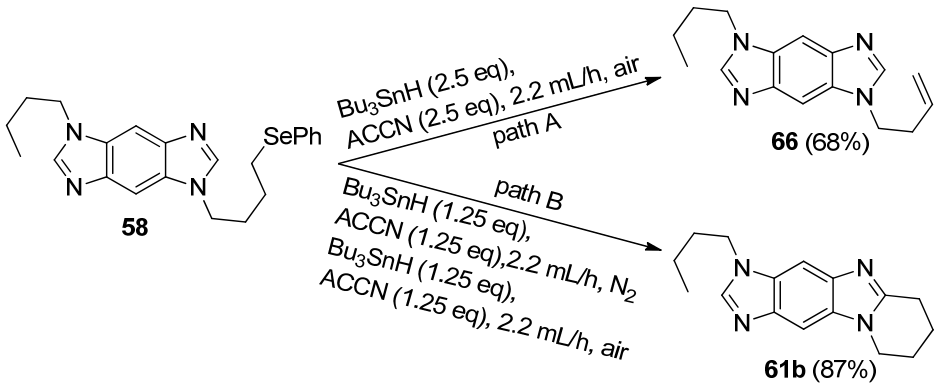

Scheme 2.35; Bu_3SnH / ACCN mediated radical reaction in air throughout (path A) and in air for the second half of the reaction only (path B).

It is known that oxygen reacts with tributyltin radicals in a fast reaction to form tributyltinperoxy radicals ($Bu_3SnOO^{\bullet}$),[45, 106] and with 2-cyanoprop-2-yl radicals (derived from the breakdown of AIBN) to form 2-cyanoprop-2-ylperoxy radicals ($Me_2C(CN)OO^{\bullet}$).[107] From our investigations, it seems that increasing the amount of added ACCN does not facilitate aromatization (on its own). Therefore it seems likely that $Bu_3SnOO^{\bullet}$ abstracts a hydrogen atom from the non-aromatic trapped π-radical intermediate to generate the rearomatized substituted product. When the concentration of oxygen is relatively high from the start, all $Bu_3Sn^{\bullet}$ may be converted to $Bu_3SnOO^{\bullet}$ which may abstract a hydrogen atom directly from the radical precursor before the cyclizing radical can form, giving rise to the alkene by-product **66** (Scheme 2.36, path A). Another possibility is that the phenylselenide is

oxidized to a selenoxide which, through *syn*-elimination, leads to the alkene **66** (Scheme 2.36, path B).[108-109]

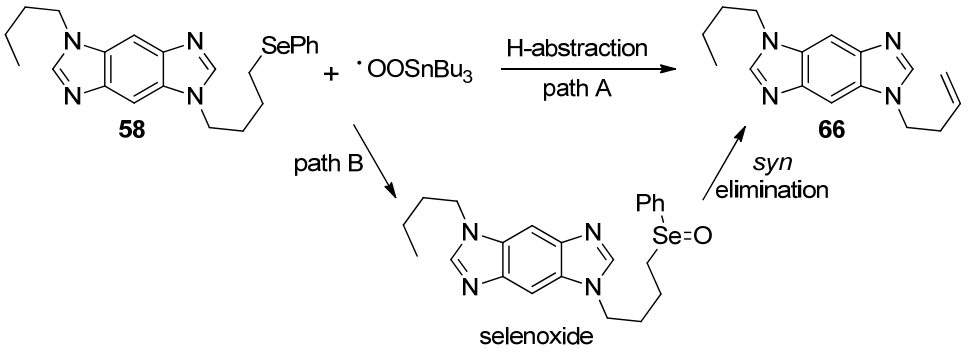

Scheme 2.36; Possible routes to terminal alkene.

Therefore it is apparent that the initial N_2 flush performed in earlier radical cyclizations was significant, as it kept the O_2 concentration low at the start of the reaction so that formation of alkene by-products did not compete with cyclization.

2.2.3 Elaboration of selected molecules to quinones

Six compounds (**55**, **60a-c**, **61b**, **63b**; Scheme 2.37) were converted to the corresponding biologically active imidazobenzimidazolequinones. Each compound was nitrated with a 1:1 mixture of concentrated nitric and sulfuric acid at 80 °C for 3 hours. Following workup and purification by column chromatography, excellent yields of mono nitrated products were obtained (Scheme 2.37). Nitration of **61b** gave an inseparable mixture of regioisomers **70a** & **70b**, both of which ultimately lead to the desired quinone, making separation unnecessary.

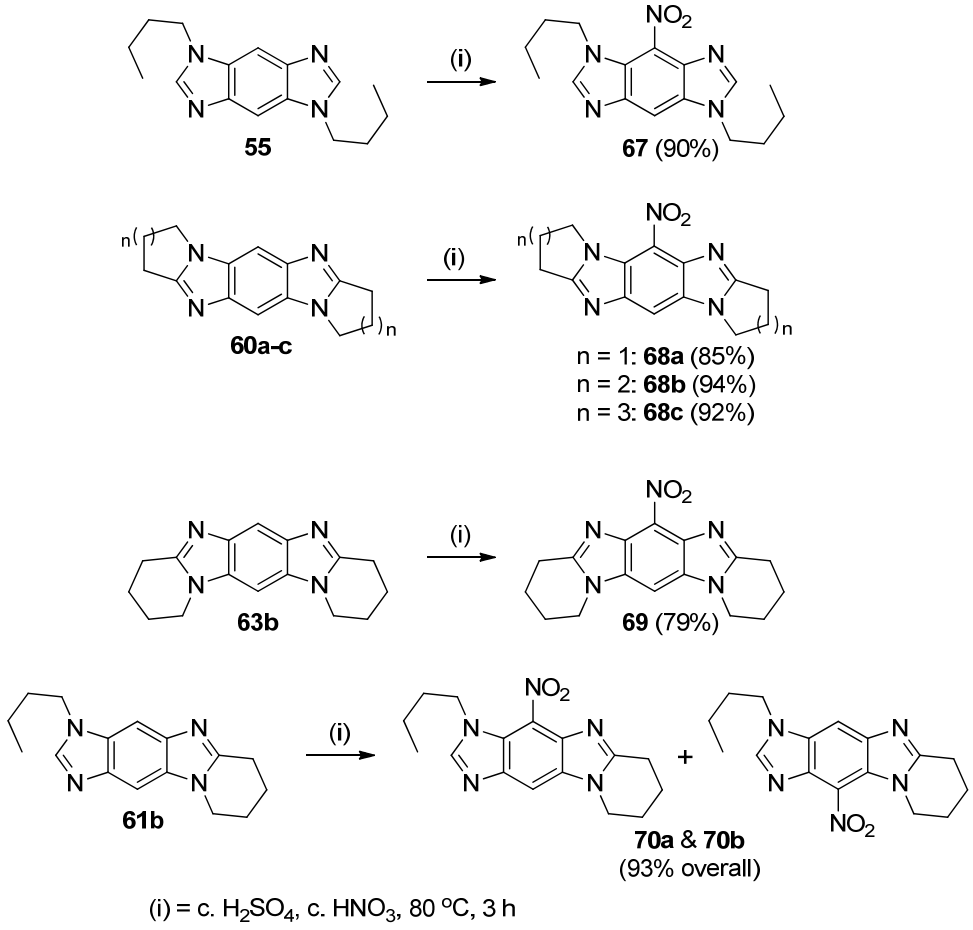

Scheme 2.37; Nitration of imidazobenzimidazoles.

Catalytic reduction to the corresponding amines used 5% palladium on activated carbon in an atmosphere of hydrogen at a pressure of 6 bar. The amine arising from reduction of the dipyridoimidazobenzimidazole **60b** (6-amino-1,2,3,4,8,9,10,11-octahydropyrido[1,2-*a*]pyrido[1′,2′:1,2]imidazo[5,4-*f*]benzimidazole) was isolated

and partially characterized, but all other amino-imidazobenzimidazoles were immediately oxidized using Frèmy's salt (potassium nitrosodisulfonate, $K_2NO(SO_3)_2$) in an aqueous monobasic potassium phosphate solution (pH 4 buffer, KH_2PO_4) to give the corresponding quinones in high yields (Scheme 2.38 & 2.39).

Reduction and Frèmy oxidation of the dipyrrolo ring fused nitro-imidazo[5,4-*f*]benzimidazole **68a** gave a 1:1 inseparable mixture of the iminoquinone **73a** and quinone **74a**. The dipyrido analogue **68b** gave the iminoquinone **73b** in an excellent yield of 91% as the sole product,[110] while the diazepino analogue **68c** gave a 2.3:1.0 mixture of iminoquinone **73c** and quinone **74c** (Scheme 2.39).

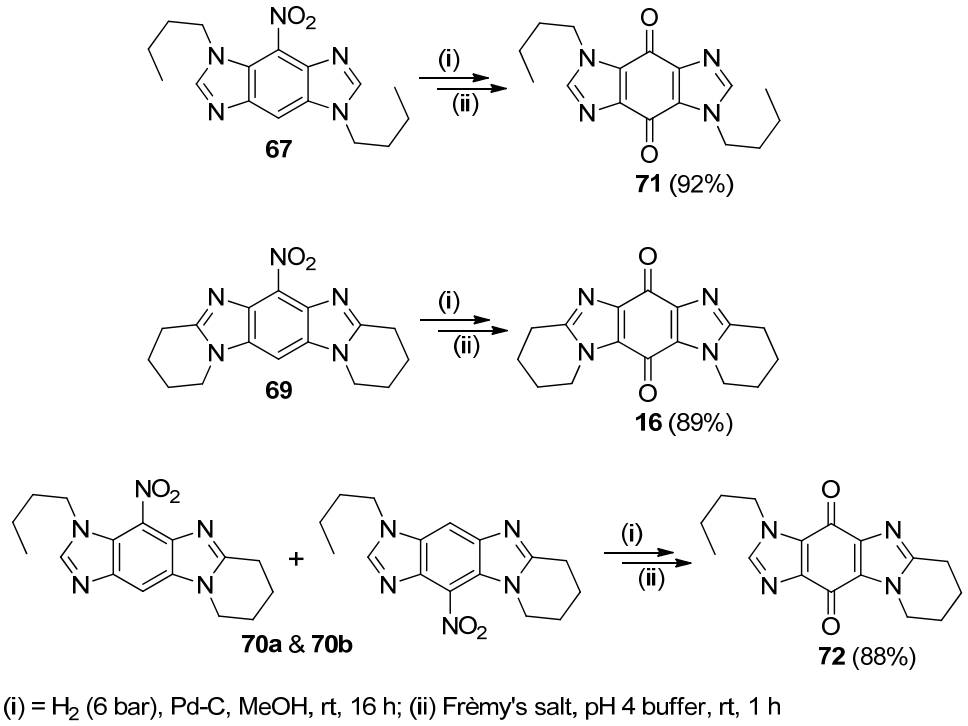

Scheme 2.38; Reduction and Frèmy oxidation to give imidazobenzimidazolequinones.

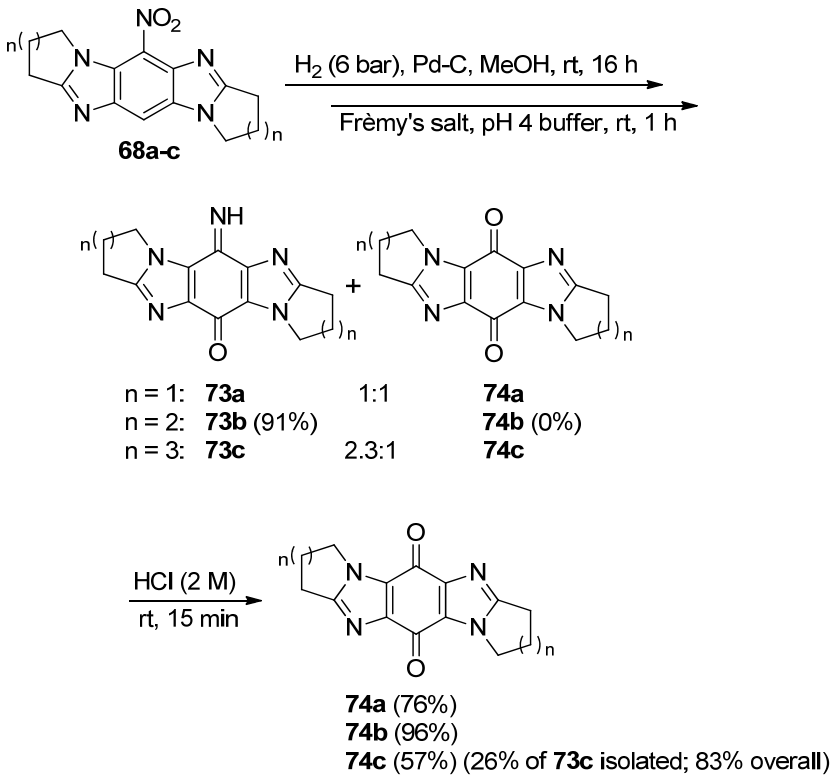

Scheme 2.39; Reduction and Frèmy oxidation of dialicyclic ring fused nitro-imidazo[5,4-*f*]benzimidazoles.

While complete separation of **73c** and **74c** was not achieved, 26% of the iminoquinone **73c** was purified and characterized with the remaining mixture converted fully to quinone **74c**. Iminoquinones were easily hydrolyzed to the corresponding quinones by stirring in dilute hydrochloric acid at room temperature for 15 minutes.

Iminobenzimidazolequinones have been isolated previously, but it was reported that internal hydrogen bonding involving the 6-acetamido and the 4-*N* of 6-acetamido-5-imino-pyrrolo[1,2-*a*]benzimidazol-8-one **75** served to stabilize the imine moiety, with analogues lacking the 6-acetamido group being unstable (Scheme 2.40).[111]

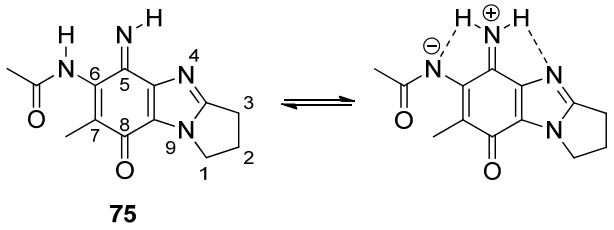

Scheme 2.40; Internal H-bonding stabilization of iminobenzimidazolequinone.

2.2.4 Nomenclature of imidazobenzimidazoles

All compounds were named according to the most recent recommendations of the International Union of Pure and Applied Chemistry (IUPAC).[112] The nomenclature of compound **60b** is explained in detail to illustrate the procedure for naming such fused polycyclic ring systems, with significant differences in the naming of other compounds highlighted.

Naming follows three main steps:

(i) Construct fusion name

(ii) Assign peripheral numbering

(iii) Assign indicated hydrogens & hydro positions

(i) *Construct fusion name:*

The parent component (red) was identified as benzimidazole (Figure 2.1) with the pyrido and imidazo rings being identified as first order components (black) and the other pyrido ring being a second order component (blue). These components are assigned based on an order of preference outlined by IUPAC.[112] The outer bonds of the parent component are labeled with alphabetic locants starting from the *N*-1 position. The atoms of the first order components are labeled with numerical locants while the atoms of the second order components are labeled with primed numerical locants (Figure 2.1).

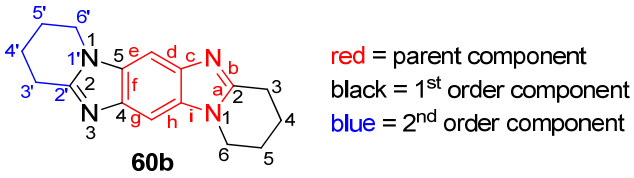

Figure 2.1; Identification and labeling of components of **60b**.

The fusion between first order components and parent components are indicated by the numerical locants of the fusion atoms in the first order component followed by the letter locant of the fusion bond in the parent component, separated by a hyphen and cited within square brackets;

pyrido[1,2-*a*]…imidazo[5,4-*f*]

The numerical locants are cited in order as they appear in the direction of the labeling of the alphabetic locants; hence, [5,4-*f*] (as opposed to [4,5-*f*]).

The fusion between second and first order components are indicated by the primed numerical locants of the fusion atoms of the second order component followed by the numerical locants of the fusion atoms of the first order component, separated by a colon and cited in square brackets:

pyrido[1′,2′:1,2]imidazo[5,4-*f*]

The combined second and first order components are now viewed as a new first order component.

The fusion name of **60b** can now be constructed with the first order components written in alphabetical order followed by the parent component;

pyrido[1,2-*a*]pyrido[1′,2′:1,2]imidazo[5,4-*f*]benzimidazole

(ii) *Assign peripheral numbering:*

Peripheral numbering is independent of any previous labeling or numbering.

The molecule is drawn with certain allowable shapes so that the largest possible number of rings lie on a horizontal axis. Numbering begins from the most counter-clockwise non-fusion atom of the ring furthest to the right in the upper right hand quadrant and proceeds in a clockwise direction. Heteroatoms are included, while fusion carbon atoms are not. Each fusion carbon atom is given the same number as the immediately preceding position, but with the addition of a letter (Figure 2.2).

If more than one orientation is equally allowed, then the following rules are applied, in order, until one orientation is preferred:[112]

(a) Give low numbers to heteroatoms as a set.

(b) Give low numbers to heteroatoms when considered in the order: 0, S, Se, Te, N, P, As, Sb, Bi, Si, Ge, Sn, Pb, B, Hg

(c) Give low numbers to fusion carbons as a set.

(d) Give low numbers to fusion rather than non-fusion atoms of the same heteroelement.

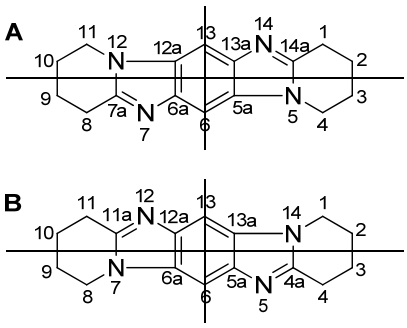

Figure 2.2; Possible orientations for peripheral numbering of **60b**.

Applying rules (a) and (b) still leaves both possible orientations. However when rule (c) is applied, orientation **B** is preferred since its fusion carbons as a set, are lower than that of orientation **A**;

Fusion carbons of **A** = 5a + 6a + 7a + 12a + 13a + 14a = 57a

Fusion carbons of **B** = 4a + 5a + 6a + 11a + 12a + 13a = 51a

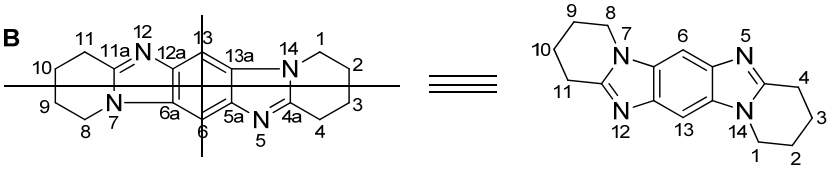

Figure 2.3; Correct peripheral numbering of **60b**.

(iii) *Assign indicated hydrogens & hydro positions;*

In the aliphatic rings, the saturated positions are identified as being hydro positions if a double bond could exist between them or as indicated hydrogens if a double bond cannot exist at that position. Hence hydro positions occur in pairs. Where possible, indicated hydrogens are placed at lower numbers and identified by an italic *H* (Figure 2.4).

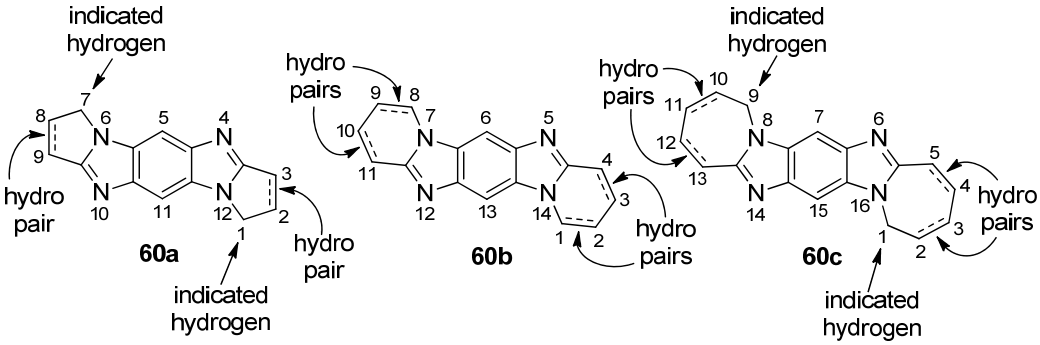

Figure 2.4; Assigning indicated hydrogens and hydro positions.

In the case of **60b**, double bonds could exist between all saturated positions, making them all hydro position with no indicated hydrogens necessary. With **60a** and **60c**, a double bond cannot exist between all saturated positions, hence the remaining positions are indicated hydrogens.

Therefore, the full names for compounds **60a-c** are:

60a; 2,3,8,9-Tetrahydro-1*H*,7*H*-pyrrolo[1,2-a]pyrrolo[1′,2′:1,2] imidazo[5,4-*f*]benzimidazole

60b; 1,2,3,4,8,9,10,11-Octahydropyrido[1,2-*a*]pyrido[1′,2′:1,2] imidazo[5,4-*f*]benzimidazole

60c; 2,3,4,5,10,11,12,13-Octahydro-1*H*,9*H*-azepino[1,2-*a*]azepino[1′,2′:1,2] imidazo[5,4-*f*]benzimidazole

The peripheral numbering of mono fused isomeric compounds (for example: **61a** and **64a**) differ so as to give lower numbers to the fusion carbons as a set (Figure 2.5).

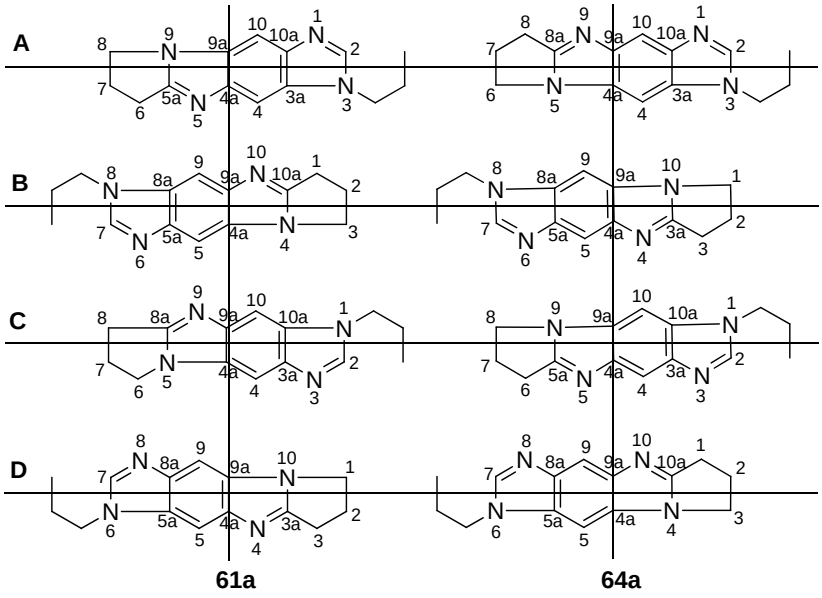

Figure 2.5; Possible orientations for peripheral numbering of isomeric mono-fused **61a** & **64a**.

Orientations **B** and **D** can be ruled out since the heteroatoms of **A** and **C** as a set are lower than that of **B** and **D**. To obtain a preferred orientation, the fusion carbons as a set must be given the lowest numbers. In the case of compound **61a**, orientation **A** is preferred while for compound **64a**, orientation **C** is preferred.

61a; A = 3a + 4a + 5a + 9a + 10a = 31a **64a; A** = 3a + 4a + 8a + 9a + 10a = 34a

61a; C = 3a + 4a + 8a + 9a + 10a = 34a **64a; C** = 3a + 4a + 5a + 9a + 10a = 31a

Therefore, the full names for compounds **61a** and **64a** are;

61a; 3-Propyl-7,8-dihydro-6*H*-imidazo[5,4-*f*]pyrrolo[1,2-*a*]benzimidazole

64a; 1-Propyl-7,8-dihydro-6*H*-imidazo[4,5-*f*]pyrrolo[1,2-*a*]benzimidazole

2.3 Conclusions

Procedures have been developed for the alkylation of imidazo[5,4-*f*(4,5-*f*)]benzimidazole **51** to give monoalkylation, dialkylation or dialkylation with different alkyl groups. Chloro-alkylating agents are shown to be superior to iodo-alkylating agents, giving higher yields with short reaction times.

The first one-pot double intramolecular homolytic aromatic substitution of primary alkyl radicals is reported, as represented by the annulation of imidazobenzimidazoles. Excellent yields are obtained for the Bu_3SnH / azo-initiator mediated double six-membered radical cyclizations onto imidazo[5,4-*f*]benzimidazole and imidazo[4,5-*f*]benzimidazole, while quaternization of the basic nitrogen atoms is required for five and seven-membered analogous alkyl radical cyclizations to proceed in reasonable yields. It was shown that the oxidative rearomatization step is facilitated by the presence of oxygen and possible explanations for the formation of alkene by-products are discussed.

A number of novel biologically active imidazobenzimidazolequinones were synthesized in high yield. Reduction and Frèmy oxidation of dialicyclic ring fused nitro-imidazo[5,4-*f*]benzimidazoles gave varying amounts of the intermediate iminoquinones, two of which were isolated and characterized and their biological activity assessed (see Chapter 4). The dipyridoiminoquinone **73b** was isolated in excellent yield as the sole product.[110]

Chapter 3

3 Synthesis of Imidazo[5,4-*f*]benzimidazolequinone Anti-Cancer Agents using Oxidative Cyclizations of *in situ* generated Amine *N*-Oxides

3.1 Introduction

3.1.1 Oxidative annulations of *ortho*-substituted *tertiary*-anilines

Meth-Cohn and Suschitzky carried out considerable work, and extensively categorized and reviewed reactions which proceed in a way which they termed the "*tertiary*-amino effect". A two step process was proposed involving initial formation of an iminium cation and a nucleophilic/anionic species, which subsequently cyclizes onto the iminium cation (Scheme 3.1).[113-114] The dipolar intermediate may be produced in a number of different ways depending on the nature of the X=Y group.

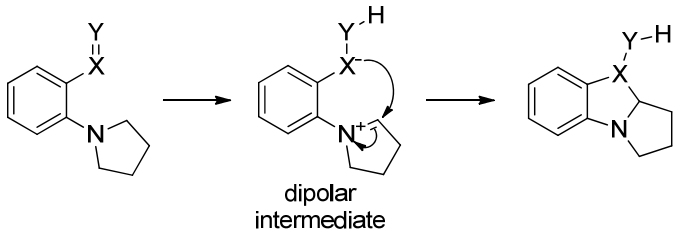

Scheme 3.1; Annulation reactions proceeding via the *tert*-amino effect.

Verboom *et al* showed that the dipolar intermediate may be formed thermally when X=Y is an alkene activated by EWGs. Heating compound **76** in toluene gave a mixture of stereoisomers **77** and **78** in 32% and 54% yield respectively. Changing the solvent to *n*-butanol had a pronounced impacted on the outcome, giving **78** in 74% yield as the sole product (Scheme 3.2).[115]

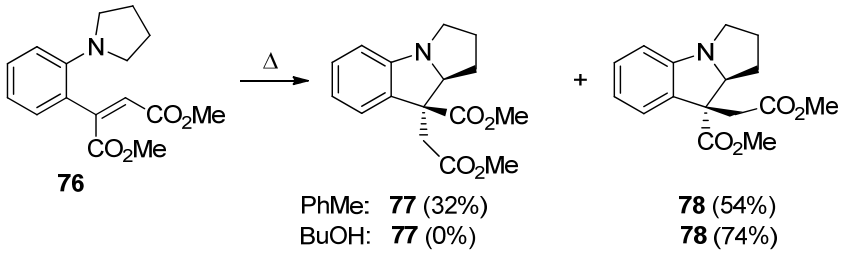

Scheme 3.2; Thermally-induced cyclization of *o*-vinylic *tert*-aniline in toluene and *n*-butanol.

The proposed mechanism involves an initial thermal sigmatropic antarafacial [1,6] hydrogen shift, producing a 1,5-dipole **79** (Scheme 3.3). This rearrangement is similar to a thermal [1,7] hydrogen shift of a triene. The dipole **79** then undergoes a

concerted disrotatory electrocyclization of the 6π-electron system (in accordance with Woodward Hoffmann rules) to form **77**. However **79** may stereomutate to the less hindered intermediate **80** which, following a concerted disrotatory cyclization, gives **78**. The polar protic solvents *n*-butanol stabilizes the 1,5-dipole **79** so as stereomutation to **80** can proceed to completion, resulting in **78** as the sole product.[115-116]

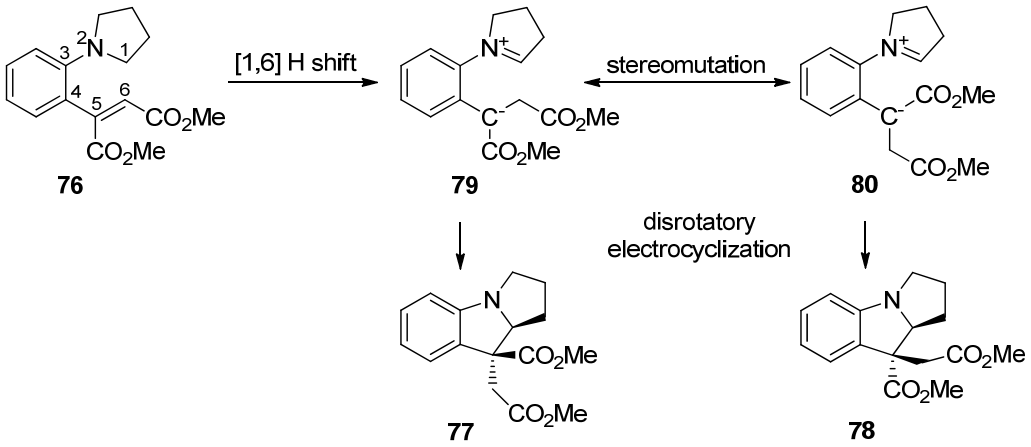

Scheme 3.3; Mechanism of thermally induced cyclization of *o*-vinylic-*t*-aniline.

When only one EWG was present on the β position, no reaction occurred (Scheme 3.4). However a second EWG on the β position caused a [1,5] hydrogen shift to occur which, following disrotatory electrocyclization, resulted in a six membered ring. Piperidinyl and morpholinyl analogues were shown to react with similarly high yields.[115]

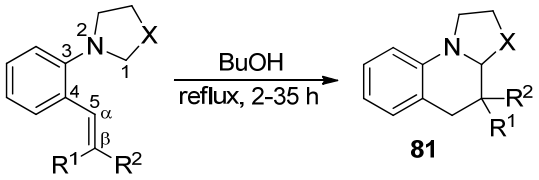

R^1	R^2	X	**81** (%)
H	CO_2Me	CH_2	No reaction
CO_2Me	CO_2Me	CH_2	67
CN	CN	CH_2	82
CN	CN	$(CH_2)_2$	78
CN	CN	OCH_2	84

Scheme 3.4; Thermally-induced cyclization of *o*-(β-substituted-vinylic)-*t*-anilines.

A similar mechanism may be invoked to explain the acid catalyzed cyclization of *o*-imino-*t*-anilines reported by Grantham, Naqui and Meth-Cohn.[117] Treatment of mixtures of *o*-pyrrolidinylaniline and various aldehydes, with a catalytic amount of acid in ethanol afforded the dihydrobenzimidazoles in high yields, which could be oxidized to the benzimidazolium salts **82** by refluxing in carbon tetrachloride or acetone for one hour (Scheme 3.5).[117]

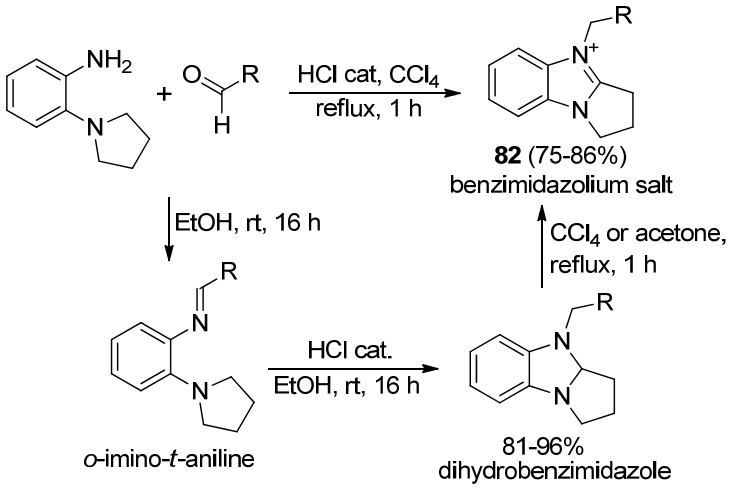

Scheme 3.5; Acid-catalyzed cyclization of *o*-imino-*t*-anilines.

Carrying out the reaction in deuterated methanol did not lead to incorporation of deuterium into the product. Therefore an intramolecular hydrogen transfer mechanism was proposed. Proton transfer from the pyrrolidine group to the imine carbon and protonation of the imine nitrogen leads to the formation of an iminium cation and a secondary amine **83** (Scheme 3.6). Nucleophilic addition of the secondary amine onto the adjacent iminium bond leads to the dihydrobenzimidazole **84** with subsequent oxidation in carbon tetrachloride or acetone leading to the benzimidazolium salts **82**.[117]

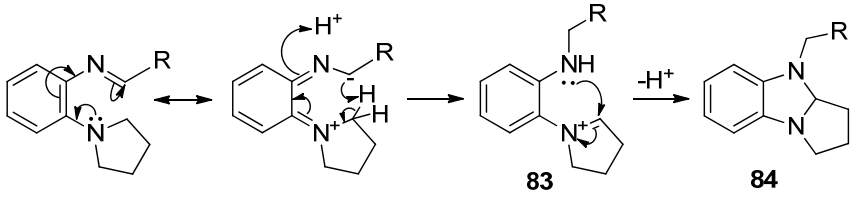

Scheme 3.6; Mechanism of acid catalyzed cyclization of *o*-imino-*t*-anilines.

If the hydrogen transfer step is viewed as a concerted sigmatropic [1,6] hydrogen shift, then this mechanism is very similar to that discussed previously, the only difference being the necessity of the acid catalyst to protonate the imine nitrogen. The same mechanism is proposed by Fielden, Meth-Cohn, and Suschitzky to account for the formation of benzimidazole *N*-oxides **86** when *o*-nitro-*t*-anilines **85** were heated at reflux in concentrated hydrochloric acid (Scheme 3.7).[118] The presence of a chloro substituent *para* to the tertiary cyclic amine enhanced yields. The size of the cyclic amine could be increased to the nine-membered azonane and non-cyclic amines reacted similarly. Yields of the benzimidazole *N*-oxides varied considerably, as did conversion, with unreacted starting material being recovered in as high as 87%.

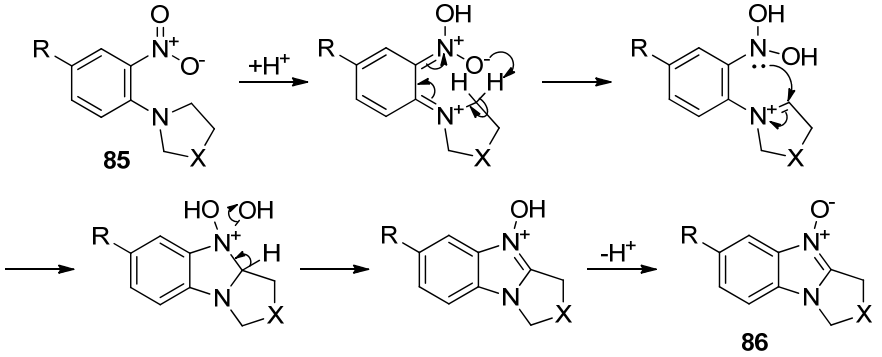

R	X	**86** (%)
H	CH_2	51
Cl	CH_2	70
NO_2	CH_2	32
CO_2H	CH_2	61
CF_3	CH_2	33
H	OCH_2	27
Cl	$(CH_2)_2$	16
Cl	$(CH_2)_3$	61
Cl	$(CH_2)_4$	52
Cl	$(CH_2)_5$	26

Scheme 3.7; Acid-catalyzed cyclization of *o*-nitro-*t*-anilines.

Use of zinc chloride as Lewis acid and acetic anhydride increased the reactivity of *o*-nitro-*t*-anilines, giving high yields of cyclization products **87**, but an acetate substituent was introduced into the aliphatic ring (Scheme 3.8).[119]

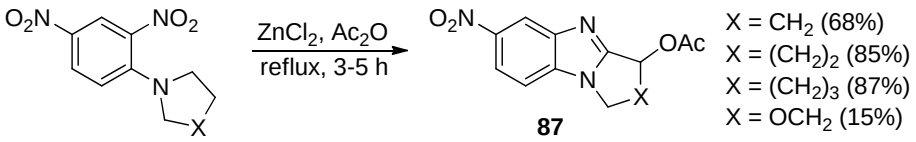

Scheme 3.8; Lewis acid promoted cyclization of *o*-nitro-*t*-anilines.

It was proposed that ring-closure may be facilitated by a complex involving the *t*-amine and the nitro group with the zinc chloride to give a benzimidazole *N*-oxide **88**, which in the presence of acetic anhydride gives the acetate substituted benzimidazole **87** (Scheme 3.9).[119]

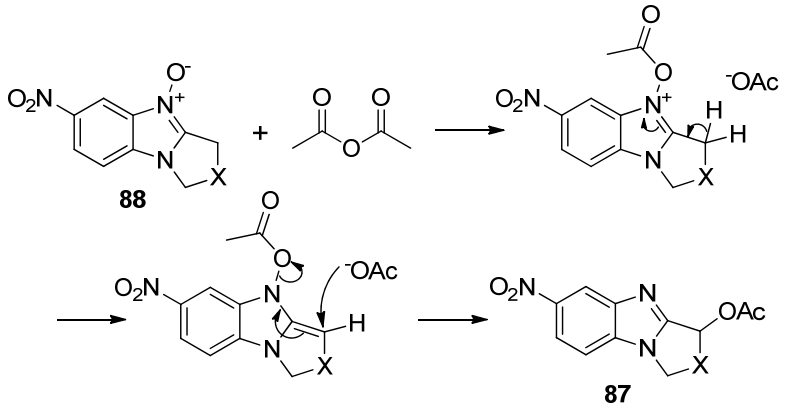

Scheme 3.9; Mechanism for formation of acetate substituted benzimidazoles from benzimidazole *N*-oxides **88**.

The reaction was later used to good effect for the preparation of a series of DNA-alkylating azamitosenes **89**, analogues of mitomycins (Figure 3.1).[111, 120-122]

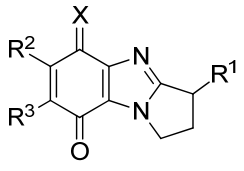

89

X	R^3	R^2	R^1
O	Me	—N◁	OAc
O	Me	—N◁	$OCONH_2$
O	Me	-NHAc	OAc
NH	Me	-NHAc	OAc
O	Me	$-N(CH_3)_2$	OAc
O	Me	$-N(CH_3)_2$	$OCONH_2$
NH	Me	$-NHCOCH_2Cl$	OAc
O	—N◁	Me	OAc

Figure 3.1; Azamitosenes prepared by Lewis acid promoted cyclization of *o*-nitro-*t*-anilines.

Meth-Cohn *et al* showed that cyclization of 4-azido-3-*t*-aminopyridines **90** could be achieved by heating at high temperature in nitrobenzene to give ring fused imidazo[4,5-*c*]pyridines **91** with yields increasing with increasing ring size. The azide moiety was introduced by diazotization of the corresponding amine followed by substitution by sodium azide (Scheme 3.10).[123]

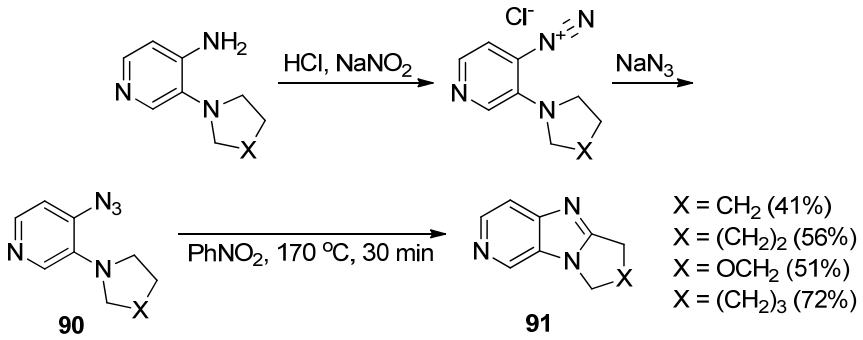

Scheme 3.10; Cyclization of 4-azido-3-*t*-aminopyridines.

Similar annulations of *t*-amines with *ortho*-azido groups were carried out by VanAllan *et al*. Introduction of the azide group was achieved by nucleophilic substitution of 2-*t*-amino-3-chloro-1,4-naphthoquinones **92** by sodium azide in DMF, with spontaneous cyclization yielding naphtha[2,3-*d*]imidazolediones **93** (Scheme 3.11).[124]

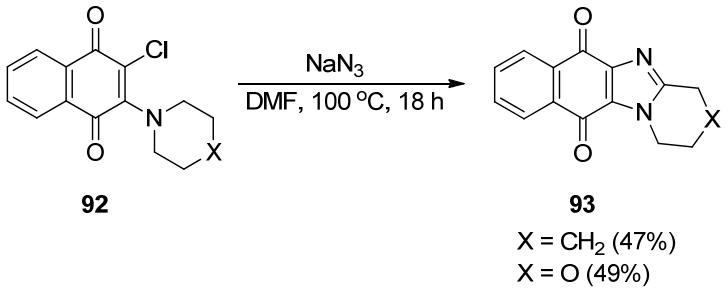

Scheme 3.11; Annulations via *ortho*-azides.

Suh *et al* used this method to prepare the quinolone analogues **17a-c** which were evaluated as anti-cancer compounds, showing higher activity than cisplatin (Scheme 3.12 (also discussed in Chapter 1).[38]

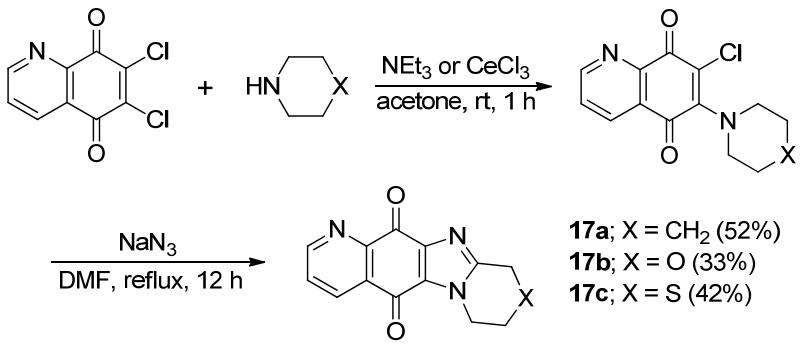

Scheme 3.12; Thermally induced cyclization of azides onto *t*-amines.

Nair and Adams reported high yields of tricyclic fused benzimidazoles **94** by treatment of *o*-*t*-amino anilines with peroxytrifluoroacetic acid (Scheme 3.13). The mechanism was thought to proceed by oxidation of the primary amine to a nitroso or hydroxylamine, followed by a cyclization onto the α-methylene carbon of the cyclic amine. An alternative pathway proceeding by oxidation of the *tert*-amine to an amine-*N*-oxide was deemed unlikely, since *N*-(2-piperidin-1-ylphenyl)benzamide **95** did not give the benzimidazole product under the same reaction conditions.[125]

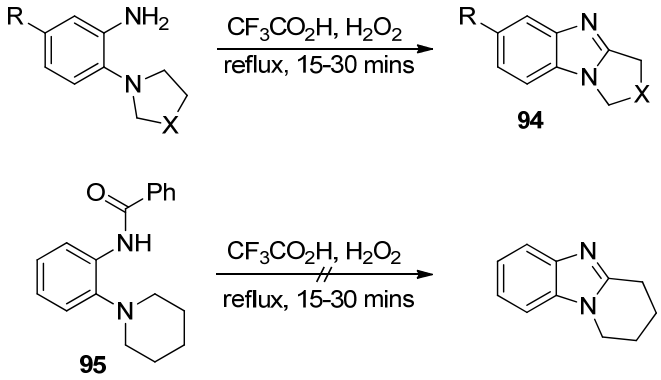

X	**94** (%)			
	R			
	H	Cl	CH_3	NO_2
CH_2	81	75	86	72
$(CH_2)_2$	58	66	60	95
$(CH_2)_3$	-	-	-	91
OCH_2	73	62	61	76

Scheme 3.13; Oxidative cyclization of *o*-cyclic amino anilines.

This report was contradicted by Meth-Cohn and Suschitzky, who found that cyclization of acyl derivatives **96** (formyl, acetyl or benzoyl) to give tricyclic benzimidazoles **97** was facilitated by peroxytrifluoroacetic acid or peroxyformic acid

(performic acid) and that the latter was as good as peroxytrifluoroacetic acid (Scheme 3.14).[105] The double annulation of *N*,*N*′-(2,4-dipiperidinyl-1,5-phenylene)diacetamide **98** was also reported, giving **63b** in 74% yield. When repeated by Skibo *et al*, the latter oxidative annulations were reported to proceed in much lower yield, with **63b** obtained in 31% yield (Scheme 3.16).[34] Compound **63b** was prepared in 81% yield via an alternative radical route presented in Chapter 2.[110]

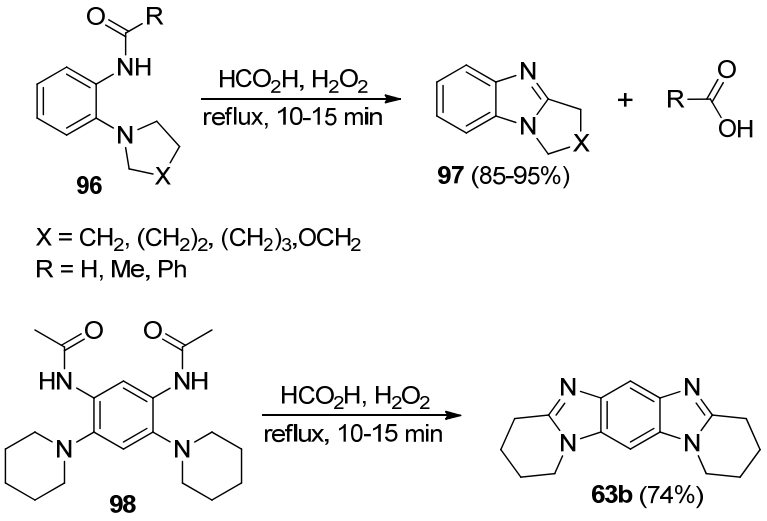

Scheme 3.14; Oxidative cyclization of *o*-*t*-amino acetanilides.

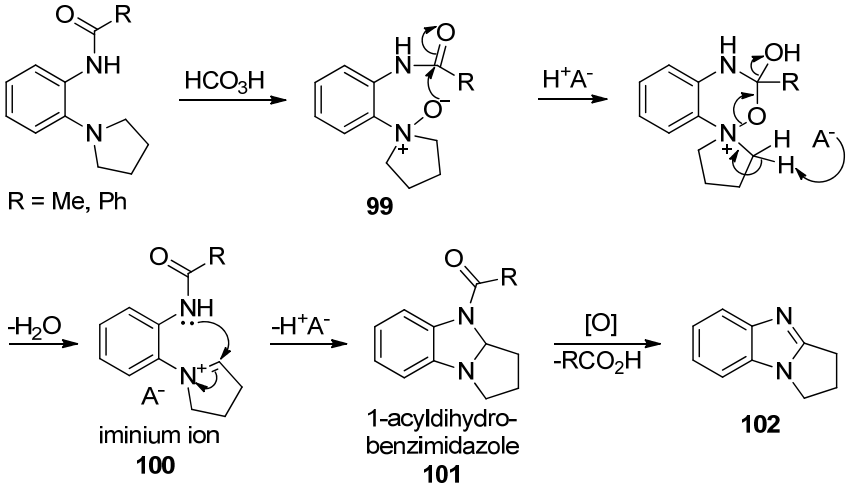

Scheme 3.15; Mechanism of oxidative cyclization of *o*-*t*-amino acetanilides proposed by Meth-Cohn.

It was shown that under the reaction conditions, aromatic amides were unchanged and that aromatic *t*-amines yielded the corresponding amine *N*-oxides. A mechanism was proposed (Scheme 3.15) similar to the Polonovski rearrangement[126] in which an *N*-oxide **99** is initially formed, and attacks the adjacent amide group. Elimination leads to an iminium ion **100** which is subjected to nucleophilic attack by the amide in

a ring closure step, leading to a 1-acyldihydrobenzimidazole **101**, with oxidation of this intermediate leading to the benzimidazole **102**.[105, 127] Support for this mechanism came from the fact that an *N*-oxide intermediate **99** (R = Ph) was isolated and treated with HCl (2 M), resulting in the formation of the corresponding benzimidazole in high yield.[127] An intermediate 1-acyldihydrobenzimidazole **101** (R = Me) was also shown to be readily oxidized to the benzimidazole by treatment with performic acid.[123]

However an anomaly exists between the experimental data reported and this proposed mechanism. As part of the characterization of the intermediate amine *N*-oxide **99** (R = Ph) a strong hydrogen bond was found to exist between the *N*-oxide oxygen and the amide NH which resulted in the carbonyl of the amide group being orientated away from the *N*-oxide.[127] Therefore attack of the *N*-oxide on the carbonyl of the amide group seems difficult and unlikely (discussed further in results and discussion). This procedure was utilized for the preparation of a series of DNA-alkylating azamitosenes **103**[33, 111, 120, 128] and topoisomerase II inhibitors **13** & **16**[34-35] (Scheme 3.16).

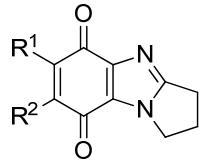

103

R^1	R^2
—N◁	H
H	—N◁
OMe	H
H	OMe
-NHAc	OMe
-NHAc	Me
$-N(CH_3)_2$	Me

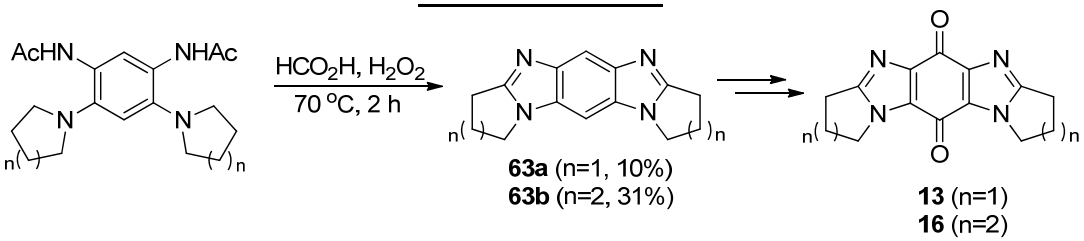

Scheme 3.16; Azamitosenes prepared by performic acid promoted cyclization of *o*-*t*-amino-acetanilide.

Using this methodology, Fahey and Aldabbagh carried out 5-8 membered cyclizations to give tricyclic fused [1,2-*a*]benzimidazoles **104** and prepared anti-cancer benzimidazolequinones **3a-c** and **4a-c** (Scheme 3.17).[26-27]

The *ortho*-*tertiary*-amino acetanilides precursors were prepared by a one-pot catalytic hydrogenation and acetylation reaction. In the case of *ortho*-nitro 7- and 8-membered *tertiary*-anilines **105**, significant amounts of alicyclic ring fused benzimidazoles were formed during the reduction and acetylation reaction (Scheme 3.18).[26]

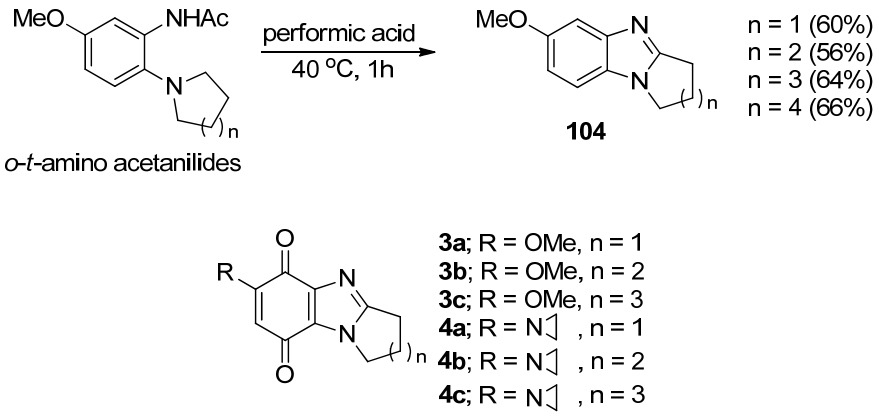

Scheme 3.17; Alicyclic ring-fused benzimidazoles and quinone analogues prepared by oxidative cyclization.

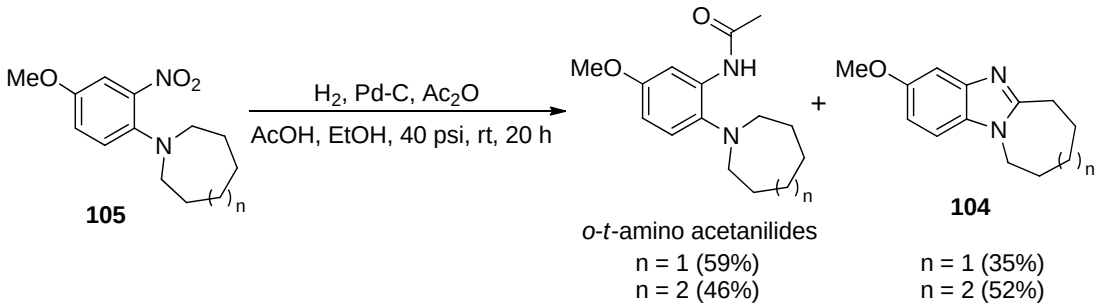

Scheme 3.18; Catalytic reduction and acetylation of *ortho*-nitro *tertiary*-anilines leading to fused [1,2-*a*]benzimidazoles.

3.1.2 Aims and objectives

- To develop a new protocol for the synthesis of ring fused imidazo[5,4-*f*]benzimidazoles via acid catalyzed oxidative cyclization of *o*-*tert*-amino acetanilides.
- To synthesize novel dialicyclic ring fused imidazo[5,4-*f*]benzimidazoles bearing heteroatoms in the aliphatic rings.
- To synthesize novel unsymmetrical dialicyclic ring fused imidazo[5,4-*f*]benzimidazoles.
- To further functionalize imidazo[5,4-*f*]benzimidazoles to the biologically active imidazo[5,4-*f*]benzimidazolequinones, which will be evaluated as anti-cancer agents (see Chapter 4).

3.1.3 Synthetic strategy

Using the appropriate 1,4-dihalo-2,5-dinitrobenzene **106**, double nucleophilic aromatic substitutions of the halogen atoms by the appropriate cyclic amine would give di-*tert*-amino substituted **107** (Scheme 3.19). Reduction and acetylation of the nitro groups of **107** would give the corresponding *N*,*N*′-(2,5-di-*t*-amino-1,4-phenylene)diacetamide **108**. Treatment with performic acid would afford the pentacyclic imidazo[5,4-*f*]benzimidazoles, which could be further functionalized to give the biologically active target imidazo[5,4-*f*]benzimidazolequinones.

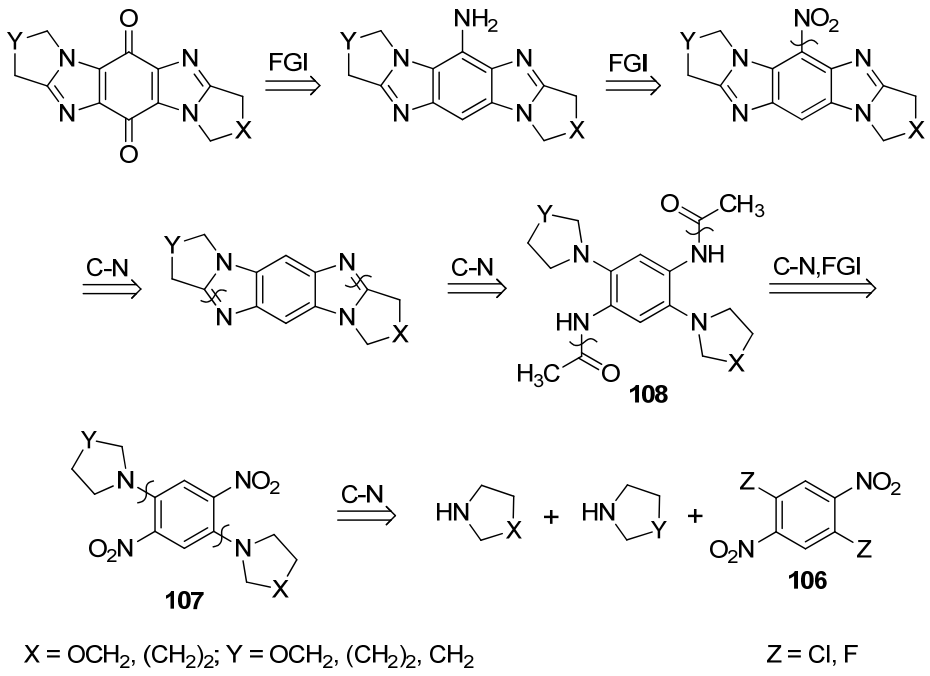

Scheme 3.19; Retrosynthetic analysis of target imidazo[5,4-*f*]benzimidazolequinones.

3.2 Results and discussion

3.2.1 Preparation of *N*,*N*′-(2,5-di-*t*-amino-1,4-phenylene)diacetamides

The synthesis of diacetamides **108** started with the commercially available 2,5-dihaloaniline, which was acetylated by stirring in acetic anhydride (Scheme 3.20). The selective nitration of the resultant *N*-(2,5-dihalophenyl)acetamide **109a**, **109b** was carried out according to a literature procedure to give *N*-(2,5-dihalo-4-nitrophenyl)acetamides **110a**, **110b** as the sole products in near quantitative overall yields (Scheme 3.20).[129] 1,4-Dichloro-2,5-dinitrobenzenes **106a** has been prepared by oxidation of 2,5-dichloro-4-nitroaniline using peroxytrifluoroacetic acid.[130] By employing the stronger methanesulfonic acid, it was possible to carry out a one pot deprotection and oxidation of **110a**, **110b** to give the desired 1,4-dihalo-2,5-dinitrobenzenes **106a**, **106b** in high yields without isolation of the intermediate anilines, thus increasing efficiency significantly.

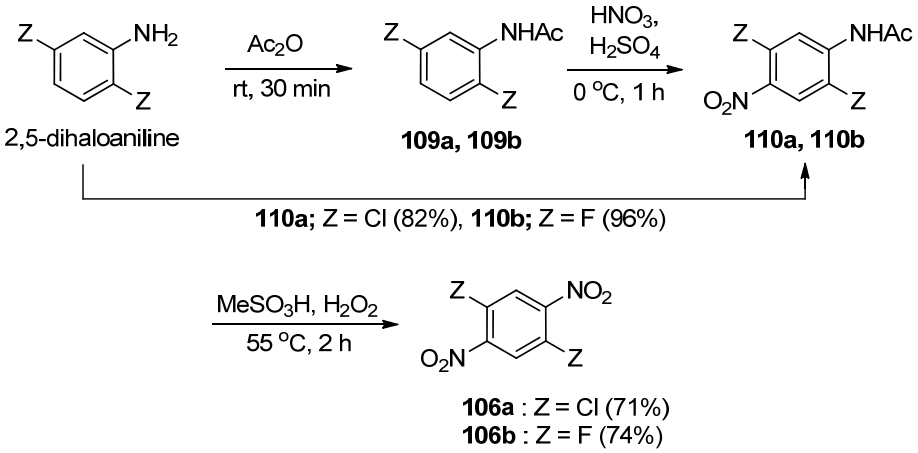

Scheme 3.20; Synthesis of 1,4-dihalo-2,5-dinitrobenzenes **106a**, **106b**.

Initially the chloro analogue **106a** was prepared and a double nucleophilic aromatic substitution reaction was attempted with excess morpholine. Only monosubstitution could be achieved. The electron donating ability of the introduced amine deactivates the aromatic system towards nucleophilic aromatic substitution; thus the second chloride could not be displaced. The rate of nucleophilic aromatic substitution onto arylhalides increases in the series Ar-I < Ar-Br < Ar-Cl << Ar-F, with the latter being 10^2-10^3 times faster than Ar-Cl.[131] Therefore the fluoro analogue **106b** was prepared

(Scheme 3.20) and treatment with excess morpholine resulted in the desired dimorpholine substituted product **107a** in excellent yield (Scheme 3.21). The different rates of substitution made it possible to introduce a different cyclic amine, allowing access to unsymmetrical target molecules. The least nucleophilic amine was introduced first, and at low temperature in the case of **107c**, followed by an excess of the second cyclic amine. In this way, two unsymmetrical analogues **107b** and **107c** were prepared in good yield (Scheme 3.21). Morpholine is the least nucleophilic of the three amines, as the oxygen inductively deactivates the nitrogen lone pair. Piperidine and pyrrolidine have very similar nucleophilicities, with pyrrolidine being slightly more nucleophilic.

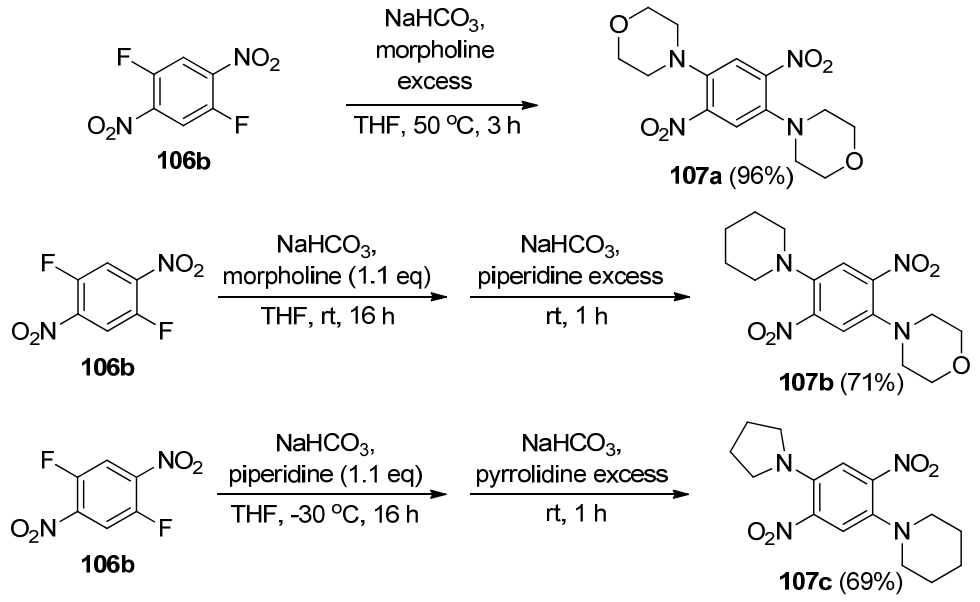

Scheme 3.21; Double nucleophilic aromatic substitutions giving symmetrical & unsymmetrical products.

Conversion to the di-acetamides **108a-c** was achieved in high yield by a one-pot catalytic hydrogenation/acetylation protocol analogous to that used by Fahey and Aldabbagh.[26] No benzimidazole products were observed under these reaction conditions, as reported by the latter authors (Scheme 3.22).

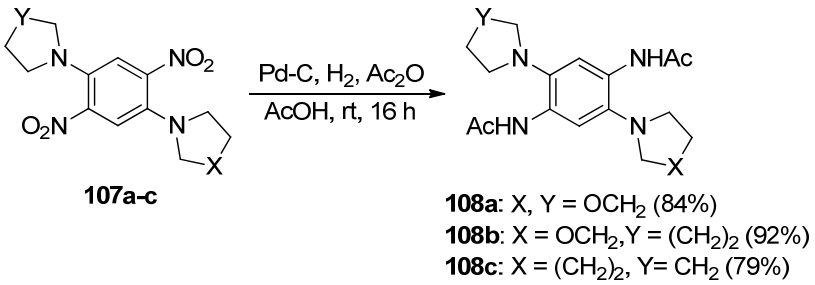

Scheme 3.22; One-pot reduction/acetylation of di-substituted dinitrobenzenes.

3.2.2 Oxidative cyclizations of *o-tert*-amino acetanilides

Initially oxidative cyclizations were carried out using formic acid and 30% hydrogen peroxide[26] and resulted in yields of less than 20% (Scheme 3.23).

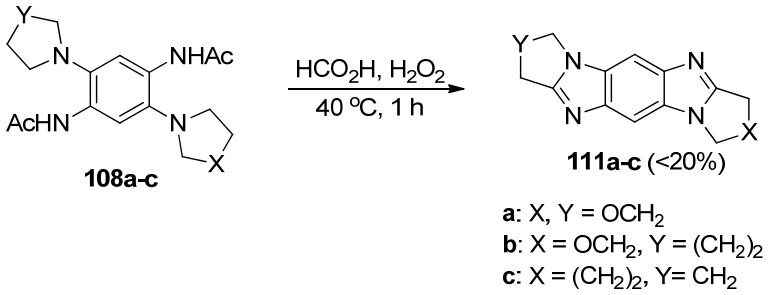

Scheme 3.23; Oxidative cyclizations of *o-t*-amino acetanilides mediated by performic acid.

Therefore alternative oxidants and conditions were explored. Treatment of **108a** with *m*-chloroperoxybenzoic acid (*m*CPBA) in acetone resulted in the precipitation of the *N*-oxide **112** (Scheme 3.24).

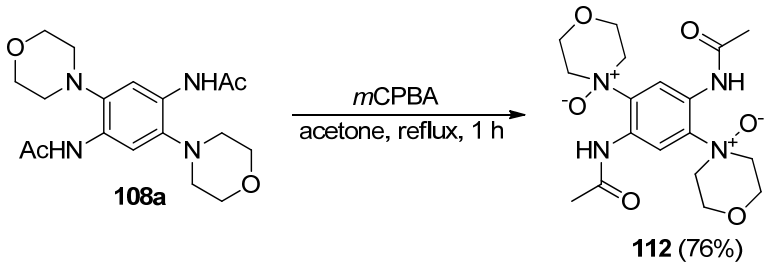

Scheme 3.24; Synthesis of di-amine *N*-oxide **112**.

Heating **112** in formic acid resulted in the formation of the partially cyclized benzimidazole **114** in high yield as the sole product (Scheme 3.25). We propose that

an acid-catalyzed cyclization occurred on one side, giving the *N*-acetyldihydrobenzimidazole intermediate **113**, which in the absence of an external oxidant was oxidized through the internal conjugated system by the second amine *N*-oxide, leading to benzimidazole **114** (Scheme 3.25).

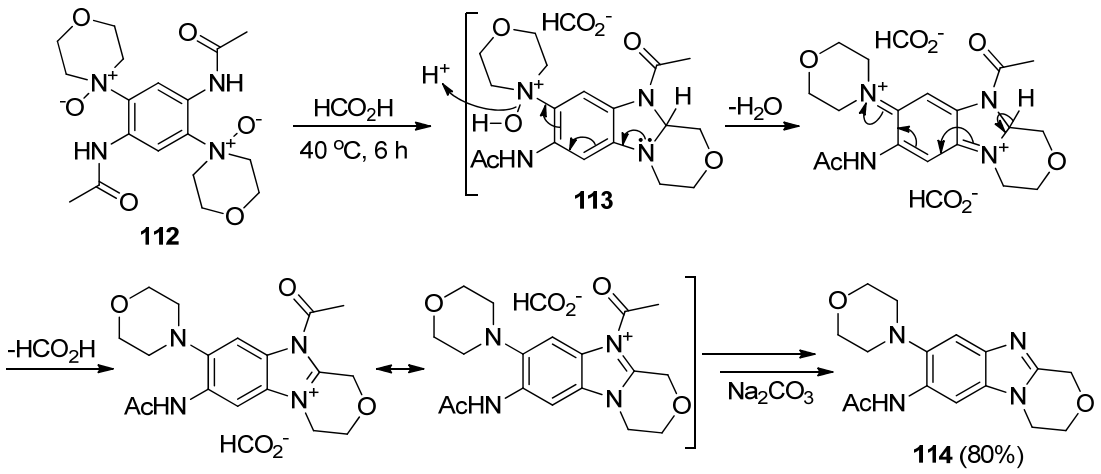

Scheme 3.25; Proposed mechanism for the formation of benzimidazole **114**.

Support for this mechanism was obtained by preparing morpholine *N*-oxide **116** and treating it with formic acid under the conditions of Scheme 3.25. *N*-oxide **116** was prepared by substitution of 1,4-dibromo-2-nitrobenzene with morpholine, followed by reduction with stannous chloride, and acetylation with acetic anhydride to give bromoacetamide **115** (83% overall), which was oxidized by *m*CPBA to *N*-oxide **116** (Scheme 3.26).

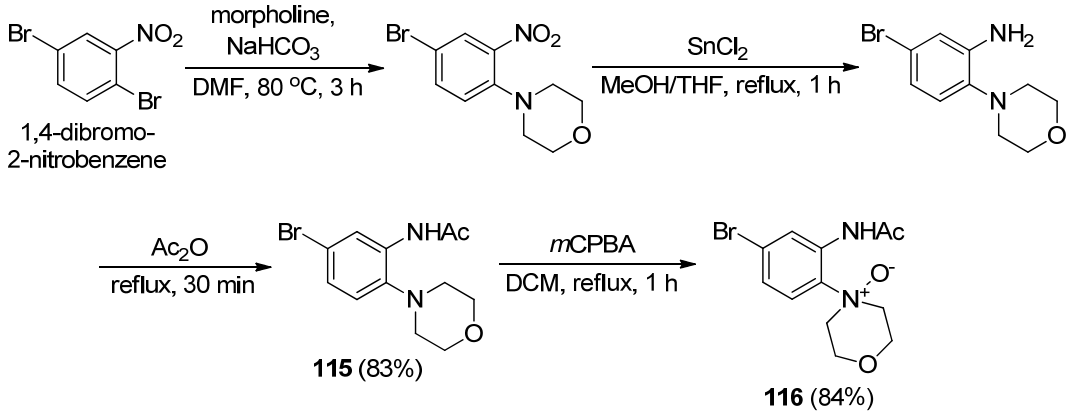

Scheme 3.26; Preparation of *N*-oxide **116**.

Treatment of *N*-oxide **116** with formic acid gave a ~1:1 mixture of benzimidazole **118** and acetamide **115** in an overall yield of 94%, indicative of amine *N*-oxide **116** acting as an intermolecular oxidant, facilitating aromatization of the *N*-acetyldihydrobenzimidazole **117** in the absence of an added oxidant (Scheme 3.27).

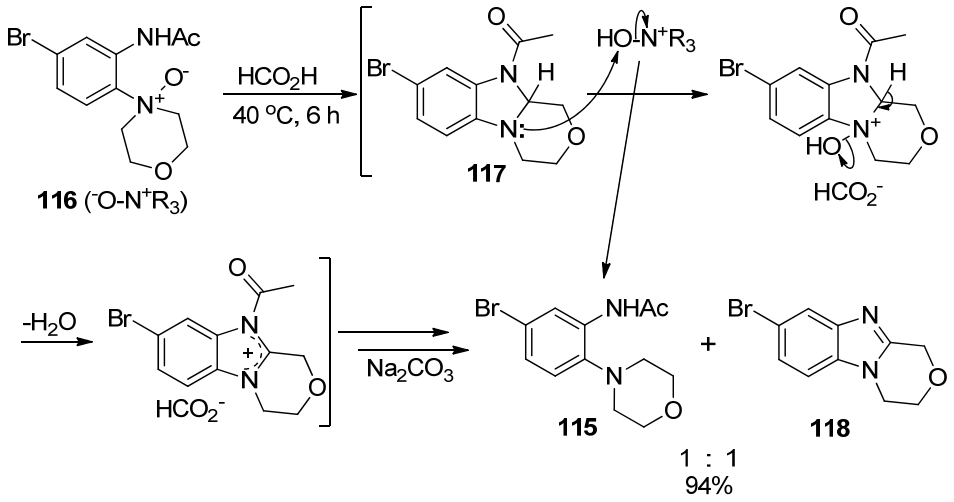

Scheme 3.27; Proposed role of morpholine-*N*-oxide as intermolecular oxidant in formic acid.

Acetamide **115** remained unchanged when heated for prolonged periods in formic acid, indicating that the formation of the amine *N*-oxide is essential. Acid is also required to facilitate the cyclization as amine *N*-oxide **116** remained unchanged when heated at reflux in acetonitrile for prolonged periods. Thus it seems that at least two equivalents of any oxidant capable of amine *N*-oxide formation would, in acidic solution, give ring fused benzimidazoles from *o*-*t*-amino acetanilides.

After surveying several oxidants in various acids, Oxone® (active form is $KHSO_5$, 3 equivalents) in 90% formic acid was the oxidizing system of choice, as it gave rise to the easiest work up, allowing isolation of cyclized products by precipitation (Scheme 3.28).

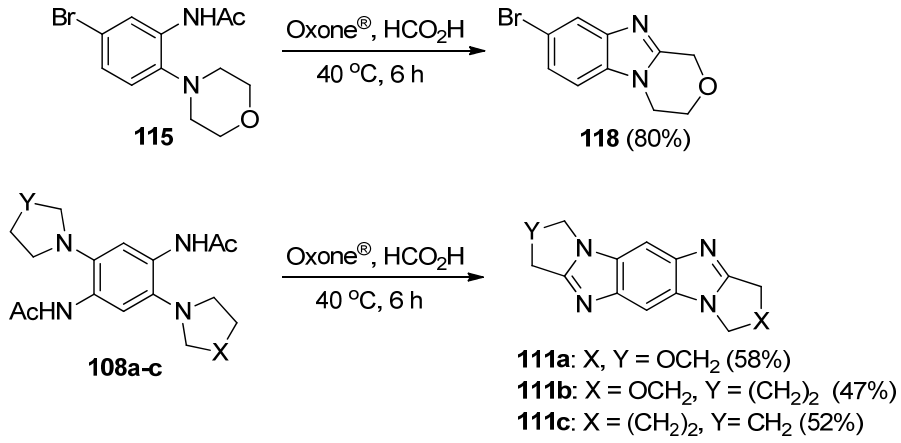

Scheme 3.28; Optimized conditions of oxidative cyclization of *o*-*t*-amino acetanilides.

Although the yields are modest, they are a significant improvement on reported yields for forming dialicyclic ring fused imidazo[4,5-*f*]benzimidazoles using formic acid and H_2O_2.[34-35]

An X-ray crystal structure of dimorpholine *N*-oxide **112** shows the carbonyl group of the amide to be orientated away from the *N*-oxide with hydrogen bonding between the *N*-oxide residues and the acetamide hydrogen (Figure 3.2 (Appendix, A.1, Table A.1)), which may account for the absence of the amide NH peak in ^{1}H NMR spectra of amine *N*-oxides prepared.

NMR analysis carried out by Meth-Cohn on *N*-(2-benzoylaminophenyl)pyrrolidine *N*-oxide **99** (Scheme 3.15, R = Ph) led to the assignment of an analogous strongly hydrogen-bonded NH.[127] The cyclization mechanism proposed by Meth-Cohn to give the pyrrolo[1,2-*a*]benzimidazole **102** (Scheme 3.15) disagrees with this molecular orientation, since it involves initial nucleophilic addition of the amine *N*-oxide onto the amide C=O.[105, 127] A new mechanism of cyclization using the hydrogen bonded orientation of the amide and amine *N*-oxide is now proposed (Scheme 3.29).

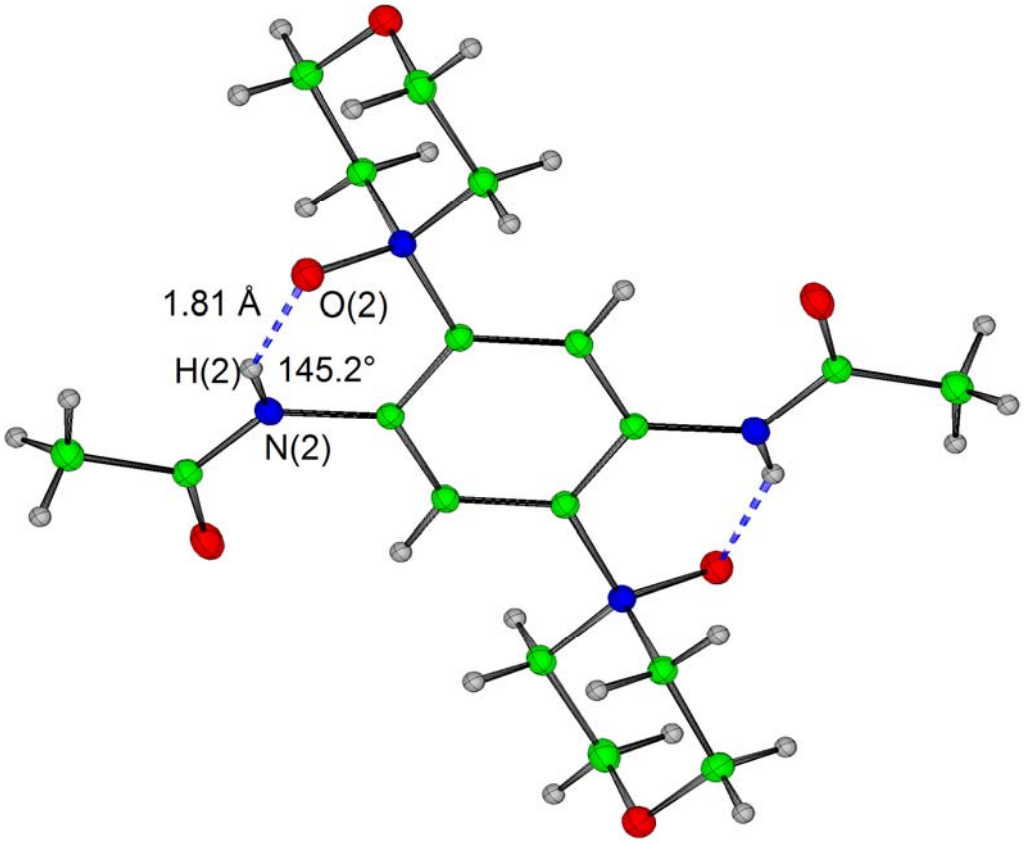

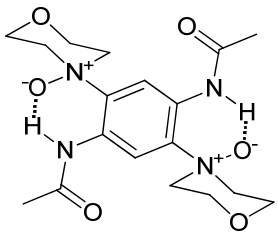

112

Figure 3.2; Crystal structure of dimorpholine-*N*-oxide **112** showing orientation of amide groups with distance between H(2) of amide and O(2) of *N*-oxide, and angle between O(2) of *N*-oxide and, H(2) and N(2) of amide.

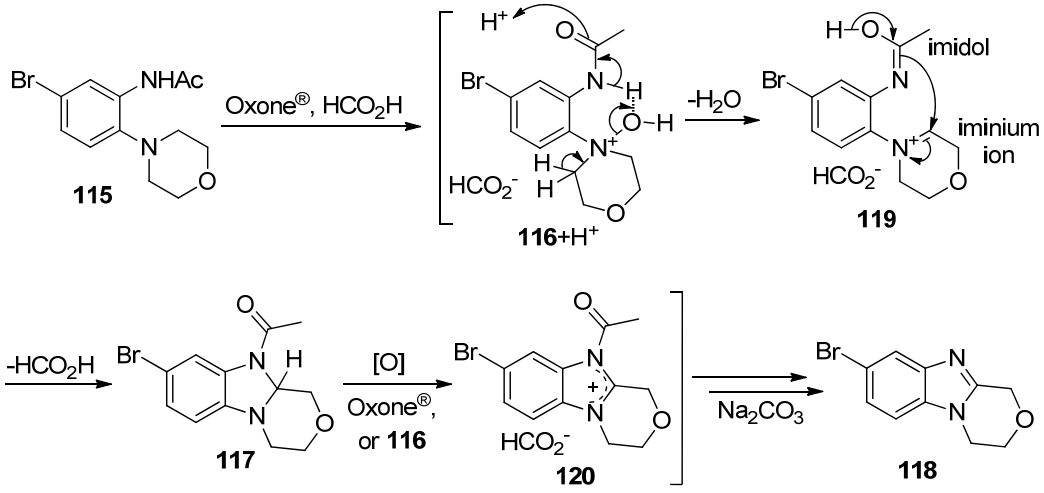

Scheme 3.29; Proposed mechanism taking into account H-bonding of *N*-oxide and amide.

The *o-tert*-amino acetanilide **115** is oxidized to the amine *N*-oxide **116**, which is protonated in the acidic solution causing the NCH_2 of the morpholine *N*-oxide ring to become acidic. This forms an iminium ion with loss of water and simultaneous tautomerism of the amide to an imidol **119**. Nucleophilic addition of the imidol onto the iminium ion gives rise to *N*-acetyldihydrobenzimidazole intermediate **117**, which is oxidized by Oxone® (or by the morpholine *N*-oxide **116**) to benzimidazolium formate **120**. Work up involving solvent evaporation and neutralization precipitates benzimidazole **118**.

3.2.3 Elaboration of imidazo[5,4-*f*]benzimidazoles to quinones

Elaboration of the three new pentacyclic ring fused imidazo[5,4-*f*]benzimidazoles **111a-c** to the corresponding quinones followed the route outlined previously (Chapter 2, Scheme 2.37 & 2.38). Each compound was nitrated with a 1:1 mixture of concentrated nitric and sulfuric acid at 80 °C for 3 hours, giving only mono-nitrated products (Scheme 3.30). The unsymmetrical imidazo[5,4-*f*]benzimidazoles **111b**, **111c** gave an inseparable mixture of regioisomers **122a**, **122b** and **123a**, **123b** respectively, which were not separated.

The nitro-imidazo[5,4-*f*]benzimidazoles were catalytically reduced to the corresponding amines using palladium in an atmosphere of hydrogen at a pressure of 6 bar. The amino-imidazo[5,4-*f*]benzimidazoles were immediately oxidized using Frèmy's salt (potassium nitrosodisulfonate, $K_2NO(SO_3)_2$) in an aqueous monobasic potassium phosphate solution (pH 4 buffer, KH_2PO_4) to give the corresponding quinones in good yield (Scheme 3.31).

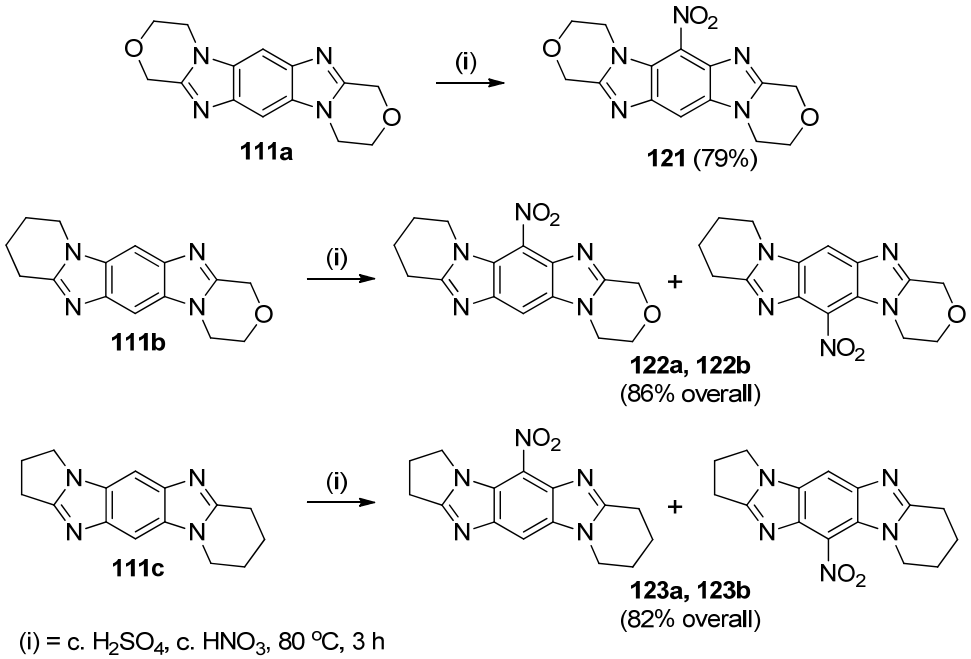

Scheme 3.30; Nitration of imidazo[5,4-*f*]benzimidazoles **111a-c**.

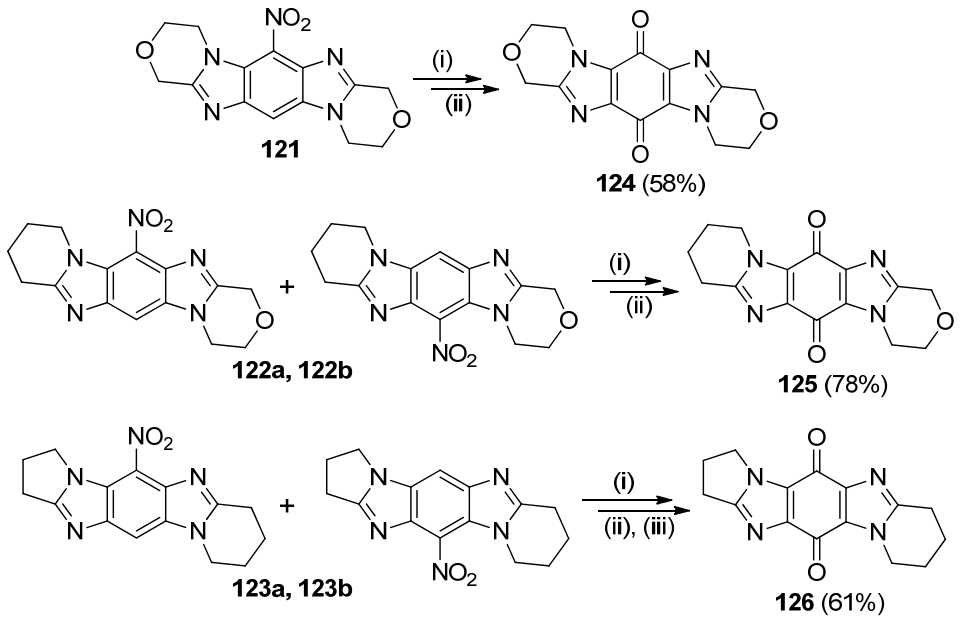

Scheme 3.31; Reduction and Frèmy oxidation to imidazo[5,4-*f*]benzimidazolequinones.

No iminoquinone (cf. Chapter 2, Scheme 2.39) was observed from the reduction and Frèmy oxidations of **121** and **122a**, **122b**. On the other hand, reduction and Frèmy oxidation of **123a**, **123b** gave an inseparable mixture containing ~30% of iminoquinone, which was hydrolyzed fully to quinone **126** using dilute HCl.

Di[1,4]oxazinoimidazo[5,4-*f*]benzimidazolequinone **124** was found to be insoluble in organic solvents, water and aqueous acids. Trifluoroacetic acid (TFA) was used to solubilize **124**, and an X-ray crystal structure was obtained of the salt formed with trifluoroacetate counter ions coordinated at the basic nitrogen atoms (7,14-*N*) of imidazo[5,4-*f*]benzimidazole (Figure 3.3 (Appendix, A.1, Table A.2)).

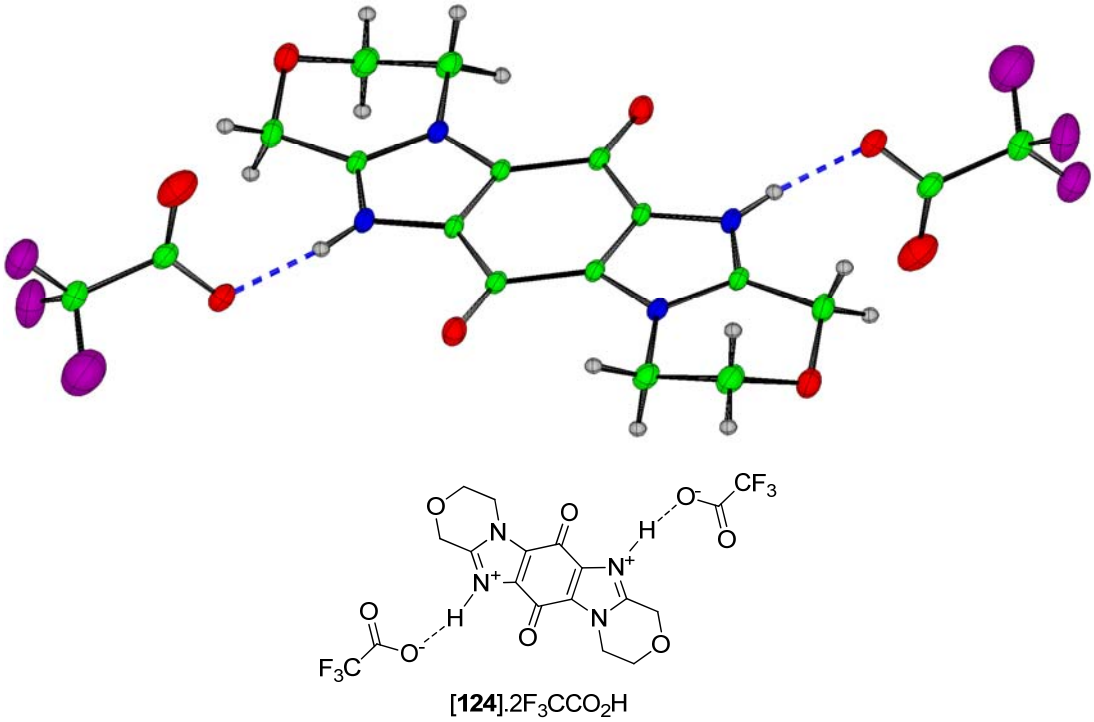

Figure 3.3; Crystal structure of 3,4,10,11-tetrahydro-1*H*,8*H*-[1,4]oxazino[4,3-*a*][1,4]oxazino[4',3':1,2]imidazo[5,4-*f*]benzimidazolium-6,13-dione di(trifluoroacetate) [**124**].$2F_3CCO_2H$.

3.2.4 Nomenclature of novel imidazo[5,4-*f*]benzimidazoles

The three main steps for naming such fused heterocycles (Chapter 2, 2.2.4) was followed: (i) Construct fusion name

(ii) Assign peripheral numbering

(iii) Assign indicated hydrogens & hydro positions

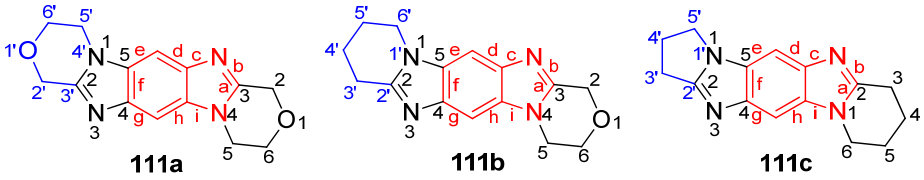

red = parent component; black = 1st order component; blue = 2nd order component

Figure 3.4; Components of imidazo[5,4-*f*]benzimidazoles **111a-c**.

(i) *Construct fusion name:*

Benzimidazole is the parent component in all three compounds. However there is a choice of benzimidazole parent components in the unsymmetrical compounds **111b** and **111c**. [1,4]Oxazino rings take preference over pyrido rings which in turn take preference over pyrrolo rings.[112] Therefore parent components are chosen so that the ring with the higher preference is the first order component, with the lower preference ring being second order (Figure 3.4).

The second order components are combined with their first order components to obtain new first order components:

111a; [1,4]oxazino[4′,3′:1,2]imidazo[5,4-*f*]

111b; pyrido[1′,2′:1,2]imidazo[5,4-*f*]

111c; pyrrolo[1′,2′:1,2]imidazo[5,4-*f*]

The fusion names can now be constructed with the first order components written in alphabetical order followed by the parent component:

111a; [1,4]oxazino[4,3-*a*][1,4]oxazino[4′,3′:1,2]imidazo[5,4-*f*]benzimidazole

111b; [1,4]oxazino[4,3-*a*]pyrido[1′,2′:1,2]imidazo[5,4-*f*]benzimidazole

111c; pyrido[1,2-*a*]pyrrolo[1′,2′:1,2]imidazo[5,4-*f*]benzimidazole

(ii) *Assign peripheral numbering:*

Peripheral numbering is independent of any previous labeling or numbering.

The molecules are drawn with certain allowable shapes so that the most possible number of rings is on a horizontal axis. Numbering begins from the most counter-clockwise non-fusion atom of the ring furthest to the right in the upper right hand quadrant and proceeds in a clockwise direction. Heteroatoms are included while fusion carbon atoms are not. Each fusion carbon atom is given the same number as the immediately preceding position but with the addition of a letter (Figure 3.5).

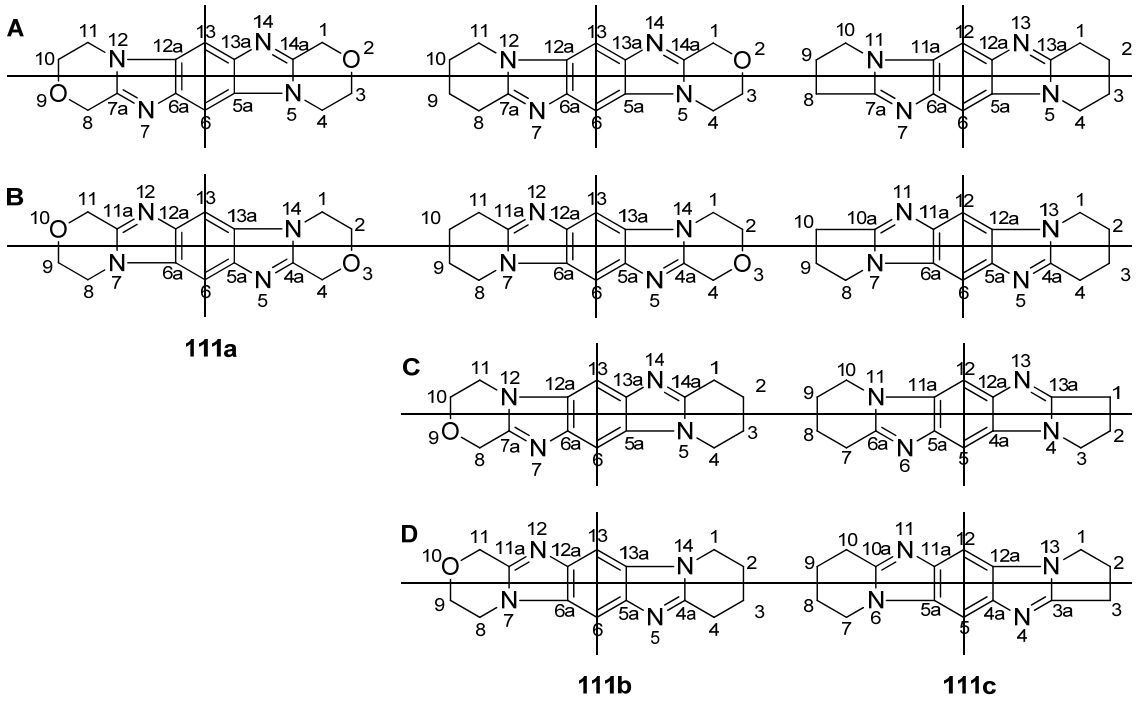

Figure 3.5; Possible orientations for peripheral numbering of compounds **111a-c**.

Since more than one orientation is equally allowed the following rules are applied, in order, until one orientation is preferred:[112]

(a) Give low numbers to heteroatoms as a set.

(b) Give low numbers to heteroatoms when considered in the order: 0, S, Se, Te, N, P, As, Sb, Bi, Si, Ge, Sn, Pb, B, Hg

(c) Give low numbers to fusion carbons as a set.

(d) Give low numbers to fusion rather than non-fusion atoms of the same heteroelement.

Applying rule (a) gives orientation **A** as the preferred orientation for compounds **111a** and **111b**, since the heteroatoms as a set are given the lowest numbers. Applying rule (a) also eliminates orientation **A** and **B** for compound **111c**, since orientation **C** and **D** gives lower numbers to the heteroatoms as a set. When rule (b) is applied orientation **C** and **D** are still equally allowed but when rule (c) is applied orientation **D** is the preferred orientation for compound **111c**.

(iii) *Assign indicated hydrogens & hydro positions:*

In the aliphatic rings the saturated positions are identified as being hydro positions if a double bond could exist between them or as indicated hydrogens if a double bond cannot exist at that position. Hence hydro positions occur in pairs. Where possible indicated hydrogens are placed at lower numbers and identified by an italic *H*. (Figure 3.6).

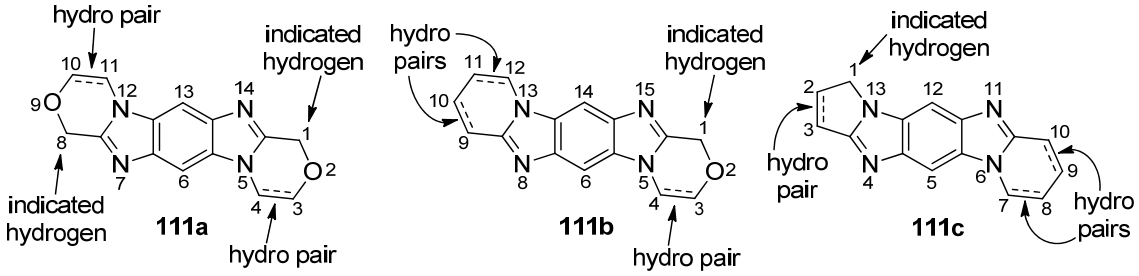

Figure 3.6; Assigning indicated hydrogen and hydro positions.

Therefore, the full names for compounds **111a-c** are:

111a; 3,4,10,11-Tetrahydro-1*H*,8*H*-[1,4]oxazino[4,3-*a*][1,4]oxazino[4′,3′:1,2] imidazo[5,4-*f*]benzimidazole

111b; 3,4,9,10,11,12-hexahydro-1*H*-[1,4]oxazino[4,3-*a*]pyrido[1′,2′:1,2] imidazo[5,4-*f*]benzimidazole

111c; 2,3,7,8,9,10-hexahydro-1*H*-pyrido[1,2-*a*]pyrrolo[1′,2′:1,2] imidazo[5,4-*f*]benzimidazole

3.3 Conclusions

Novel symmetrical and unsymmetrical pentacyclic imidazo[5,4-*f*]benzimidazoles with and without fused [1,4]oxazino rings have been synthesized using oxidative cyclizations of *o*-*tert*-amino acetanilides mediated by Oxone® in formic acid. This oxidizing system was shown to be superior to the literature procedures which use hydrogen peroxide in formic acid.[26, 34]

It was shown that at least two equivalents of any oxidant capable of amine *N*-oxide formation would, in acidic solution, give alicyclic ring fused benzimidazoles from *o*-*tert*-amino acetanilides. In the absence of an added oxidant, the amine *N*-oxide intermediates were shown to be able to act as an oxidant, facilitating the aromatization of the *N*-acetyldihydrobenzimidazoles to give the corresponding benzimidazoles.

A mechanism has been proposed, alternative to that proposed by Meth-Cohn[105] (Scheme 3.15), which takes into account the observed H-bonding of the amide NH and the *N*-oxide oxygen.

Imidazo[5,4-*f*]benzimidazoles were further functionalized to the corresponding quinones giving three new biologically active ring fused imidazo[5,4-*f*]benzimidazolequinones.

Chapter 4

4 Cytotoxicity Evaluation of Alicyclic Ring-Fused Imidazo[5,4-*f*]benzimidazolequinones

4.1 Introduction

The enzyme NAD(P)H:quinone oxidoreductase 1 (NQO1) is known to be over expressed in many human tumor cell lines.[132-134] The rational design of NQO1 substrates is important in targeting cancerous tissues expressing high levels of NQO1 leading to controlled toxicity. Skibo and co-workers showed that dialicyclic ring fused imidazo[4,5-*f*]benzimidazolequinones **13** and **16** (Figure 4.1) were excellent NQO1 substrates. When tested under the Development Therapeutics Program National Cancer Institute 60 human tumor cell line screen (see later), compound **13** showed moderate activity with a high specificity towards human melanoma cell lines, although no correlation to NQO1 was observed. Its biological response pattern was unlike that of any other compound in the NCI database, suggesting an unknown mode of action.[34] Cytotoxicity evaluation of dipyridoimidazo[4,5-*f*]benzimidazolequinone **16** was not reported.[35]

As part of this PhD, ten novel imidazo[5,4-*f*]benzimidazolequinones were prepared (Figure 4.1) and evaluated as anti-cancer compounds, along with the known dipyridoimidazo[4,5-*f*]benzimidazolequinone **16**, which was prepared using a novel synthetic route discussed in Chapter 2.

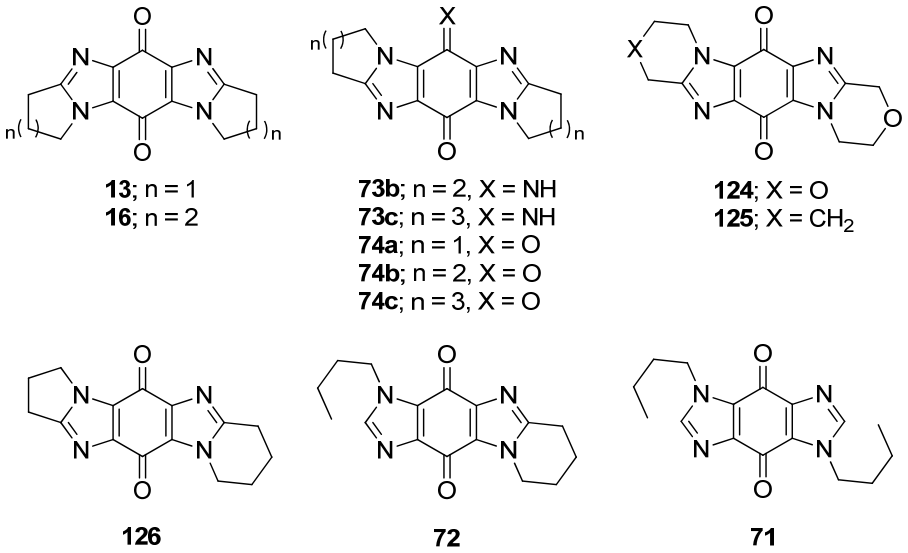

Figure 4.1; Novel series of imidazo[5,4-*f*]benzimidazolequinones with literature imidazo[4,5-*f*]benzimidazolequinones.

4.1.1 NAD(P)H:quinone oxidoreductase 1 (NQO1)

NQO1, also known as DT-diaphorase (EC 1.6.5.2), is a ubiquitous flavoenzyme which catalyzes the two-electron reduction of many quinones to their corresponding hydroquinones. NQO1 was isolated in 1958 by Ernster and Navazio and initially named DT-diaphorase for its ability to efficiently use both diphosphopyridine (NADH (nicotinamide adenine dinucleotide)) or triphosphopyridine (NADPH (nicotinamide adenine dinucleotide phosphate)) nucleotide electron donor cofactors (Scheme 4.1).[135] Traditionally NQO1 has been regarded as a detoxification, enzyme catalyzing the reduction of exogenous quinones to non-toxic hydroquinones.

NQO1 has a flavin adenine dinucleotide (FAD) redox cofactor that remains bound to the NQO1 protein during the catalytic cycle, and undergoes reduction by NAD(P)H (Scheme 4.1).

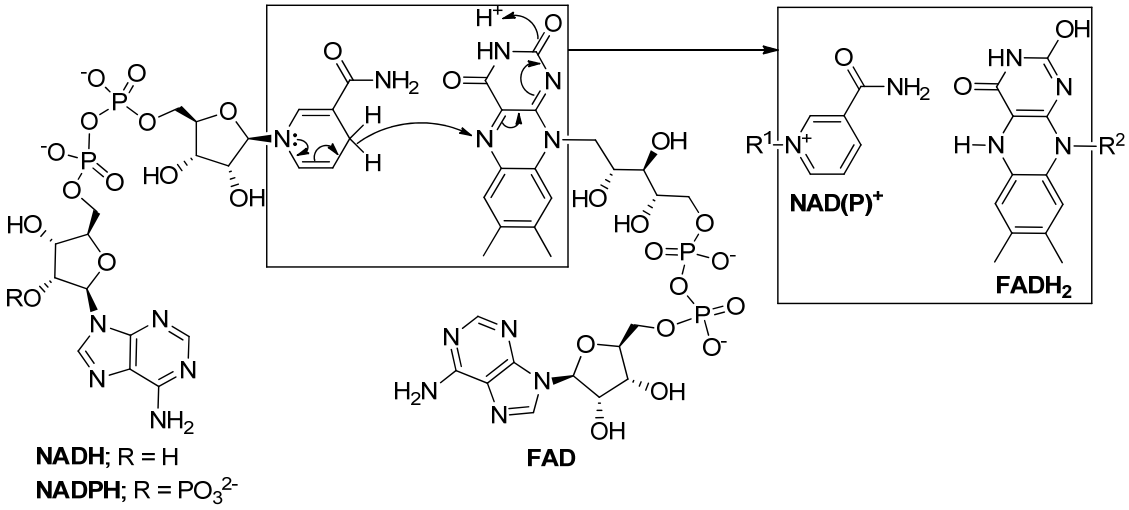

Scheme 4.1; Reduction of FAD cofactor to $FADH_2$ by NAD(P)H in the active site of NQO1.

The NQO1 mechanism of action is described as a ping-pong mechanism, as both NAD(P)H and the quinone substrate must independently occupy the same binding site. The catalytic cycle begins with the formation of a NQO1-FAD-NAD(P)H complex. The FAD cofactor is reduced to $FADH_2$ by NAD(P)H, and the resulting $NAD(P)^+$ is lost. The quinone substrate now enters the active site and is reduced to a hydroquinone by $FADH_2$. The substrate is then expelled as the hydroquinone, which regenerates the NQO1 enzyme.[12, 136]

4.1.2 Cytotoxicity evaluation using the MTT assay

New imidazo[5,4-*f*]benzimidazolequinones **71**, **72**, **74b**, **74c**, **125** & **126**, iminoquinone **73b**, and literature imidazo[4,5-*f*]benzimidazolequinone **16** were evaluated using two human cancer cell lines known to express high levels of NQO1 (cervical (HeLa, CCL-2)[132] and prostate (DU-145)[133]) and one human normal skin fibroblast cell line (GM00637). These evaluations were carried out within the Aldabbagh group by fellow group member Sarah Bonham using the MTT (3-(4,5-dimethylthiazol-2-yl)-2,5-diphenyltetrazolium bromide) colorimetric assay.[137] Cells are incubated in the presence of the test compound for a set period of time (72 h in this case) before addition of a solution of MTT. The yellow MTT is reduced to the purple formazan by mitochondrial reductase enzymes (Scheme 4.2). This reduction can only take place in metabolically active cells. Therefore the amount of formazan produced is directly related to the number of viable (living) cells. The amount of purple formazan can be quantified by measuring the absorbance using a spectrophotometer. The percentage cell viability can be determined by comparing the amount of formazan produced by the cells treated with the test compound in a particular solvent, to the amount of formazan produced by the control cells treated with the solvent alone. This process is repeated for different concentrations of the test compound, so that a dose response curve can be produced. From this dose response curve, an IC_{50} (concentration of compound required to inhibit cell viability by 50%) is determined, which is a measure of the cytotoxicity of the compound.

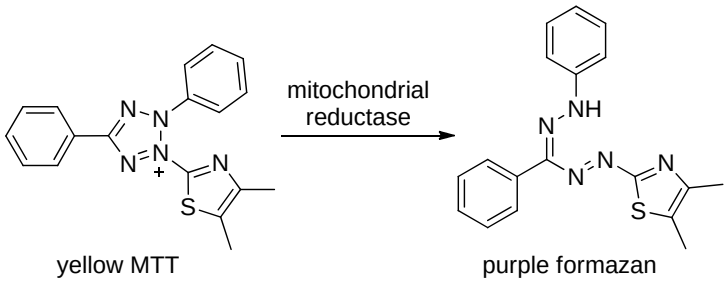

Scheme 4.2; Reduction of MTT to the purple formazan by viable cells.

4.1.3 DTP NCI-60 human tumor cell line screen

Operating since 1990 under the Development Therapeutics Program (DTP), the US National Cancer Institute (NCI) provides a free cytotoxicity screening service for compounds with potential anticancer activity. The screen utilizes 60 different human tumor cell lines, representing cancers of the lung, colon, brain, ovary, breast, prostate, kidney, and leukemia and melanoma.[138-139] Software known as COMPARE can be accessed on the DTP NCI website (http://dtp.nci.nih.gov/), which allows results to be compared to all other data accumulated within the NCI database.[139]

The number and variety of cell lines used means that each test compound will have a complex biological response pattern which can be compared to that of other test compounds. Compounds which possess similar mechanisms of toxicity will have similar biological response patterns; the COMPARE program can quantify the degree of similarity as a Pearson correlation coefficient. Correlation coefficients fall between -1 and +1, with -1 indicating a perfect inverse correlation, zero indicating no correlation at all and +1 indicating a perfect direct correlation.[140] A correlation coefficient of 0.3-0.5 is generally accepted as being weak to moderate, 0.5-0.7 as being moderate to strong and above 0.7 strong to very strong.

It is possible to determine the mode of action of new compounds if their biological response patterns are similar to that of compounds whose modes of action are known. It is also possible to assign a mode of action to a test compound if the biological response pattern correlates to the activity of a known molecular target. A molecular target is a protein, enzyme, gene or any other cellular molecule whose presence within the 60 cell line panel has been identified and quantified by the NCI.[138-139, 141]

Correlations to compounds of unknown mode of action also provide valuable information. By comparing the chemical structures of the compounds, common structural features can be identified, which may be responsible for the common biological response patterns displayed. If an active compound does not correlate to any known compound, then a new mode of action can be assigned. To date NCI has gathered data on over 200,000 compounds and identified and quantified over 12,000 molecular targets.

Selected imidazo[5,4-*f*]benzimidazolequinones **72**, **74a**, **74b**, **125** and iminoquinones **73b**, **73c** were submitted to the NCI for *in vitro* testing under the DTP NCI-60 screening program. NQO1 has been identified by the NCI as an important molecular target and its activity has been measured within each of the human cancer cell lines (Figure 4.2).[133] Therefore the cytotoxicity profile of each compound can be correlated to NQO1 activity, thereby quantifying specificity to this molecular target. The prostate cancer cell line DU-145 used in the MTT cytotoxicity evaluations (section 4.1.2) is also one of the 60 cancer cell lines used in the DTP NCI-60 cell screen.

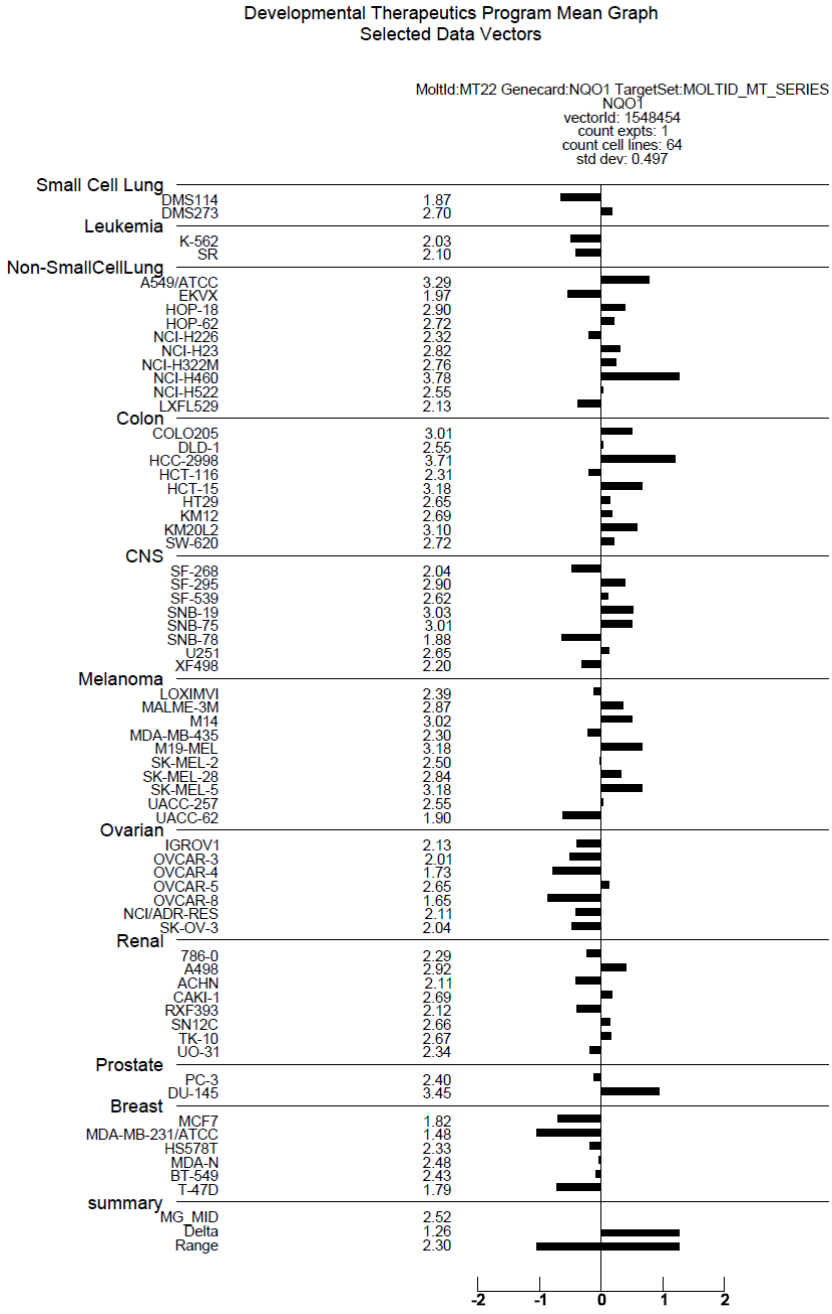

Figure 4.2; Levels of NQO1 activity in the DTP NCI-60 cell panel.[133]

4.1.4 Computational docking

Computational docking studies were carried out through collaboration with the Computational Chemistry and Biology Group, Facultad de Química, UdelaR, Montevideo 11800, Uruguay. All molecular modeling was performed by Dr. Patricia Saenz-Méndez using the Molecular Operating Environment (MOE) 2009.10 program.[142] MOE is a molecular modeling program which is specifically designed to deal with large biological molecules.

The NQO1 crystal structure has two homodimers, each of which is made of two interlocked monomers. The physiological unit of the quinone reductase consists of a dimer,[143] which was thus employed in the computational modeling.

All imidazo[5,4-*f*]benzimidazolequinones, iminoquinone **73b** and literature imidazo[4,5-*f*]benzimidazolequinones **13** and **16** were computationally docked into the active site of human NQO1 (PDB code 1D4A).[144] There have been no reports in literature of a comprehensive docking study of mitomycin C (MMC) into the active site of NQO1. As a result the first computational docking study of MMC as an NQO1 substrate is presented, along with that of the imidazobenzimidazolequinones, in order to assess the relationship between cytotoxicity and substrate-enzyme interactions.

4.1.5 Aims and objectives

- To carry out cytotoxicity evaluation of the novel series of imidazo[5,4-*f*]benzimidazolequinones using the MTT assay on human normal skin fibroblast cells (GM00637) and two cancer cell lines known to over express the quinone reducing enzyme NQO1: cervical (HeLa) and prostate (DU-145) cancer.
- To conduct structure-activity relationship studies to assess how the different structural features (i-v) affect cytotoxicity.

  (i) Isomer [5,4-*f*] v [4,5-*f*]

  (ii) Quinone moiety v iminoquinone

  (iii) Alicyclic ring size (pyrrolo v pyrido v azepino)

  (iv) Alicyclic ring fusion (di-fused v mono-fused v non-fused)

  (v) Pyrido ring v oxazino ring

- To evaluate selected imidazo[5,4-*f*]benzimidazolequinones using the DTP NCI-60 screening program so that correlations can be made to NQO1 and any other molecular targets.
- To carry out computational docking of the imidazobenzimidazolequinones into the active site of NQO1 in order to assess the relationship between cytotoxicity and substrate-enzyme interactions.

4.2 Results and discussion

4.2.1 Toxicity towards human normal cells and cancer cell lines using the MTT assay

Compounds **16**, **71**, **72**, **73b**, **74b**, **74c**, **125** & **126** were evaluated against the three human cell lines (cervical (HeLa) and prostate cancer (DU-145), and normal skin fibroblast (GM00637)). Each cell line was treated with 0.1-5.0 μM solutions of the test compound and with MMC in parallel as a positive control. The activity of each compound was quantified by determining IC_{50} values using GraphPad Prism software, v. 5.02 (GraphPad Inc., San Diego, CA, USA) (Table 3 (Appendix, A.2)).

Table 3; Biological evaluation: IC_{50} values (μM).[a]

Entry	Compound	Cell Lines		
		GM00637	HeLa CCL-2	DU-145
1	**MMC**	0.46 ± 0.09	0.27 ± 0.16	0.17 ± 0.02
2	**16**	> 5.0	3.33 ± 0.47	1.73 ± 0.23
3	**71**	1.05 ± 0.15	0.44 ± 0.04	1.34 ± 0.06
4	**72**	2.12 ± 0.04	1.28 ± 0.05	1.35 ± 0.11
5	**73b**	3.63 ± 0.52	1.55 ± 0.35	0.30 ± 0.01
6	**74b**	> 5.0	1.67 ± 0.05	1.99 ± 0.39
7	**74c**	> 5.0	1.78 ± 0.19	4.46 ± 0.16
8	**125**	0.60 ± 0.03	0.58 ± 0.03	0.66 ± 0.02
9	**126**	1.27 ± 0.05	0.95 ± 0.10	0.79 ± 0.05

[a] IC_{50} represents the compound concentration required for reduction of mean cell viability to 50% of the control value after incubation for 72 h at 37 °C, as determined using the MTT assay.

These compounds were chosen so that chemical structure-activity relationships could be conducted in order to assess how the different structural features impact on cytotoxicity. Comparisons were made to dipyridoimidazo[5,4-*f*]benzimidazolequinone **74b**, which was viewed as the parent molecule.

The cytotoxicities of compounds bearing the following structural features were contrasted;

(i) Isomer [5,4-*f*] v [4,5-*f*]

(ii) Quinone v iminoquinone moiety

(iii) Alicyclic fused ring size (pyrrolo v pyrido v azepino)

(iv) Alicyclic ring fusion (di-fused v mono-fused v non-fused)

(v) Pyrido ring v oxazino ring

(i) *Contrasting the cytotoxicities of dipyridoimidazo[5,4-f]benzimidazolequinone* **74b** *against its [4,5-f] analogue* **16**.

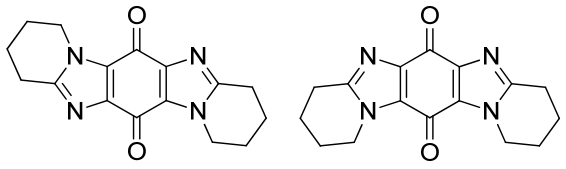

	74b	**16**
GM00637	> 5.0	> 5.0
HeLa CCL-2	1.67 ± 0.05	3.33 ± 0.47
DU-145	1.99 ± 0.39	1.73 ± 0.23

Although Skibo and co-workers previously prepared dipyridoimidazo[4,5-*f*]benzimidazolequinone **16**, no toxicity evaluation was reported.[35] Both isomers **16** and **74b** showed negligible toxicity towards the normal skin fibroblast cell line (GM00637) in the concentration range 0.1-5 μM (Table 3, entry 2 & 6), which may be of therapeutic advantage. Imidazo[5,4-*f*]benzimidazolequinone **74b** was more toxic towards both HeLa and DU-145 cancer cell lines compared to the normal human skin fibroblast cell line (Table 3, entry 6). Isomer **16** also showed greater toxicity towards the cancer cell lines than the normal cell line, but was about twice less potent towards the HeLa cell line than its novel isomer **74b** (entry 2).

(ii) *Contrasting the cytotoxicities of dipyridoimidazo[5,4-f]benzimidazolequinone* **74b** *against its iminoquinone analogue* **73b**.

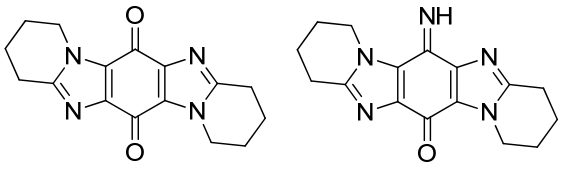

	74b	**73b**
GM00637	> 5.0	3.63 ± 0.52
HeLa CCL-2	1.67 ± 0.05	1.55 ± 0.35
DU-145	1.99 ± 0.39	0.30 ± 0.01

The 6-iminodipyridoimidazo[5,4-*f*]benzimidazol-13-one **73b** showed enhanced cytotoxicity towards all three cell lines (Table 3, entry 5) compared to dipyridoimidazo[5,4-*f*]benzimidazolequinone **74b** (entry 6). The iminoquinone **73b** showed particularly high cytotoxicity towards the prostate cancer cell line (DU-145), being the most active of all imidazobenzimidazoles evaluated (IC_{50} = 0.30 μM) with toxicity towards HeLa cells being similar to that of quinone analogue **74b**. Iminoquinone **73b** was about 12 times more toxic towards the prostate cancer cell line than towards normal cells.

(iii) *Assessment of the influence of the fused alicyclic ring size by contrasting the cytotoxicities of imidazo[5,4-f]benzimidazolequinones containing pyrrolo* (**126**)*, pyrido* (**74b**) *and azepino* (**74c**) *fused rings.*

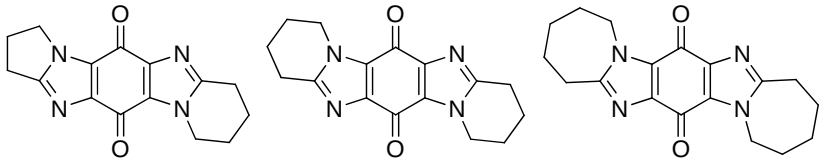

	126	**74b**	**74c**
GM00637	1.27 ± 0.05	> 5.0	> 5.0
HeLa CCL-2	0.95 ± 0.10	1.67 ± 0.05	1.78 ± 0.19
DU-145	0.79 ± 0.05	1.99 ± 0.39	4.46 ± 0.16

Dipyrroloimidazo[5,4-*f*]benzimidazolequinone **74a** was not evaluated due to poor solubility in organic and aqueous solvents, although pyridopyrroloimidazo[5,4-*f*]benzimidazolequinone **126** allowed the influence on cytotoxicity of the five-membered fused alicyclic ring to be assessed. The pyrrolo-fused compound **126** was

more cytotoxic towards all three cell lines tested than dipyrido fused analogue **74b** with some specificity towards the two cancer cell lines. Like the other dialicyclic ring-fused quinones, diazepinoimidazo[5,4-*f*]benzimidazolequinone **74c** showed greater toxicity towards the cancer cell lines compared to the normal skin fibroblast cell line, but was less toxic towards cancer cell lines than dipyrido fused analogue **74b**. There is a clear trend of increased potency towards cancer cell lines with a decrease in the size of the fused alicyclic ring from seven to five-membered. For example, pyridopyrroloimidazo[5,4-*f*]benzimidazolequinone **126** is 5-6 times more potent towards DU-145 cells than diazepino analogue **74c**. In agreement with this trend in potency, previous studies by the Aldabbagh group showed pyrrolo[1,2-*a*]benzimidazolequinones to be more cytotoxic towards GM00637 cells than six and seven-membered alicyclic ring-fused analogues.[27]

(iv) *Assessment of the influence of alicyclic ring fusion by contrasting the cytotoxicities of dipyridoimidazo[5,4-f]benzimidazolequinone* **74b** *against its mono-fused analogue* **72** *and its non-fused analogue* **71**.

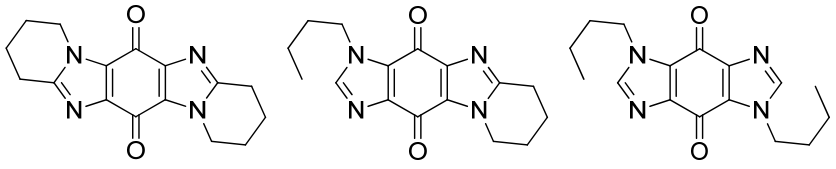

	74b	**72**	**71**
GM00637	> 5.0	2.12 ± 0.04	1.05 ± 0.15
HeLa CCL-2	1.67 ± 0.05	1.28 ± 0.05	0.44 ± 0.04
DU-145	1.99 ± 0.39	1.35 ± 0.11	1.34 ± 0.06

Decreasing the extent of alicyclic ring fusion from the fully fused system **74b** to its analogue containing only one fused pyrido ring **72** to the non-fused **71** containing no alicyclic fused rings resulted in increased toxicity towards all three cell lines. Although 1,5-dibutylimidazo[5,4-*f*]benzimidazol-4,8-dione **71** was the most potent, it did not show specificity towards the cancer cell lines, although marginally greater toxicity towards the cervical cancer cell line (HeLa, IC_{50} = 0.44 μM) was observed. Analogue **72** with one fused pyrido ring was also most cytotoxic towards HeLa cells (IC_{50} = 1.28 μM), although less so than dibutylimidazo[5,4-*f*]benzimidazol-4,8-dione **71**. Similarly it has been reported that benzimidazolequinones containing fused

aromatic rings are less toxic towards the cell lines evaluated in this study than the corresponding non-fused 2-aryl substituted benzimidazole-4,7-diones analogues.[31]

(v) *Assessment of the influence of an oxygen atom in the alicyclic ring by contrasting the cytotoxicities of dipyridoimidazo[5,4-f]benzimidazolequinone* **74b** *against its oxazinopyrido analogue* **125**.

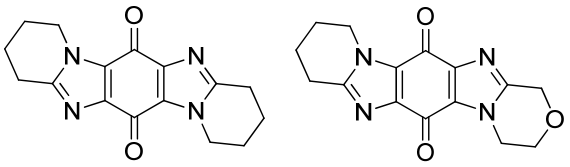

	74b	**125**
GM00637	> 5.0	0.60 ± 0.03
HeLa CCL-2	1.67 ± 0.05	0.58 ± 0.03
DU-145	1.99 ± 0.39	0.66 ± 0.02

Dioxazinoimidazo[5,4-*f*]benzimidazolequinone **124** was not evaluated due to poor solubility in organic and aqueous solvents, although oxazinopyridoimidazo[5,4-*f*]benzimidazolequinone **125** allowed the influence on cytotoxicity of an oxygen atom in the alicyclic ring to be assessed. Oxazinopyridoimidazo[5,4-*f*]benzimidazolequinone **125** was more cytotoxic against all three cell lines than the dipyrido analogue **74b** (Table 3, entry 6 & 8), but lacked specificity towards the cancer cell lines with IC_{50} values of similar magnitude for each cell line. Compound **125** was more cytotoxic towards the human normal fibroblast cell line (GM00637: IC_{50} = 0.60 μM) than all other imidazobenzimidazolequinone compounds tested in the series, while quinone **74b** was evaluated as being non-toxic towards the same cell line at concentrations of up to 5μM. Therefore, the presence of an oxygen atom in the alicyclic ring increases cytotoxicity against all cell lines evaluated.

4.2.2 Toxicity towards cancer cell lines using the DTP NCI-60 cell screening program

The DTP NCI-60 is a two-stage screening process beginning with the evaluation of all compounds against 60 human tumor cell lines, representing 9 major histological tissue types, at a single dose of 10 μM. The output of the single dose is reported as a mean growth % graph. Compounds which exhibit significant growth inhibition are evaluated against the 60 cell panel at five different concentrations, giving three further parameters of toxicity: GI_{50} (concentration of compound required to inhibit cell growth by 50%), TGI (concentration of compound required to totally inhibit cell growth) and LC_{50} (concentration of compound required to kill 50% of cells). Six imidazo[5,4-*f*]benzimidazole (**72**, **73b**, **73c**, **74a**, **74b** & **125**) were submitted for *in vitro* cytotoxicity evaluation by the DTP NCI-60 screening program (Figure 4.3).

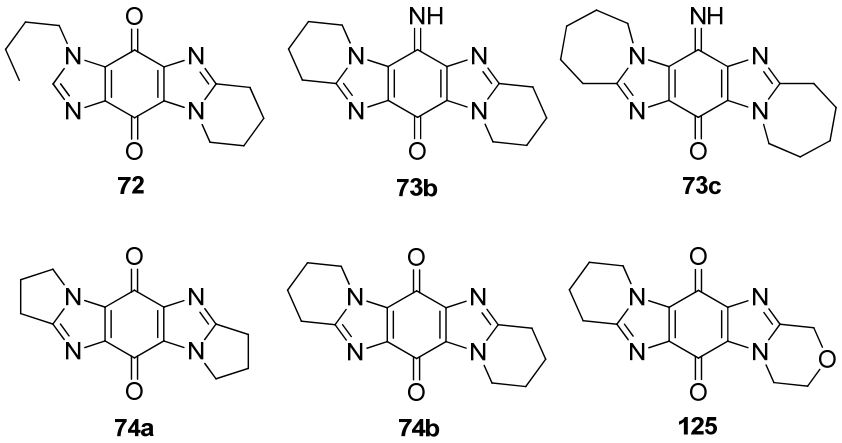

Figure 4.3; Imidazo[5,4-*f*]benzimidazoles submitted to the DTP NCI-60 screen.

The results of the single dose screen for the six submitted compounds are presented in Figure 4.4 as the average percentage growth for each histological tissue type (Appendix, A.3). Generally the results of the NCI-60 screen indicate a lower potency for compounds than that indicated by the MTT assays, although different cell lines and conditions are used. Further, in the NCI-60 screen, the cultivated cells are incubated with the test compounds for a shorter period (48 h) than in the case of the MTT assays (72 h) carried out at NUI Galway. While both data sets are not directly comparable, the trends observed from the activity of molecules relative to each other are comparable.

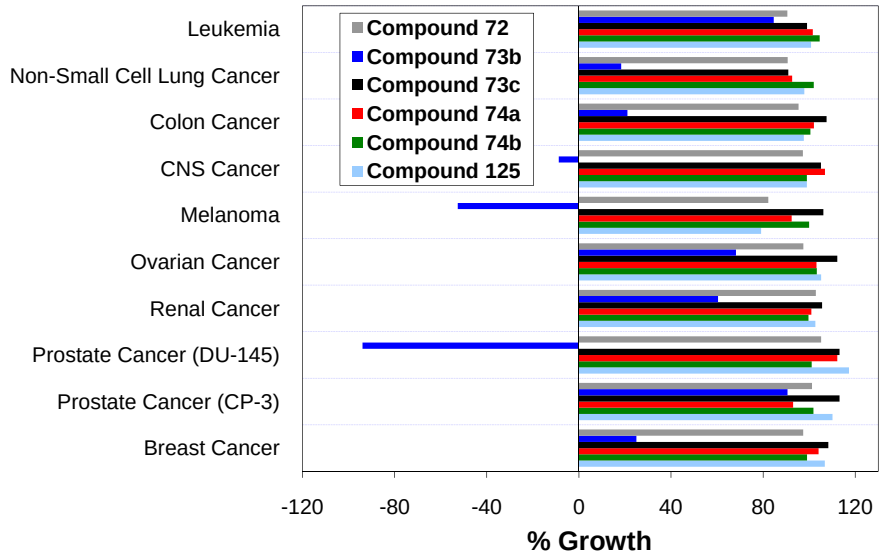

Figure 4.4; Average % growth after treatment with **72**, **73b**, **73c**, **74a**, **74b** & **125**.

In agreement with the MTT cytotoxicity evaluations, iminoquinone **73b** was highly potent towards the DU-145 cell line. The latter compound has a complex biological response pattern showing significant toxicity towards cell lines within cancer types which otherwise showed a low response. The two prostate cancer cell lines (DU-145, CP-3) are shown separately to exemplify the variation observed between different cell lines within the same cancer type (Figure 4.4). The diazepino iminoquinone **73c** showed a marked decrease in activity compared to its dipyrido iminoquinone analogue **73b**, with a complete loss of specificity towards the DU-145 prostate cancer cell line. This may be ascribed to a decrease in toxicity with increase in fused alicyclic ring size, a trend also observed in the results of MTT assays (see above).

The mean growth percent for each compound assessed by the NCI-60 is shown in Table 4 and is a measure of overall activity against all cancer cell lines. Four compounds (**72**, **73b**, **74b** & **125**) were evaluated by both the MTT assay and by the NCI-60 screen. The results of the MTT assays indicate that compound **125** was most active on the cancer cell lines followed by **73b** and **72**, with **74b** being least active of the four. With the exception of compound **125**, the results of the NCI-60 screen showed the same trend, with **73b** being most active followed by **72** and **125**, with **74b** being least active.

Table 4; Mean growth percent of compounds evaluated by the NCI-60 screen.

Compound	Mean growth %
72	94
73b	24
73c	106
74a	100
74b	101
125	98

Of all six compounds submitted, only iminoquinone **73b** was deemed active enough under the test conditions to proceed with testing at five concentration levels (100, 10, 1, 0.1, 0.01 μM), the results of which are presented in Figure 4.5a (Appendix, A.3).

Iminoquinone **73b** had a varying biological response pattern showing an overall high activity on melanoma. The two prostate cell lines are again shown separately to highlight the specificity towards the DU-145 cell line. While the iminoquinone **73b** was almost inactive on the CP-3 prostate cancer cell line (inactivity; $-\log GI_{50} < 4$), it showed a high degree of activity on the DU-145 cell line. This is in agreement with the MTT assay results where **73b** was found to be over 12 times more active on the DU-145 prostate cell line than on the normal skin fibroblast cell line GM00637 and over five times more active than on the cervical cancer cell line HeLa CCL-2.[110] Figure 4.5b shows the average NQO1 activity for each cancer type with the prostate cancer cell lines shown separately.[133] It is clear that the difference in toxicity towards the two prostate cell lines is related to the levels of NQO1 activity in those cell lines. The DU-145 cell line has significantly higher NQO1 activity than the CP-3 cell line, and compound **73b** displays significantly greater toxicity towards the DU-145 prostate cell line than the CP-3 cell line.

An overall trend of increased cytotoxicity with increased levels of NQO1 activity can be seen when comparing Figures 4.5a and 4.5b, and this trend was examined further using the COMPARE program.

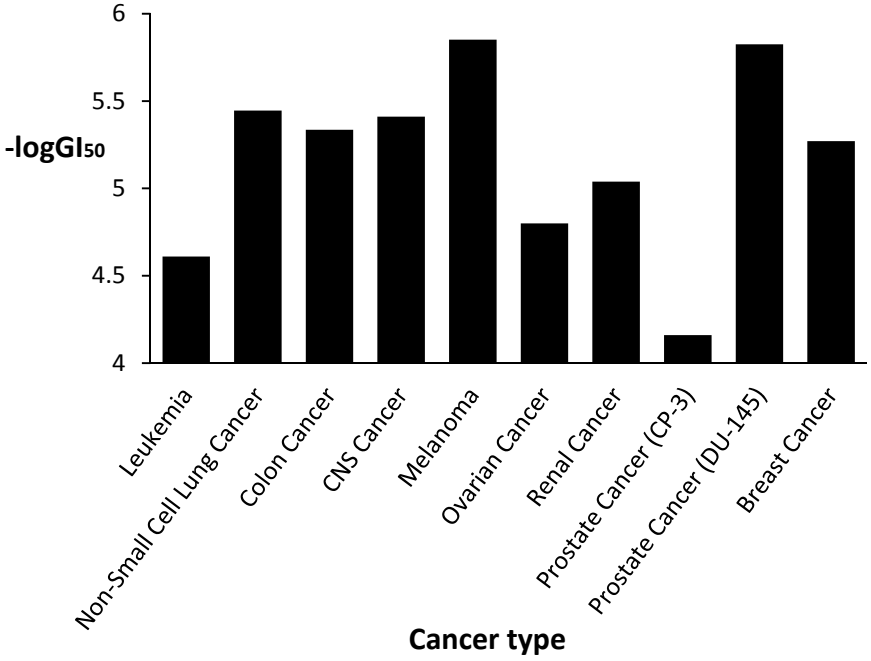

Figure 4.5a; Average -logGI_{50} of **73b** for each cancer type.

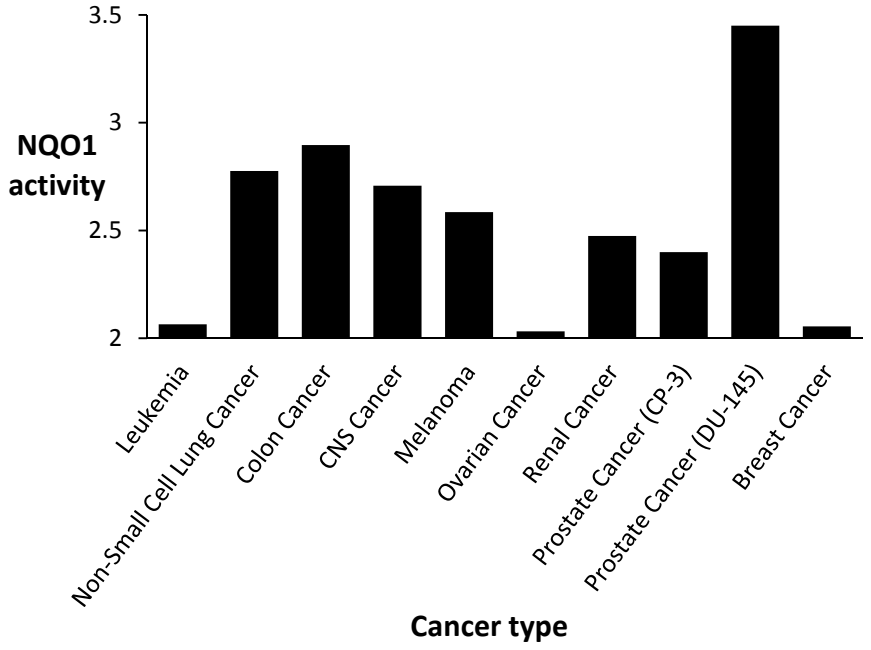

Figure 4.5b; Average NQO1 activity for each cancer type.

4.2.2.1 COMPARE analysis

COMPARE analysis was carried out using the one-dose pre-screen data for all compounds submitted, as well as the five-dose testing results for iminoquinone **73b**. Using the one dose pre-screen data, only iminoquinone **73b** showed correlation to NQO1, albeit with a moderate correlation of 0.45. However, four of the six submitted compounds (**72**, **73c**, **74a**, **125**) showed correlation to another important molecular target TP53 (Figure 4.6 (Appendix, A.4)). This gene encodes protein p53, which functions as a transcription factor. Its level is altered in response to cellular stresses such as DNA damage, spindle damage, toxic chemicals or hypoxia. The p53 protein regulates a large number of genes that control a number of key tumor suppressing functions such as cell cycle arrest, DNA repair and apoptosis.[145] Whilst the activation of p53 often leads to apoptosis, p53 inactivation facilitates tumor progression. MDM2 is a ubiquitin ligase that binds p53 and targets it for proteasomal degradation.[145] Of the four compounds that showed correlation to TP53, three also showed correlation to MDM2 (**72**, **73c**, **125**; Figure 4.6 (Appendix, A.4)). The imidazo[5,4-*f*]benzimidazolequinones may induce p53 activation and expression, or may interact with MDM2 to inhibit the degradation of p53. Given the important role of TP53 in tumor suppression, the correlations observed here are worthy of future investigation.

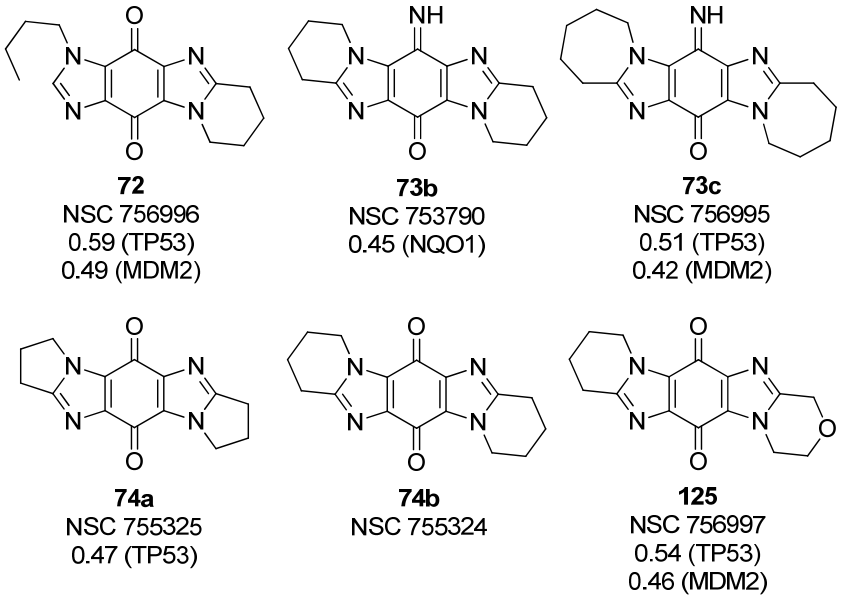

Figure 4.6; COMPARE analysis of the one dose pre-screen data.

When the five-dose testing results for iminoquinone **73b** were analyzed using COMPARE a higher correlation of 0.51 to NQO1 was obtained (Figure 4.7). The clinically used quinone drug mitomycin C is known to be reductively activated by NQO1 and has the highest correlation of the 171 standard agents at the NCI. However with only a moderate correlation of 0.43, compound **73b** compares favorably. The biological response pattern of iminoquinone **73b** was also compared to that of all compounds tested by the NCI. The two highest correlations obtained were to compounds **127** and **128**,[146] with coefficients of 0.87 and 0.77 respectively (Figure 4.7 (Appendix, A.4)). Compound **127** had a correlation of 0.64 to NQO1, the second highest of all synthetic compounds in the NCI compound database while compound **128** had a correlation of 0.47. Compound **129** had the highest correlation to NQO1 of all compounds in the NCI with a correlation coefficient of 0.67. Compound **127** and **128** possess structural similarities to **73b** and therefore it is possible to determine which structural characteristics exert the greatest influence on the activity of such molecules. All three molecules have the iminoquinone motif incorporated in some way. All three are flat aromatic molecules with π-stacking capabilities and all have additional groups or positions with hydrogen bonding capabilities.

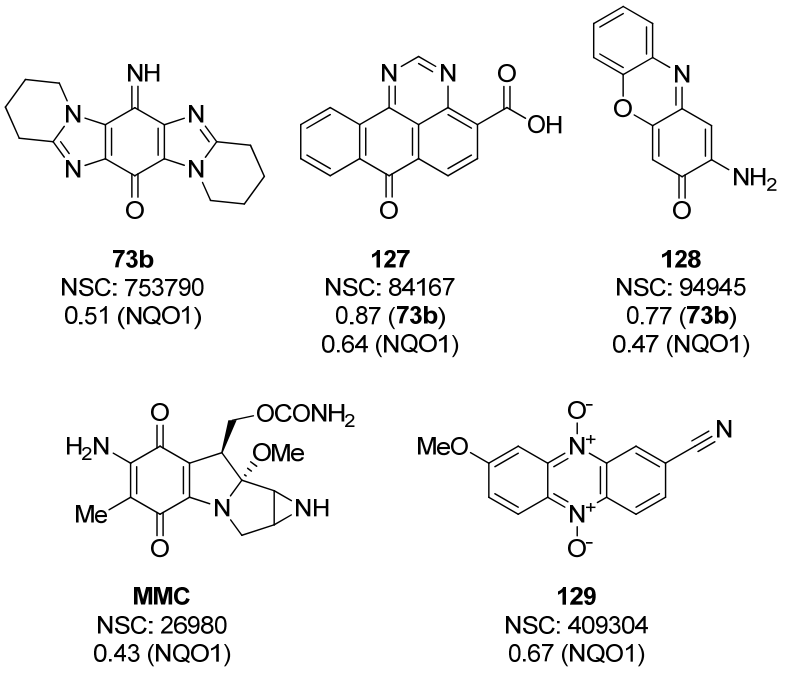

Figure 4.7; COMPARE analysis of five dose data for dipyrido iminoquinone **73b**.

The results obtained here confirm that NQO1 has a significant role to play in the mode of action of compound **73b**. However, with a moderate to good correlation obtained, it seems that other factors also influence its activity. From the excellent correlations obtained between **73b** and compounds **127** and **128**, it seems that the most significant structural feature of compound **73b** is the iminoquinone moiety and the synthesis of analogues bearing this moiety would be of interest in the future.

4.2.3 Computational docking

After each member of the novel series of imidazo[5,4-*f*]benzimidazolequinones was docked into the active site of human NQO1, relaxation / minimization of the enzyme-substrate complex was carried out (for details see Experimental Section), and the interaction energies were calculated (Table 5).

Table 5; Interaction energies of quinone substrates with NQO1

Entry	Complex with NQO1	Interaction energy (I.E.)[a] (kcal.mol^{-1})
1	**MMC**	-88.35
2	**13**	-74.28
3	**16**	-63.02
4	**71**	-65.12
5	**72**	-69.91
6	**73b**	-63.99
7	**74a**	-53.57
8	**74b**	-76.75
9	**74c**	-61.91
10	**124**	-69.63
11	**125**	-66.12
12	**126**	-56.24

[a] I.E. = $E_{complex} - (E_{enz} + E_{ligand})$.

In all cases, the interaction between the quinone substrate and NQO1 lowered the total energy considerably, leading to stable complexes. The most favorable docking energy was obtained for MMC (Table 5, Entry 1), in agreement with experimental IC_{50} trends obtained by the MTT cytotoxicity evaluations (Table 3). However, no clear correlation could be established between the computed interaction energies (I.E.) and the experimental IC_{50} values determined by the MTT assays. For example, for both cancer cell lines, **73b** displays a higher cytotoxicity than **74b**, and these observations are not reproduced by the docking interaction energies. One possible explanation is that binding is not the only factor accounting for the observed cytotoxicities.

With that in mind, the models were improved for seven of the substrate-enzyme complexes (**MMC**, **16**, **71**, **73b**, **74b**, **124** & **125**). With the exception of quinone **124**, all of these quinones were evaluated using the MTT assay. Starting from complexes derived from docking, MD (molecular dynamics) simulation and a

final energy minimization, the refined models were built using the LigX interface in MOE.[142] In these calculations the protein atoms far from the substrate were constrained not to move while receptor atoms in the active site and the quinone substrate in the active site were treated as flexible. The active site was defined as a distance of 8 Å from the substrate. An energy minimization was performed (rms gradient of 0.01 kcal mol^{-1} $Å^{-1}$) subject to these restraints. Several 2D and 3D properties were calculated after energy minimization, including the binding affinity (the estimated binding energy reported in units of pKi), the results of which are shown in Table 6.

The binding energy is not the only factor to be taken into account when explaining or predicting biological activity of the quinones. The substrate-protein complex must be stabilized (i.e. have a high binding affinity), but the substrate must also bind in a proper orientation. Ideally, the $C_{quinone}$-N5 distance should be less than 5 Å in order to permit the hydride transfer from the reduced $FADH_2$ group to the quinone substrate (Scheme 4.3). Starting from the refined models, the active site was analyzed and the $C_{quinone}$-N5 distance was measured (Table 6).

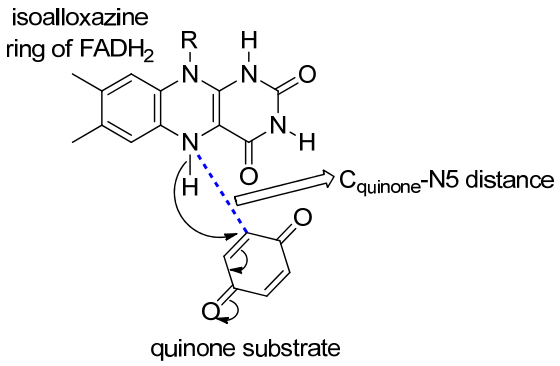

Scheme 4.3; Hydride transfer from $FADH_2$ N5 to the quinone substrate.

Table 6; Affinity of quinone substrates with NQO1, and key substrate-N5 distance.

Entry	Complex with NQO1	Binding affinity (pKi)	$dC_{quinone}$-N5 (Å)
1	**MMC**	8.60	3.89
2	**16**	6.43	8.02
3	**71**	7.45	5.25
4	**73b**	7.41	5.09
5	**74b**	7.33	4.34
6	**124**	7.98	4.47
7	**125**	6.45	6.00

The refined models generally reproduced the observed trends for the cytotoxicity against the HeLa CCL-2 cell line, except for **125**, which displayed a slightly lower binding affinity and greater $C_{quinone}$-N5 distance than expected.

MMC was found to bind with the highest affinity and the shortest distance to the N5 of the $FADH_2$ isoalloxazine ring, and therefore is calculated to be the most easily reduced by NQO1. A detailed representation of the MMC-NQO1 active site is shown in Figure 4.8.

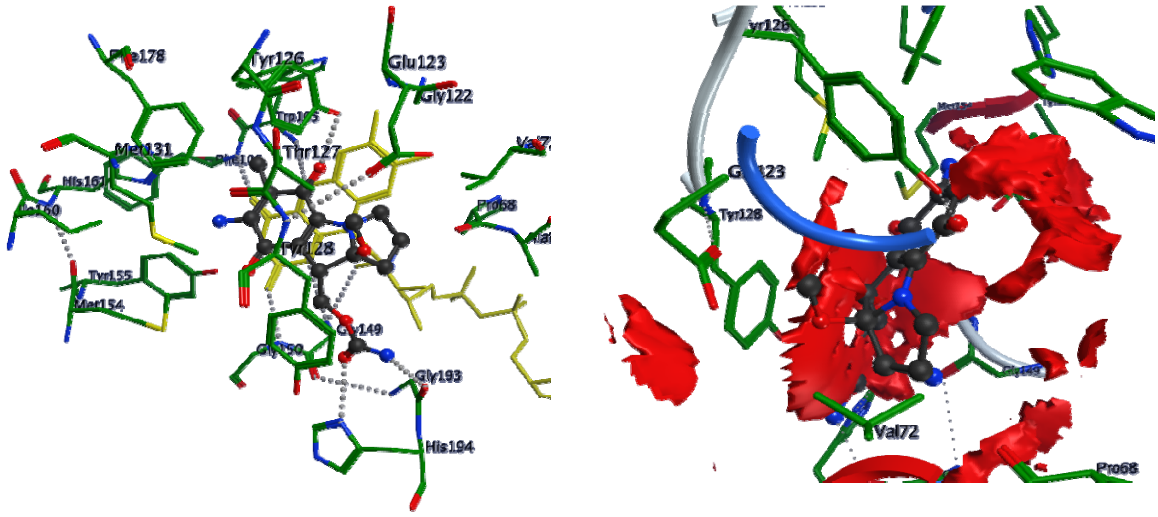

Figure 4.8; (Left) Molecular model of MMC docked into the active site of NQO1. Hydrogen bonds are shown as dashed lines and the FAD cofactor is shown in yellow; (Right) Hydrophobic contact surface between MMC and NQO1.

Three residues hydrogen-bond to MMC (namely Gly193, His194 and Tyr126), holding it in a favorable position for reduction to occur. The His194 residue is reported to play an important role in the interaction of quinone substrates with NQO1.[147-148] The oxygen atom of the carbamate side chain of MMC hydrogen-bonds to this residue, influencing the position of the quinone substrate in the active site so that the reactive carbon is located 3.89 Å from N5 of the $FADH_2$. The Trp105 and Tyr128 residues provide a pocket on one side of the active site towards which MMC displays favorable hydrophobic contacts (Figure 4.8 (Right)).

Previously reported NQO1 docking studies found imidazo[4,5-*f*]benzimidazole **16** to be an excellent substrate for NQO1.[35] The results of computational docking studies carried out here show quinone **16** to have a low affinity and a large $C_{quinone}$-N5 distance. A π-cation interaction between the imidazole ring of **16** and the proton atoms in His194 is observed which flips the molecular plane, placing **16** perpendicular to the isoalloxazine ring plane.

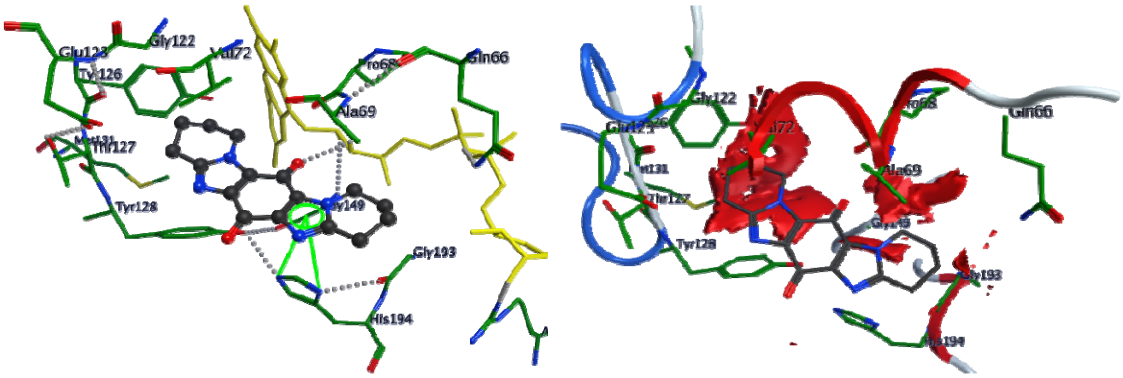

Figure 4.9; (Left) Molecular model of quinone **16** docked into the active site of NQO1. Hydrogen bonds are shown as dashed lines, π-arene-cation interactions are shown in green and the FAD cofactor is shown in yellow; (Right) Hydrophobic contact surface between **16** and NQO1 (Tyr126 and Tyr128).

This orientation gives rise to a very large $C_{quinone}$-N5 distance (8.02 Å; almost double that for structural isomer **74b**; 4.34 Å), which hampers hydride transfer (Figure 4.9 (Left)). The hydrophobic contacts are also less stabilizing than the interactions observed for MMC (Figure 4.9 (Right)). The lower affinity and greater $C_{quinone}$-N5 distance for imidazo[4,5-*f*]benzimidazolequinone **16** suggests that the [5,4-*f*] isomer **74a** is a better NQO1 substrate.

For the non-ring fused compound **71**, the docking studies predict a slightly lower binding affinity and larger $C_{quinone}$-N5 distance than expected from its cytotoxicity towards HeLa cells. Polar interactions between **71** and NQO1 are shown in Figure 4.10 (Left).

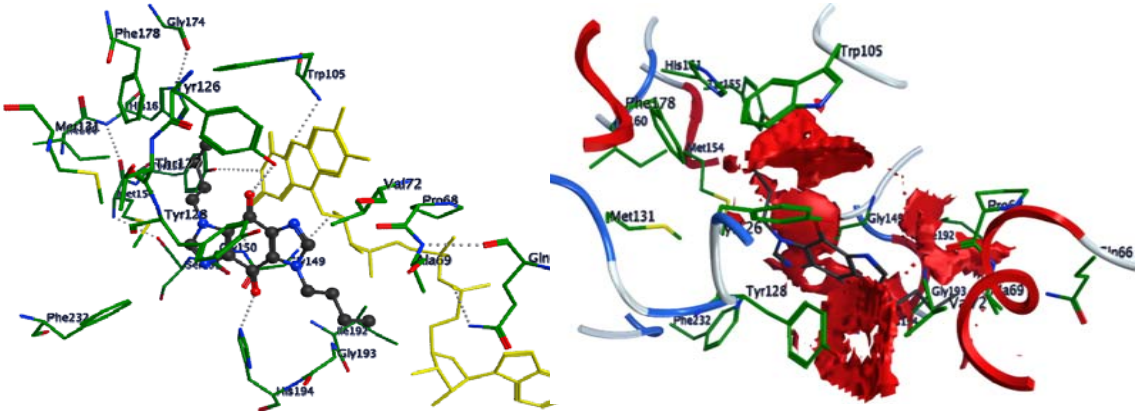

Figure 4.10; (Left) Molecular model of quinone **71** docked into the active site of NQO1. Hydrogen bonds are shown as dashed lines, and the FAD cofactor is shown in yellow; (Right) Hydrophobic contact surface between **71** and NQO1 (Tyr128 and Trp105).

Even though the docking affinity is lower than expected, compound **71** interacts with His194 and Tyr126 through hydrogen bonding. As mentioned, His194 plays a particularly important role in the interaction of substrates with NQO1. Therefore, compound **71** is well positioned for reduction. In addition, the hydrophobic contacts are reasonably favorable, as shown in Figure 4.10 (Right).

Similar analysis of the active site of quinone **125**-NQO1 complex revealed that even though two hydrogen bonds are observed, His194 is not involved in the interactions. The Tyr128 and Tyr126 residues hold quinone **125** in a totally different orientation to that observed for MMC, increasing the $C_{quinone}$-N5 distance to 6.00 Å (Figure 4.11 (Left)). The hydrophobic contacts of quinone **125** within the active site are also diminished (Figure 4.11 (Right)).

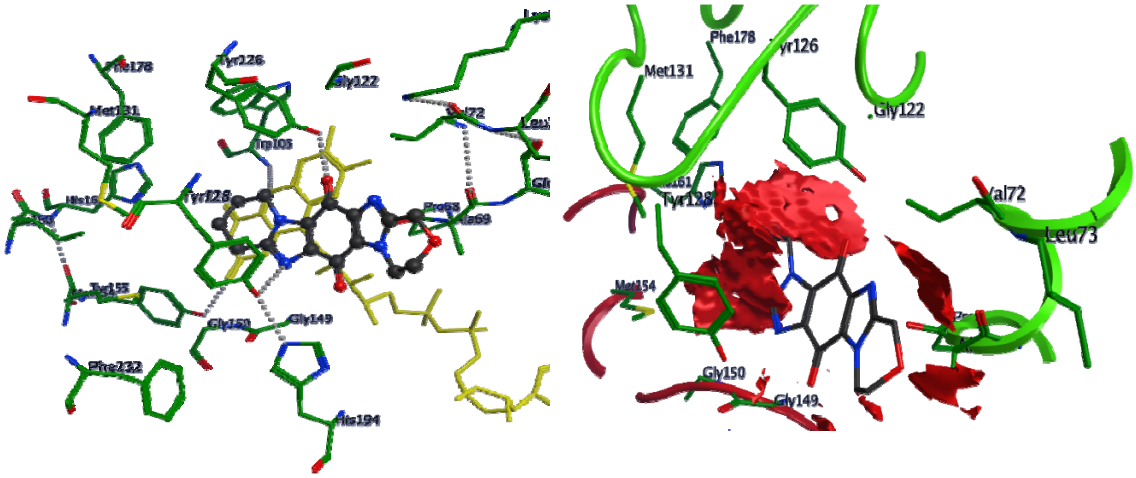

Figure 4.11; (Left) Molecular model of quinone **125** docked into the active site of NQO1. Hydrogen bonds are shown as dashed lines and the FAD cofactor is shown in yellow; (Right) Hydrophobic contact surface between **125** and NQO1 (Tyr126 and Tyr128).

The computational docking results suggest that quinone **125** adopts an unfavorable position within the NQO1 active site, making hydride transfer less favorable than expected. Therefore alternative pathways for cellular response may account for the activity of quinone **125**. These results seem to be substantiated by the cytotoxicity evaluations carried out by the DTP NCI-60 screening program, in which no correlation to NQO1 was observed.

Docking simulations performed on an isolated protein structure cannot fully explain the differences in observed cytotoxicities, since other factors come into play, such as cellular uptake, interactions with other macromolecules and metabolism. However it offers insight into the interactions between the quinones and NQO1, and can assist in the design of more potent and selective compounds.

4.3 Conclusions

MTT cytotoxicity evaluations showed that imidazo[5,4-*f*]benzimidazolequinone **74b** was marginally more toxic and selective towards the cancer cell lines than the isomeric [4,5-*f*] **16** analogue. Computational docking studies showed the novel [5,4-*f*] compound **74b** to be a better NQO1 substrate with a greater binding affinity and a shorter $C_{quinone}$-N5 distance than the isomeric [4,5-*f*] **16**.

Altering the fused alicyclic ring size in the MTT evaluations influenced cytotoxicity in a manner that followed a clear trend. Cytotoxicity increased as the fused ring-size decreased. The DTP NCI-60 evaluations showed the same trend when dipyrido iminoquinone **73b** was compared to the diazepino iminoquinone **73c**.

MTT evaluations also showed a clear trend when comparing fused alicyclic ring compounds to their open chain analogues. The open chain analogue was most cytotoxic, followed by its mono ring-fused analogue which in turn was more potent than the dialicyclic ring-fused compound. However the dialicyclic ring-fused compounds displayed greater selectivity towards the cancer cell lines.

MTT evaluations found that incorporation of an oxygen atom into the fused alicyclic ring increased cytotoxicity across all cell lines. Computational docking of quinone **125** revealed a low binding affinity and large $C_{quinone}$-N5 distance which suggested inefficient reduction. The DTP-NCI-60 screen revealed a correlation to the tumor suppression gene TP53 with no correlation to NQO1, suggesting an alternative mechanism of cytotoxicity.

When comparing the quinone moiety to the iminoquinone moiety, the MTT evaluations found an increased potency along with a high degree of selectivity towards the DU-145 prostate cell line. The DTP NCI-60 evaluations corroborated these findings and a good correlation to NQO1 was observed. Excellent correlations were obtained to other NQO1 substrates which contained the iminoquinone moiety, highlighting its significance with regard to NQO1 selectivity.

The first comprehensive docking study of mitomycin C into NQO1 showed a high binding affinity and short $C_{quinone}$-N5 distance, influenced by hydrogen bonding of the carbamate group with the His194 residue, resulting in efficient hydride transfer. This may partly explain the high potency of MMC towards cancer the cell lines evaluated.

Chapter 5

5 Experimental Section

5.1 General

5.1.1 Materials and methods

All commercially available reagents were used without purification unless otherwise stated. Dimethylformamide (DMF) and toluene were freshly distilled over CaH_2. Thin layer chromatography (TLC) was carried out on aluminium-backed plates coated with silica gel (Merck Kieselgel 60 F_{254}). Flash chromatography and dry column vacuum chromatography[149-150] were carried out using Merck Kieselgel 60H silica gel (particle size 0.040-0.060 mm) and Merck Kieselgel silica gel 60 (particle size 0.015-0.040 mm) respectively, using the specified eluent.

5.1.2 Instrumental

Melting points were measured on a Stuart Scientific melting point apparatus SMP3. Infrared spectra were recorded using a Perkin-Elmer Spec 1 with ATR attached. NMR spectra were recorded using a Joel GXFT 400 MHz instrument equipped with a DEC AXP 300 computer workstation. All chemical shifts are expressed in parts per million (ppm) downfield from trimethylsilane as internal standard except for quinone **124** which is reported relative to DSS (4,4-dimethyl-4-silapentane-1-sulfonic acid sodium salt) as internal standard. NMR assignments of new compounds were supported by DEPT and ^{1}H-^{13}C NMR 2D spectra. High resolution mass spectra for compounds **53a-c**, **54a-c**, **60b**, **60c**, **63b**, **63c**, **73b** & **74b** were carried out at the University College London, Mass Spectroscopy Facility using a Thermo Finnigan MAT900xp operating in chemical ionization (CI) mode with methane as the carrier gas or elctrospray ionization (ESI). Accurate masses were calculated against reference 'heptacosa'. High resolution mass spectra for all other compounds were carried out at NUI Galway using ESI on a Waters LCT Premier XE spectrometer by manual peak matching. The precision of all accurate mass measurements are better than 5 ppm. Elemental analysis was carried out on a Perkin–Elmer 2400 Series II analyzer. HPLC chromatograms were obtained using an Agilent Technologies 1200 series instrument with UV detector at the specified settings. Hydrogenation reactions were carried out using a Parr® 5500 Series Compact reactor.

5.2 Experimental for Chapter 2

Experiment 1: Synthesis of 1*H*,5(7)*H*-imidazo[5,4-*f*(4,5-*f*)]benzimidazole (51)

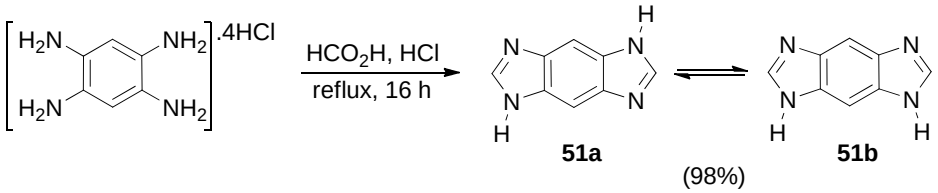

1,2,4,5-Benzenetetraamine tetrahydrochloride (1.00 g, 3.5 mmol), formic acid (90%, 50 mL) and HCl (37%, 10 mL) were heated at reflux for 16 h. The cooled solution was evaporated and Na_2CO_3 (5%, 50 mL) added. The precipitate was collected, washed with water and dried to give ~1:1 mixture of the two tautomers of the *title compound* **51** (0.542 g, 98%); pale brown solid; mp > 350 °C (lit.,[92] > 300 °C); δ_H (400 MHz; DMSO-d_6) 7.49 (1H, bs, 8-H, **51b**), 7.65 (2H, bs, 4,8-H, **51a**), 7.78 (1H, bs, 4-H, **51b**), 8.14 (4H, s, 2,6-H), 12.17 (4H, bs, *N*-H).

5.2.1 General procedure for the synthesis of ω-chloroalkyl phenylselenide

Sodium borohydride (1.110 g, 29.3 mmol) was added to a stirring solution of diphenyl diselenide (3.000 g, 9.6 mmol) in EtOH (600 mL) at room temperature. After the color change of yellow to colorless the temperature was reduced to -10 °C. 1-Chloro-*ω*-iodoalkane (19.7 mmol) was added and the solution stirred for 2 h. The solution was evaporated, HCl (2 M, 50 mL) added and extracted with CH_2Cl_2 (6 x 50 mL). The combined organic extracts were dried ($MgSO_4$) and evaporated to give the *ω*-chloroalkyl phenylselenide as a colorless oil which required no further purification.

Experiment 2: Synthesis of 3-chloropropyl phenylselenide (52a)

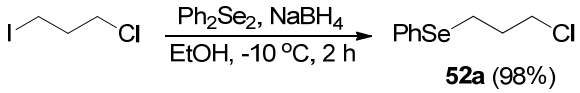

52a (98%)

Following general procedure 5.2.1, sodium borohydride (1.110 g, 29.3 mmol), diphenyl diselenide (3.000 g, 9.6 mmol) and 1-Chloro-3-iodopropane (4.013 g, 19.7 mmol) gave the *title compound* **52a** (4.395 g, 98%); colorless oil; δ_H 2.09-2.16 (2H, m, CH_2), 3.04 (2H, t, *J* 7.1, CH_2SePh), 3.64 (2H, t, *J* 6.3, CH_2Cl), 7.24-7.33 (3H, m, Ph-H), 7.50-7.54 (2H, m, Ph-H); δ_C 24.66 (CH_2SePh), 32.73 (CH_2), 44.46 (CH_2Cl), 127.22 (Ph-CH), 129.30 (Ph-CH), 129.66 (C), 132.93 (Ph-CH).

Experiment 3: Synthesis of 4-chlorobutyl phenylselenide (52b)

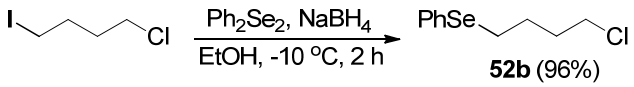

52b (96%)

Following general procedure 5.2.1, sodium borohydride (1.110 g, 29.3 mmol), diphenyl diselenide (3.000 g, 9.6 mmol) and 1-chloro-4-iodobutane (4.289 g, 19.7 mmol) gave the *title compound* **52b** (4.571 g, 96%); colorless oil; δ_H 1.82-1.94 (4H, m, CH_2CH_2), 2.94 (2H, t, *J* 6.8, CH_2SePh), 3.51 (2H, t, *J* 6.2, CH_2Cl), 7.24-7.33 (3H, m, Ph-H), 7.53-7.59 (2H, m, Ph-H); δ_C 27.08 (CH_2), 27.60 (CH_2), 32.73 (CH_2), 44.71 (CH_2Cl), 127.01 (Ph-CH), 129.38 (Ph-CH), 130.65 (C), 132.64 (Ph-CH).

Experiment 4: Synthesis of 5-chloropentyl phenylselenide (52c)

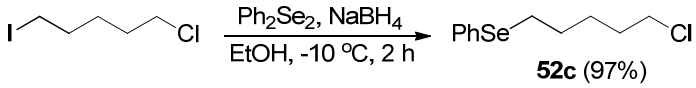

Following general procedure 5.2.1, sodium borohydride (1.110 g, 29.3 mmol), diphenyl diselenide (3.000 g, 9.6 mmol) and 1-chloro-5-iodopentane (4.565 g, 19.7 mmol) gave the *title compound* **52c** (4.879 g, 97%); colorless oil; δ_H 1.51-1.60 (2H, m, CH_2), 1.68-1.81 (4H, m, CH_2CH_2), 2.90 (2H, t, *J* 7.3, CH_2SePh), 3.50 (2H, t, *J* 6.4, CH_2Cl), 7.20-7.29 (3H, m, Ph-H), 7.46-7.51 (2H, m, Ph-H); δ_C 27.15 (CH_2SePh), 27.66 (CH_2), 29.52 (CH_2), 32.14 (CH_2), 44.93 (CH_2Cl), 126.89 (Ph-CH), 129.15 (Ph-CH), 130.41 (C), 132.66 (Ph-CH).

5.2.2 General procedure for the synthesis of 1,5(7)-di(*ω*-(phenylselano)alkyl) imidazo[5,4-*f*(4,5-*f*)]benzimidazoles radical precursors

Imidazo[5,4-*f*(4,5-*f*)]benzimidazole **51** (0.790 g, 5.0 mmol) and sodium hydride (0.252 g, 10.5 mmol) were heated in DMF (50 mL) at 120 °C for 10 min. *ω*-Chloroalkyl phenylselenide (10.5 mmol) was added and the mixture stirred for 1 h. The cooled reaction mixture was evaporated, CH_2Cl_2 added and filtered. The filtrate was evaporated and the residue purified by dry column vacuum chromatography with gradient elution of EtOAc and MeOH to give the separated 1,5-di(*ω*-(phenylselano)alkyl)imidazo[5,4-*f*]benzimidazole **53a-c** and 1,7-di(*ω*-(phenylselano)alkyl)imidazo[4,5-*f*]benzimidazole isomers **54a-c**.

Experiment 5: Synthesis of 1,5-di(3-(phenylselano)propyl)imidazo[5,4-*f*]benzimidazole (53a) and 1,7-di(3-(phenylselano)propyl)imidazo[4,5-*f*]benzimidazole (54a)

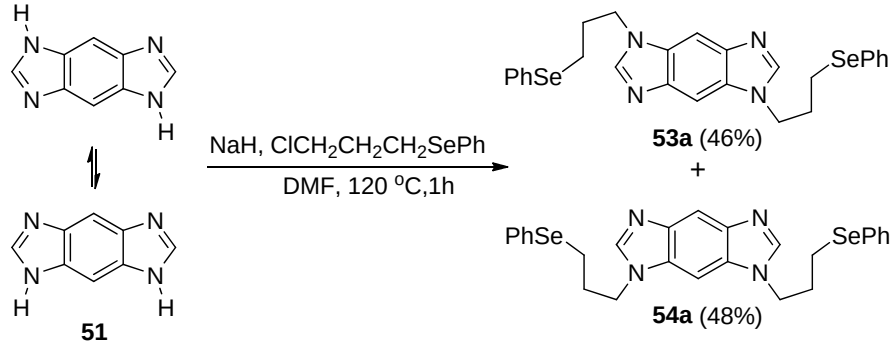

Following general procedure 5.2.2, imidazo[5,4-*f*(4,5-*f*)]benzimidazole **51** (0.790 g, 5.0 mmol), sodium hydride (0.252 g, 10.5 mmol) and 3-chloropropyl phenylselenide **52a** (2.450 g, 10.5 mmol) gave the *title compound* **53a** and **54a**.

1,5-Di(3-(phenylselano)propyl)imidazo[5,4-*f*]benzimidazole (53a): (1.271 g, 46%); white solid; R_f 0.49 (EtOAc-MeOH 9:1); mp 144-146 °C; ν_{max} (neat/ cm^{-1}) 3080, 2928, 1576, 1518, 1495, 1476, 1437, 1381, 1357, 1313, 1218, 1162, 1127, 1070, 1043, 1020; δ_H (400 MHz, $CDCl_3$) 2.17-2.24 (4H, m, CH_2), 2.76 (4H, t, *J* 6.7, CH_2SePh), 4.29 (4H, t, *J* 6.6, NCH_2), 7.18-7.21 (6H, m, Ph-H), 7.41-7.44 (4H, m, Ph-H), 7.68 (2H, s, 4,8-H), 7.85 (2H, s, 2,6-H); δ_C (100 MHz, $CDCl_3$) 24.0 (CH_2SePh), 28.9 (CH_2), 44.0 (NCH_2), 98.9 (4,8-CH), 127.1 (Ph-CH), 128.8 (C), 129.0 (Ph-CH), 131.1 (C), 132.8 (Ph-CH), 141.4 (3a,7a-C), 144.1 (2,6-CH); *m/z* (ESI) 555.0557 ($[M+H]^+$, $C_{26}H_{27}N_4{}^{80}Se^{80}Se$ requires 555.0566).

1,7-Di(3-(phenylselano)propyl)imidazo[4,5-*f*]benzimidazole (54a): (1.326 g, 48%); white solid; R_f 0.39 (EtOAc-MeOH 9:1); mp 89-91 °C; ν_{max} (neat, cm^{-1}) 3359, 3093, 2921, 2851, 1639, 1576, 1524, 1493, 1476, 1435, 1364, 1292, 1232, 1213, 1159, 1113, 1070, 1020, 1000; δ_H (400 MHz, $CDCl_3$) 2.14-2.22 (4H, m, CH_2), 2.77 (4H, t, *J* 6.9, CH_2SePh), 4.25 (4H, t, *J* 6.6, NCH_2), 7.16-7.21 (7H, m, Ph-H & 8-H), 7.38-7.43 (4H, m, Ph-H), 7.81 (2H, s, 2,6-H), 8.17 (1H, s, 4-H); δ_C (100 MHz, $CDCl_3$) 24.3 (CH_2SePh), 29.3 (CH_2), 44.2 (NCH_2), 88.5 (8-CH), 110.5 (4-CH), 127.4

(Ph-CH), 129.1 (C), 129.4 (Ph-CH), 132.0 (C), 133.0 (Ph-CH), 141.2 (3a,4a-C), 143.8 (2,6-CH); *m/z* (ESI) 555.0576 ($[M+H]^+$, $C_{26}H_{27}N_4{}^{80}Se^{80}Se$ requires 555.0566).

Experiment 6: Synthesis of 1,5-di(4-(phenylselano)butyl)imidazo[5,4-*f*]benzimidazole (53b) and 1,7-di(4-(phenylselano)butyl)imidazo[4,5-*f*]benzimidazole (54b)

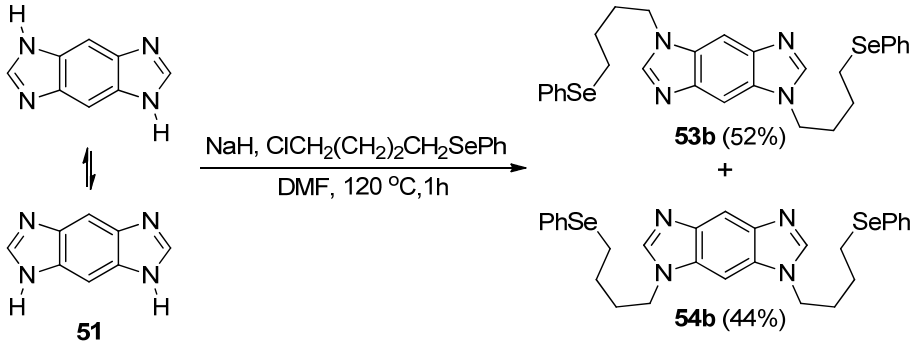

Following general procedure 5.2.2, imidazo[5,4-*f*(4,5-*f*)]benzimidazole **51** (0.790 g, 5.0 mmol), sodium hydride (0.252 g, 10.5 mmol) and 4-chlorobutyl phenylselenide **52b** (2.600 g, 10.5 mmol) gave the *title compound* **53b** and **54b**.

1,5-Di(4-(phenylselano)butyl)imidazo[5,4-*f*]benzimidazole (53b): (1.509 g, 52%); white solid; R_f 0.50 (EtOAc-MeOH 9:1); mp 156-158 °C; ν_{max} (neat, cm^{-1}) 3074, 2930, 1797, 1579, 1521, 1477, 1446, 1356, 1236, 1212, 1124, 1072, 1022; δ_H (400 MHz, $CDCl_3$) 1.67-1.74 (4H, m, CH_2), 2.00-2.01 (4H, m, CH_2), 2.86 (4H, t, *J* 7.2, CH_2SePh), 4.18 (4H, t, *J* 7.1, NCH_2), 7.19-7.24 (6H, m, Ph-H), 7.39-7.43 (4H, m, Ph-H), 7.70 (2H, s, 4,8-H), 7.86 (2H, s, 2,6-H); δ_C (100 MHz, $CDCl_3$) 27.2 (CH_2SePh), 27.3 (CH_2), 29.4 (CH_2), 44.9 (NCH_2), 99.2 (4,8-CH), 127.1 (Ph-CH), 129.2 (Ph-CH), 129.8 (C), 131.5 (C), 133.0 (Ph-CH), 141.7 (3a,7a-C), 144.2 (2,6-CH); *m/z* (CI) 583.0853 ($[M+H]^+$, $C_{28}H_{31}N_4{}^{80}Se{}^{80}Se$ requires 583.0879).

1,7-Di(4-(phenylselano)butyl)imidazo[4,5-*f*]benzimidazole (54b): (1.277 g, 44%); white solid; R_f 0.40 (EtOAc-MeOH 9:1); mp 125-127 °C; ν_{max} (neat, cm^{-1}) 3345, 2922, 1579, 1524, 1500, 1364, 1283, 1212, 1111, 1071, 1022; δ_H (400 MHz, $CDCl_3$) 1.68-1.76 (4H, m, CH_2), 2.01-2.08 (4H, m, CH_2), 2.87 (4H, t, *J* 7.0, CH_2SePh), 4.15 (4H, t, *J* 7.1, NCH_2), 7.14-7.19 (7H, m, Ph-H & 8-H), 7.36-7.39 (4H, m, Ph-H), 7.81 (2H, s, 2,6-H), 8.18 (1H, s, 4-H); δ_C (100 MHz, $CDCl_3$) 27.2 (CH_2SePh), 27.3 (CH_2), 29.2 (CH_2), 44.7 (NCH_2), 88.4 (8-CH), 110.6 (4-CH), 127.2 (Ph-CH), 129.2 (Ph-

CH), 129.7 (C), 132.0 (C), 133.0 (Ph-CH), 141.3 (3a,4a-C), 143.6 (2,6-CH); *m/z* (CI) 583.0857 ($[M+H]^+$, $C_{28}H_{31}N_4{}^{80}Se^{80}Se$ requires 583.0879).

Experiment 7: Synthesis of 1,5-di(5-(phenylselano)pentyl)imidazo[5,4-*f*]benzimidazole (53c) and 1,7-di(5-(phenylselano)pentyl)imidazo[4,5-*f*]benzimidazole (54c)

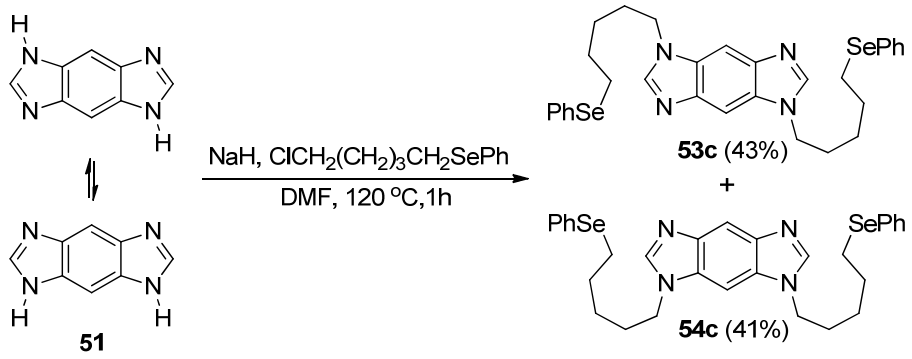

Following general procedure 5.2.2, imidazo[5,4-*f*(4,5-*f*)]benzimidazole **51** (0.790 g, 5.0 mmol), sodium hydride (0.252 g, 10.5 mmol) and 5-chloropentyl phenylselenide **52c** (2.747 g, 10.5 mmol) gave the *title compound* **53c** and **54c**.

1,5-Di(5-(phenylselano)pentyl)imidazo[5,4-*f*]benzimidazole (53c): (1.308 g, 43%); white solid; R_f 0.50 (EtOAc-MeOH 9:1); mp 115-117 °C; ν_{max} (neat, cm^{-1}) 3033, 2934, 2853, 1702, 1574, 1517, 1492, 1475, 1446, 1356, 1331, 1269, 1224, 1203, 1165, 1125, 1072, 1021; δ_H (400 MHz, $CDCl_3$) 1.41-1.49 (4H, m, CH_2), 1.69-1.77 (4H, m, CH_2), 1.89-1.96 (4H, m, CH_2), 2.86 (4H, t, *J* 7.3, CH_2SePh), 4.20 (4H, t, *J* 6.9, NCH_2), 7.22-7.27 (6H, m, Ph-H), 7.44-7.47 (4H, m, Ph-H), 7.71 (2H, s, 4,8-H), 7.91 (2H, s, 2,6-H); δ_C (100 MHz, $CDCl_3$) 26.9 (CH_2), 27.4 (CH_2SePh), 28.9 (CH_2), 29.6 (CH_2), 45.1 (NCH_2), 99.1 (4,8-CH), 126.9 (Ph-CH), 129.0 (Ph-CH), 130.1 (C), 131.4 (C), 132.6 (Ph-CH), 141.6 (3a,7a-C), 144.1 (2,6-CH); *m/z* (CI) 611.1177 ($[M+H]^+$, $C_{30}H_{35}N_4{}^{80}Se^{80}Se$ requires 611.1192).

1,7-Di(5-(phenylselano)pentyl)imidazo[4,5-*f*]benzimidazole (54c): (1.248 g, 41%); white solid; R_f 0.40 (EtOAc-MeOH 9:1); mp 78-81 °C; ν_{max} (neat, cm^{-1}) 3089, 2936, 1577, 1522, 1477, 1446, 1361, 1288, 1261, 1211, 1142, 1107, 1070, 1021; δ_H (400 MHz, $CDCl_3$) 1.43-1.51 (4H, m, CH_2), 1.70-1.77 (4H, m, CH_2), 1.87-1.95 (4H, m, CH_2), 2.86 (4H, t, *J* 7.2, CH_2SePh), 4.17 (4H, t, *J* 7.1, NCH_2), 7.17-7.28 (7H, m, Ph-H & 8-H), 7.42-7.46 (4H, m, Ph-H), 7.88 (2H, s, 2,6-H), 8.20 (1H, s, 4-H); δ_C

(100 MHz, $CDCl_3$) 27.0 (CH_2), 27.5 (CH_2SePh), 29.0 (CH_2), 29.7 (CH_2), 45.1 (NCH_2), 88.5 (8-CH), 110.2 (4-CH), 126.9 (Ph-CH), 129.2 (Ph-CH), 130.2 (C), 132.0 (C), 132.6 (Ph-CH), 140.9 (3a,4a-C), 143.7 (2,6-CH); *m/z* (CI) 611.1185 ($[M+H]^+$, $C_{30}H_{35}N_4{}^{80}Se^{80}Se$ requires 611.1192).

Experiment 8: Synthesis of 1-butyl-5(7)*H*-imidazo[5,4-*f*(4,5-*f*)]benzimidazole (57)

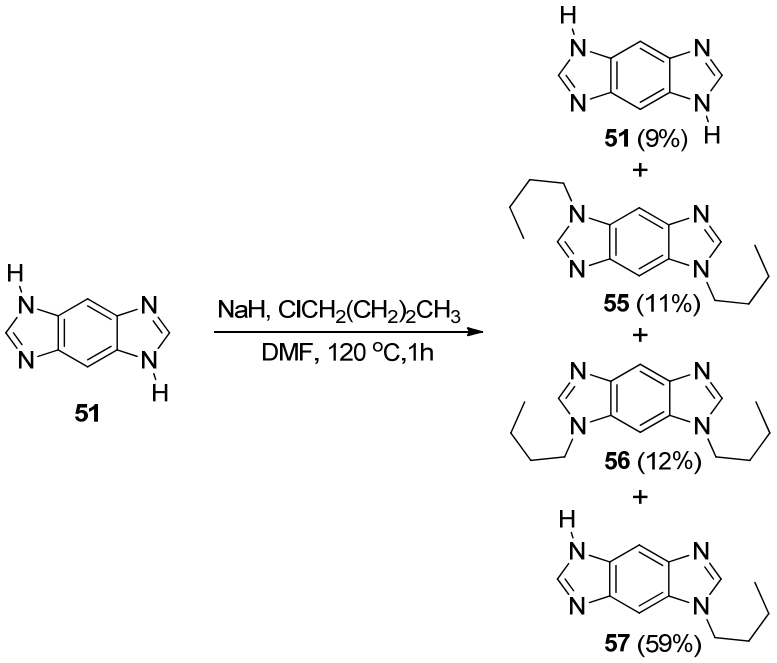

Imidazo[5,4-*f*(4,5-*f*)]benzimidazole **51** (0.500 g, 3.2 mmol) and sodium hydride (84 mg, 3.5 mmol) were heated in DMF (50 mL) at 120 °C for 10 min. 1-Chlorobutane (0.322 g, 3.5 mmol) was added and the mixture stirred for 1 h. The cooled reaction mixture was evaporated, CH_2Cl_2 added and filtered. The solids were washed with water to yield a small amount of the starting material **51** (45 mg, 9%). The filtrate was evaporated and the residue purified by dry column vacuum chromatography with gradient elution of EtOAc and MeOH, yielding the separated 1,5-dibutylimidazo[5,4-*f*]benzimidazole **55**, 1,7-dibutylimidazo[4,5-*f*]benzimidazole **56** and 1-butyl-5(7)*H*-imidazo[5,4-*f*(4,5-*f*)]benzimidazole **57** in an overall yield of 91%.

1,5-Dibutylimidazo[5,4-*f*]benzimidazole (55): (94 mg, 11%); white solid; R_f 0.42 (EtOAc-MeOH 9:1); mp 209-211 °C; ν_{max} (neat, cm^{-1}) 3093, 3032, 2960, 2930, 2875, 1734, 1516, 1491, 1448, 1370, 1354, 1289, 1223, 1198, 1166, 1117; δ_H (400 MHz, $CDCl_3$) 0.94 (6H, t, *J* 7.4, CH_3), 1.32-1.41 (4H, m, CH_2), 1.87-1.94 (4H, m, CH_2), 4.22 (4H, t, *J* 7.1, NCH_2), 7.73 (2H, s, 4,8-H), 7.93 (2H, s, 2,6-H); δ_C (100 MHz, $CDCl_3$) 13.7 (CH_3), 20.1 (CH_2), 31.6 (CH_2), 45.1 (NCH_2), 99.1 (4,8-CH),

131.6 (C), 141.7 (C), 144.3 (2,6-CH); *m/z* (ESI) 271.1937 ($[M+H]^+$, $C_{16}H_{23}N_4$ requires 271.1923).

1,7-Dibutylimidazo[4,5-*f*]benzimidazole (56): (0.103 g, 12%); white solid; R_f 0.26 (EtOAc-MeOH 9:1); mp 86-87 °C; ν_{max} (neat, cm^{-1}) 3405, 3226, 3087, 2957, 2930, 2872, 1637, 1525, 1492, 1464, 1450, 1363, 1277, 1262, 1210, 1202, 1137, 1109, 1093, 1010; δ_H (400 MHz, $CDCl_3$) 0.97 (6H, t, *J* 7.4, CH_3), 1.35-1.44 (4H, m, CH_2), 1.87-1.94 (4H, m, CH_2), 4.21 (4H, t, *J* 7.1, NCH_2), 7.21 (1H, s, 8-H), 7.92 (2H, s, 2,6-H), 8.19 (1H, s, 4-H); δ_C (100 MHz, $CDCl_3$) 13.7 (CH_3), 20.2 (CH_2), 31.5 (CH_2), 45.0 (NCH_2), 88.3 (8-CH), 110.4 (4-CH), 132.1 (C), 141.1 (C), 143.7 (2,6-CH); *m/z* (ESI) 271.1916 ($[M+H]^+$, $C_{16}H_{23}N_4$ requires 271.1923).

1-Butyl-5(7)*H*-imidazo[5,4-*f*(4,5-*f*)]benzimidazole (57): (0.400 g, 59%); white solid; R_f 0.88 (EtOAc-MeOH 4:1); mp >350 °C; ν_{max} (neat, cm^{-1}) 3072, 2935, 1577, 1508, 1476, 1446, 1436, 1371, 1284, 1225, 1210, 1136, 1115, 1059, 1021; δ_H (400 MHz, $CDCl_3$) 0.94 (3H, t, *J* 7.4, CH_3), 1.32-1.42 (2H, m, CH_2), 1.87-1.94 (2H, m, CH_2), 4.21 (2H, t, *J* 7.1, NCH_2), 7.68 (1H, bs, Ar-H), 7.92 (1H, bs, Ar-H), 7.95 (1H, s, Ar-H), 8.15 (1H, s, Ar-H); δ_C (100 MHz, $CDCl_3$) 13.7 (CH_3), 20.2 (CH_2), 31.6 (CH_2), 45.2 (NCH_2), 131.9 (C), 141.7 (C), 141.9 (CH), 144.1 (CH); *m/z* (ESI) 215.1291 ($[M+H]^+$, $C_{12}H_{15}N_4$ requires 215.1297).

Experiment 9: Synthesis of 1-butyl-5-(4-(phenylselano)butyl)imidazo[5,4-*f*]benzimidazole (58) and 1-butyl-7-(4-(phenylselano)butyl)imidazo[4,5-*f*]benzimidazole (59)

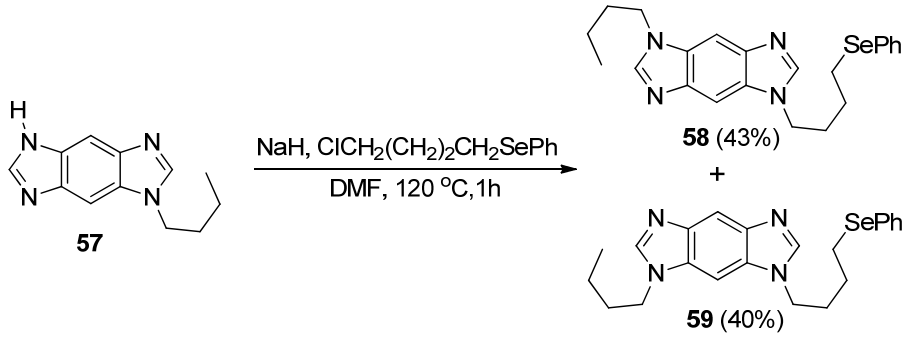

1-Butyl-5(7)*H*-imidazo[5,4-*f*(4,5-*f*)]benzimidazole **57** (0.833 g, 3.9 mmol) and sodium hydride (0.103 g, 4.3 mmol) were heated in DMF (50 mL) at 120 °C for 10 min. 4-Chlorobutyl phenylselenide **52b** (1.065 g, 4.3 mmol) was added and the mixture stirred for 1 h. The cooled reaction mixture was evaporated, CH_2Cl_2 added and filtered. The filtrate was evaporated and the residue purified by dry column vacuum chromatography with gradient elution of EtOAc and MeOH to give the separated 1-butyl-5-(4-(phenylselano)butyl)imidazo[5,4-*f*]benzimidazole **58** and 1-butyl-7-(4-(phenylselano)butyl)imidazo[4,5-*f*]benzimidazole **59**.

1-Butyl-5-(4-(phenylselano)butyl)imidazo[5,4-*f*]benzimidazole (58): (0.705 g, 43%); white solid; R_f 0.32 (EtOAc-MeOH 9:1); mp 287-293 °C; ν_{max} (neat, cm^{-1}) 3244, 2956, 1647, 1525, 1490, 1447, 1359, 1287, 1173, 1115, 1082; δ_H (400 MHz, $CDCl_3$) 0.94 (3H, t, *J* 7.4, CH_3), 1.31-1.41 (2H, m, CH_2), 1.67-1.75 (2H, m, CH_2), 1.86-1.93 (2H, m, CH_2), 2.00-2.08 (2H, m, CH_2), 2.87 (2H, t, *J* 7.1, CH_2SePh), 4.17-4.23 (4H, m, NCH_2), 7.16-7.24 (3H, m, Ph-H), 7.40-7.44 (2H, m, Ph-H), 7.72 (1H, s, 4 or 8-H), 7.74 (1H, s, 4 or 8-H), 7.88 (1H, s, 2 or 6-H), 7.95 (1H, s, 2 or 6-H); δ_C (100 MHz, $CDCl_3$) 13.7 (CH_3), 20.1 (CH_2), 27.2 (CH_2SePh), 27.3, 29.4, 31.5 (all CH_2), 44.8, 45.1 (NCH_2), 99.0, 99.2 (4,8-CH), 127.1 (Ph-CH), 129.2 (Ph-CH), 129.8, 131.4, 131.6 (all C), 132.9 (Ph-CH), 141.6 (C), 141.7 (C), 144.1, 144.3 (2,6-CH); *m/z* (ESI) 427.1399 ($[M+H]^+$, $C_{22}H_{27}N_4{}^{80}Se$ requires 427.1401).

1-Butyl-7-(4-(phenylselano)butyl)imidazo[4,5-*f*]benzimidazole (59): (0.663 g, 40%); white solid; R_f 0.11 (EtOAc-MeOH 9:1); mp 78-80 °C; ν_{max} (neat, cm^{-1}) 3374, 3100, 2956, 2930, 2871, 1718, 1683, 1636, 1577, 1524, 1493, 1477, 1456, 1436, 1362, 1263, 1211, 1144, 1112, 1064, 1021; δ_H (400 MHz, $CDCl_3$) 0.94 (3H, t, *J* 7.4, CH_3), 1.30-1.40 (2H, m, CH_2), 1.66-1.73 (2H, m, CH_2), 1.83-1.90 (2H, m, CH_2), 1.99-2.06 (2H, m, CH_2), 2.87 (2H, t, *J* 7.0, CH_2SePh), 4.10-4.20 (4H, m, NCH_2), 7.15-7.23 (4H, m, Ph-H & 8-H), 7.34-7.39 (2H, m, Ph-H), 7.81 (1H, s, 2 or 6H), 7.89 (1H, s, 2 or 6-H), 8.20 (1H, s, 4-H); δ_C (100 MHz, $CDCl_3$) 13.7 (CH_3), 20.1 (CH_2), 27.1 (CH_2), 27.2 (CH_2SePh), 29.1 (CH_2), 31.4 (CH_2), 44.6, 45.0 (NCH_2), 88.5 (8-CH), 110.2 (4-CH), 127.1 (Ph-CH), 129.2 (Ph-CH), 129.6, 131.8, 132.0 (all C), 132.8 (Ph-CH), 141.11(2 X C), 143.5, 143.7 (2,6-CH); *m/z* (ESI) 427.1386 ($[M+H]^+$, $C_{22}H_{27}N_4{}^{80}Se$ requires 427.1401).

Experiment 10: Synthesis of 1,5-dibutylimidazo[5,4-*f*]benzimidazole (55) and 1,7-dibutylimidazo[4,5-*f*]benzimidazole (56)

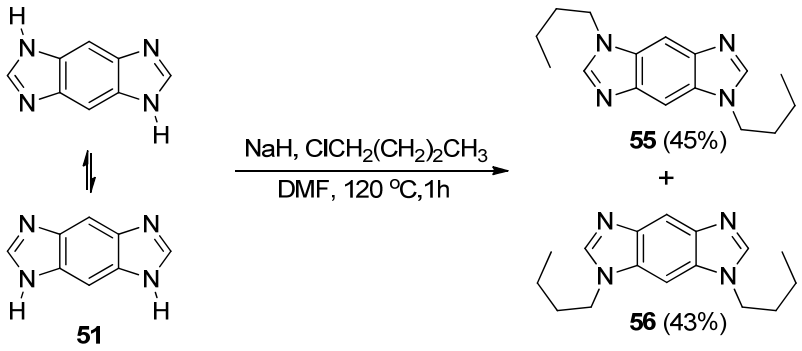

Imidazo[5,4-*f*(4,5-*f*)]benzimidazole **51** (0.751 g, 4.8 mmol) and sodium hydride (0.242 g, 10.1 mmol) were heated in DMF (50 mL) at 120 °C for 10 min. 1-Chlorobutane (0.935 g, 10.5 mmol) was added and the mixture stirred for 1 h. The cooled reaction mixture was evaporated, CH_2Cl_2 added and filtered. The filtrate was evaporated and the residue purified by dry column vacuum chromatography with gradient elution of EtOAc and MeOH giving the separated isomers 1,5-butylimidazo[5,4-*f*]benzimidazole **55** (0.576 g, 45%) and 1,7-butylimidazo[4,5-*f*]benzimidazole **56** (0.552 g, 43%).

(see Experiment 8 for characterization)

5.2.3 One-pot double homolytic aromatic substitution methods

Method 1: Radical cyclizations without activation;

To a solution of 1,5(7)-di(*ω*-(phenylselano)alkyl)imidazo[5,4-*f*(4,5-*f*)]benzimidazole (0.6 mmol) in toluene (50 mL) at reflux, and open to the air (initially flushed with N_2, with drying tube placed on top of condenser), was added a solution of ACCN (0.733 g, 3.0 mmol) and Bu_3SnH (0.873 g, 3.0 mmol) in toluene (50 mL) using a syringe pump at a rate of 2.2 mL/h.

Method 2: Radical cyclizations with activation using camphorsulfonic acid;

To a solution of 1,5(7)-di(*ω*-(phenylselano)alkyl)imidazo[5,4-*f*(4,5-*f*)]benzimidazole (0.6 mmol) and camphorsulfonic acid (CSA) (0.302 g, 1.3 mmol) in toluene (50 mL) at reflux, and open to the air (initially flushed with N_2, with drying tube placed on top of condenser), was added a solution of ACCN (0.733 g, 3.0 mmol) and Bu_3SnH (0.873 g, 3.0 mmol) in toluene (50 mL) using a syringe pump at a rate of 2.2 mL/h.

Method 3: Radical cyclizations with activation using acetic anhydride;

To a solution of 1,5(7)-di(*ω*-(phenylselano)alkyl)imidazo[5,4-*f*(4,5-*f*)]benzimidazole (0.6 mmol) and acetic anhydride (0.123 mL, 1.3 mmol) in toluene (50 mL) at reflux, and open to the air (initially flushed with N_2, with drying tube placed on top of condenser), was added a solution of ACCN (0.733 g, 3.0 mmol) and Bu_3SnH (0.873 g, 3.0 mmol) in toluene (50 mL) using a syringe pump at a rate of 2.2 mL/h.

General work up and purification for methods 1-3:

The cooled reaction mixture was left in sunlight for 3 h and extracted with AcOH (80%, 5 x 20 mL). The combined acid extracts were washed with petroleum ether (3 x 20 mL) and evaporated. Na_2CO_3 (5%, 50 mL) was added to the acid residue and extracted with CH_2Cl_2 (5 x 50 mL). The combined organic extracts were dried (Na_2SO_4), evaporated and the residue purified by dry column vacuum chromatography with gradient elution of EtOAc and MeOH.

One-pot double five-membered radical cyclizations onto imidazo[5,4-*f*]benzimidazole

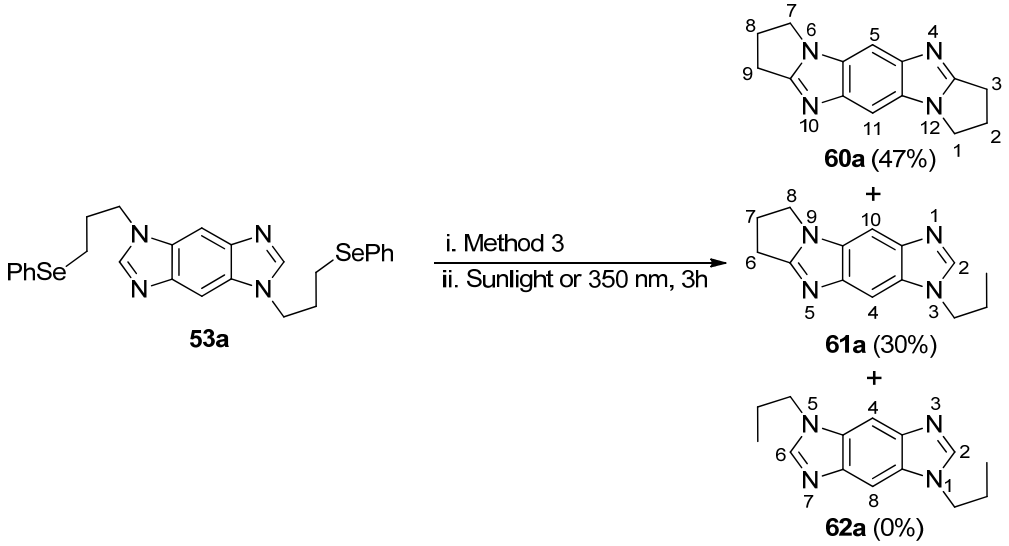

Experiment 11: Following method 1, using **53a** and after purification by chromatography, **60a** (46 mg, 32%), **61a** (45 mg, 31%) and **62a** (14 mg, 10%) were obtained.

Experiment 12: Following method 2, using **53a** an intractable mixture was obtained.

Experiment 13: Following method 3, using **53a** and after purification by chromatography, **60a** (67 mg, 47%) and **61a** (43 mg, 30%) were obtained.

2,3,8,9-Tetrahydro-1*H*,7*H*-pyrrolo[1,2-*a*]pyrrolo[1′,2′:1,2]imidazo[5,4-*f*]benzimidazole (60a): white solid; R_f 0.24 (CH_2Cl_2-Et_2O-MeOH 7:2:1); mp 295-305 °C decomp; ν_{max} (neat, cm^{-1}) 3009, 2942, 2895, 1546, 1489, 1434, 1411, 1347, 1324, 1267, 1161, 1100; δ_H (400 MHz, $CDCl_3$) 2.77-2.84 (4H, m, 2,8-CH_2), 3.19 (4H, t, *J* 7.6, 3,9-CH_2), 4.22 (4H, t, *J* 7.1, 1,7-CH_2), 7.59 (2H, s, 5,11-H); δ_C (100 MHz, $CDCl_3$) 23.9 (3,9-CH_2), 26.0 (2,8-CH_2), 43.0 (1,7-CH_2), 98.5 (5,11-CH), 129.6 (5a,11a-C), 145.5 (4a,10a-C), 161.7 (3a,9a-C); *m/z* (ESI) 239.1307 ($[M+H]^+$, $C_{14}H_{15}N_4$ requires 239.1297).

3-Propyl-7,8-dihydro-6*H*-imidazo[5,4-*f*]pyrrolo[1,2-*a*]benzimidazole (61a): white solid; R_f 0.32 (CH_2Cl_2-Et_2O-MeOH 7:2:1); mp 210-213 °C; ν_{max} (neat, cm^{-1}) 3019, 2935, 1538, 1493, 1444, 1418, 1357, 1291, 1222, 1189, 1163, 1110, 1056; δ_H (400 MHz, $CDCl_3$) 0.97 (3H, *t*, J 7.3, CH_3), 1.92-2.01 (2H, m, CH_2CH_3), 2.71-2.79 (2H, m, 7-CH_2), 3.11 (2H, t, *J* 7.6, 6-CH_2), 4.15-4.21 (4H, m, NCH_2), 7.63 (2H, s, 4,10-H), 7.92 (1H, s, 2-H); δ_C (100 MHz, $CDCl_3$) 11.4 (CH_3), 22.8 (CH_2), 23.8 (6-CH_2), 25.9 (CH_2), 42.9, 46.9 (NCH_2), 98.4 (CH), 98.9 (CH), 130.0 (C), 131.0 (C), 140.6 (C), 143.5 (2-CH), 146.6 (C), 162.4 (5a-C); *m/z* (ESI) 241.1452 ($[M+H]^+$, $C_{14}H_{17}N_4$ requires 241.1453).

1,5-Dipropylimidazo[5,4-*f*]benzimidazole (62a): white solid; R_f 0.39 (CH_2Cl_2-Et_2O-MeOH 7:2:1); mp 205-208 °C; ν_{max} (neat, cm^{-1}) 3091, 3025, 2960, 2930, 2874, 1741, 1518, 1491, 1450, 1382, 1361, 1312, 1227, 1208, 1167, 1113, 1084; δ_H (400 MHz, $CDCl_3$) 0.94 (6H, t, *J* 7.3, CH_3), 1.90-1.99 (4H, m, CH_2), 4.18 (4H, t, *J* 7.1, NCH_2), 7.72 (2H, s, 4,8-H); 7.93 (2H, s, 2,6-H); δ_C (100 MHz, $CDCl_3$) 11.3 (CH_3), 22.7 (CH_2), 46.9 (NCH_2), 99.0 (4,8-CH), 131.4 (4a,8a-C), 141.6 (3a,7a-C), 144.2 (2,6-CH); *m/z* (ESI) 243.1618 ($[M+H]^+$, $C_{14}H_{19}N_4$ requires 243.1610).

One-pot double six-membered radical cyclizations onto imidazo[5,4-*f*]benzimidazole

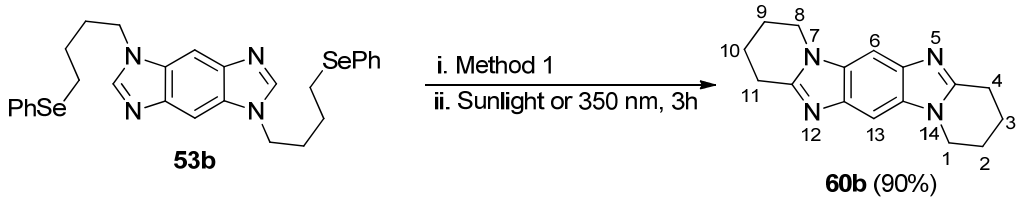

Experiment 14: Following method 1, using **53b** and after purification by chromatography, **60b** (0.144 g, 90%) was obtained.

1,2,3,4,8,9,10,11-Octahydropyrido[1,2-*a*]pyrido[1′,2′:1,2]imidazo[5,4-*f*]benzimidazole (60b): white solid; R_f 0.23 (CH_2Cl_2-Et_2O-MeOH 7:2:1); mp 285-295 °C decomp (lit.[104] > 300 °C); ν_{max} (neat, cm^{-1}) 2942, 1534, 1488, 1445, 1417, 1362, 1316, 1279, 1259, 1190, 1165, 1130, 1092; δ_H (400 MHz, $CDCl_3$) 2.02-2.08 (4H, m, CH_2), 2.15-2.21 (4H, m, CH_2), 3.16 (4H, t, *J* 6.4, 4,11-CH_2), 4.14 (4H, t, *J* 6.1, 1,8-CH_2), 7.55 (2H, s, 6,13-H); δ_C (100 MHz, $CDCl_3$) 20.5 (CH_2), 22.6 (CH_2), 25.4 (4,11-CH_2), 42.8 (1,8-CH_2), 96.9 (6,13-CH), 132.1 (6a,13a-C), 138.1 (5a,12a-C), 152.4 (4a,11a-C); *m/z* (CI) 267.1605 ($[M+H]^+$, $C_{16}H_{19}N_4$ requires 267.1610).

One-pot double seven-membered radical cyclizations onto imidazo[5,4-*f*]benzimidazole

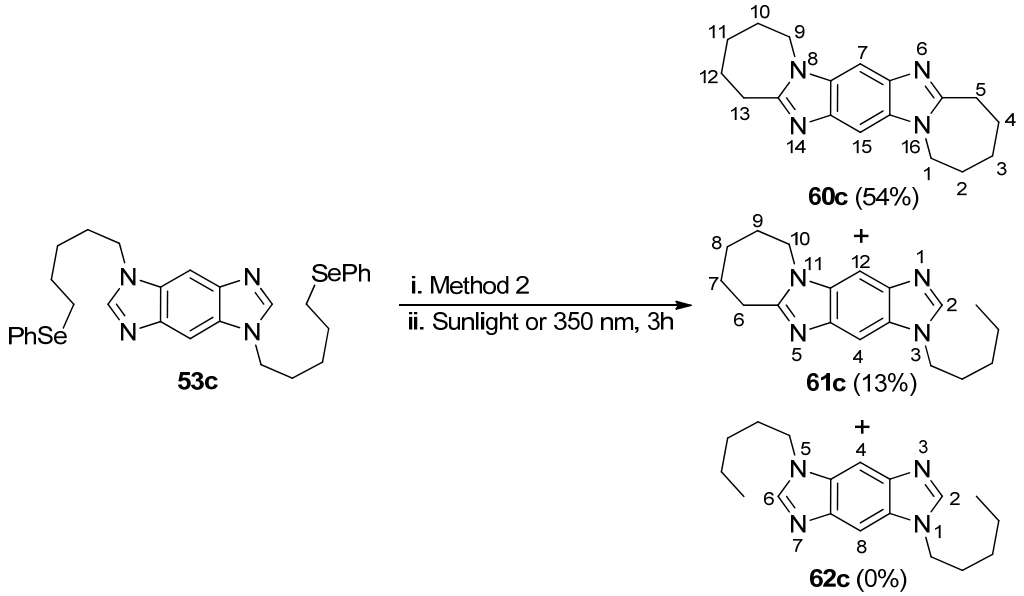

Experiment 15: Following method 1, using **53c** and after purification by chromatography, **60c** (51 mg, 29%), **61c** (57 mg, 32%) and **62c** (15 mg, 8%) were obtained.

Experiment 16: Following method 2, using **53c** and after purification by chromatography, **60c** (95 mg, 54%) and **61c** (23 mg, 13%) were obtained.

Experiment 17: Following method 3, using **53c** and after purification by chromatography, **60c** (60 mg, 34%) and **61c** (55 mg, 31%) were obtained.

2,3,4,5,10,11,12,13-Octahydro-1*H*,9*H*-azepino[1,2-*a*]azepino[1′,2′:1,2]imidazo[5,4-*f*]benzimidazole (60c): white solid; R_f 0.38 (CH_2Cl_2-Et_2O-MeOH 7:2:1); mp 275-285 °C decomp; ν_{max} (neat, cm^{-1}) 2931, 2850, 1534, 1478, 1440, 1414, 1365, 1311, 1256, 1178, 1157, 1116, 1085; δ_H (400 MHz, $CDCl_3$) 1.78-1.91 (8H, m, CH_2), 1.92-1.98 (4H, m, CH_2), 3.11 (4H, t, *J* 5.6, 5,13-CH_2), 4.19 (4H, t, *J* 5.0, 1,9-CH_2), 7.46 (2H, s, 7,15-H); δ_C (100 MHz, $CDCl_3$) 25.7 (CH_2), 28.8 (CH_2), 30.5 (5,13-CH_2), 31.0 (CH_2), 44.7 (1,9-CH_2), 97.1 (7,15-CH),

133.2 (7a,15a-C), 139.5 (6a,14a-C), 158.2 (5a,13a-C); *m/z* (CI) 295.1916 ($[M+H]^+$, $C_{18}H_{23}N_4$ requires 295.1923).

3-Pentyl-7,8,9,10-tetrahydro-6*H*-azepino[1,2-*a*]imidazo[5,4-*f*]benzimidazole (61c): white solid; R_f 0.43 (CH_2Cl_2-Et_2O-MeOH 7:2:1); mp 198-200 °C; ν_{max} (neat, cm^{-1}) 2924, 2855, 1528, 1476, 1447, 1358, 1313, 1260, 1205, 1188, 1118; δ_H (400 MHz, $CDCl_3$) 0.87 (3H, t, *J* 6.9, CH_3), 1.29-1.37 (4H, m, CH_2), 1.80-2.00 (8H, m, CH_2), 3.13 (2H, t, *J* 5.7, 6-CH_2), 4.19-4.23 (4H, m, NCH_2), 7.61 (2H, s, 4,12-H), 7.91 (1H, s, 2-H); δ_C (100 MHz, $CDCl_3$) 14.0 (CH_3), 22.3, 25.7, 28.8, 29.0, 29.2 (all CH_2), 30.5 (6-CH_2), 31.0 (CH_2), 44.7, 45.4 (NCH_2), 98.0 (CH), 98.2 (CH), 131.1, 133.7, 140.3, 141.0 (all C), 143.6 (2-CH), 158.9 (5a-C); *m/z* (ESI) 297.2091 ($M+H^+$, $C_{18}H_{25}N_4$ requires 297.2079).

1,5-Dipentylimidazo[5,4-*f*]benzimidazole (62c): white solid, R_f 0.49 (CH_2Cl_2-Et_2O-MeOH 7:2:1); mp 161-162 °C; ν_{max} (neat, cm^{-1}) 2923, 2855, 1715, 1517, 1494, 1452, 1375, 1357, 1318, 1222, 1194, 1164, 1118, 1061, 1029; δ_H (400 MHz, $CDCl_3$) 0.77 (6H, t, *J* 6.9, CH_3), 1.17-1.28 (8H, m, CH_2), 1.77-1.85 (4H, m, CH_2), 4.10 (4H, t, *J* 7.1, NCH_2), 7.64 (2H, s, 4,8-H), 7.85 (2H, s, 2,6-H); δ_C (100 MHz, $CDCl_3$) 13.9 (CH_3), 22.2, 29.0, 29.1 (all CH_2), 45.3 (NCH_2), 99.0 (4,8-CH), 131.5 (4a,8a-C), 141.6 (3a,7a-C), 144.2 (2,6-CH); *m/z* (ESI) 299.2238 ($[M+H]^+$, $C_{18}H_{27}N_4$ requires 299.2236).

One-pot double five-membered radical cyclizations onto imidazo[4,5-*f*]benzimidazole

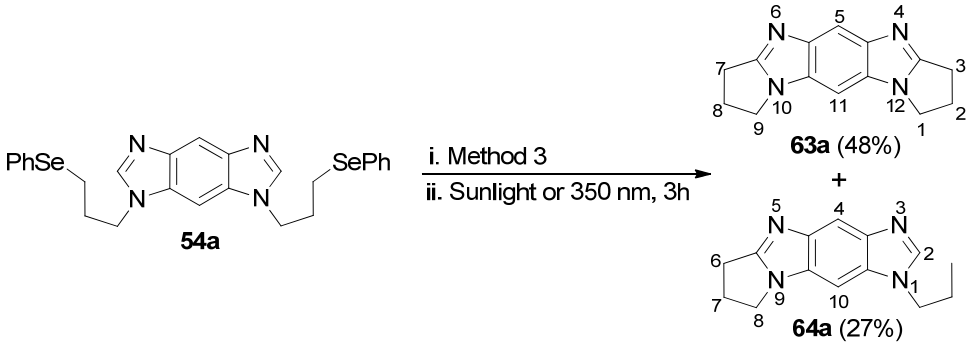

Experiment 18: Following method 3, using **54a** and after purification by chromatography, **63a** (69 mg, 48%) and **64a** (40 mg, 27%) were obtained.

2,3,8,9-Tetrahydro-1*H*,7*H*-pyrrolo[1,2-*a*]pyrrolo[1′,2′:1,2]imidazo[4,5-*f*]benzimidazole (63a): white solid; R_f 0.22 (CH_2Cl_2-Et_2O-MeOH 7:2:1); mp 266-268 °C decomp (lit.[34] 240 °C decomp); ν_{max} (neat, cm^{-1}) 3229, 2956, 1644, 1543, 1490, 1431, 1352, 1300, 1228, 1117; δ_H (400 MHz, $CDCl_3$) 2.64-2.71 (4H, m, 2,8-CH_2), 3.02 (4H, t, *J* 7.7, 3,7-CH_2), 4.06 (4H, t, *J* 7.1, 1,9-CH_2), 7.04 (1H, s, 11-H), 7.95 (1H, s, 5-H); δ_C (100 MHz, $CDCl_3$) 23.8 (3,7-CH_2), 26.1 (2,8-CH_2), 42.8 (1,9-CH_2), 88.7 (11-CH), 108.9 (5-CH), 129.5 (10a,11a-C), 145.6 (4a,5a-C), 161.2 (3a,6a-C); *m/z* (ESI) 239.1300 ($[M+H]^+$, $C_{14}H_{15}N_4$ requires 239.1297).

1-Propyl-7,8-dihydro-6*H*-imidazo[4,5-*f*]pyrrolo[1,2-*a*]benzimidazole (64a): (40 mg, 27%) white solid; R_f 0.30 (CH_2Cl_2-Et_2O-MeOH 7:2:1); mp 168-171 °C; ν_{max} (neat, cm^{-1}) 3351, 3079, 2927, 1641, 1544, 1513, 1492, 1453, 1423, 1356, 1322, 1298, 1253, 1215, 1115; δ_H (400 MHz, $CDCl_3$) 0.98 (3H, t, *J* 7.6, CH_3), 1.91-2.00 (2H, m, C$H_2$$CH_3$), 2.70-2.78 (2H, m, 7-$CH_2$), 3.09 (2H, t, *J* 7.8, 6-CH_2), 4.12-4.17 (4H, m, NCH_2), 7.16 (1H, s, 10-H), 7.89 (1H, s, 4-H), 8.08 (1H, s, 2-H); δ_C (100 MHz, $CDCl_3$) 11.5 (CH_3), 22.9 (CH_2), 23.8 (6-CH_2), 26.1 (CH_2), 42.9 (NCH_2), 47.0 (NCH_2), 88.5 (10-CH), 109.7 (4-CH), 130.6, 131.1, 140.7 (all C), 143.2 (2-CH), 146.2 (C), 161.9 (5a-C); *m/z* (ESI) 241.1457 ($[M+H]^+$, $C_{14}H_{17}N_4$ requires 241.1453).

One-pot double six-membered radical cyclizations onto imidazo[4,5-*f*]benzimidazole

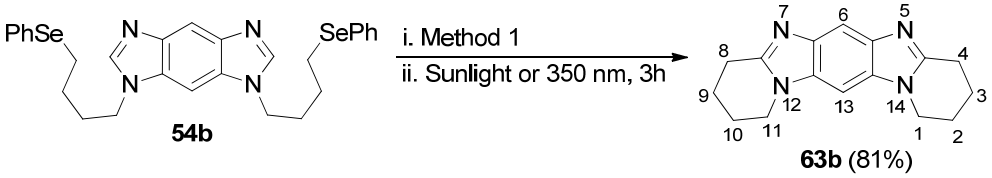

Experiment 19: Following method 1, using **54b** and after purification by chromatography, **63b** (0.129 g, 81%) was obtained.

1,2,3,4,8,9,10,11-Octahydropyrido[1,2-*a*]pyrido[1′,2′:1,2]imidazo[4,5-*f*]benzimidazole (63b): white solid; R_f 0.20 (CH_2Cl_2-Et_2O-MeOH 7:2:1); mp 266-270 °C decomp (lit.[35] 104-108 °C); ν_{max} (neat, cm^{-1}) 3372, 2950, 2891, 1659, 1635, 1526, 1487, 1438, 1417, 1365, 1313, 1255, 1238, 1151, 1134; δ_H (400 MHz, $CDCl_3$) 1.99-2.05 (4H, m, CH_2), 2.12-2.18 (4H, m, CH_2), 3.09 (4H, t, *J* 6.3, 4,8-CH_2), 4.07 (4H, t, *J* 6.0, 1,11-CH_2), 7.02 (1H, s, 13-H), 7.95 (1H, s, 6-H); δ_C (100 MHz, $CDCl_3$) 20.9 (CH_2), 22.9 (CH_2), 25.8 (4,8-CH_2), 42.6 (1,11-CH_2), 87.1 (13-CH), 107.4 (6-CH), 132.0 (12a,13a-C), 139.9 (5a,6a-C), 151.8 (4a,7a-C); *m/z* (CI) 267.1595 ($[M+H]^+$, $C_{16}H_{19}N_4$ requires 267.1610).

One-pot double seven-membered radical cyclizations onto imidazo[4,5-*f*]benzimidazole

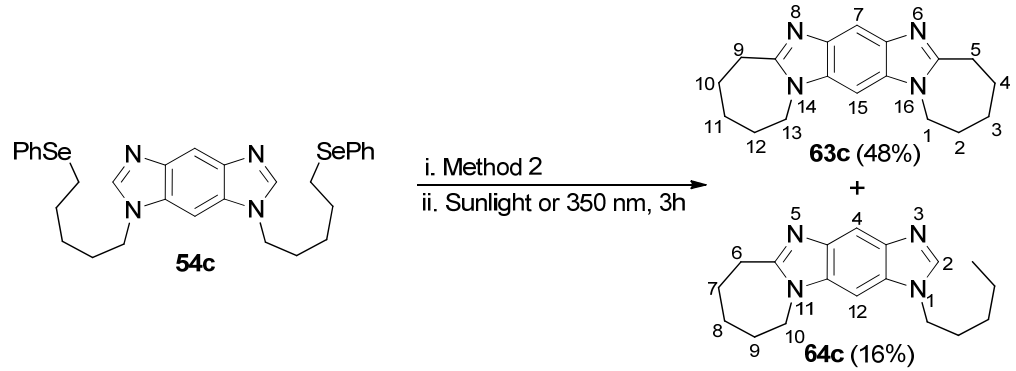

Experiment 20: Following method 2, using **54c** and after purification by chromatography only **63c** (85 mg, 48%) and **64c** (29 mg, 16%) were obtained.

2,3,4,5,10,11,12,13-Octahydro-1*H*,9*H*-azepino[1,2-*a*]azepino[1′,2′:1,2]imidazo[4,5-*f*]benzimidazole (63c): white solid; R_f 0.32 (CH_2Cl_2-Et_2O-MeOH 7:2:1); mp 214-217 °C decomp; ν_{max} (neat, cm^{-1}) 3377, 2928, 2852, 1638, 1527, 1470, 1447, 1422, 1367, 1345, 1323, 1230, 1200, 1140; δ_H (400 MHz, $CDCl_3$) 1.79-1.97 (12H, m, CH_2), 3.11 (4H, t, *J* 5.6, 5,9-CH_2), 4.18 (4H, t, *J* 5.1, 1,13-CH_2), 7.00 (1H, s, 15-H), 7.95 (1H, s, 7-H); δ_C (100 MHz, $CDCl_3$) 25.7 (CH_2), 28.9 (CH_2), 30.4 (5,9-CH_2), 31.0 (CH_2), 44.7 (1,13-CH_2), 87.0 (15-CH), 108.0 (7-CH), 133.3 (14a,15a-C), 139.1 (6a,7a-C), 157.6 (5a,8a-C); *m/z* (ESI) 295.1911 ($[M+H]^+$, $C_{18}H_{23}N_4$ requires 295.1923).

1-Pentyl-7,8,9,10-tetrahydro-6*H*-azepino[1,2-*a*]imidazo[4,5-*f*]benzimidazole (64c): colorless oil; R_f 0.41 (CH_2Cl_2-Et_2O-MeOH 7:2:1); ν_{max} (neat, cm^{-1}) 2926, 2855, 1638, 1535, 1510, 1489, 1448, 1365, 1286, 1254, 1220, 1193, 1126; δ_H (400 MHz, $CDCl_3$) 0.89 (3H, t, *J* 6.9, CH_3), 1.31-1.39 (4H, m, CH_2), 1.82-1.96 (8H, m, CH_2), 3.11 (2H, t, *J* 5.6, 6-CH_2), 4.16-4.21 (4H, m, NCH_2), 7.10 (1H, s, 12-H), 7.88 (1H, s, 4-H), 8.07 (1H, s, 2-H); δ_C (100 MHz, $CDCl_3$) 14.0 (CH_3), 22.3, 25.7, 28.9, 29.1, 29.2 (all CH_2), 30.5 (6-CH_2), 31.0 (CH_2), 44.8, 45.3 (NCH_2), 87.6 (12-CH), 109.2 (4-CH), 131.3, 134.1, 139.7, 140.7 (all C), 143.2 (2-CH), 158.2 (5a-C); *m/z* (ESI) 297.2089 ($[M+H]^+$, $C1_8H_{25}N_4$ requires 297.2079).

Experiment 21: Synthesis of 1-(but-3-en-1-yl)-5-butylimidazo[5,4-*f*]benzimidazole (66)

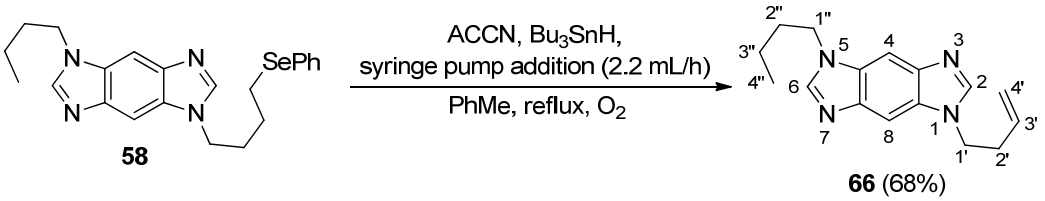

To a solution of 1-butyl-5-(4-(phenylselano)butyl)imidazo[5,4-*f*]benzimidazole **58** (0.300g, 0.7 mmol) in toluene (50 mL) at reflux, and open to the air (no initial N_2 flush, no drying tube), was added a solution of ACCN (0.440 g, 1.8 mmol) and Bu_3SnH (0.524 g, 1.8 mmol) in toluene (50 mL) using a syringe pump at a rate of 2.2 mL/h. The cooled reaction mixture was extracted with AcOH (80%, 5 x 20 mL), the combined extracts washed with petroleum ether (3 x 20 mL), and evaporated. Na_2CO_3 solution (5%, 50 mL) was added to the acidic residue, and extracted with CH_2Cl_2 (5 x 50 mL). The combined organic extracts were dried (Na_2SO_4), evaporated and the residue purified by dry column vacuum chromatography with a gradient elution of EtOAc and MeOH to give the *title compound* **66** (0.129 g, 68%); white solid; R_f 0.41 (EtOAc-MeOH 9:1); δ_H (400 MHz, $CDCl_3$) 0.97 (3H, t, *J* 7.4, CH_3), 1.35-1.44 (2H, m, CH_2), 1.89-1.97 (2H, m, CH_2), 2.65-2.71 (2H, m, CH_2), 4.25 (2H, t, *J* 7.1, NCH_2), 4.31 (2H, t, *J* 7.0, NCH_2), 5.01-5.11 (2H, m, 4′-CH), 5.74-5.85 (1H, tdd, *J* 6.9, 10.2, 17.0, 3′-CH), 7.76 (2H, s, 4, 8-H), 7.95 (1H, s, 2 or 6-H), 7.97 (1H, s, 2 or 6-H). (Not characterized further)

Experiment 22: Synthesis of 3-butyl-6,7,8,9-tetrahydroimidazo[5,4-*f*]pyrido[1,2-*a*]benzimidazole (61b)

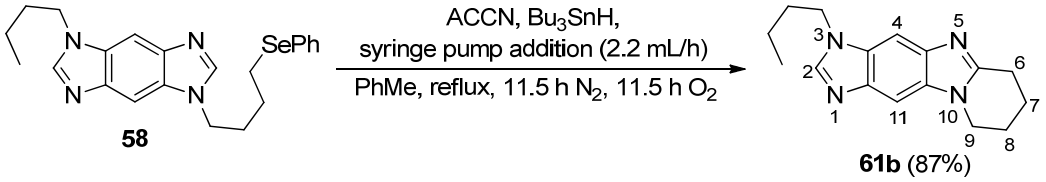

To a solution of 1-butyl-5-(4-(phenylselano)butyl)imidazo[5,4-*f*]benzimidazole **58** (0.600g, 1.4 mmol) in toluene (50 mL) at reflux under N_2, was added a solution of ACCN (0.855 g, 3.5 mmol) and Bu_3SnH (1.019 g, 3.5 mmol) in toluene (50 mL) using a syringe pump at a rate of 2.2 mL/h. After ~11.5 h the reaction was allowed to proceed in the open air. The cooled reaction mixture was extracted with AcOH (80%, 5 x 20 mL), the combined extracts washed with petroleum ether (3 x 20 mL), and evaporated. Na_2CO_3 solution (5%, 50 mL) was added to the acidic residue, and extracted with CH_2Cl_2 (5 x 50 mL). The combined organic extracts were dried (Na_2SO_4), evaporated and the residue purified by dry column vacuum chromatography with a gradient elution of EtOAc and MeOH to give the *title compound* **61b** (0.329 g, 87%); white solid; R_f 0.33 (EtOAc-MeOH 9:1); mp 238-240 °C; ν_{max} (neat, cm^{-1}) 2924, 2856, 1529, 1477, 1447, 1358, 1314, 1259, 1189, 1119, 1084; δ_H (400 MHz, $CDCl_3$) 0.92 (3H, t, *J* 7.4, CH_3), 1.28-1.38 (2H, m, CH_2), 1.84-1.91 (2H, m, CH_2), 1.99-2.05 (2H, m, CH_2), 2.12-2.18 (2H, m, CH_2), 3.10 (2H, t, *J* 6.4, 6-CH_2), 4.11 (2H, t, *J* 6.1, NCH_2), 4.20 (2H, t, *J* 7.1, NCH_2), 7.58 (1H, s, 4 or 11-H), 7.60 (1H, s, 4 or 11-H), 7.89 (1H, s, 2-H); δ_C (100 MHz, $CDCl_3$) 13.7 (CH_3), 20.1 (CH_2), 20.9 (CH_2), 22.8 (CH_2), 25.8 (6-CH_2), 31.6 (CH_2), 42.6, 45.1 (NCH_2), 97.7, 98.3 (4,11-CH), 131.5, 132.5 , 140.6 , 140.8 (all C), 143.5 (2-CH), 153.1 (5a-CH); *m/z* (ESI) 269.1759 ($[M+H]^+$, $C_{16}H_{21}N_4$ requires 269.1766).

5.2.4 General procedure for the nitration of imidazo[5,4-*f*(4,5-*f*)]benzimidazoles

Imidazo[5,4-*f*(4,5-*f*)]benzimidazoles (1.0 mmol) were heated in concentrated H_2SO_4 (10 mL) and HNO_3 (10 mL) at 80 °C for 3 h. The cooled mixture was diluted with water (100 mL), neutralized with solid Na_2CO_3, and extracted with CH_2Cl_2 (5 x 50 mL). The combined organic extracts were dried (Na_2SO_4), evaporated and the residue purified by dry column vacuum chromatography with gradient elution of EtOAc (or CH_2Cl_2) and MeOH.

Experiment 23: Synthesis of 1,5-dibutyl-4-nitro-imidazo[5,4-*f*]benzimidazole (67)

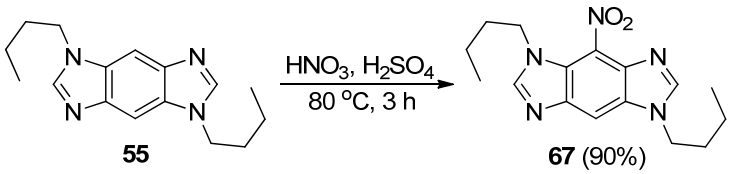

Following general procedure 5.2.4, 1,5-dibutylimidazo[5,4-*f*]benzimidazole **55** (0.200 g, 0.7 mmol) gave the *title compound* **67** (0.210 g, 90 %); yellow solid; R_f 0.44 (EtOAc-MeOH 9:1); mp 155-156 °C; ν_{max} (neat, cm^{-1}) 3109, 2949, 2929, 2870, 1763, 1526 (NO_2), 1512, 1498, 1485, 1464, 1436, 1369 (NO_2), 1349, 1333, 1317, 1280, 1230, 1200, 1191, 1125, 1087; δ_H (400 MHz, $CDCl_3$) 0.86 (3H, t, *J* 7.4, CH_3), 0.93 (3H, t, *J* 7.4, CH_3), 1.15-1.25 (2H, m, CH_2), 1.30-1.39 (2H, m, CH_2), 1.58-1.66 (2H, m, CH_2), 1.85-1.92 (2H, m, CH_2), 4.26 (2H, t, *J* 7.1, NCH_2), 4.32 (2H, t, *J* 7.2, NCH_2), 7.97 (1H, s, 2 or 6-H), 7.99 (1H, s, 8-H), 8.07 (1H, s, 2 or 6-H); δ_C (100 MHz, $CDCl_3$) 13.56 (CH_3), 13.58 (CH_3), 19.8, 20.1, 31.7, 32.3 (all CH_2), 45.5, 47.8 (NCH_2), 105.7 (8-CH), 123.4, 125.9, 131.7, 135.9, 143.7 (all C), 146.4, 147.5 (2,6-CH); *m/z* (ESI) 316.1769 ($[M+H]^+$, $C_{16}H_{22}N_5O_2$ requires 316.1774).

Experiment 24: Synthesis of 5-nitro-2,3,8,9-tetrahydro-1*H*,7*H*-pyrrolo[1,2-*a*]pyrrolo[1′,2′:1,2]imidazo[5,4-*f*]benzimidazole (68a)

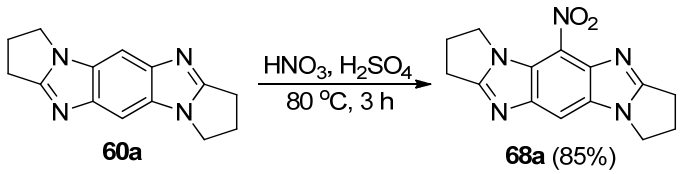

Following general procedure 5.2.4, 2,3,8,9-tetrahydro-1*H*,7*H*-pyrrolo[1,2-*a*]pyrrolo[1′,2′:1,2]imidazo[5,4-*f*]benzimidazole **60a** (0.150 g, 0.6 mmol) gave the *title compound* **68a** (0.152 g, 85%); yellow solid; R_f 0.52 (CH_2Cl_2-MeOH 9:1); mp 245-247 °C; ν_{max} (neat, cm^{-1}) 3225, 1647, 1566, 1522 (NO_2), 1484, 1452, 1409, 1346 (NO_2), 1298, 1271, 1211, 1187, 1117, 1055; δ_H (400 MHz, $CDCl_3$) 2.67-2.74 (2H, m, 2 or 8-CH_2), 2.77-2.85 (2H, m, 2 or 8-CH_2), 3.11 (2H, t, *J* 7.8, 3 or 9-CH_2), 3.21 (2H, t, *J* 7.7, 3 or 9-CH_2), 4.23 (2H, t, *J* 7.1, 1 or 7-CH_2), 4.54 (2H, t, *J* 7.2, 1 or 7-CH_2), 7.72 (1H, s, 11-H); δ_C (100 MHz, $CDCl_3$) 23.7, 24.4 (3,9-CH_2), 25.8, 26.1 (2,8-CH_2), 43.6, 48.0 (1,7-CH_2), 106.5 (11-CH), 123.7, 124.8, 129.9, 140.2, 146.5 (all C), 164.1, 165.2 (3a,9a-C); *m/z* (ESI) 284.115 ($[M+H]^+$, $C_{14}H_{14}N_5O_2$ requires 284.1147).

Experiment 25: Synthesis of 6-nitro-1,2,3,4,8,9,10,11-octahydropyrido[1,2-*a*]pyrido[1′,2′:1,2]imidazo[5,4-*f*]benzimidazole (68b)

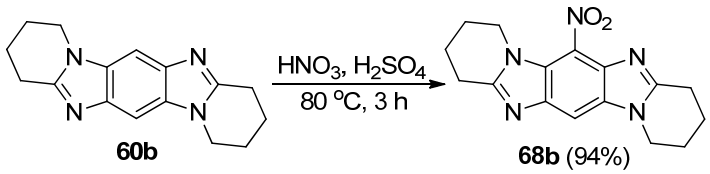

Following general procedure 5.2.4, 1,2,3,4,8,9,10,11-octahydropyrido[1,2-*a*]pyrido[1′,2′:1,2]imidazo[5,4-*f*]benzimidazole **60b** (0.240 g, 0.9 mmol) gave the *title compound* **68b** (0.263 g, 94%); yellow solid; R_f 0.48 (EtOAc-MeOH 9:1); mp 230-236 °C decomp; ν_{max} (neat, cm^{-1}) 2952, 1735, 1542, 1514 (NO_2), 1478, 1431, 1415, 1360 (NO_2), 1335, 1310, 1272, 1255, 1205, 1170, 1145, 1076, 1043; δ_H (400 MHz, $CDCl_3$) 2.01-2.29 (8H, m, CH_2), 3.13-3.22 (4H, m, 4,11-CH_2), 4.12-4.21 (4H, m, 1,8-CH_2), 7.69 (1H, s, 13-H); δ_C (100 MHz, $CDCl_3$) 20.1, 20.5, 22.5, 23.2 (all CH_2), 26.0, 26.4 (4,11-CH_2), 43.0, 45.7, (1,8-CH_2), 102.8 (13-CH), 124.5, 124.6, 132.5, 134.1, 141.0 (all C), 154.4, 155.4 (4a,11a-C); *m/z* (ESI) 312.1460 ($[M+H]^+$, $C_{16}H_{18}N_5O_2$ requires 312.1461).

Experiment 26: Synthesis of 7-nitro-2,3,4,5,10,11,12,13-octahydro-1*H*,9*H*-azepino[1,2-*a*]azepino[1′,2′:1,2]imidazo[5,4-*f*]benzimidazole (68c)

Following general procedure 5.2.4, 2,3,4,5,10,11,12,13-octahydro-1*H*,9*H*-azepino[1,2-*a*]azepino[1′,2′:1,2]imidazo[5,4-*f*]benzimidazole **60c** (0.172 g, 0.6 mmol) gave the *title compound* **68c** (0.182 g, 92%); yellow solid; R_f 0.17 (EtOAc-MeOH 9:1); mp 278-280 °C; ν_{max} (neat, cm^{-1}) 3029, 2938, 2923, 2849, 1545, 1520 (NO_2), 1480, 1468, 1442, 1410, 1348 (NO_2), 1305, 1254, 1215, 1190, 1135, 1088, 1045; δ_H (400 MHz, $CDCl_3$) 1.74-1.99 (12H, m, 2,3,4,10,11,12-CH_2), 3.10 (2H, t, *J* 5.3, 5 or 13-CH_2), 3.16 (2H, t, *J* 5.6, 5 or 13-CH_2), 4.05-4.15 (2H, m, 1 or 9-CH_2), 4.19 (2H, t, *J* 4.9, 1 or 9-CH_2), 7.64 (1H, s, 15-H); δ_C (100 MHz, $CDCl_3$) 25.3, 25.4, 28.1, 28.6, 30.1, 30.4, 30.5, 30.8 (all CH_2), 45.1, 46.8 (1,9-CH_2), 103.2 (15-CH), 124.4, 125.1, 133.2, 133.9, 140.8 (all C), 161.0, 161.1 (5a,13a-C); *m/z* (ESI) 340.1783 ($[M+H]^+$, $C_{18}H_{22}N_5O_2$ requires 340.1774).

Experiment 27: Synthesis of 6-nitro-1,2,3,4,8,9,10,11-octahydropyrido[1,2-*a*]pyrido[1′,2′:1,2]imidazo[4,5-*f*]benzimidazole (69)

Following general procedure 5.2.4, 1,2,3,4,8,9,10,11-octahydropyrido[1,2-*a*]pyrido[1′,2′:1,2]imidazo[4,5-*f*]benzimidazole **63b** (0.200 g, 0.7 mmol) gave the title compound **69** (0.186 g, 79%) as a yellow solid; R_f 0.27 (CH_2Cl_2-MeOH 9:1); mp 240-250 °C decomp; ν_{max} (neat, cm^{-1}) 3321, 2951, 1486 (NO_2), 1444, 1417, 1364, 1335 (NO_2), 1310, 1270, 1242, 1162, 1027; δ_H (400 MHz, $CDCl_3$) 2.02-2.08 (4H, m, CH_2), 2.16-2.21 (4H, m, CH_2), 3.19 (4H, t, *J* 6.4, 4,8-CH_2), 4.14 (4H, t, *J* 6.2, 1,11-CH_2), 7.34 (1H, s, 13-H); δ_C (100 MHz, $CDCl_3$) 20.5 (CH_2), 22.5 (CH_2), 26.0 (4,8-CH_2), 43.0, (1,11-CH_2), 94.1 (13-CH), 127.7 (6-C), 132.7 (C), 134.6 (C), 155.4, (4a, 7a-C); *m/z* (ESI) 312.1474 ($[M+H]^+$, $C_{16}H_{18}N_5O_2$ requires 312.1461).

Experiment 28: Synthesis of 3-butyl-4(11)-nitro-6,7,8,9-tetrahydroimidazo[5,4-*f*]pyrido[1,2-*a*]benzimidazole (70a, 70b)

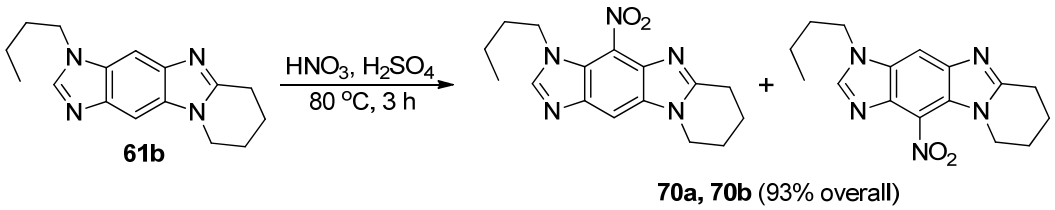

Following general procedure 5.2.4, 3-butyl-6,7,8,9-tetrahydroimidazo[5,4-*f*]pyrido[1,2-*a*]benzimidazole **61b** (0.300 g, 1.1 mmol) gave a mixture of 3-butyl-4-nitro- and 3-butyl-11-nitro-6,7,8,9-tetrahydroimidazo[5,4-*f*]pyrido[1,2-*a*]benzimidazole **70a**, **70b** (0.324 g, 93%) which were not separated.

5.2.5 General procedure for the synthesis of imidazo[5,4-*f*(4,5-*f*)]benzimidazolequinones

A mixture of nitro-imidazo[5,4-*f*]benzimidazole (0.6 mmol) and Pd-C (5%, 20 mg) in MeOH (100 mL) was stirred under 6 bar H_2 at room temperature for 16 h. The mixture was filtered, evaporated and aqueous pH 4 buffer solution (monobasic potassium phosphate, KH_2PO_4, 0.2 M, 50 mL) added. A separate solution of Frèmy's salt (potassium nitrosodisulfonate, $K_2NO(SO_3)_2$, 1.8 mmol) in KH_2PO_4 (0.2 M, 50 mL) was added, and the mixture stirred at room temperature for 1 h. The reaction mixture was extracted with CH_2Cl_2 (5 x 50 mL), the combined organic extracts dried (Na_2SO_4) and evaporated. Unless otherwise stated, HCl (2 M, 50 mL) was added to the residue (to hydrolyze intermediate iminoquinone to quinone) and the solution stirred for 15 min. The acid solution was neutralized with solid Na_2CO_3 and extracted with CH_2Cl_2 (5 x 50 mL). The combined organic extracts were dried (Na_2SO_4), evaporated and the residue purified by dry column vacuum chromatography with a gradient elution of EtOAc (or CH_2Cl_2) and MeOH.

Experiment 29: Synthesis of 1,5-dibutylimidazo[5,4-*f*]benzimidazol-4,8-dione (71)

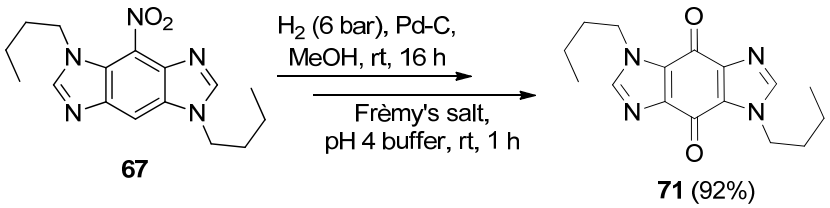

Following general procedure 5.2.5, 1,5-dibutyl-4-nitro-imidazo[5,4-*f*]benzimidazole **67** (0.202 g, 0.6 mmol), Pd-C (5%, 20 mg) and Frèmy's salt (0.483 g, 1.8 mmol) gave the *title compound* **71** (0.168 g, 92%) with no iminoquinone present, therefore acid hydrolysis was not necessary; yellow solid; R_f 0.44 (EtOAc-MeOH 9:1); mp 213-214 °C; ν_{max} (neat, cm^{-1}) 3068, 2957, 2932, 2871, 1665 (C=O), 1515, 1489, 1459, 1385, 1336, 1217, 1185, 1065, 1033; δ_H (400 MHz, $CDCl_3$) 0.92 (6H, t, *J* 7.4, CH_3), 1.28-1.37 (4H, m, CH_2), 1.78-1.85 (4H, m, CH_2), 4.35 (4H, t, *J* 7.2, NCH_2), 7.64 (2H, s, 2,6-H); δ_C (100 MHz, $CDCl_3$) 13.6 (CH_3), 19.7 (CH_2), 32.6 (CH_2), 47.1 (NCH_2), 131.0 (C), 142.9 (2,6-CH), 143.5 (C), 172.2 (C=O); *m/z* (ESI) 301.1656 ($[M+H]^+$, $C_{16}H_{21}N_4O_2$ requires 301.1665); elemental analysis calcd (%) for $C_{16}H_{20}N_4O_2$: C 63.98, H 6.71, N 18.65; found: C 63.60, H 6.85, N 18.31.

Experiment 30: Synthesis of 1,2,3,4,8,9,10,11-octahydropyrido[1,2-*a*]pyrido[1′,2′:1,2]imidazo[4,5-*f*]benzimidazol-6,13-dione (16)

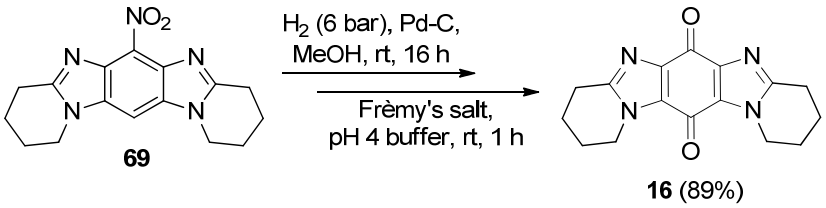

Following general procedure 5.2.5, 6-nitro-1,2,3,4,8,9,10,11-octahydropyrido[1,2-*a*]pyrido[1′,2′:1,2]imidazo[4,5-*f*]benzimidazole **69** (0.158 g, 0.6 mmol), Pd-C (5%, 20 mg) and Frèmy's salt (0.483 g, 1.8 mmol) gave the *title compound* **16** (0.134 g, 89%) with no iminoquinone present, therefore acid hydrolysis was not necessary; yellow solid; R_f 0.30 (EtOAc-MeOH 9:1); mp 221-223 °C decomp (lit.[35] > 260 °C); ν_{max} (neat, cm^{-1}) 2941, 1675, 1652 (C=O), 1493, 1442, 1421, 1331, 1295, 1163, 1073, 1039; δ_H (400 MHz, $CDCl_3$) 1.94-2.09 (8H, m, CH_2), 2.98 (4H, t, *J* 6.4, 4,8-CH_2), 4.32 (4H, t, *J* 6.0, 1,11-CH_2); δ_C (100 MHz, $CDCl_3$) 19.8 (CH_2), 22.4 (CH_2), 25.0 (4,8-CH_2), 45.5 (1,11-CH_2), 130.3 (12a,13a-C), 142.5 (5a,6a-C), 151.4 (4a,7a-C), 169.8 (13-C=O), 175.5 (6-C=O); *m/z* (ESI) 297.1352 ($[M+H]^+$, $C_{16}H_{17}N_4O_2$ requires 297.1355).

Experiment 31: Synthesis of 3-butyl-6,7,8,9-tetrahydroimidazo[5,4-*f*]pyrido[1,2-*a*]benzimidazol-4,11-dione (72)

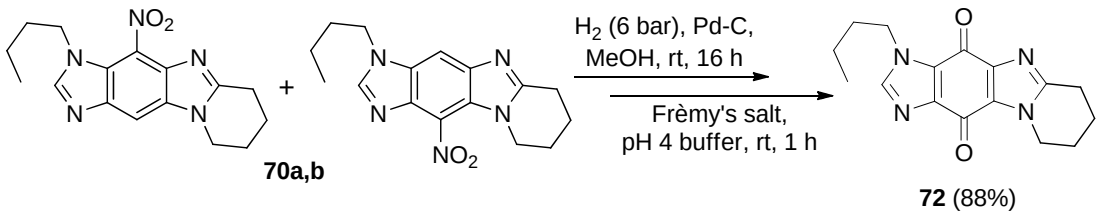

70a,b

72 (88%)

Following general procedure 5.2.5, 3-butyl-4-nitro- and 3-butyl-11-nitro-6,7,8,9-tetrahydroimidazo[5,4-*f*]pyrido[1,2-*a*]benzimidazole **70a,b** (0.324 g, 1.0 mmol), Pd-C (5%, 32 mg) and Frèmy's salt (0.805 g, 3.0 mmol) gave the *title compound* **72** (0.273 g, 88%)with no iminoquinone present, therefore acid hydrolysis was not necessary; yellow solid; R_f 0.17 (EtOAc-MeOH 9:1); mp 216-217 °C; ν_{max} (neat, cm^{-1}) 3190, 2955, 2871, 1678, 1656 (C=O), 1512, 1488, 1473, 1425, 1377, 1334, 1299, 1266, 1253, 1222, 1193, 1072, 1052; δ_H (400 MHz, $CDCl_3$) 0.92 (3H, t, *J* 7.4, CH_3), 1.29-1.38 (2H, m, CH_2), 1.77-1.84 (2H, m, CH_2), 1.93-2.07 (4H, m, CH_2), 2.96 (2H, t, *J* 6.4, 6-CH_2), 4.31-4.35 (4H, m, NCH_2), 7.60 (1H, s, 2-H); δ_C (100 MHz, $CDCl_3$) 13.6 (CH_3), 19.72, 19.75, 22.2 (all CH_2), 25.1 (6-CH_2), 32.4 (CH_2), 45.7, 47.0 (NCH_2), 130.66, 130.71, 142.15 (all C), 142.5 (2-CH), 143.2 (C), 151.6 (C), 171.9, 172.1 (C=O); *m/z* (ESI) 299.1497 ($[M+H]^+$, $C_{16}H_{19}N_4O_2$ requires 299.1508).

Experiment 32: Synthesis of 2,3,8,9-tetrahydro-1*H*,7*H*-pyrrolo[1,2-*a*]pyrrolo[1′,2′:1,2]imidazo[5,4-*f*]benzimidazol-5,11-dione (74a)

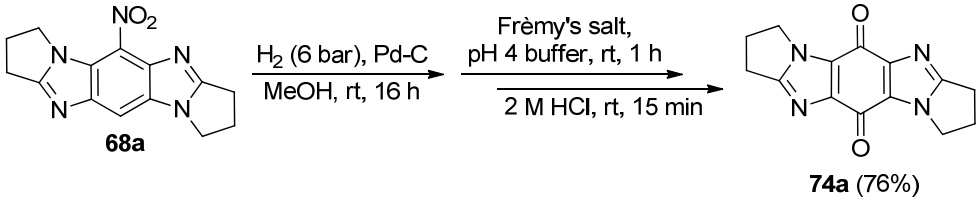

Following general procedure 5.2.5, 5-nitro-2,3,8,9-tetrahydro-1*H*,7*H*-pyrrolo[1,2-*a*]pyrrolo[1′,2′:1,2]imidazo[5,4-*f*]benzimidazole **68a** (92 mg, 0.3 mmol), Pd-C (5%, 10 mg) and Frèmy's salt (0.242 g, 0.9 mmol) gave a ~1:1 mixture of iminoquinone **73a** and quinone **74a** which was hydrolyzed without separation with HCl as per general procedure 5.2.5 to give the *title compound* **74a** (66 mg, 76%); yellow solid; R_f 0.55 (CH_2Cl_2-MeOH 9:1); mp >350 °C; ν_{max} (neat, cm^{-1}) 3316, 2990, 2957, 1663 (C=O), 1514, 1485, 1438, 1403, 1356, 1301, 1267, 1225, 1214, 1200, 1179, 1040; δ_H (400 MHz, $CDCl_3$) 2.69-2.76 (4H, m, 2,8-CH_2), 2.96 (4H, t, *J* 7.6, 3,9-CH_2), 4.29 (4H, t, *J* 7.2, 1,7-CH_2); δ_C (100 MHz, $CDCl_3$) 23.0 (3,9-CH_2), 26.5 (2,8-CH_2), 45.4 (1,7-CH_2), 130.7, 145.8, 160.2 (all C), 171.8 (C=O); *m/z* (ESI) 269.1047 ($[M+H]^+$, $C_{14}H_{13}N_4O_2$ requires 269.1039).

Experiment 33: Synthesis of 6-imino-1,2,3,4,8,9,10,11-octahydropyrido[1,2-*a*]pyrido[1′,2′:1,2]imidazo[5,4-*f*]benzimidazol-13-one (73b)

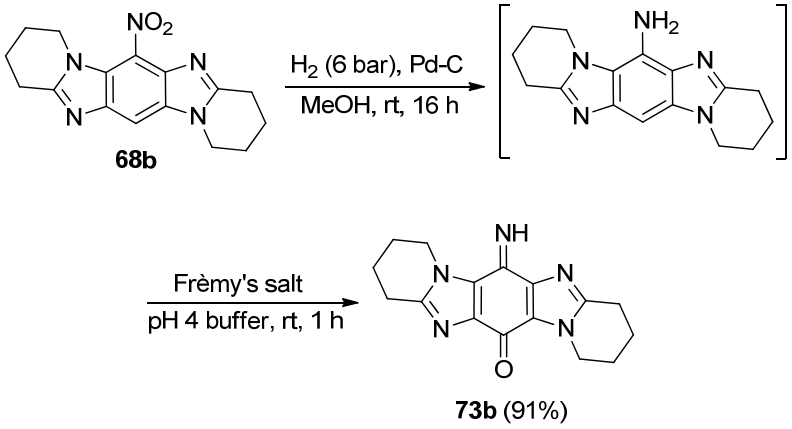

6-Nitro-1,2,3,4,8,9,10,11-octahydropyrido[1,2-*a*]pyrido[1′,2′:1,2]imidazo[5,4-*f*]benzimidazole **68b** (0.275 g, 0.9 mmol) was catalytically reduced with Pd-C (10%, 25 mg) as per general procedure 5.2.5 to give 6-amino-1,2,3,4,8,9,10,11-octahydropyrido[1,2-*a*]pyrido[1′,2′:1,2]imidazo[5,4-*f*]benzimidazole as a brown residue; δ_H (400 MHz, $CDCl_3$) 1.97-2.08 (4H, m, CH_2), 2.10-2.20 (4H, m, CH_2), 3.10-3.06 (4H, m, 4,11-CH_2), 4.07 (2H, t, *J* 6.1, NCH_2), 4.36 (2H, bs, NH_2), 4.62 (2H, t, *J* 6.1, NCH_2), 6.97 (1H, s, 13-H); Oxidation with Frèmy's salt (0.725 g, 2.7 mmol) as per general procedure 5.2.5 gave the *title compound* **73b** (with no quinone present) which was purified and characterized before acid hydrolysis (0.238 g, 91%); yellow solid; R_f 0.30 (EtOAc-MeOH 9:1); mp 230-240 °C decomp; ν_{max} (neat, cm^{-1}) 2948, 2867, 1656, (C=O), 1515, 1494, 1442, 1425, 1405, 1377, 1336, 1306, 1272, 1219, 1167, 1075, 1042; δ_H (400 MHz, $CDCl_3$) 1.93-2.08 (8H, m, CH_2), 2.92-3.00 (4H, m, 4,11-CH_2), 4.37-4.43 (4H, m, 1,8-CH_2), 10.55 (1H, s, NH); δ_C (100 MHz, $CDCl_3$) 19.9, 20.0, 22.3, 22.7 (all CH_2), 25.0, 25.3 (4,11-CH_2), 45.4, 46.5, (1,8-CH_2), 126.0 (C), 131.5 (C), 139.7 (2 x C), 150.2 (2 x C), 155.5 (C=N), 172.0 (C=O); *m/z* (ESI) 296.1502 ($[M+H]^+$, $C_{16}H_{18}N_5O$ requires 296.1511).

Experiment 34: Synthesis of 1,2,3,4,8,9,10,11-octahydropyrido[1,2-*a*]pyrido[1′,2′:1,2]imidazo[5,4-*f*]benzimidazol-6,13-dione (74b)

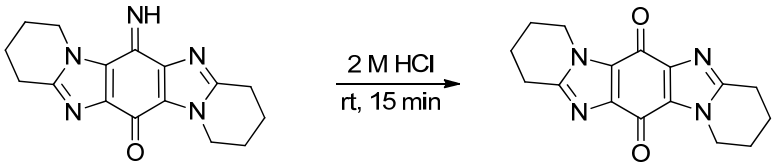

73b **74b** (96%)

6-Imino-1,2,3,4,8,9,10,11-octahydropyrido[1,2-*a*]pyrido[1′,2′:1,2]imidazo[5,4-*f*]benzimidazol-13-one **73b** (0.238 g, 0.8 mmol) was dissolved in HCl (50 mL, 2 M) and stirred for 15 min. The solution was neutralized with solid Na_2CO_3 and extracted using CH_2Cl_2 (6 x 50 mL). The combined organic extracts were dried (Na_2SO_4), evaporated and the residue purified by dry column vacuum chromatography to give the *title compound* **74b** (0.229 g, 96%); yellow solid; R_f 0.32 (EtOAc-MeOH 9:1); mp 265-275 °C decomp; ν_{max} (neat, cm^{-1}) 2948, 1655 (C=O), 1493, 1377, 1336, 1305, 1218, 1076, 1042; δ_H (400 MHz, $CDCl_3$) 1.98-2.10 (8H, m, CH_2), 2.99 (4H, t, *J* 6.2, 4,11-CH_2), 4.35 (4H, t, *J* 5.9, 1,8-CH_2); δ_C (100 MHz, $CDCl_3$) 19.8 (CH_2), 22.2 (CH_2), 25.1 (4,11-CH_2), 45.6 (1,8-CH_2), 130.2 (6a,13a-C), 141.8 (5a,12a-C), 151.4 (4a,11a-C), 171.6 (C=O); *m/z* (ESI) 297.1365 ($[M+H]^+$, $C_{16}H_{17}N_4O_2$ requires 297.1352).

Experiment 35: Synthesis of 7-imino-2,3,4,5,10,11,12,13-octahydro-1*H*,9*H*-azepino[1,2-*a*]azepino[1′,2′:1,2]imidazo[5,4-*f*]benzimidazol-15-one (73c) and 2,3,4,5,10,11,12,13-octahydro-1*H*,9*H*-azepino[1,2-*a*]azepino[1′,2′:1,2]imidazo[5,4-*f*]benzimidazol-7,15-dione (74c)

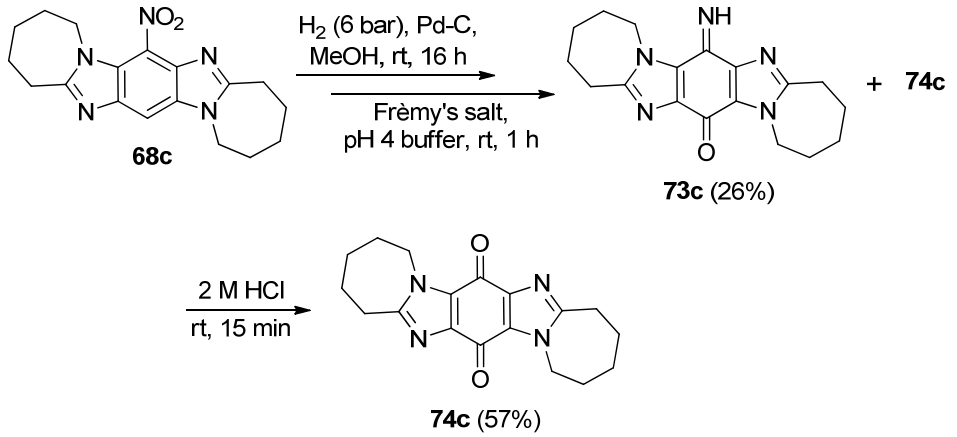

Following general procedure 5.2.5, 7-nitro-2,3,4,5,10,11,12,13-octahydro-1*H*,9*H*-azepino[1,2-*a*]azepino[1′,2′:1,2]imidazo[5,4-*f*]benzimidazole **68c** (0.138 g, 0.4 mmol), Pd-C (5%, 14 mg) and Frèmy's salt (0.322 g, 1.2 mmol) gave a ~2.3:1 mixture of iminoquinone **73c** and quinone **74c** respectively. The mixture was columned prior to acid hydrolysis and while separation was not achieved, a pure sample of the *title compound* **73c** was obtained. The remaining mixture was hydrolyzed with HCl as per general procedure 5.2.5 to give the *title compound* **74c.**

7-Imino-2,3,4,5,10,11,12,13-octahydro-1*H*,9*H*-azepino[1,2-*a*]azepino[1′,2′:1,2]imidazo[5,4-*f*]benzimidazol-15-one (73c): (34 mg, 26%); yellow solid; R_f 0.60 (CH_2Cl_2-MeOH 9:1); mp 260-265 °C decomp; ν_{max} (neat, cm^{-1}) 2940, 2918, 2887, 2842, 1650 (C=O), 1611, 1518, 1495, 1474, 1439, 1412, 1386, 1356, 1349, 1319, 1278 , 1261, 1228, 1090, 1073, 1042, 1009; δ_H (400 MHz, $CDCl_3$) 1.62-1.90 (12H, m, 2,3,4,10,11,12-CH_2), 2.91 (2H, t, *J* 5.7, 5 or 13-CH_2), 2.97 (2H, t, *J* 5.6, 5 or 13-CH_2), 4.57-4.66 (2H, m, 1 or 9-CH_2), 4.76-4.88 (2H, m, 1 or 9-CH_2), 10.69 (1H, s, NH); δ_C (100 MHz, $CDCl_3$) 25.2, 25.3, 28.4, 29.5, 29.6, 30.95, 31.03 (all CH_2), 45.9, 46.4 (1,9-CH_2), 126.2, 131.9, 139.4, 156.4, 156.7, 156.9 (all C), 173.0 (C=O); *m/z* (ESI) 324.1827($[M+H]^+$, $C_{18}H_{22}N_5O$ requires 324.1824).

2,3,4,5,10,11,12,13-octahydro-1*H*,9*H*-azepino[1,2-*a*]azepino[1′,2′:1,2]imidazo[5,4-*f*]benzimidazol-7,15-dione (74c): (75 mg, 57%); yellow solid; R_f 0.62 (CH_2Cl_2-MeOH 9:1); mp 340-346 °C decomp; ν_{max} (neat, cm^{-1}) 2950, 2919, 2886, 2842, 1654 (C=O), 1523, 1492, 1474, 1437, 1373, 1357, 1346, 1318, 1280, 1241, 1227, 1180, 1093, 1076, 1055, 1016; δ_H (400 MHz, $CDCl_3$) 1.69-1.94 (12H, m, CH_2), 2.99 (4H, t, *J* 5.6, 5,13-CH_2), 4.56-4.64 (4H, m, 1,9-CH_2); δ_C (100 MHz, $CDCl_3$) 25.0 (CH_2), 28.2 (CH_2), 29.4 (5,13-CH_2), 30.9 (CH_2), 46.0 (1,9-CH_2), 130.5, 141.4, 157.8 (all C), 172.7 (C=O); *m/z* (ESI) 325.1652 ($[M+H]^+$, $C_{18}H_{21}N_4O_2$ requires 325.1665).

5.3 Experimental for Chapter 3

Experiment 36: Synthesis of 1,4-difluoro-2,5-dinitrobenzene (106b)

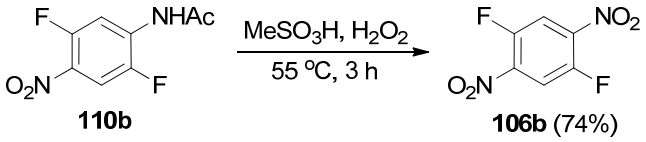

110b **106b** (74%)

N-(2,5-difluoro-4-nitrophenyl)acetamide **110b** was prepared according to the literature procedure by Kosynkin *et al*.[129]

H_2O_2 (30 wt%, 11.95 mL, 0.116 mol) was added drop wise to a solution of *N*-(2,5-difluoro-4-nitrophenyl)acetamide **110b** (2.500 g, 11.6 mmol) in $MeSO_3H$ (90%, 40 mL) and the solution heated at 55 °C for 3 h. The cooled solution was poured onto ice and the precipitate collected, washed with water and dried to give the *title compound* **106b** (1.745 g, 74%); yellow solid; mp 103-104 °C; ν_{max} (neat, cm^{-1}) 3075, 1547 (NO_2), 1498, 1412, 1343 (NO_2), 1292, 1199, 1108, 1059, 1033; δ_H 8.06 (2H, t, *J* 7.5); δ_C 116.5-117.0 (m, CH), 140.1-140.4 (m, CNO_2), 150.7 (dd, *J* 268.7, 5.5, CF); *m/z* (ESI) 202.9911 ($[M-H]^-$, $C_6HN_2O_4F_2$ requires 202.9904).

Experiment 37: Synthesis of 4,4'-(2,5-dinitro-1,4-phenylene)dimorpholine (107a)

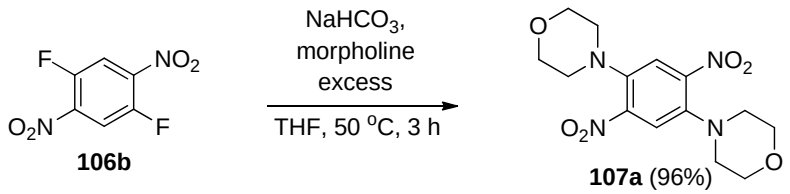

1,4-Difluoro-2,5-dinitrobenzene **106b** (0.793 g, 3.9 mmol), $NaHCO_3$ (1.638 g, 19.5 mmol) and morpholine (1.37 mL, 15.6 mmol) were heat in THF (30 mL) at 50 °C for 3 h. Water (100 mL) was added and the precipitate collected, washed with water and dried to give the *title compound* **107a** (1.262 g, 96%); red solid; mp 236-237 °C; ν_{max} (neat, cm^{-1}) 2974, 2859, 2838, 1528, 1501 (NO_2), 1409, 1378, 1358 (NO_2), 1324, 1300, 1283, 1249, 1230, 1210, 1109, 1064, 1055; δ_H (400 MHz, $CDCl_3$) 3.01 (8H, t, *J* 4.6, NCH_2), 3.82 (8H, t, *J* 4.6, OCH_2), 7.49 (2H, s); δ_C (100 MHz, $CDCl_3$) 52.2 (NCH_2), 66.7 (OCH_2), 118.7 (CH), 140.4 (C), 146.2 (C); *m/z* (ESI) 339.1290 ($[M+H]^+$, $C_{14}H_{19}N_4O_6$ requires 339.1305).

Experiment 38: Synthesis of 4-(2,5-dinitro-4-piperidin-1-ylphenyl)morpholine (107b)

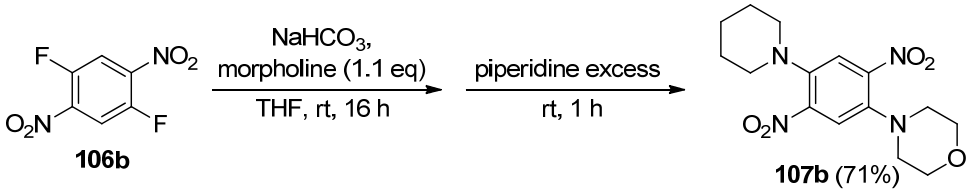

1,4-Difluoro-2,5-dinitrobenzene **106b** (0.600 g, 2.9 mmol), $NaHCO_3$ (1.218 g, 14.5 mmol) and morpholine (0.28 mL, 3.2 mmol) were stirred in THF (30 mL) at room temperature for 16 h. Piperidine (2.87 mL, 29.0 mmol) was added and the mixture stirred for 1 h. Water (100 mL) was added, the precipitate was collected and purified by flash chromatography with petroleum ether and acetone (19:1) as eluent to give the *title compound* **107b** (0.702 g, 71%); red solid; R_f 0.12 (Pet. ether-Acetone 9:1); mp 175-176 °C; ν_{max} (neat, cm^{-1}) 2936, 2855, 1530, 1516 (NO_2), 1499, 1407, 1379, 1351 (NO_2), 1323, 1253, 1226, 1210, 1113, 1066, 1049, 1030; δ_H (400 MHz, $CDCl_3$) 1.53-1.63 (2H, m, CH_2), 1.65-1.73 (4H, m, CH_2), 2.97 (8H, t, *J* 4.8, NCH_2), 3.80 (4H, t, *J* 4.5, OCH_2), 7.41 (1H, s), 7.50 (1H, s); δ_C (100 MHz, $CDCl_3$) 23.8 (CH_2), 25.9 (CH_2), 52.5, 53.0 (NCH_2), 66.9 (OCH_2), 117.9, 119.3 (CH), 138.6, 142.3, 144.7, 147.2 (all C); *m/z* (ESI) 337.1503 ($[M+H]^+$, $C_{15}H_{21}N_4O_5$ requires 337.1512).

Experiment 39: Synthesis of 1-(2,5-dinitro-4-(pyrrolidin-1-yl)phenyl)piperidine (107c)

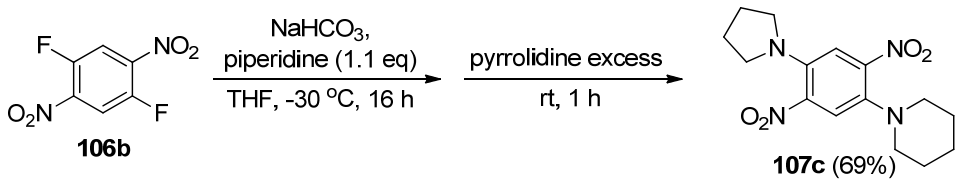

Piperidine (0.41 mL, 4.1 mmol) was added to 1,4-difluoro-2,5-dinitrobenzene **106b** (0.750 g, 3.7 mmol) and $NaHCO_3$ (1.554 g, 18.5 mmol) in THF (30 mL) at -30 °C and the mixture stirred for 16 h. Pyrrolidine (3.04 mL, 37.0 mmol) was added and the mixture stirred at room temperature for 1 h. Water (100 mL) was added, the precipitate collected and purified by flash chromatography with petroleum ether and acetone (19:1) as eluent to give the *title compound* **107c** (0.818 g, 69%); red solid; R_f 0.22 (Pet. ether-Acetone 9:1); mp 162-164 °C; ν_{max} (neat, cm^{-1}) 2946, 2856, 1630, 1534 (NO_2), 1497, 1449, 1360, 1306 (NO_2), 1264, 1248, 1221, 1211, 1106, 1032; δ_H (400 MHz, $CDCl_3$) 1.49-1.56 (2H, m, CH_2), 1.63-1.70 (4H, m, CH_2), 1.96-2.02 (4H, m, CH_2), 2.85 (4H, t, *J* 5.3, NCH_2), 3.18 (4H, t, *J* 6.5, NCH_2), 7.14 (1H, s), 7.54 (1H, s); δ_C (100 MHz, $CDCl_3$) 23.9, 25.8, 26.3 (all CH_2), 50.6, 54.4 (NCH_2), 111.7, 120.7 (CH), 135.5, 138.1, 138.5, 148.8 (all C); *m/z* (ESI) 321.1578 ($[M+H]^+$, $C_{15}H_{21}N_4O_4$ requires 321.1563).

5.3.1 General procedure for the reduction and acetylation of dinitrobenzenes to give diacetamides

2,5-Dinitrobenzenes **107a-c** (5.3 mmol), Pd-C (5%, 0.178 g) and Ac_2O (5.0 mL, 53.0 mmol) in glacial AcOH (50 mL) were stirred under 6 bar of H_2 at room temperature for 16 h. The mixture was filtered, evaporated, Na_2CO_3 (5%, 50 mL) added and stirred for 1 h. The precipitate was collected, washed with water, and dried to give **108a-c**.

Experiment 40: Synthesis of *N*,*N'*-(2,5-dimorpholin-4-yl-1,4-phenylene)diacetamide (108a)

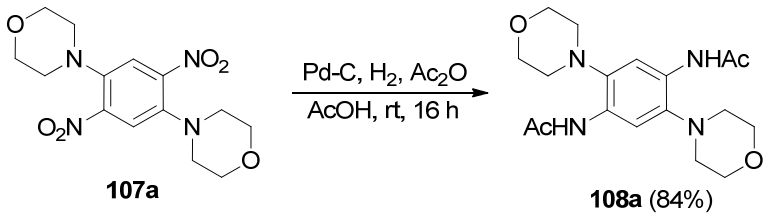

Following general procedure 5.3.1, 4,4'-(2,5-Dinitro-1,4-phenylene)dimorpholine **107a** (1.785 g, 5.3 mmol), Pd-C (5%, 0.178 g) and Ac_2O (5.00 mL, 53.0 mmol) gave the *title compound* **108a** (1.606 g, 84%); white solid; mp 266-268 °C; ν_{max} (neat, cm^{-1}) 3341, 2969, 2843, 1677 (C=O), 1525, 1418, 1368, 1294, 1259, 1229, 1179, 1113, 1071, 1057, 1007; δ_H (400 MHz, $CDCl_3$) 2.19 (6H, s, CH_3), 2.85 (8H, t, *J* 4.5, NCH_2), 3.84 (8H, t, *J* 4.5, OCH_2), 8.27 (2H, s), 8.42 (2H, bs, disappears with D_2O, NH); δ_C (100 MHz, $CDCl_3$) 25.0 (CH_3), 52.6 (NCH_2), 67.7 (OCH_2), 112.4 (CH), 129.6 (C), 137.8 (C), 168.1 (C=O); *m/z* (ESI) 385.1847 ($[M+Na]^+$, $C_{18}H_{26}N_4O_4Na$ requires 385.1852).

Experiment 41: Synthesis of *N*,*N*′-(2-morpholin-4-yl-5-piperidin-1-yl-1,4-phenylene)diacetamide (108b)

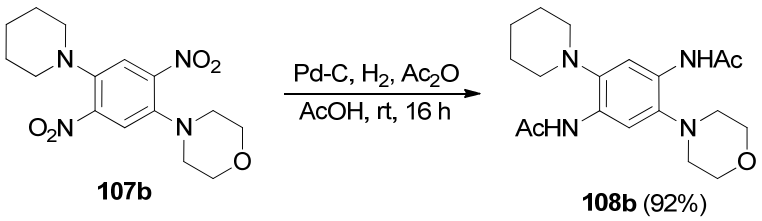

Following general procedure 5.3.1, 4-(2,5-dinitro-4-piperidin-1-ylphenyl)morpholine **107b** (0.433 g, 1.3 mmol), Pd-C (5%, 44 mg) and Ac_2O (1.23 mL, 13.0 mmol) gave the *title compound* **108b** (0.431 g, 92%); white solid; mp 230-240 °C decomp; ν_{max} (neat, cm^{-1}) 3265, 2853, 2491 1661 (C=O), 1528, 1451, 1414, 1376, 1298, 1245, 1197, 1115, 1071, 1053, 1035, 1017; δ_H (400 MHz, $CDCl_3$) 1.53-1.61 (2H, m, CH_2), 1.64-1.73 (4H, m, CH_2), 2.18 (6H, s, CH_3), 2.77 (4H, t, *J* 5.2, NCH_2), 2.85 (4H, t, *J* 4.5, NCH_2), 3.84 (4H, t, *J* 4.5, OCH_2), 8.23 (1H, s), 8.26 (1H, s), 8.43 (1H, bs, disappears with D_2O, NH), 8.50 (1H, bs, disappears with D_2O, NH); δ_C (100 MHz, $CDCl_3$) 24.0 (CH_2), 25.0 (CH_3), 27.0 (CH_2), 52.7, 53.8 (NCH_2), 67.7 (OCH_2), 112.0 (CH), 112.2 (CH), 129.4, 129.7, 137.1, 139.7 (all C), 168.0, 168.1 (C=O); *m/z* (ESI) 359.2082 ($[M-H]^-$, $C_{19}H_{29}N_4O_3$ requires 359.2083).

Experiment 42: Synthesis of *N*,*N*′-(2-piperidin-1-yl-5-pyrrolidin-1-yl-1,4-phenylene)diacetamide (108c)

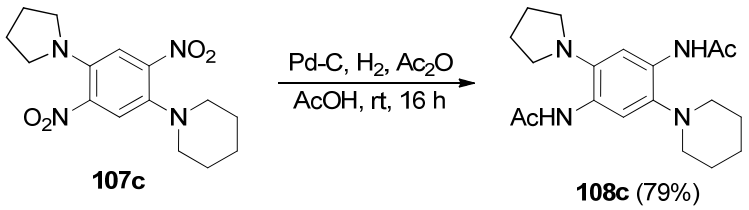

107c **108c** (79%)

Following general procedure 5.3.1, 1-(2,5-dinitro-4-(pyrrolidin-1-yl)phenyl)piperidine **107b** (1.061 g, 3.3 mmol), Pd-C (5%, 0.111 g) and Ac_2O (3.11 mL, 33.0 mmol) gave the *title compound* **108c** (0.898 g, 79%); white solid; mp 214-216 °C; ν_{max} (neat, cm^{-1}) 3318, 2937, 2809, 1663 (C=O), 1526, 1475, 1411, 1366, 1295, 1239, 1216, 1108, 1033, 1014; δ_H (400 MHz, $CDCl_3$) 1.50-1.61 (2H, m, CH_2); 1.66-1.72 (4H, m, CH_2), 1.89-1.96 (4H, m, CH_2), 2.17 (6H, s, CH_3), 2.77 (4H, t, *J* 5.1, NCH_2), 2.95-3.05 (4H, m, NCH_2), 8.12 (1H, s), 8.18 (1H, bs, disappears with D_2O, NH), 8.24 (1H, s), 8.53 (1H, bs, disappears with D_2O, NH); δ_C (100 MHz, $CDCl_3$) 24.1 (CH_2), 24.5 (CH_2), 25.0 (CH_3), 27.1 (CH_2), 52.8, 53.8 (NCH_2), 110.9, 112.9 (CH), 129.1, 129.8, 136.8, 138.4 (all C), 168.0, 168.1 (C=O); *m/z* (ESI) 343.2126 ($[M-H]^-$, $C_{19}H_{27}N_4O_2$ requires 343.2134).

Experiment 43: Synthesis of *N,N′*-[2,5-bis(4-oxidomorpholin-4-yl)-1,4-phenylene]diacetamide (112)

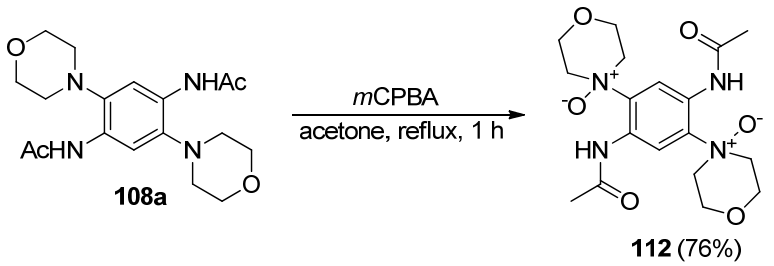

N,N′-(2,5-Dimorpholin-4-yl-1,4-phenylene)diacetamide **108a** (0.204 g, 0.6 mmol) and *m*CPBA (70%, 0.740 g, 3.0 mmol) were heated in acetone at reflux for 1 h. The resultant white precipitate was collected, washed with acetone and dried to give the *title compound* **112** (0.168 g, 76%); white solid; mp 234-236 °C; ν_{max} (neat, cm^{-1}) 3512, 3223, 2973, 2940, 1655 (C=O), 1532, 1475, 1428, 1404, 1301, 1247, 1118, 1054 (N-O), 1033, 1019; δ_H (400 MHz, $CDCl_3$) 2.20 (6H, s, CH_3), 3.47 (4H, d, *J* 10.6), 3.87-3.95 (8H, m), 4.65 (4H, t, *J* 12.8), 9.13 (2H, s), NH not observed; δ_C (100 MHz, $CDCl_3$) 25.7 (CH_3), 61.6 (CH_2), 66.3 (CH_2), 113.1 (CH), 130.2 (C), 138.9 (C), 169.3 (C=O); *m/z* (ESI) 395.1912 ($[M+H]^+$, $C_{18}H_{27}N_4O_6$ requires 395.1931).

Experiment 44: Synthesis of *N*-(8-morpholin-4-yl-3,4-dihydro-1*H*-[1,4]oxazino[4,3-*a*]benzimidazol-7-yl)acetamide (114)

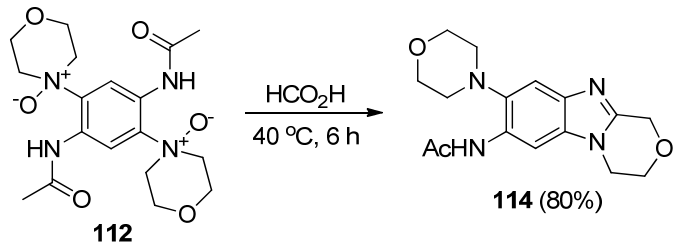

N,*N*'-[2,5-Bis(4-oxidomorpholin-4-yl)-1,4-phenylene]diacetamide **112** (0.150 g, 0.4 mmol) was heated in HCO_2H (20 mL) at 40 °C for 6 h. The mixture was evaporated and Na_2CO_3 (5%, 50 mL) added. The precipitate was collected, washed with water and dried to give the *title compound* **114** (96 mg, 80%); white solid; mp 251-252 °C; ν_{max} (neat, cm^{-1}) 2957, 2846, 1672 (C=O), 1591, 1507, 1471, 1459, 1365, 1338, 1242, 1164, 1108, 1097, 1046, 1033; δ_H (400 MHz, $CDCl_3$) 2.24 (3H, s, CH_3), 2.85-2.92 (4H, m, 3′,5′-CH_2), 3.86-3.91 (4H, m, 2′,6′-CH_2), 4.13-4.18 (4H, m, 3,4-CH_2), 4.98 (2H, s, 1-CH_2), 7.52 (1H, s), 8.47 (1H, s), 8.88 (1H, bs, disappears with D_2O, NH); δ_C (100 MHz, $CDCl_3$) 25.2 (CH_3), 42.3 (4-CH_2), 53.5 (3′,5′-CH_2), 64.1 (3-CH_2), 65.6 (1-CH_2), 67.9 (2′,6′-CH_2), 99.7 (CH), 111.9 (CH), 129.6, 131.6, 137.6, 138.5, 148.2 (all C), 168.2 (C=O); *m/z* (ESI) 315.1456 ($[M-H]^-$, $C_{16}H_{19}N_4O_3$ requires 315.1457).

Experiment 45: Synthesis of *N*-(5-bromo-2-morpholin-4-ylphenyl)acetamide (115)

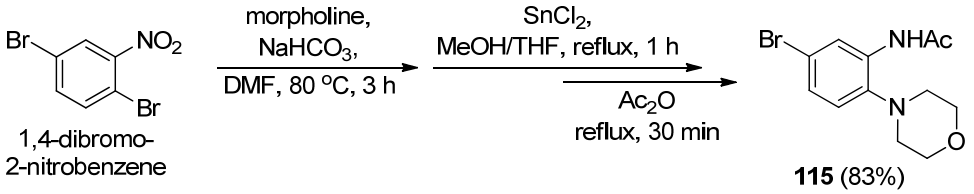

1,4-Dibromo-2-nitrobenzene (2.000 g, 7.1 mmol), $NaHCO_3$ (2.982 g, 35.5 mmol) and morpholine (3.10 mL, 35.5 mmol) were heated in DMF at 80 °C for 1 h. The cooled mixture was evaporated, water (100 mL) added and extracted with EtOAc (5 x 50 mL). The combined organic extracts were washed with water (3 x 50 mL), dried (Na_2SO_4) and evaporated. $SnCl_2.2H_2O$ (8.010 g, 35.5 mmol) was added to the residue in MeOH and THF (1:1, 50 mL) and the mixture heated at reflux for 1 h. The cooled mixture was evaporated, neutralized with NaOH (5 M) and the precipitate collected. The precipitate was dissolved in MeOH (50 mL), Ac_2O added (6.71 mL, 71.0 mmol) and stirred at reflux for 30 minutes. The cooled reaction mixture was evaporated, ice-water added (200 mL) and stirred for 3 h. The precipitate was collected, washed with water and dried to give the *title compound* **115** (1.766 g, 83%); white solid; mp 139-141 °C; ν_{max} (neat, cm^{-1}) 3332, 2951, 1683 (C=O), 1507, 1410, 1374, 1226, 1112, 1033; δ_H (400 MHz, $CDCl_3$) 2.19 (3H, s, CH_3), 2.82 (4H, t, *J* 4.6, NCH_2), 3.84 (4H, t, *J* 4.6, OCH_2), 7.00 (1H, d, *J* 8.5, 3-H), 7.16 (1H, dd, *J* 8.5, 2.2, 4-H), 8.42 (1H, bs, disappears with D_2O, NH), 8.55 (1H, d, *J* 2.2, 6-H); δ_C (100 MHz, $CDCl_3$) 25.1 (CH_3), 52.6 (NCH_2), 67.6 (OCH_2), 119.2 (C), 122.2 (3-CH), 122.4 (6-CH), 126.7 (4-CH), 134.8 (C), 139.5 (C), 168.1 (C=O); *m/z* (ESI) 297.0237 ($[M-H]^-$, $C_{12}H_{14}N_2O_2{}^{79}Br$ requires 297.0239).

Experiment 46: Synthesis of *N*-[5-bromo-2-(4-oxidomorpholin-4-yl)phenyl]acetamide (116)

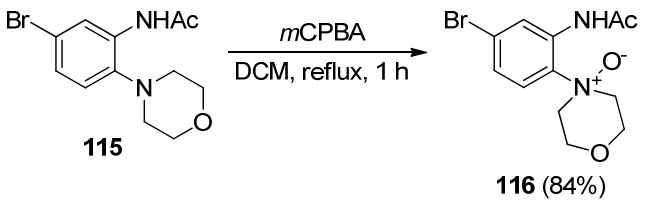

N-(5-Bromo-2-morpholin-4-ylphenyl)acetamide **115** (0.342 g, 1.1 mmol) and *m*CPBA (70%, 0.678 g, 2.75 mmol) were heated in CH_2Cl_2 (40 mL) at reflux for 1 h. The cooled reaction mixture was washed with Na_2CO_3 (5%, 3 x 50 mL), dried (Na_2SO_4) and evaporated give *title compound* **116** (0.302 g, 84%); white solid; mp 164-166 °C; ν_{max} (neat, cm^{-1}) 2969, 2492, 1655 (C=O), 1590, 1514, 1443, 1409, 1370, 1286, 1226, 1106 (N-O), 1020; δ_H (400 MHz, $CDCl_3$) 2.12 (3H, s, CH_3), 3.44 (2H, d, *J* 11.0), 3.72-3.85 (4H, m), 4.57-4.64 (2H, m), 7.12 (1H, dd, *J* 8.9, 2.2, 4-H), 7.16 (1H, d, *J* 8.9, 3-H), 8.78 (1H, d, *J* 2.2, 6-H), NH not observed; δ_C (100 MHz, $CDCl_3$) 25.6 (CH_3), 61.6 (NCH_2), 65.9 (OCH_2), 119.2 (3-CH), 124.0 (C), 125.4 (4-CH), 126.0 (6-CH), 136.5 (C), 138.3 (C), 168.8 (C=O); *m/z* (ESI) 313.0188 ($[M-H]^-$, $C_{12}H_{14}N_2O_3{}^{79}Br$ requires 313.0176).

Experiment 47: Acid catalyzed cyclization of *N*-[5-bromo-2-(4-oxidomorpholin-4-yl)phenyl]acetamide

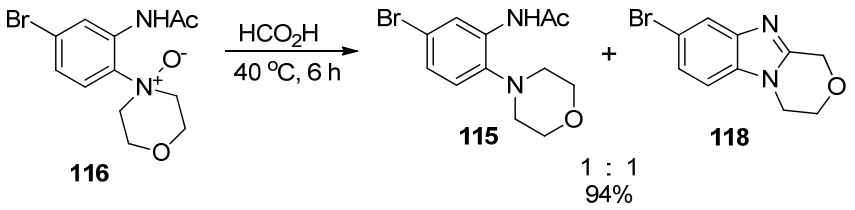

N-[5-bromo-2-(4-oxidomorpholin-4-yl)phenyl]acetamide **116** (0.329 g, 1.0 mmol) was heated in HCO_2H (90%, 30 mL) at 40 °C for 6 h. The mixture was evaporated, Na_2CO_3 (5%, 50 mL) and extracted with CH_2Cl_2 (5 x 50 mL). The combined organic extracts were dried (Na_2SO_4) and evaporated to give a ~1:1 mixture of *N*-(5-Bromo-2-morpholin-4-ylphenyl)acetamide **115** and 8-bromo-3,4-dihydro-1*H*-[1,4]oxazino[4,3- a]benzimidazole **118** (0.271 g, overall 94%).

5.3.2 General procedure for the synthesis of ring-fused benzimidazoles from *o-tert*-amino acetanilides

Oxone® (1.844, 3 mmol) and *o-tert*-amino acetanilides (1.5 mmol) were heated in HCO_2H (90%, 30 mL) at 40 °C for 6 h. The mixture was evaporated, water (50 mL) added and the solution neutralized with solid Na_2CO_3. The precipitate was collected, washed with water and dried to give ring fused benzimidazoles.

Experiment 48: Synthesis of 8-bromo-3,4-dihydro-1*H*-[1,4]oxazino[4,3-*a*]benzimidazole (118)

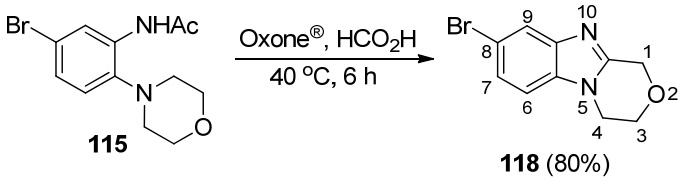

Following general procedure 5.3.2, *N*-(5-bromo-2-morpholin-4-ylphenyl)acetamide **115** (0.250 g, 0.8 mmol) and Oxone® (1.475 g, 2.4 mmol) gave the *title compound* **118** (0.170 g, 80%); white solid; mp 213-214 °C; ν_{max} (neat, cm^{-1}) 3037, 2976, 2937, 1520, 1481 1432, 1407, 1369, 1333, 1317, 1170, 1112, 1091, 1049; δ_H (400 MHz, $CDCl_3$) 4.11-4.22 (4H, m, 3,4-CH_2), 5.01 (2H, s, 1-CH_2), 7.19 (1H, d, *J* 8.5, 6-H), 7.36 (1H, dd, *J* 8.5, 1.4, 7-H), 7.84 (1H, s, 9-H); δ_C (100 MHz, $CDCl_3$) 42.2, 63.9 (3,4-CH_2), 65.5 (1-CH_2), 110.0 (6-CH), 115.6 (C), 122.5 (9-CH), 125.5 (7-CH), 133.1, 144.1, 149.0 (all C); *m/z* (ESI) 254.9957 ($[M+H]^+$, $C_{10}H_{10}N_2O^{81}Br$ requires 254.9956).

Experiment 49: Synthesis of 3,4,10,11-tetrahydro-1*H*,8*H*-[1,4]oxazino[4,3-*a*][1,4]oxazino[4',3':1,2]imidazo[5,4-*f*]benzimidazole (111a)

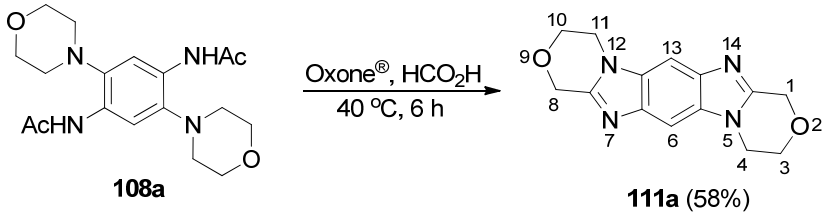

108a **111a** (58%)

Following general procedure 5.3.2, *N,N'*-(2,5-dimorpholin-4-yl-1,4-phenylene)diacetamide **108a** (0.642 g, 1.8 mmol) and Oxone® (6.640 g, 10.8 mmol) gave the *title compound* **111a** (0.282 g, 58%); white solid; mp >350 °C; ν_{max} (neat, cm^{-1}) 3137, 1541, 1490, 1447, 1426, 1353, 1336, 1275, 1191, 1149, 1106, 1099; δ_H (400 MHz, $CDCl_3$) 4.21-4.27 (8H, m, CH_2CH_2), 5.06 (4H, s, 1,8-CH_2), 7.58 (2H, s, 6,13-H); δ_C (100 MHz, $CDCl_3$) 42.2 (CH_2), 64.2 (CH_2), 65.7 (1,8-CH_2), 97.7 (6,13-CH), 132.1, 139.9, 148.9 (all C); *m/z* (ESI) 271.1199 ($[M+H]^+$, $C_{14}H_{15}N_4O_2$ requires 271.1195).

Experiment 50: Synthesis of 3,4,8,9,10,11-hexahydro-1*H*-[1,4]oxazino[4,3-*a*]pyrido[1',2':1,2]imidazo[5,4-*f*]benzimidazole (111b)

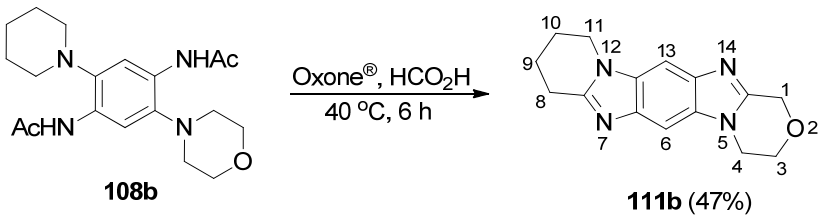

Following general procedure 5.3.2, *N,N'*-(2-morpholin-4-yl-5-piperidin-1-yl-1,4-phenylene)diacetamide **108b** (0.495 g, 1.4 mmol) and Oxone® (5.164 g, 8.4 mmol) gave the *title compound* **111b** (0.177 g, 47%); white solid; mp 330-340 °C decomp; ν_{max} (neat, cm^{-1}) 2944, 1537, 1486, 1445, 1417, 1360, 1280, 1187, 1147, 1089; δ_H (400 MHz, $CDCl_3$) 2.01-2.07 (2H, m, CH_2), 2.14-2.20 (2H, m, CH_2), 3.11 (2H, t, *J* 6.3, 8-CH_2), 4.13 (2H, t, *J* 6.1, 11-CH_2) 4.20-4.25 (4H, m, 3,4-CH_2), 5.04 (2H, s, 1-CH_2), 7.52 (1H, s), 7.53 (1H, s); δ_C (100 MHz, $CDCl_3$) 19.5, 21.4 (9,10-CH_2), 24.4 (8-CH_2), 40.8 (4-CH_2), 41.3 (11-CH_2), 62.8 (3-CH_2), 64.4 (1-CH_2), 95.5, 97.7 (6,13-CH), 130.4, 131.4, 138.1, 138.8, 146.9, 151.4 (all C); *m/z* (ESI) 269.1391 ($[M+H]^+$, $C_{15}H_{17}N_4O_2$ requires 269.1402).

Experiment 51: Synthesis of 2,3,7,8,9,10-hexahydro-1*H*-pyrido[1,2-*a*]pyrrolo[1',2':1,2]imidazo[5,4-*f*]benzimidazole (111c)

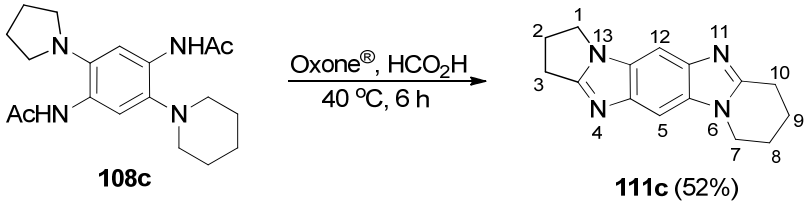

108c **111c** (52%)

Following general procedure 5.3.2, *N,N'*-(2-piperidin-1-yl-5-pyrrolidin-1-yl-1,4-phenylene)diacetamide **108c** (0.467g, 1.4 mmol) and Oxone® (5.164 g, 8.4 mmol) gave the *title compound* **111c** (0.184 g, 52%); white solid; mp 280-290 °C decomp; ν_{max} (neat, cm^{-1}) 2941, 1541, 1484, 1443, 1433, 1412, 1353, 1334, 1313, 1265, 1162, 1131, 1097; δ_H (400 MHz, $CDCl_3$) 2.00-2.02 (2H, m, CH_2), 2.12-2.20 (2H, m, CH_2), 2.70-2.77 (2H, m, 2-CH_2), 3.07-3.12 (4H, m, 3,10-CH_2), 4.11-4.17 (4H, m, 1,7-CH_2), 7.49 (1H, d, *J* 0.7, 5 or 12-H), 7.51 (1H, d, *J* 0.7, 5 or 12-H); δ_C (100 MHz, $CDCl_3$) 20.9, 22.8, 23.9, 25.8 (all CH_2), 26.0 (2-CH_2), 42.6, 43.0 (1,7-CH_2), 97.7 (5,12-CH), 130.0, 132.0, 140.0, 145.7, 152.3, 161.7 (all C); *m/z* (ESI) 253.1453 ($[M+H]^+$, $C_{14}H_{17}N_4$ requires 253.1453).

Experiment 52: Synthesis of 6-nitro-3,4,10,11-tetrahydro-1*H*,8*H*-[1,4]oxazino[4,3-*a*][1,4]oxazino[4',3':1,2]imidazo[5,4-*f*]benzimidazole (121)

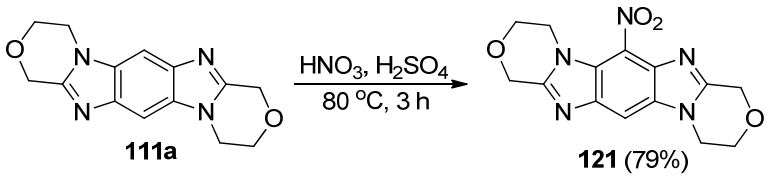

3,4,10,11-Tetrahydro-1*H*,8*H*-[1,4]oxazino[4,3-*a*][1,4]oxazino[4',3':1,2]imidazo[5,4-*f*]benzimidazole **111a** (0.321 g, 1.2 mmol) was heated in concentrate H_2SO_4 (10 mL) and HNO_3 (5 mL) at 80 °C for 3 h. The cooled mixture was diluted with water (100 mL) and neutralized with solid Na_2CO_3. The precipitate was collected, washed with water and dried to give the *title compound* **121** (0.299 g, 79%); yellow solid; mp >350 °C; ν_{max} (neat, cm^{-1}) 3021, 2867, 1501 (NO_2), 1435, 1356 (NO_2), 1331, 1273, 1210, 1116, 1095, 1054; δ_H (400 MHz, $CDCl_3$) 4.18 (2H, t, *J* 5.4, CH_2), 4.27 (4H, s, CH_2CH_2), 4.33 (2H, m, CH_2), 5.09 (2H, s, 1 or 8-CH_2), 5.13 (2H, s, 1 or 8-CH_2), 7.84 (1H, s, 13-H); δ_C (100 MHz, $CDCl_3$) 42.5, 45.6, 63.8, 64.4 (all CH_2), 65.7, 65.8 (1,8-CH_2), 104.1 (13-CH), 125.0, 125.1, 132.3, 134.5, 141.3, 151.1, 152.1 (all C); *m/z* (ESI) 316.1031 ($[M+H]^+$, $C_{14}H_{14}N_5O_4$ requires 316.1046).

Experiment 53: Synthesis of 3,4,10,11-Tetrahydro-1*H*,8*H*-[1,4]oxazino[4,3-*a*][1,4]oxazino[4',3':1,2]imidazo[5,4-*f*]benzimidazol-6,13-dione (124)

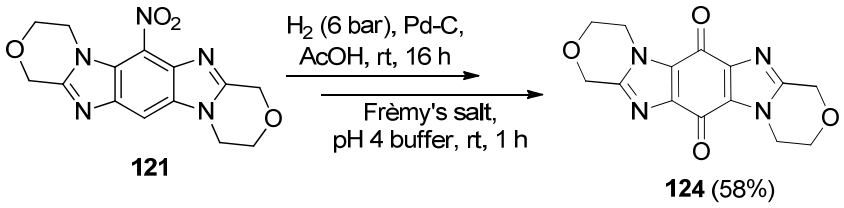

6-Nitro-3,4,10,11-tetrahydro-1*H*,8*H*-[1,4]oxazino[4,3-a][1,4]oxazino[4',3':1,2]imidazo[5,4-*f*]benzimidazole **121** (0.726 g, 2.3 mmol) and Pd-C (5%, 73 mg) were stirred under 6 bar of H_2 in glacial AcOH (50 mL) at room temperature for 16 h. The mixture was filtered, evaporated, and KH_2PO_4 (0.2 M, 100 mL) added. A separate solution of Frèmy's salt (1.852 g, 6.9 mmol) in KH_2PO_4 (0.2 M, 50 mL,) was added, and the mixture stirred at room temperature for 1 h. The precipitate was collected, washed with water and dried to give the *title compound* **124** (0.401 g, 58%): yellow solid; mp >350 °C; ν_{max} (neat, cm^{-1}) 2949, 1664 (C=O), 1502, 1485, 1439, 1369, 1128, 1104, 1051; δ_H (400 MHz, F_3CCO_2H) 4.66 (4H, bs, 4,11-CH_2), 5.00 (4H, bs), 5.59 (4H, bs); δ_C (100 MHz, F_3CCO_2H) 48.7 (4,11-CH_2), 64.4 (CH_2), 65.0 (CH_2), 132.0 (C), 134.3 (C), 152.1 (all C), 167.0 (C=O); *m/z* (ESI) 301.0937 ($[M+H]^+$, $C_{14}H_{13}N_4O_4$ requires 301.0937).

Experiment 54: Synthesis of 3,4,8,9,10,11-hexahydro-1*H*-[1,4]oxazino[4,3-*a*]pyrido[1',2':1,2]imidazo[5,4-*f*]benzimidazol-6,13-dione (125)

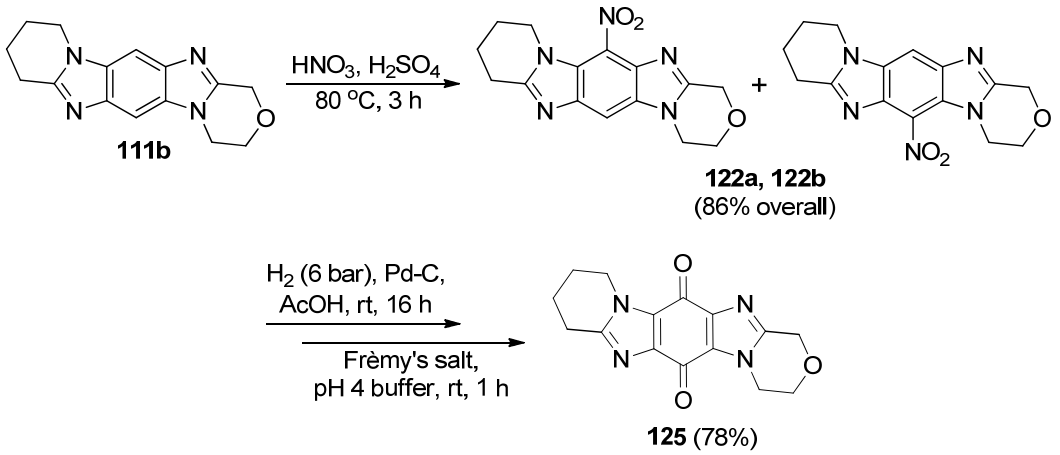

3,4,8,9,10,11-Hexahydro-1*H*-[1,4]oxazino[4,3-*a*]pyrido[1',2':1,2]imidazo[5,4-*f*]benzimidazole **111b** (0.381 g, 1.4 mmol) was heated in concentrated H_2SO_4 (10 mL) and HNO_3 (5 mL) at 80 °C for 3 h. The cooled mixture was diluted with water (100 mL), neutralized with solid Na_2CO_3, and extracted with CH_2Cl_2 (5 x 50 mL). The combined organic extracts were dried (Na_2SO_4) and evaporated to give a mixture of nitro isomers **122a**, **122b** (0.383 g, 86% overall), which were stirred under 6 bar of H_2 in glacial AcOH (50 mL) with Pd-C (5%, 38 mg) at room temperature for 16 h. The mixture was filtered, evaporated and KH_2PO_4 (0.2 M, 100 mL) added. A separate solution of Frèmy's salt (0.966 g, 3.6 mmol) in KH_2PO_4 (0.2 M, 50 mL,) was added, and the mixture stirred at room temperature for 1 h. Extraction with CH_2Cl_2 (5 x 50 mL), drying (Na_2SO_4) and evaporation gave only the quinone *title compound* **125** which was recrystallized from water (0.284 g, 78%): yellow solid; m.p. >350 °C; ν_{max} (neat, cm^{-1}) 2953, 2869, 1657 (C=O), 1496, 1479, 1433, 1374, 1315, 1302, 1249, 1223, 1136, 1116, 1099, 1071, 1045; δ_H (400 MHz, $CDCl_3$) 1.98-2.09 (4H, m, 9,10-CH_2), 2.98 (2H, t, *J* 6.2, 8-CH_2), 4.16 (2H, t, *J* 5.1, 3-CH_2), 4.32 (2H, t, *J* 5.9, 11-CH_2), 4.38 (2H, t, *J* 5.1, 4-CH_2), 4.94 (2H, s, 1-CH_2); δ_C (100 MHz, $CDCl_3$) 19.7, 22.2 (9,10-CH_2), 25.1 (8-CH_2), 45.0 (4-CH_2), 45.7 (11-CH_2), 63.5 (3-CH_2), 65.0 (1-CH_2), 130.3, 130.5, 141.6, 141.7, 147.7, 151.9 (all-C), 171.3, 171.4 (C=O); *m/z* (ESI) 299.1148 ($[M+H]^+$, $C_{15}H_{15}N_4O_3$ requires 299.1144); elemental analysis calcd (%) for $C_{15}H_{14}N_4O_3$: C 60.40, H 4.73, N 18.78; found: C 60.00, H 4.64, N 18.80.

Experiment 55: Synthesis of 2,3,7,8,9,10-hexahydro-1*H*-pyrido[1,2-*a*]pyrrolo[1′,2′:1,2]imidazo[5,4-*f*]benzimidazol-5,12-dione (126)

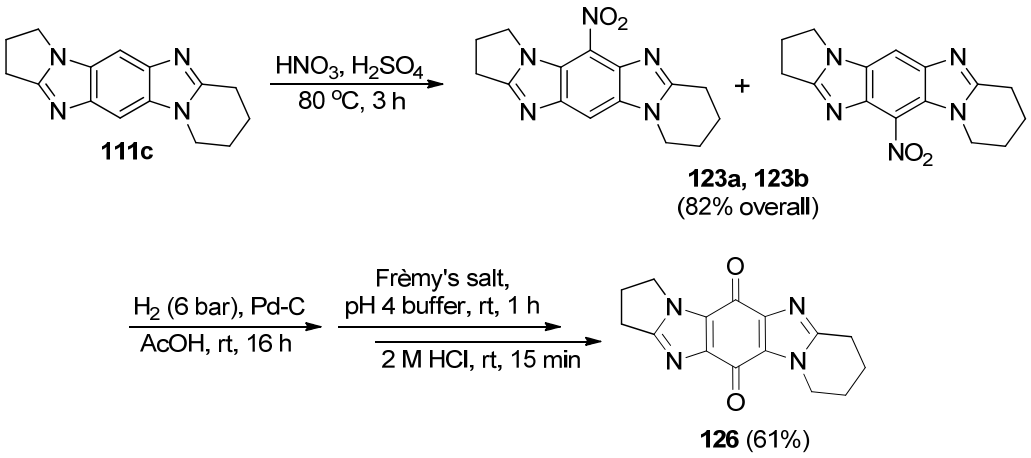

2,3,7,8,9,10-Hexahydro-1*H*-pyrido[1,2-*a*]pyrrolo[1',2':1,2]imidazo[5,4-*f*]benzimidazole **111c** (0.100 g, 0.4 mmol) was heated in concentrated H_2SO_4 (10 mL) and HNO_3 (5 mL) at 80 °C for 3 h. The cooled mixture was diluted with water (100 mL), neutralized with solid Na_2CO_3, and extracted with CH_2Cl_2 (5 x 50 mL). The combined organic extracts were dried (Na_2SO_4) and evaporated to give a mixture of nitro isomers **123a**, **123b** (97 mg, 82% overall), which were stirred under 6 bar of H_2 in glacial AcOH (50 mL) with Pd-C (5%, 38 mg) at room temperature for 16 h. The mixture was filtered, evaporated and KH_2PO_4 (0.2 M, 100 mL) added. A separate solution of Frèmy's salt (0.966 g, 3.6 mmol) in KH_2PO_4 (0.2 M, 50 mL,) was added, and the mixture stirred at room temperature for 1 h. Extraction with CH_2Cl_2 (5 x 50 mL), drying (Na_2SO_4) and evaporation gave a mixture of compounds containing ~30% of iminoquinone. HCl (2 M, 50 mL) was added to the residue and the solution stirred for 15 min. The acid solution was neutralized with solid Na_2CO_3 and extracted with CH_2Cl_2 (5 x 50 mL). The combined organic extracts were dried (Na_2SO_4), evaporated and recrystallized from water to give the *title compound* **126** (56 mg, 61%); yellow solid; mp >350 °C; ν_{max} (neat, cm^{-1}) 2952, 2871, 1654 (C=O), 1482, 1440, 1404, 1375, 1302, 1270, 1222, 1164, 1072, 1043; δ_H (400 MHz, $CDCl_3$) 1.96-2.08 (4H, m, 8,9-CH_2), 2.68-2.76 (2H, m, 2-CH_2), 2.93-2.99 (4H, m, 3,10-CH_2), 4.28 (2H, t, *J* 7.2, 1 or 7-CH_2), 4.34 (2H, t, *J* 5.9, 1 or 7-CH_2); δ_C (100 MHz, $CDCl_3$) 19.8, 22.3 (8,9-CH_2), 23.1, 25.1 (3,10-CH_2), 26.5 (2-CH_2), 45.4, 45.7 (1,7-CH_2),

129.9, 130.8, 141.3, 146.3, 151.4, 160.3 (all-C), 171.2, 171.9 (C=O); *m/z* (ESI) 283.1187 ($[M+H]^+$, $C_{15}H_{15}N_4O_2$ requires 283.1195).

5.4 Experimental for Chapter 4

5.4.1 Cell culture and cytotoxicity evaluation

5.4.1.1 Cell lines

An SV40-transformed normal human skin fibroblast cell line (repository number GM00637) was obtained from the National Institute for General Medical Sciences (NIGMS) Human Genetic Cell Repository (Coriell Institute for Medical Research, New Jersey, USA). The HeLa cervical cancer cell line (repository number CCL-2) was obtained from the American Type Culture Collection (ATCC). The DU-145 prostate cancer cell line (ATCC repository number HTB-81) was obtained from Prof. R.W.G Watson, School of Medicine & Medical Science, University College Dublin, Ireland.

5.4.1.2 Cell culture

The SV40-transformed normal human skin fibroblast cell line (GM00637) was grown in minimum essential media (MEM) Eagle-Earle BSS supplemented with 15% heat-inactivated fetal bovine serum (FBS), penicillin-streptomycin, 2 mM L-glutamine, 2x essential and non-essential amino acids, and vitamins. HeLa-CCL-2 cervical cancer cells were grown in Dulbecco's modified Eagle's medium (DMEM) supplemented with 10% heat-inactivated fetal bovine serum, penicillin-streptomycin, 2 mM L-glutamine, and MEM non-essential amino acids. DU-145 prostate cancer cells were grown in RPMI-1640 medium supplemented with 10% heat-inactivated fetal bovine serum, penicillin-streptomycin and 2 mM L-glutamine.

5.4.1.3 Cytotoxicity measurement using the MTT assay

Cell viability was determined using the MTT colorimetric assay.[137] Normal cells were plated into 96-well plates at a density of 10,000 cells per well (200 μL per

well), and allowed to adhere over a period of 24 h. HeLa cells were plated into 96-well plates at a density of 1000 cells per well (100 μL per well) and allowed to adhere over a period of 24 h. DU-145 cells were plated into 96-well plates at a density of 2000 cells per well (200 μL per well) and allowed to adhere over a period of 24 h.

Compound solutions were applied in ethanol or ethanol/H_2O (1% final concentration in well), and the plates were incubated at 37 °C under a humidified atmosphere containing 5% CO_2 for 72 h. Control cells were exposed to an equivalent concentration of ethanol or ethanol/H_2O alone. **MMC** (Sigma) solutions were applied in DMSO (1% final concentration in well) and the plates were incubated at 37 °C under a humidified atmosphere containing 5% CO_2 for 72 h. Control cells were exposed to an equivalent concentration of DMSO alone. MTT (20 μL, 5 mg/ml solution) was added, and the cells were incubated for another 3 h. The supernatant was removed carefully by pipetting. The resultant MTT formazan crystals were dissolved in 100 μL of DMSO and absorbance was determined on a plate reader at 550 nm with a reference at 690 nm. Cell viability is expressed as a percentage of the EtOH/H_2O, EtOH or DMSO-only treated value. Dose–response curves were analysed by nonlinear regression analysis and IC_{50} values were estimated using GraphPad Prism software, v. 5.02 (GraphPad Inc., San Diego, CA, USA).

5.4.2 Computational methods

The crystallographic coordinates of human NQO1 (1D4A) were obtained from the RCSB Protein Data Bank. The physiological dimer was employed in all calculations, prior adding of hydrogen atoms to the protein and the prostetic group (FAD), assigning the appropriate ionization state at pH 7. The ligands were built in MOE. All structures of ligands, enzyme model (NQO1 physiological dimer) and enzyme-ligand complexes were geometry minimized using the AMBER99 molecular mechanics force field[151] to within an rms gradient of 0.05 kcal mol^{-1} $Å^{-1}$. Throughout, all systems were also surrounded by a distance distance dependent dielectric model of bulk water ($E_{SOL} = 0$, $E_{ELECTROSTATIC} = q_i q_j / 4\pi\varepsilon_0 r_{ij}^2$). To obtain a relaxed geometry of the initial receptor, a short molecular dynamics (MD)

simulations was performed, followed by a final energy minimization step. The MD simulation of the NQO1 dimer was performed using a canonical ensemble (NVT), with initial temperature 150 K; heating for 50 ps; simulation temperature 300 K; duration 500 ps; time step 1 fs; temperature response 1 ps; pressure response 0.5 ps and constraint tolerance $1x10^{-9}$ ps. After the MD simulation, a final energy minimization was performed. The resulting protein model was used in the docking studies.

Possible active sites in the receptor model were identified by using Alpha Site Finder.[152] Once defined, ligands were docked into the enzyme retaining 500 poses using the alpha triangle placement methodology with affinity ΔG as scoring function as implemented in MOE. In the docking studies, flexible ligand structures were generated using a Monte Carlo algorithm, whereas the receptor was held fixed according to the minimized geometries.

Best scored binding orientations for each ligand were energy minimized, subjected to MD simulation using the same settings as above and finally energy minimized, using in all stages the AMBER99 force field. The potential energy of the final complex was calculated ($E_{complex}$). The ligand was then moved away from the protein, the non-interacting system energy minimized, and the potential energy of the separated moieties calculated ($E_{enz} + E_{ligand}$). Substracting this from $E_{complex}$ gives the interaction energy (I.E.) reported herein. Several properties were calculated for each best scored complex, using the LigX procedure,[142] such as the affinity, hydrogen bond interactions, van der Waals interactions and π-π interactions.

References

[1] W. A. Denny, *Cancer Invest.* **2004**, *22*, 604-619.

[2] J. Scaife, D. Kerr, in *Anticancer Therapeutics*, 1st ed., Missailidis, S., John Wiley & Sons Ltd, **2008**, pp. 97-100.

[3] A. P. Francisco, M. D. J. Perry, R. Moreira, E. Mendes, in *Anticancer Therapeutics*, 1st ed., Missailidis, S., John Wiley & Sons Ltd, **2008**, pp. 137-138.

[4] F. J. Alcaín, J. M. Villalba, *Expert Opin. Ther. Patents* **2007**, *17*, 649-665.

[5] W. A. Denny, *Expert Opin. Ther. Patents* **2005**, *15*, 635-646.

[6] X. Shi, S. M. Mandel, M. S. Platz, *J. Am. Chem. Soc.* **2007**, *129*, 4542-4550.

[7] M. Jaffar, I. J. Stratford, *Expert Opin. Ther. Patents* **1999**, *9*, 1371-1380.

[8] F. Jiang, Q. Weng, R. Sheng, Q. Xia, Q. He, B. Yang, Y. Hu, *Arch. Pharm. Chem. Life Sci.* **2007**, *340*, 258-263.

[9] S. R. McKeown, R. L. Cowen, K. J. Williams, *J. Clin. Oncol.* **2007**, *19*, 427-442.

[10] L. Garuti, M. Roberti, D. Pizzirani, *Mini-Rev. Med. Chem.* **2007**, *7*, 481-489.

[11] M. Jaffar, N. Abou-Zeid, L. Bai, I. Mrema, I. Robinson, R. Tanner, I. Stratford, *Current Drug Del.* **2004**, *1*, 345-350.

[12] M. A. Colucci, C. J. Moody, G. D. Couch, *Org. Biomol. Chem.* **2008**, *6*, 637-656.

[13] G. S. Kumar, R. Lipman, J. Cummings, M. Tomasz, *Biochem.* **1997**, *36*, 14128-14136.

[14] A. S. Cotterill, C. J. Moody, R. J. Mortimer, C. L. Norton, N. O'Sullivan, M. A. Stephens, N. R. Stradiotto, E. Swann, I. J. Stratford, *J. Med. Chem.* **1994**, *37*, 3834-3843.

[15] M. A. Naylor, E. Swann, S. A. Everett, M. Jaffar, J. Nolan, N. Robertson, S. D. Lockyer, K. B. Patel, M. F. Dennis, M. R. L. Stratford, P. Wardman, G. E. Adams, C. J. Moody, I. J. Stratford, *J. Med. Chem.* **1998**, *41*, 2720-2731.

[16] H. D. Beall, S. Winski, E. Swann, A. R. Hudnott, A. S. Cotterill, N. O'Sullivan, S. J. Green, R. Bien, D. Siegel, D. Ross, C. J. Moody, *J. Med. Chem.* **1998**, *41*, 4755-4766.

[17] M. Hernick, C. Flader, R. F. Borch, *J. Med. Chem.* **2002**, *45*, 3540-3548.

[18] M. Hernick, R. F. Borch, *J. Med. Chem.* **2003**, *46*, 148-154.

[19] E. B. Skibo, W. G. Schulz, *J. Med. Chem.* **1993**, *36*, 3050-3055.

[20] E. B. Skibo, A. Jamil, B. Austin, D. Hansen, A. Ghodousi, *Org. Biomol. Chem.* **2010**, *8*, 1577-1587.

[21] A. Ghodousi, X. Huang, Z. Cheng, E. B. Skibo, *J. Med. Chem.* **2004**, *47*, 90-100.

[22] J. O'Shaughnessy, F. Aldabbagh, *Synthesis* **2005**, *7*, 1069-1076.

[23] J. O'Shaughnessy, D. Cunningham, P. Kavanagh, D. Leech, P. McArdle, F. Aldabbagh, *Synlett* **2004**, *13*, 2382-2384.

[24] S. Hehir, L. O'Donovan, M. P. Carty, F. Aldabbagh, *Tetrahedron* **2008**, *64*, 4196-4203.

[25] M. Lynch, S. Hehir, P. Kavanagh, D. Leech, J. O'Shaughnessy, M. P. Carty, F. Aldabbagh, *Chem. Eur. J.* **2007**, *13*, 3218-3226.

[26] K. Fahey, F. Aldabbagh, *Tetrahedron Lett.* **2008**, *49*, 5235-5237.

[27] K. Fahey, L. O'Donovan, M. Carr, M. P. Carty, F. Aldabbagh, *Eur. J. Med. Chem.,* **2010**, *45*, 1873-1879.

[28] L. O'Donovan, M. P. Carty, F. Aldabbagh, *Chem. Commun.* **2008**, 5592-5594.

[29] S. Bonham, L. O'Donovan, M. P. Carty, F. Aldabbagh, *Org. Biomol. Chem* **2011**, DOI: 10.1039/C1031OB05694H.

[30] L. Garuti, M. Roberti, D. Pizzirani, A. Pession, E. Leoncini, V. Cenci, S. Hrelia, *Il Farmaco* **2004**, *59*, 663-668.

[31] E. Moriarty, M. Carr, S. Bonham, M. P. Carty, F. Aldabbagh, *Eur. J. Med. Chem.* **2010**, *45*, 3762-3769.

[32] W. G. Schulz, I. Islam, E. B. Skibo, *J. Med. Chem.* **1995**, *38*, 109-118.

[33] R. Zhou, E. B. Skibo, *J. Med. Chem.* **1996**, *39*, 4321-4331.

[34] W. G. Schulz, E. B. Skibo, *J. Med. Chem.* **2000**, *43*, 629-638.

[35] A. Suleman, E. B. Skibo, *J. Med. Chem.* **2002**, *45*, 1211-1220.

[36] C. Asche, *Mini-Rev. Med. Chem.* **2005**, *5*, 449-467.

[37] A. Bolognese, G. Correale, M. Manfra, A. Lavecchia, O. Mazzoni, E. Novellino, P. La Colla, G. Sanna, R. Loddo, *J. Med. Chem.* **2004**, *47*, 849-858.

[38] M.-E. Suh, M.-J. Kang, H.-W. Yoo, S.-Y. Park, C.-O. Lee, *Bioorg. Med. Chem.* **2000**, *8*, 2079-2083.

[39] M.-E. Suh, M.-J. Kang, S.-Y. Park, *Bioorg. Med. Chem.* **2001**, *9*, 2987-2991.

[40] U. Pindur, M. Haber, K. Sattler, *J. Chem. Educ.* **1993**, *70*, 263-269.

[41] A. Bodely, L. F. Liu, M. Israel, R. Seshadri, Y. Koseki, F. C. Giuliani, S. Kirschenbaum, R. Silber, M. Potmesil, *Cancer Res.* **1989**, *49*, 5969-5978.

[42] J. S. Kim, H.-J. Lee, M.-E. Suh, H.-Y. P. Choo, S. K. Lee, H. J. Park, C. Kim, S. W. Park, C.-O. Lee, *Bioorg. Med. Chem.* **2004**, *12*, 3683-3686.

[43] B. R. Copp, C. M. Ireland, L. R. Barrows, *J. Org. Chem.* **1991**, *56*, 4596-4597.

[44] H. Hoang, X. Huang, E. B. Skibo, *Org. Biomol. Chem.* **2008**, *6*, 3059-3064.

[45] W. R. Bowman, J. M. D. Storey, *Chem. Soc. Rev.* **2007**, *36*, 1803-1822.

[46] G. J. Rowlands, *Tetrahedron* **2009**, *65*, 8603-8655.

[47] F. Aldabbagh, W. R. Bowman, *Tetrahedron Lett.* **1997**, *38*, 3793-3794.

[48] S. Caddick, K. Aboutayab, R. I. West, *J. Chem. Soc., Chem. Commun.* **1995**, 1353-1354.

[49] S. Caddick, K. Aboutayab, K. Jenkins, R. I. West, *J. Chem. Soc., Perkin Trans. 1* **1996**, 675-682.

[50] F. Aldabbagh, W. R. Bowman, *Tetrahedron* **1999**, *55*, 4109-4122.

[51] S. Caddick, C. L. Shering, S. N. Wadman, *Tetrahedron* **2000**, *56*, 465-473.

[52] M. L. E. N. da Mata, W. B. Motherwell, F. Ujjainwalla, *Tetrahedron Lett.* **1997**, *38*, 137-140.

[53] M. L. E. N. da Mata, W. B. Motherwell, F. Ujjainwalla, *Tetrahedron Lett.* **1997**, *38*, 141-114.

[54] W. B. Motherwell, A. M. K. Pennell, *J. Chem. Soc., Chem. Commun.* **1991**, 877-879.

[55] D. L. J. Clive, S. Kang, *Tetrahedron Lett.* **2000**, *41*, 1315-1319.

[56] D. L. J. Clive, S. Kang, *J. Org. Chem.* **2001**, *66*, 6083-6091.

[57] M. A. Clyne, F. Aldabbagh, *Org. Biomol. Chem.* **2006**, *4*, 268-277.

[58] P. J. Bunyan, D. H. Hey, *J. Chem. Soc.* **1960**, 3787-3790.

[59] B. B. Snider, R. Mohan, S. A. Kates, *J. Org. Chem.* **1985**, *50*, 3659-3661.

[60] L. J. Johnston, J. Lusztyk, D. D. M. Wayner, A. N. Abeywickreyma, A. L. J. Beckwith, J. C. Scaiano, K. U. Ingold, *J. Am. Chem. Soc.* **1985**, *107*, 4594-4596.

[61] F. Minisci, F. Fontana, G. Pianese, Y. M. Yan, *J. Org. Chem.* **1993**, *58*, 4207-4211.

[62] M. Ballestri, C. Chatgilialoglu, M. Guerra, A. Guerrini, M. Lucarini, G. Seconi, *J. Chem. Soc. Perkin Trans. 2* **1993**, 421-425.

[63] A. L. Castelhano, D. Griller, *J. Am. Chem. Soc.* **1982**, *104*, 3655-3659.

[64] F. Minisci, E. Vismara, F. Fontana, *J. Org. Chem.* **1989**, *54*, 5224-5227.

[65] D. P. Curran, C. P. Jasperse, M. J. Totleben, *J. Org. Chem.* **1991**, *56*, 7169-7172.

[66] J. Clayden, N. Greeves, S. Warren, P. Wothers, in *Organic Chemistry*, 1st ed., Oxford University Press, **2000**, pp. 1020-1052.

[67] J. C. Scaiano, L. C. Stewart, *J. Am. Chem. Soc.* **1983**, *105*, 3609-3614.

[68] A. Citterio, F. Minisci, O. Porta, G. Sesana, *J. Am. Chem. Soc.* **1977**, *99*, 7960-7968.

[69] L. J. Johnston, J. C. Scaiano, K. U. Ingold, *J. Am, Chem. Soc.* **1984**, *106*, 4877-4881.

[70] T. Shono, I. Nishiguchi, *Tetrahedron* **1974**, *30*, 2183-2190.

[71] V. Martínez-Barrasa, A. G. de Viedma, C. Burgos, J. Alvarez-Builla, *Org. Lett.* **2000**, *2*, 3933-3935.

[72] P. T. F. McLoughlin, M. A. Clyne, F. Aldabbagh, *Tetrahedron* **2004**, *60*, 8065-8071.

[73] A. Fiumana, K. Jones, *Tetrahedron Lett.* **2000** *41*, 4209-4211.

[74] D. C. Harrowven, M. I. T. Nunn, D. R. Fenwick, *Tetrahedron Lett.* **2002**, *43*, 3185-3187.

[75] D. C. Harrowven, I. L. Guy, L. Nanson, *Angew. Chem. Int. Ed.* **2006**, *45*, 2242 -2245.

[76] D. C. Harrowven, B. J. Sutton, S. Coulton, *Tetrahedron* **2002**, *58*, 3387-3400.

[77] D. C. Harrowven, B. J. Sutton, S. Coulton, *Org. Biomol. Chem.* **2003**, *1*, 4047-4057.

[78] W. R. Bowman, H. Heaney, B. M. Jordan, *Tetrahedron* **1991**, *47*, 10119–10128.

[79] F. Aldabbagh, M. A. Clyne, *Lett. Org. Chem.* **2006**, *3*, 510-513.

[80] D. P. Curran, A. I. Keller, *J. Am. Chem. Soc.* **2006**, *128*, 13706-13707.

[81] F. Minisci, E. Vismara, F. Fontana, *Heterocycles* **1989**, *28*, 489-519.

[82] A. L. J. Beckwith, J. M. D. Storey, *J. Chem. Soc., Chem. Commun.* **1995**, 977-978.

[83] J. M. D. Storey, M. M. Ladwa, *Tetrahedron Lett.* **2006**, *47*, 381-383.

[84] G. Pavé, S. Usse-Versluys, M.-C. Viaud-Massuard, G. Guillaumet, *Org. Lett.* **2003**, *5*, 4253-4256.

[85] F. Gagosz, C. Moutrille, S. Z. Zard, *Org. Lett.* **2002**, *4*, 2707-2709.

[86] F. Gagosz, S. Z. Zard, *Org. Lett.* **2002**, *4*, 4345-4348.

[87] Y. M. Osornio, L. D. Miranda, R. Cruz-Almanza, J. M. Muchowski, *Tetrahedron Lett.* **2004**, *45*, 2855-2858.

[88] F. Aldabbagh, W. R. Bowman, E. Mann, A. M. Z. Slawin, *Tetrahedron* **1999**, *55*, 8111-8128.

[89] F. Aldabbagh, W. R. Bowman, E. Mann, *Tetrahedron Lett.* **1997**, *38*, 7937-7940.

[90] S. M. Allin, W. R. S. Barton, W. R. Bowman, T. McInally, *Tetrahedron Lett.* **2002**, *43*, 4191-4193.

[91] S. M. Allin, W. R. S. Barton, W. R. Bowman, E. Bridge, M. R. J. Elsegood, T. McInally, V. McKee, *Tetrahedron* **2008**, *64*, 7745-7758.

[92] A. J. Boydston, K. A. Williams, C. W. Bielawski, *J. Am. Chem. Soc.* **2005**, *127*, 12496-12497.

[93] A. J. Boydston, P. D. Vu, O. L. Dykhno, V. Chang, A. R. Wyatt, A. S. Stockett, E. T. Ritschdorff, J. B. Shear, C. W. Bielawski, *J. Am. Chem. Soc.* **2008**, *130*, 3143-3156.

[94] D. P. Curran, A. A. Martin-Esker, S.-B. Ko, M. Newcomb, *J. Org. Chem.* **1993**, *58*, 4691-4695.

[95] W. R. Bowman, P. T. Stephenson, N. K. Terrett, A. R. Young, *Tetrahedron* **1995**, *51*, 7959-7980.

[96] D. L. J. Clive, W. Yang, *Chem. Commun.* **1996**, 1605-1606.

[97] M. Koreeda, Y. Wang, L. Zhang, *Org. Lett.* **2002**, *4*, 3329-3332.

[98] M.-L. Bennasar, T. Roca, F. Ferrando, *Tetrahedron Lett.* **2004**, *45*, 5605-5609.

[99] M.-L. Bennasar, T. Roca, F. Ferrando, *Org. Lett.* **2006**, *8*, 561-564.

[100] W. R. Bowman, A. J. Fletcher, J. M. Pedersen, P. J. Lovell, M. R. J. Elsegood, E. H. López, V. McKee, G. B. S. Potts, *Tetrahedron* **2007**, *63*, 191-203.

[101] B. Sjorberg, S. Herdevall, *Acta Chem. Scand.* **1958**, *12*, 1347-1348.

[102] S. M. Allin, W. R. Bowman, R. Karim, S. S. Rahman, *Tetrahedron* **2006**, *62*, 4306-4316.

[103] M.-L. Bennasar, T. Roca, R. Griera, J. Bosch, *J. Org. Chem.* **2001**, *66*, 7547-7551.

[104] I. Baxter, D. W. Cameron, *J. Chem. Soc. (C)* **1968**, 1747-1752.

[105] O. Meth-Cohn, H. Suschitsky, *J. Chem. Soc.* **1963**, 4666-4669.

[106] I. P. Beletskaya, A. S. Sigeev, V. A. Kuzmin, A. S. Tatikolov, L. Hevesi, *J. Chem. Soc., Perkin Trans. 2* **2000**, 107-109.

[107] W. K. Busfieid, l. D. Jenkins, P. VanLe, *Polym. Bull.* **1997**, *38*, 149-155.

[108] D. N. Jones, D. Mundy, R. D. Whitehouse, *Chem. Commun.* **1970**, 86-87.

[109] H. J. Reich, J. M. Renga, I. L. Reich, *J. Am. Chem. Soc.* **1975**, *97*, 5434-5447.

[110] V. Fagan, S. Bonham, M. P. Carty, F. Aldabbagh, *Org. Biomol. Chem.* **2010**, *8*, 3149-3156.

[111] I. Islam, E. B. Skibo, *J. Org. Chem.* **1990**, *55*, 3195-3205.

[112] G. P. Moss, *Pure & Appl. Chem* **1998**, *70*, 143-216.

[113] O. Meth-Cohn, H. Suschitzky, *Adv. Heterocycl. Chem.* **1972**, *14*, 211-278.

[114] O. Meth-Cohn, *Adv. Heterocycl. Chem.* **1996**, *65*, 1-37.

[115] W. Verboom, D. N. Reinhoudt, R. Visser, S. Harkema, *J. Org. Chem.* **1984**, *49*, 269-276.

[116] D. N. Reinhoudt, G. W. Visser, W. Verboom, P. H. Benders, M. L. M. Pennings, *J. Am. Chem. Soc.* **1983**, *105*, 4775-4781.

[117] R. K. Grantham, O. Meth-Cohn, M. A. Naqui, *J. Chem. Soc. (C)* **1969**, 1438-1443.

[118] R. Fielden, O. Meth-Cohn, H. Suschitzky, *J. Chem. Soc., Perkin Trans. 1* **1973**, 696-701.

[119] R. K. Grantham, O. Meth-Cohn, *J. Chem. Soc. (C)* **1969**, 70-74.

[120] I. Islam, E. B. Skibo, *J. Med. Chem.* **1991**, *34*, 2954-2961.

[121] E. B. Skibo, W. G. Schulz, *J. Med. Chem.* **1993**, *36*, 3050-3055.

[122] E. B. Skibo, I. Islam, M. J. Heileman, W. G. Schulz, *J. Med. Chem.* **1994**, *37*, 78-92.

[123] O. Meth-Cohn, R. K. Smalley, H. Suschitzky, *J. Chem. Soc.* **1963**, 1666-1669.

[124] J. A. VanAllan, G. A. Reynolds, R. E. Adel, *J. Org. Chem.* **1963**, *28*, 524-527.

[125] M. D. Nair, R. Adams, *J . Am. Chem. Soc.* **1961**, *83*, 3518-3521.

[126] M. Polonovski, *Bull. Soc. Chim. Fra.* **1927**, *41*, 1186-1190.

[127] O. Meth-Cohn, *J. Chem. Soc. (C)* **1971**, 1356-1357.

[128] E. B. Skibo, S. Gordon, L. Bess, R. Boruah, M. J. Heileman, *J. Med. Chem.* **1997**, *40*, 1327-1339.

[129] D. V. Kosynkin, J. M. Tour, *Org. Lett.* **2001**, *3*, 993-995.

[130] R. Adams, M. D. Nair, *J . Am. Chem. Soc.* **1956**, *78*, 5932-5938.

[131] J. Clayden, N. Greeves, S. Warren, P. Wothers, in *Organic Chemistry*, 1st ed., Oxford University Press, **2000**, pp. 589-595.

[132] R. I. Bello, C. Gómez-Díaz, F. Navarro, F. J. Alcaín, J. M. Villalba, *J. Biol. Chem.* **2001**, *276*, 44379-44384.

[133] S. A. Fitzsimonns, P. Workman, M. Grever, K. Paull, R. Camalier, A. D. Lewis, *J. Natl. Cancer Inst.* **1996**, *88*, 259-269.

[134] J. M. Kolesar, S. C. Pritchard, K. M. Kerr, K. Kim, M. C. Nicolson, H. McLeod, *Int. J. Oncol.* **2002**, *21*, 1119-1124.

[135] L. Ernster, F. Navazio, *Acta Chem. Scand.* **1958**, *12*, 595-602.

[136] R. Li, M. A. Bianchet, P. Talalay, L. M. Amzel, *Proc. Natl. Acad. Sci. USA* **1995**, *92*, 8846-8850.

[137] T. Mosmann, *J. Immunol. Methods* **1983**, *65*, 55-63.

[138] R. H. Shoemaker, *Nat. Rev. Cancer* **2006**, *6*, 813-823.

[139] M. R. Boyd, K. D. Paull, *Drug Dev. Res.* **1995**, *34*, 91-109

[140] K. D. Paull, C. M. Lin, L. Malspeis, E. Hamel, *Cancer Res.* **1992**, *52*, 3892-3900.

[141] A. Wallqvist, A. A. Rabow, R. H. Shoemaker, E. A. Sausville, D. G. Covell, *Bioinformatics* **2003**, *19*, 2212-2224.

[142] in *Chemical Computing Group*, version 2009.10 ed., Montreal, QC, **2009**.

[143] M. A. Bianchet, M. Faig, L. M. Amzel, *Methods Enzymol.* **2004**, *382*, 144-174.

[144] M. Faig, M. A. Bianchet, P. Talalay, S. Chen, S. Winski, D. Ross, L. M. Amzel, *Proc. Natl. Acad. Sci. U.S.A.* **2000**, *97*, 3177-3182.

[145] L. Bai, W.-G. Zhu, *J. Cancer Mol.* **2006**, *2*, 141-153.

[146] A. Bolognese, G. Correale, M. Manfra, A. Lavecchia, O. Mazzoni, E. Novellino, V. Barone, A. Pani, E. Tramontano, P. La Colla, C. Murgioni, I. Serra, G. Setzu, R. Loddo, *J. Med. Chem.* **2002**, *45*, 5205-5216.

[147] S. Chen, K. Wu, D. Zhang, M. Sherman, R. Knox, C. S. Yang, *Molecular Pharmacol.* **1999**, *56*, 272-278.

[148] X. Huang, A. Suleman, E. B. Skibo, *Bioorg. Chem.* **2000**, *28*, 324-337.

[149] L. M. Harwood, *Aldrichim. Acta.* **1985**, *18*, 25.

[150] D. S. Pedersen, C. Rosenbohm, *Synthesis* **2001**, 2431-2434.

[151] J. W. Ponder, D. A. Case, *Adv. Protein Chem.* **2003**, *66*, 27-85.

[152] H. Edelsbrunner, M. Facello, R. Fu, J. Liang, in *Proceedings of the 28th Hawaii International Conference on Systems Science*, **1995**, pp. 256–264.

Appendix

A.1 X-Ray crystallographic data

Table A.1; X-ray crystallographic data and structure refinement for *N*,*N'*-[2,5-Bis(4-oxidomorpholin-4-yl)-1,4-phenylene]diacetamide **112**.

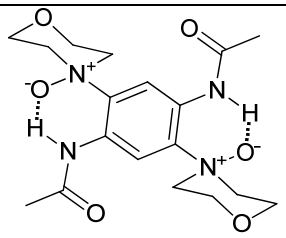

112

CCDC reference number	816319
Empirical formula	$C_{18}H_{26}N_4O_6.H_2O$
Formula weight	412.44
Temperature	297.7 K
Wavelength	0.7107 Å
Crystal system	Monoclinic
Space group	$P2_1/c$
Unit cell dimensions	a = 9.5842(4)Å
	b = 13.9491(5)Å β = 99.019(4)º
	c = 7.4995(3)Å
Volume	990.23(7) $Å^3$
Z	2
Density (calculated)	1.383 Mg/m^3
Absorption coefficient	0.107 mm^{-1}
F(000)	440
Crystal size	0.35 x 0.30 x 0.18 mm
Theta range for data collection	2.9154 to 29.0433 º.
Index ranges	-9<=h<=9; -11<=k<=19; -12<=l<=12
Reflections collected	4418
Independent reflections	1805 [R_{int} = 0.0177]
Reflections observed (>2σ)	1406
Data Completeness	0.999
Absorption correction	Semi-empirical from equivalents
Max. and min. transmission	1.00000 and 0.99824
Refinement method	Full-matrix least-squares on F^2
Data / restraints / parameters	1805 / 1 / 142
Goodness-of-fit on F^2	1.110
Final R indices [I>2σ(I)]	R_1 = 0.0450 wR_2 = 0.1385
R indices (all data)	R_1 = 0.0604 wR_2 = 0.1516
Largest diff. peak and hole	0.242 and -0.167 e.$Å^{-3}$

Table A.2; X-ray crystallographic data and structure refinement for 3,4,10,11-tetrahydro-1*H*,8*H*-[1,4]oxazino[4,3-*a*][1,4]oxazino[4',3':1,2]imidazo[5,4-*f*]benzimidazolium-6,13-dione di(trifluoroacetate) [**124**].2F_3CCO_2H.

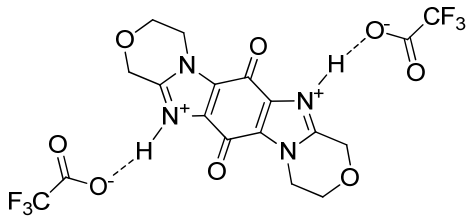

[**124**].2F_3CCO_2H

CCDC reference number	816444
Empirical formula	$C_{18}H_{14}F_6N_4O_8$
Formula weight	528.33
Temperature	295.2 K
Wavelength	0.7107 Å
Crystal system	Triclinic
Space group	P-1
Unit cell dimensions	a = 8.0719(8)Å α = 88.162(10)º
	b = 8.0863(10)Å β = 81.560(9)º
	c = 8.7199(10)Å γ = 67.525(10)º
Volume	520.06(10) $Å^3$
Z	1
Density (calculated)	1.687 Mg/m^3
Absorption coefficient	0.166 mm^{-1}
F(000)	268
Crystal size	0.50 x 0.45 x 0.15 mm
Theta range for data collection	3.0447 to 28.9983 º.
Index ranges	-10<=h<=5; -10<=k<=10; -11<=l<=11
Reflections collected	3921
Independent reflections	1911 [R_{int} = 0.0280]
Reflections observed (>2σ)	1248
Data Completeness	0.998
Absorption correction	Semi-empirical from equivalents
Max. and min. transmission	1.00000 and 0.92247
Refinement method	Full-matrix least-squares on F^2
Data / restraints / parameters	1911 / 0 / 163
Goodness-of-fit on F^2	1.038
Final R indices [I>2σ(I)]	R_1 = 0.0620 wR_2 = 0.1502
R indices (all data)	R_1 = 0.1001 wR_2 = 0.1771
Largest diff. peak and hole	0.412 and -0.318 e.$Å^{-3}$

A.2 MTT assay cell viability graphs

1,2,3,4,8,9,10,11-Octahydropyrido[1,2-*a*]pyrido[1′,2′:1,2]imidazo[4,5-*f*]benzimidazol-6,13-dione (16)

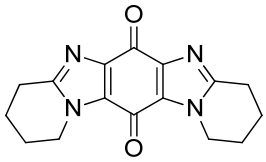

16

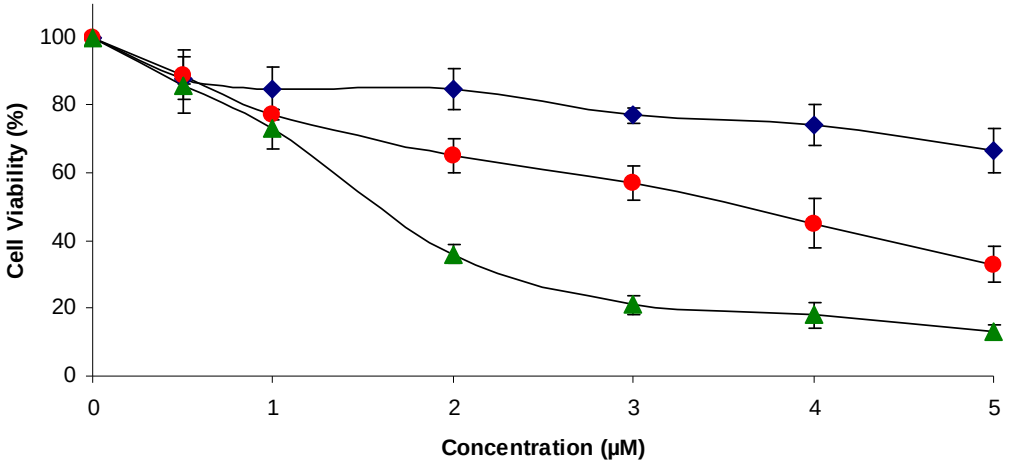

Figure A.1; Viability of normal human skin fibroblast (GM00637) (♦), HeLa (CCL-2) (●) and DU145 (HTB-81) (▲) cell lines determined using the MTT assay following treatment with 1,2,3,4,8,9,10,11-octahydropyrido[1,2-*a*] pyrido[1′,2′:1,2]imidazo[4,5-*f*]benzimidazol-6,13-dione **16** under aerobic conditions for 72 h at 37°C. Each data point is the mean of at least three independent experiments. The lines shown are trend lines.

1,5-Dibutylimidazo[5,4-*f*]benzimidazol-4,8-dione (71)

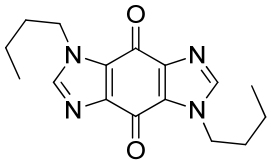

71

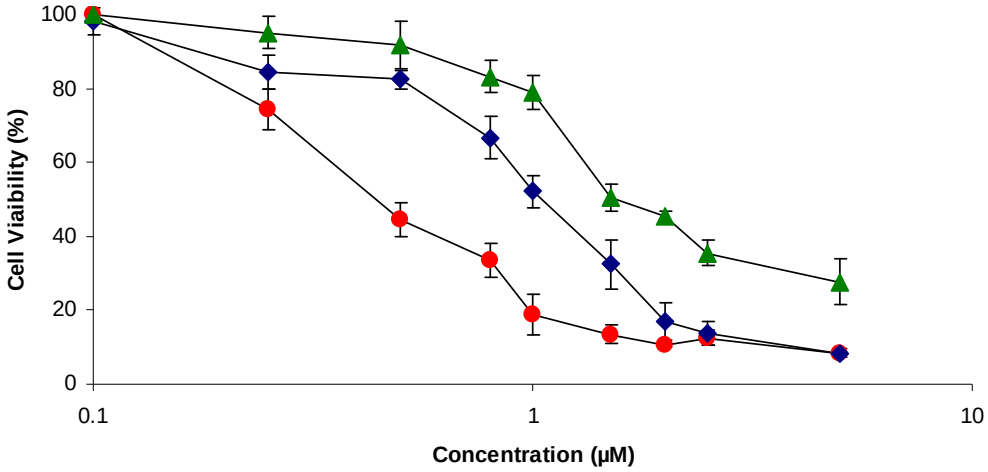

Figure A.2; Viability of normal human skin fibroblast (GM00637) (♦), HeLa (CCL-2) (●) and DU145 (HTB-81) (▲) cell lines determined using the MTT assay following treatment with 1,5-dibutylimidazo[5,4-*f*]benzimidazol-4,8-dione **71** under aerobic conditions for 72 h at 37°C. Each data point is the mean of at least three independent experiments. The lines shown are trend lines.

3-Butyl-6,7,8,9-tetrahydroimidazo[5,4-*f*]pyrido[1,2-*a*]benzimidazol-4,11-dione (72)

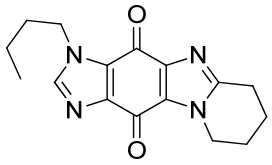

72

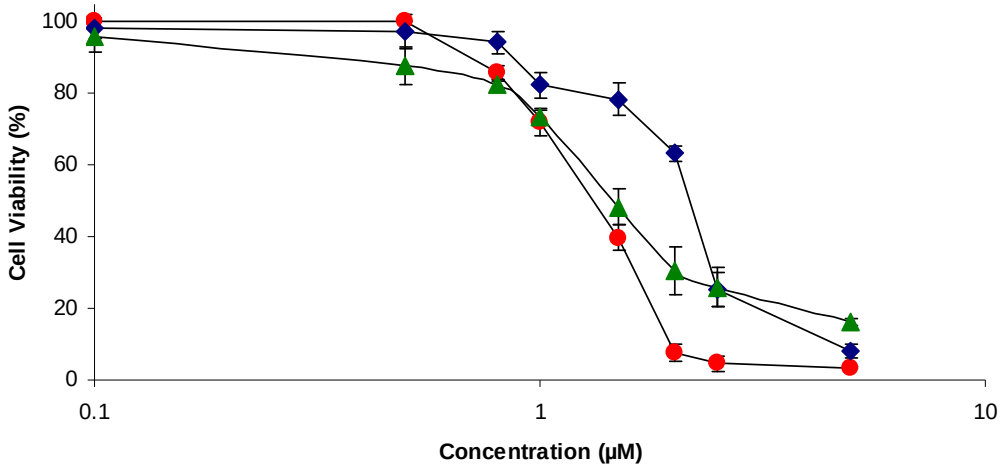

Figure A.3; Viability of normal human skin fibroblast (GM00637) (♦), HeLa (CCL-2) (●) and DU145 (HTB-81) (▲) cell lines determined using the MTT assay following treatment with 3-butyl-6,7,8,9-tetrahydro-imidazo[5,4-*f*]pyrido[1,2-*a*]benzimidazol-4,11-dione **72** under aerobic conditions for 72 h at 37°C. Each data point is the mean of at least three independent experiments. The lines shown are trend lines.

6-Imino-1,2,3,4,8,9,10,11-octahydropyrido[1,2-*a*]pyrido[1′,2′:1,2]imidazo[5,4-*f*]benzimidazol-13-one (73b)

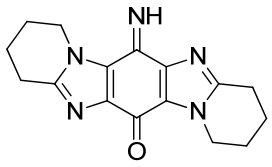

73b

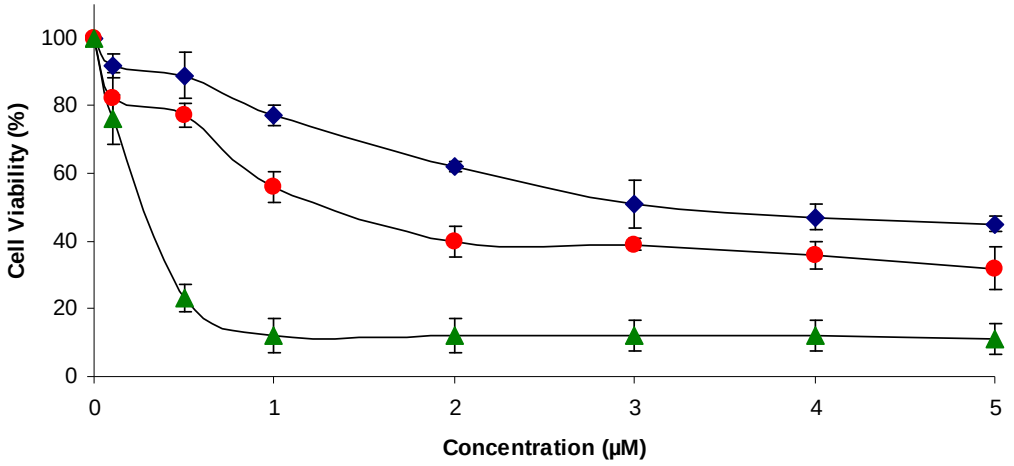

Figure A.4; Viability of normal human skin fibroblast (GM00637) (♦), HeLa (CCL-2) (●) and DU145 (HTB-81) (▲) cell lines determined using the MTT assay following treatment with 6-imino-1,2,3,4,8,9,10,11-octahydropyrido[1,2-*a*] pyrido[1′,2′:1,2]imidazo[5,4-*f*]benzimidazol-13-one **73b** under aerobic conditions for 72 h at 37°C. Each data point is the mean of at least three independent experiments. The lines shown are trend lines.

1,2,3,4,8,9,10,11-Octahydropyrido[1,2-*a*]pyrido[1′,2′:1,2]imidazo[5,4-*f*]benzimidazol-6,13-dione (74b)

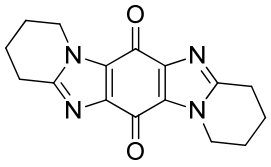

74b

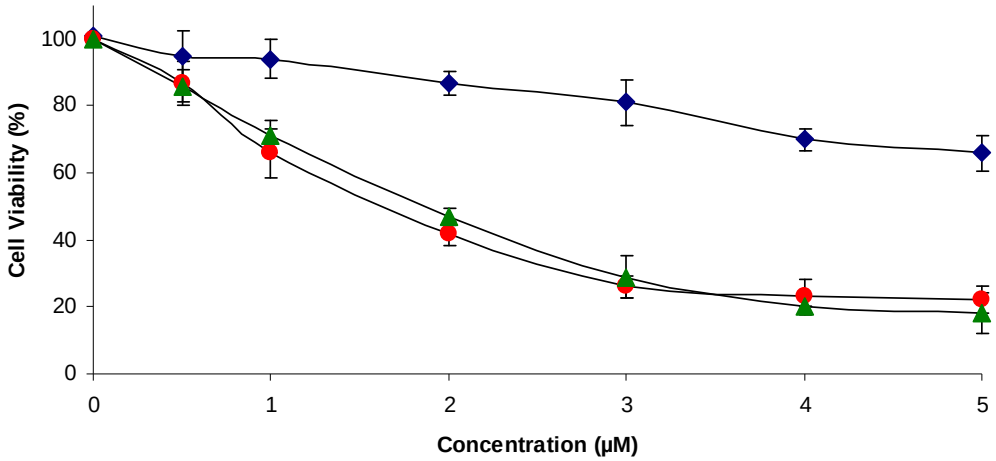

Figure A.5; Viability of normal human skin fibroblast (GM00637) (♦), HeLa (CCL-2) (●) and DU145 (HTB-81) (▲) cell lines determined using the MTT assay following treatment with 1,2,3,4,8,9,10,11-octahydropyrido[1,2-*a*] pyrido[1′,2′:1,2]imidazo[5,4-*f*]benzimidazol-6,13-dione **74b** under aerobic conditions for 72 h at 37°C. Each data point is the mean of at least three independent experiments. The lines shown are trend lines.

2,3,4,5,10,11,12,13-Octahydro-1*H*,9*H*-azepino[1,2-*a*]azepino[1′,2′:1,2]imidazo[5,4-*f*]benzimidazol-7,15-dione (74c)

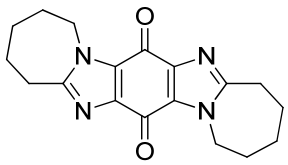

74c

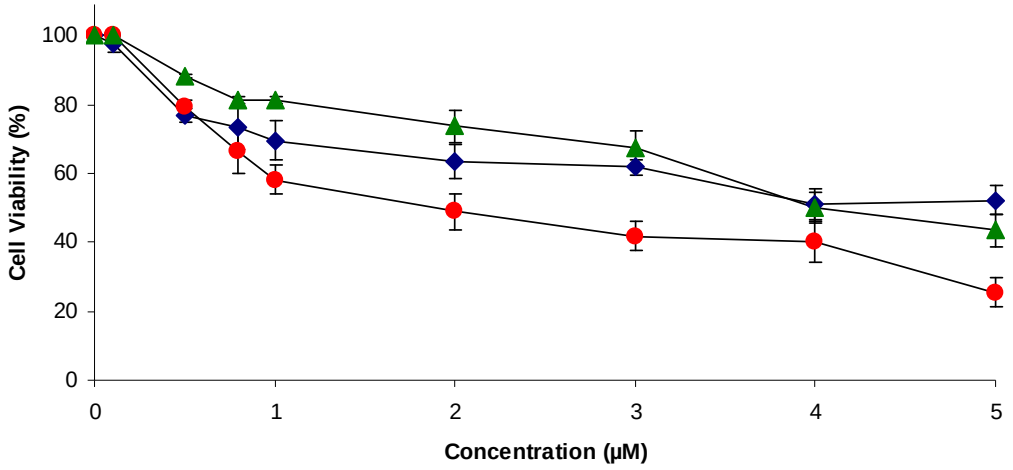

Figure A.6; Viability of normal human skin fibroblast (GM00637) (♦), HeLa (CCL-2) (●) and DU145 (HTB-81) (▲) cell lines determined using the MTT assay following treatment with 2,3,4,5,10,11,12,13-octahydro-1*H*,9*H*-azepino[1,2-*a*]azepino[1′,2′:1,2]imidazo[5,4-*f*]benzimidazol-7,15-dione **74c** under aerobic conditions for 72 h at 37°C. Each data point is the mean of at least three independent experiments. The lines shown are trend lines.

3,4,8,9,10,11-Hexahydro-1*H*-[1,4]oxazino[4,3-*a*]pyrido[1',2':1,2]imidazo[5,4-*f*]benzimidazol-6,13-dione (125)

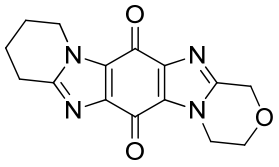

125

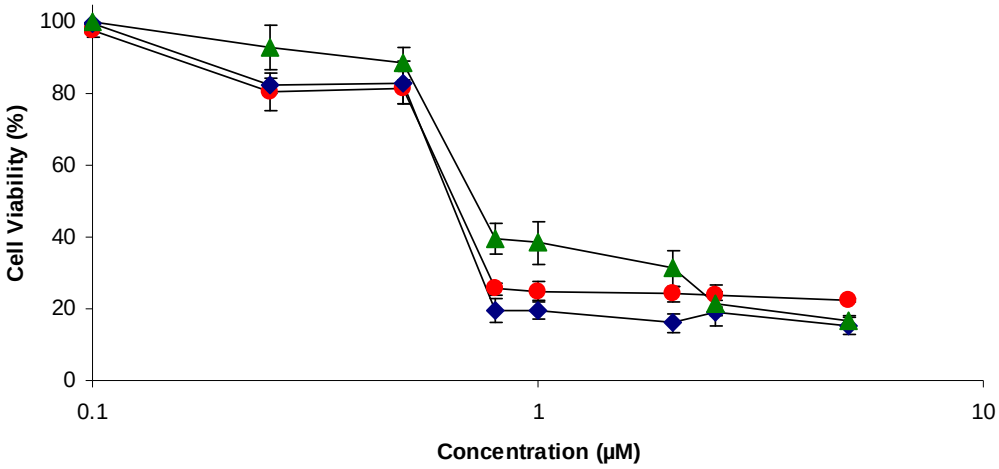

Figure A.7; Viability of normal human skin fibroblast (GM00637) (♦) HeLa (CCL-2) (●) and DU145 (HTB-81) (▲) cell lines cell lines determined using the MTT assay following treatment with 3,4,8,9,10,11-hexahydro-1*H*-[1,4]oxazino[4,3-*a*]pyrido[1′,2′:1,2]imidazo[5,4-*f*]benzimidazol-6,13-dione **125** under aerobic conditions for 72 h at 37°C. Each data point is the mean of at least three independent experiments. The lines shown are trend lines.

2,3,7,8,9,10-hexahydro-1*H*-pyrido[1,2-*a*]pyrrolo[1′,2′:1,2]imidazo[5,4-*f*]benzimidazol-5,12-dione (126)

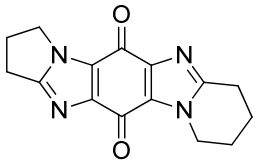

126

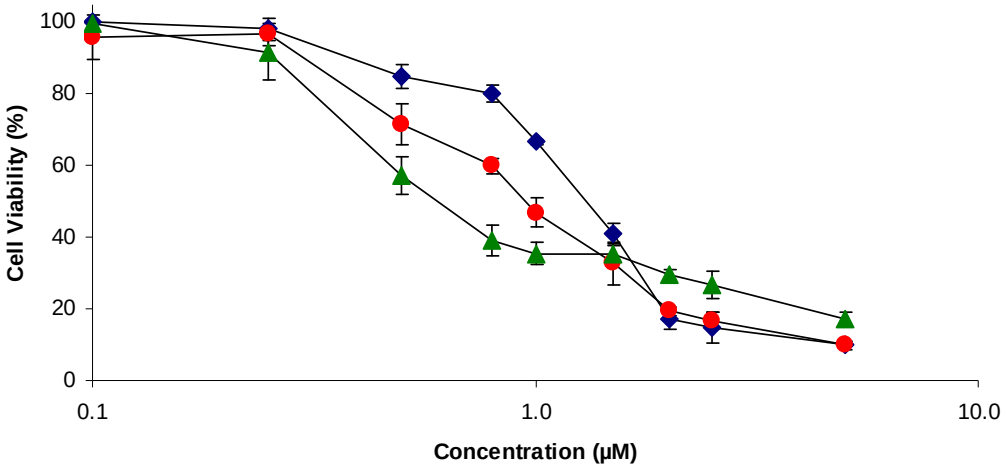

Figure A.8; Viability of normal human skin fibroblast (GM00637) (♦) HeLa (CCL-2) (●) and DU145 (HTB-81) (▲) cell lines cell lines determined using the MTT assay following treatment with 2,3,7,8,9,10-hexahydro-1*H*-pyrido[1,2-*a*]pyrrolo[1′,2′:1,2]imidazo[5,4-*f*]benzimidazol-5,12-dione **126** under aerobic conditions for 72 h at 37°C. Each data point is the mean of at least three independent experiments. The lines shown are trend lines.

A.3 DTP NCI-60 mean growth percent graphs

3-Butyl-6,7,8,9-tetrahydroimidazo[5,4-*f*]pyrido[1,2-*a*]benzimidazol-4,11-dione (72)

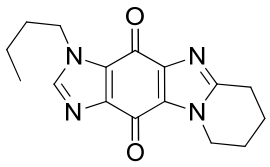

NSC 756996

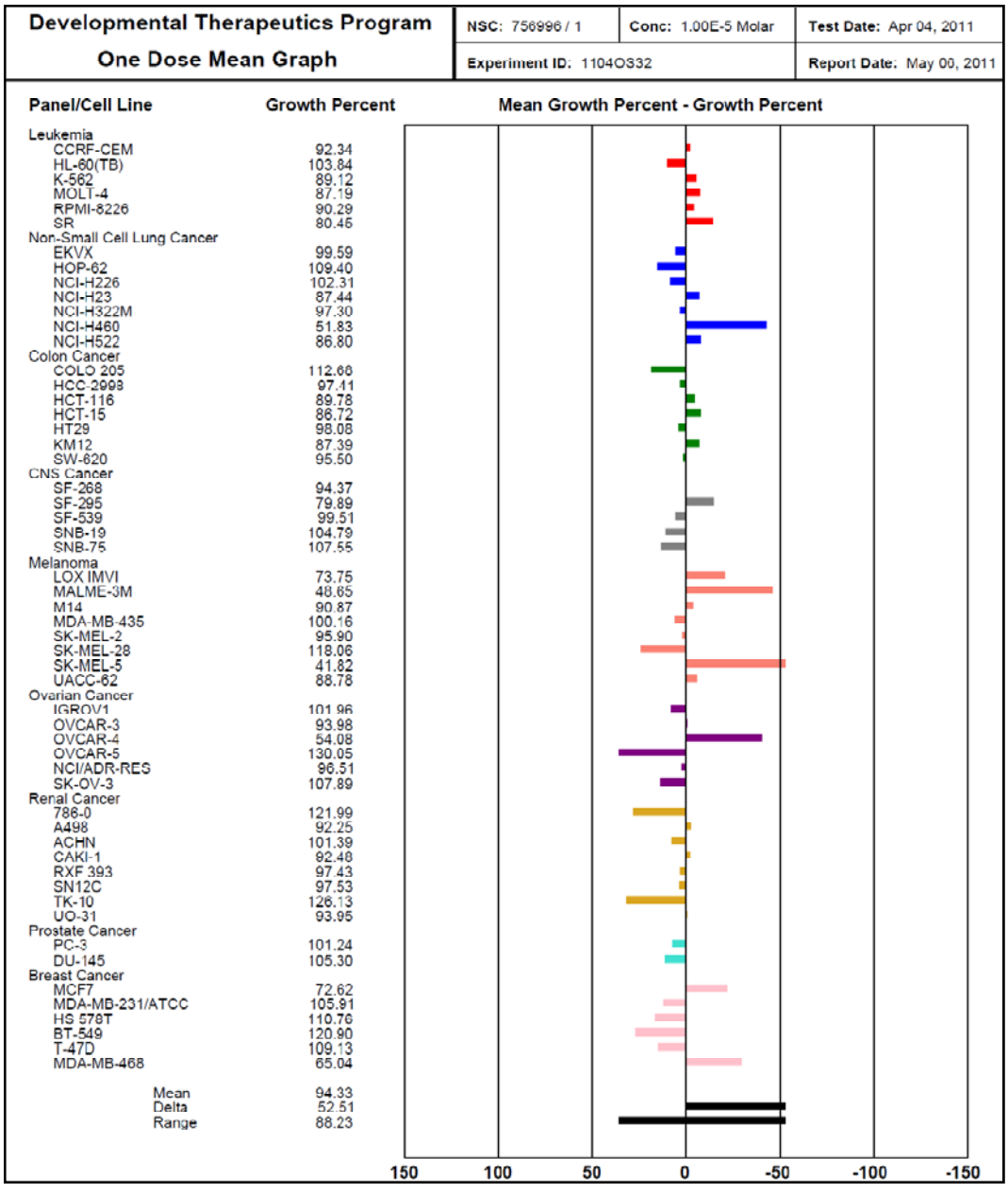

Developmental Therapeutics Program	NSC: 756996 / 1	Conc: 1.00E-5 Molar	Test Date: Apr 04, 2011
One Dose Mean Graph	Experiment ID: 1104OS32		Report Date: May 06, 2011

Panel/Cell Line	Growth Percent
Leukemia	
CCRF-CEM	92.34
HL-60(TB)	103.84
K-562	89.12
MOLT-4	87.19
RPMI-8226	90.29
SR	80.45
Non-Small Cell Lung Cancer	
EKVX	99.59
HOP-62	109.40
NCI-H226	102.31
NCI-H23	87.44
NCI-H322M	97.30
NCI-H460	51.83
NCI-H522	86.80
Colon Cancer	
COLO 205	112.66
HCC-2998	97.41
HCT-116	89.78
HCT-15	86.72
HT29	98.08
KM12	87.39
SW-620	95.50
CNS Cancer	
SF-268	94.37
SF-295	79.89
SF-539	99.51
SNB-19	104.79
SNB-75	107.55
Melanoma	
LOX IMVI	73.75
MALME-3M	48.65
M14	90.87
MDA-MB-435	100.16
SK-MEL-2	95.90
SK-MEL-28	118.06
SK-MEL-5	41.82
UACC-62	88.78
Ovarian Cancer	
IGROV1	101.96
OVCAR-3	93.98
OVCAR-4	54.08
OVCAR-5	130.05
NCI/ADR-RES	96.51
SK-OV-3	107.89
Renal Cancer	
786-0	121.99
A498	92.25
ACHN	101.39
CAKI-1	92.48
RXF 393	97.43
SN12C	97.53
TK-10	126.13
UO-31	93.95
Prostate Cancer	
PC-3	101.24
DU-145	105.30
Breast Cancer	
MCF7	72.62
MDA-MB-231/ATCC	105.91
HS 578T	110.76
BT-549	120.90
T-47D	109.13
MDA-MB-468	65.04
Mean	94.33
Delta	52.51
Range	88.23

Mean Growth Percent - Growth Percent

150 100 50 0 -50 -100 -150

6-Imino-1,2,3,4,8,9,10,11-octahydropyrido[1,2-*a*]pyrido[1′,2′:1,2]imidazo[5,4-*f*]benzimidazol-13-one (73b)

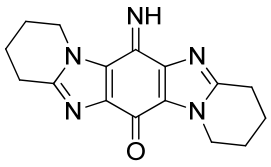

NSC 753790

Developmental Therapeutics Program

One Dose Mean Graph

NSC: 753790 / 1	Conc: 1.00E-5 Molar	Test Date: Jul 26, 2010
Experiment ID: 1007OS90		Report Date: Oct 15, 2010

Panel/Cell Line	Growth Percent
Leukemia	
CCRF-CEM	92.92
HL-60(TB)	96.34
K-562	81.43
MOLT-4	85.39
RPMI-8226	82.23
SR	69.53
Non-Small Cell Lung Cancer	
A549/ATCC	-30.65
EKVX	95.60
HOP-62	52.30
NCI-H226	57.10
NCI-H23	-70.36
NCI-H322M	27.71
NCI-H460	4.62
NCI-H522	10.51
Colon Cancer	
COLO 205	-88.60
HCC-2998	87.31
HCT-116	65.82
HCT-15	6.18
HT29	-13.67
KM12	66.70
SW-620	23.70
CNS Cancer	
SF-268	71.34
SF-295	-85.69
SF-539	-21.72
SNB-19	30.00
SNB-75	-97.04
U251	50.65
Melanoma	
LOX IMVI	-68.04
M14	-95.62
MDA-MB-435	-82.54
SK-MEL-2	82.74
SK-MEL-28	-67.22
SK-MEL-5	-98.00
UACC-257	-6.60
UACC-62	-85.09
Ovarian Cancer	
OVCAR-3	98.43
OVCAR-4	96.21
OVCAR-5	-57.79
OVCAR-8	91.47
NCI/ADR-RES	85.71
SK-OV-3	95.03
Renal Cancer	
786-0	88.99
A498	52.05
ACHN	69.43
CAKI-1	88.78
RXF 393	94.79
SN12C	-86.09
TK-10	128.36
UO-31	46.94
Prostate Cancer	
PC-3	90.55
DU-145	-93.91
Breast Cancer	
MCF7	-6.98
MDA-MB-231/ATCC	82.60
HS 578T	-28.65
BT-549	-37.18
T-47D	71.89
MDA-MB-468	68.06
Mean	24.00
Delta	122.00
Range	226.36

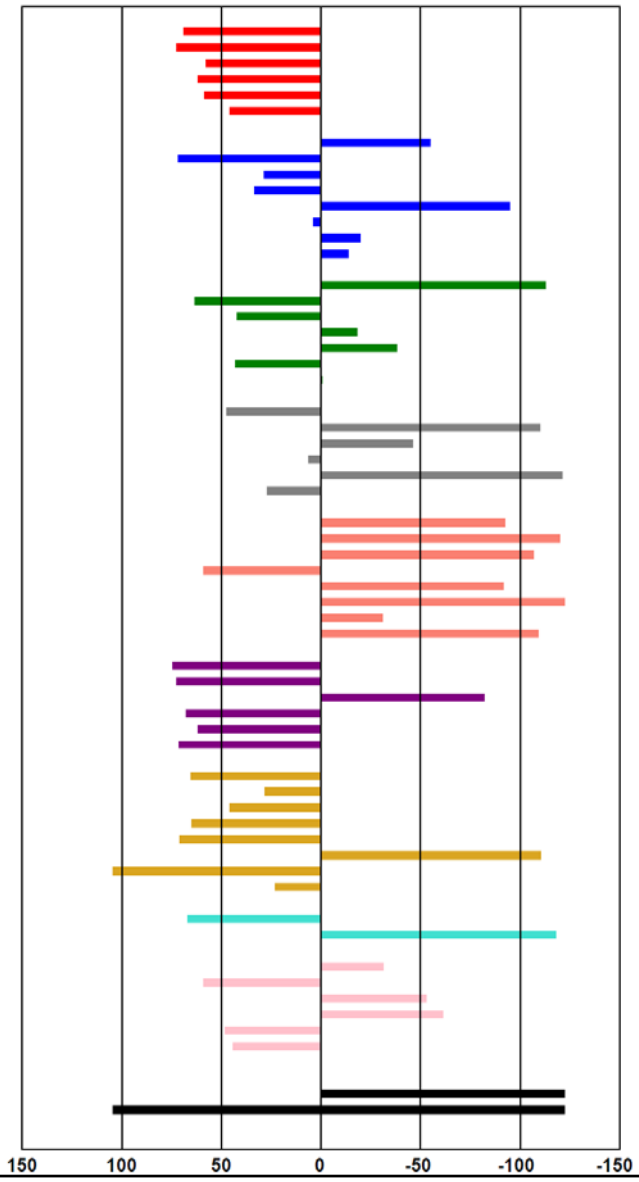

6-Imino-1,2,3,4,8,9,10,11-octahydropyrido[1,2-*a*]pyrido[1′,2′:1,2]imidazo[5,4-*f*]benzimidazol-13-one (73b) (5 Dose testing)

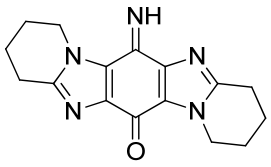

NSC 753790

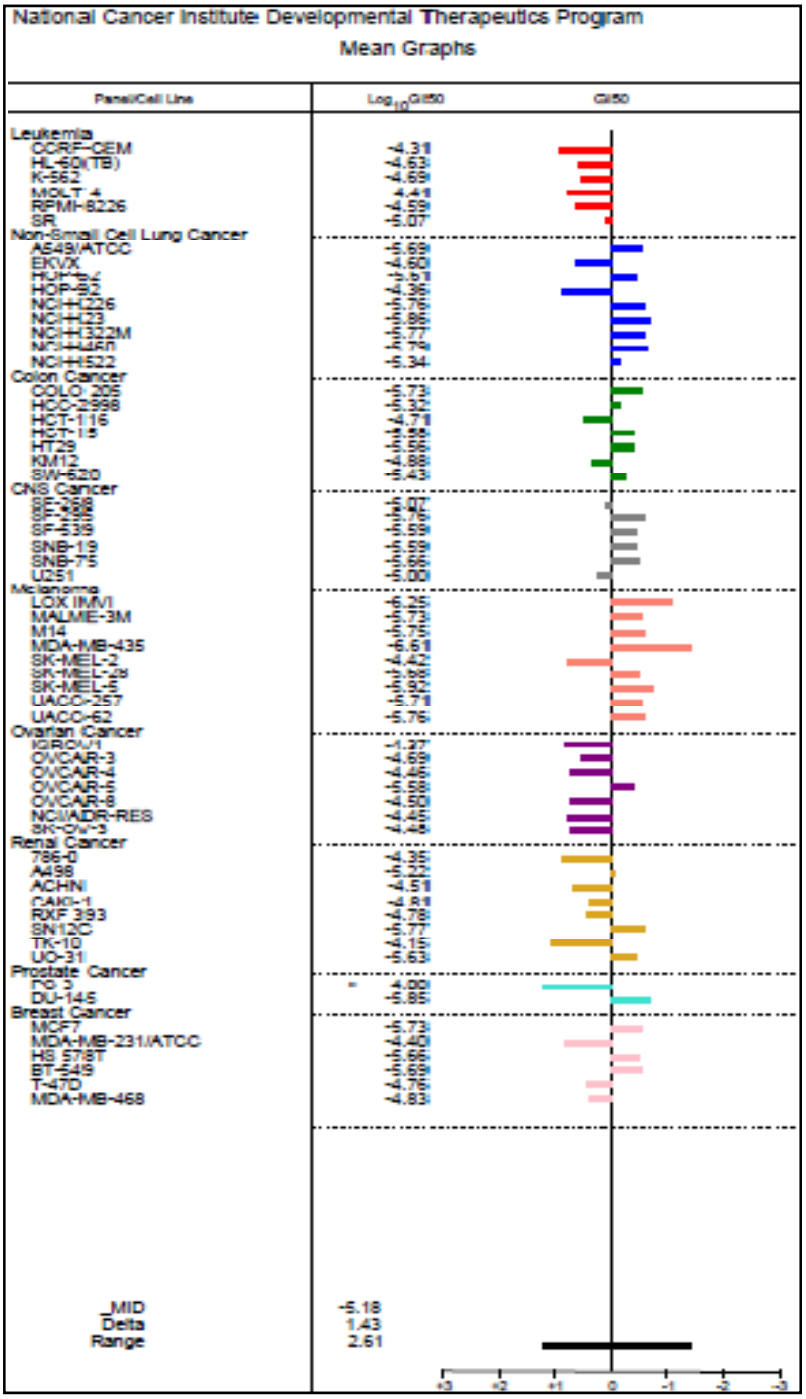

7-Imino-2,3,4,5,10,11,12,13-octahydro-1*H*,9*H*-azepino[1,2-*a*]azepino[1′,2′:1,2]imidazo[5,4-*f*]benzimidazol-15-one (73c)

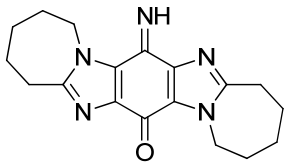

NSC 756995

Developmental Therapeutics Program

One Dose Mean Graph

NSC: 756995 / 1	Conc: 1.00E-5 Molar	Test Date: Apr 04, 2011
Experiment ID: 1104OS32		Report Date: May 06, 2011

Panel/Cell Line	Growth Percent
Leukemia	
CCRF-CEM	104.45
HL-60(TB)	103.28
K-562	102.03
MOLT-4	93.73
RPMI-8226	99.11
SR	91.79
Non-Small Cell Lung Cancer	
EKVX	102.84
HOP-62	121.77
HOP-92	126.16
NCI-H226	98.25
NCI-H23	97.32
NCI-H322M	109.57
NCI-H460	92.57
NCI-H522	90.90
Colon Cancer	
HCC-2998	112.19
HCT-116	107.20
HCT-15	109.05
HT29	105.86
KM12	105.97
SW-620	104.97
CNS Cancer	
SF-268	108.00
SF-295	93.85
SF-539	105.41
SNB-19	113.27
SNB-75	104.89
Melanoma	
LOX IMVI	92.00
MALME-3M	103.35
M14	108.14
MDA-MB-435	110.69
SK-MEL-2	117.92
SK-MEL-28	117.98
SK-MEL-5	98.69
UACC-62	110.42
Ovarian Cancer	
IGROV1	129.59
OVCAR-3	110.94
OVCAR-4	93.24
OVCAR-5	122.82
NCI/ADR-RES	110.20
SK-OV-3	106.74
Renal Cancer	
786-0	120.00
A498	91.57
ACHN	104.79
CAKI-1	95.10
RXF 393	101.92
SN12C	106.21
TK-10	141.83
UO-31	83.65
Prostate Cancer	
PC-3	113.24
DU-145	113.23
Breast Cancer	
MCF7	94.48
MDA-MB-231/ATCC	117.19
HS 578T	112.26
BT-549	109.99
T-47D	115.93
MDA-MB-468	99.84
Mean	106.33
Delta	22.68
Range	58.18

Mean Growth Percent - Growth Percent

150 100 50 0 -50 -100 -150

2,3,8,9-Tetrahydro-1*H*,7*H*-pyrrolo[1,2-*a*]pyrrolo[1′,2′:1,2]imidazo[5,4-*f*]benzimidazol-5,11-dione (74a)

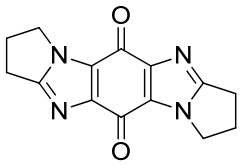

NSC 755325

Developmental Therapeutics Program	NSC: 755325 / 1	Conc: 1.00E-5 Molar	Test Date: Dec 20, 2010
One Dose Mean Graph	Experiment ID: 1012OS74		Report Date: Jan 26, 2011

Panel/Cell Line	Growth Percent
Leukemia	
CCRF-CEM	105.93
HL-60(TB)	101.79
K-562	103.12
MOLT-4	103.75
RPMI-8226	96.85
SR	97.86
Non-Small Cell Lung Cancer	
A549/ATCC	96.08
EKVX	84.07
HOP-62	112.71
NCI-H226	95.19
NCI-H23	91.34
NCI-H322M	100.56
NCI-H460	67.44
NCI-H522	93.35
Colon Cancer	
COLO 205	122.51
HCC-2998	104.86
HCT-116	93.94
HCT-15	99.71
HT29	100.46
KM12	84.70
SW-620	108.14
CNS Cancer	
SF-268	101.06
SF-295	99.37
SF-539	113.89
SNB-19	105.63
SNB-75	116.55
U251	104.64
Melanoma	
LOX IMVI	78.75
M14	96.60
MDA-MB-435	102.47
SK-MEL-2	85.16
SK-MEL-28	126.36
SK-MEL-5	64.03
UACC-257	79.27
UACC-62	106.67
Ovarian Cancer	
IGROV1	112.66
OVCAR-3	103.55
OVCAR-4	105.29
OVCAR-5	103.41
OVCAR-8	98.71
NCI/ADR-RES	93.98
SK-OV-3	104.68
Renal Cancer	
786-0	112.12
A498	88.07
ACHN	104.08
CAKI-1	94.12
RXF 393	113.99
SN12C	104.22
TK-10	109.69
UO-31	81.47
Prostate Cancer	
PC-3	93.04
DU-145	112.21
Breast Cancer	
MCF7	95.97
MDA-MB-231/ATCC	107.96
HS 578T	121.31
T-47D	106.28
MDA-MB-468	88.88
Mean	100.01
Delta	35.98
Range	62.33

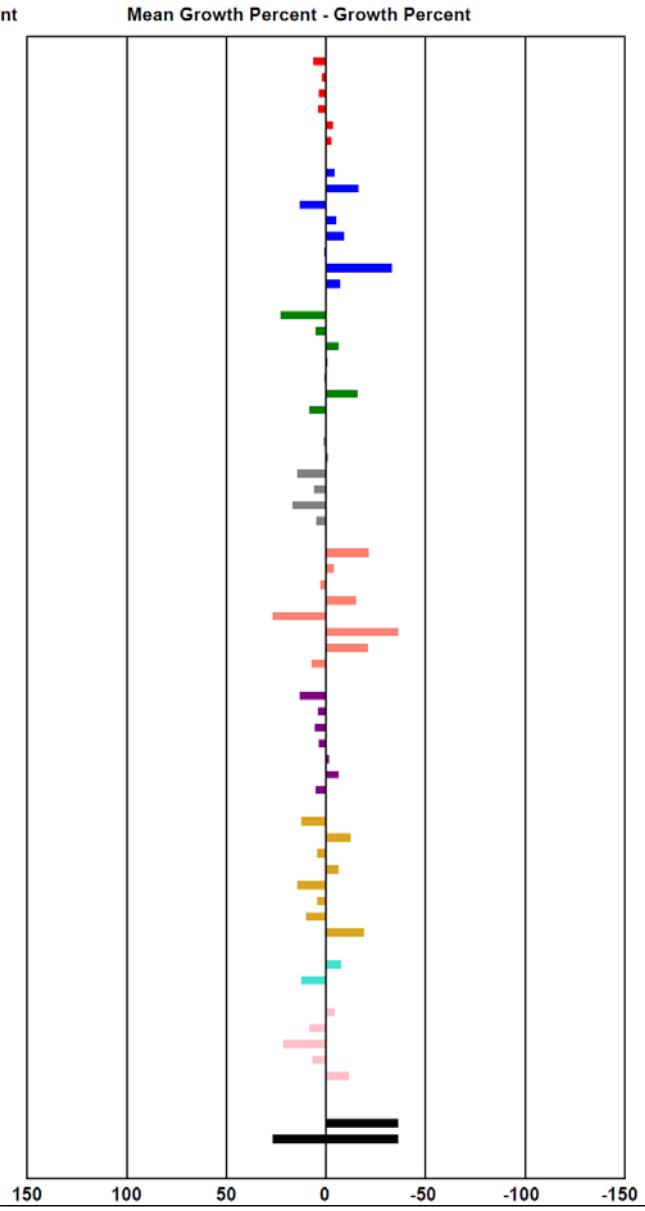

1,2,3,4,8,9,10,11-Octahydropyrido[1,2-*a*]pyrido[1′,2′:1,2]imidazo[5,4-*f*]benzimidazol-6,13-dione (74b)

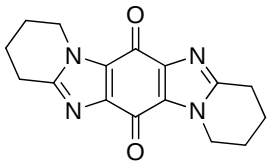

NSC 755324

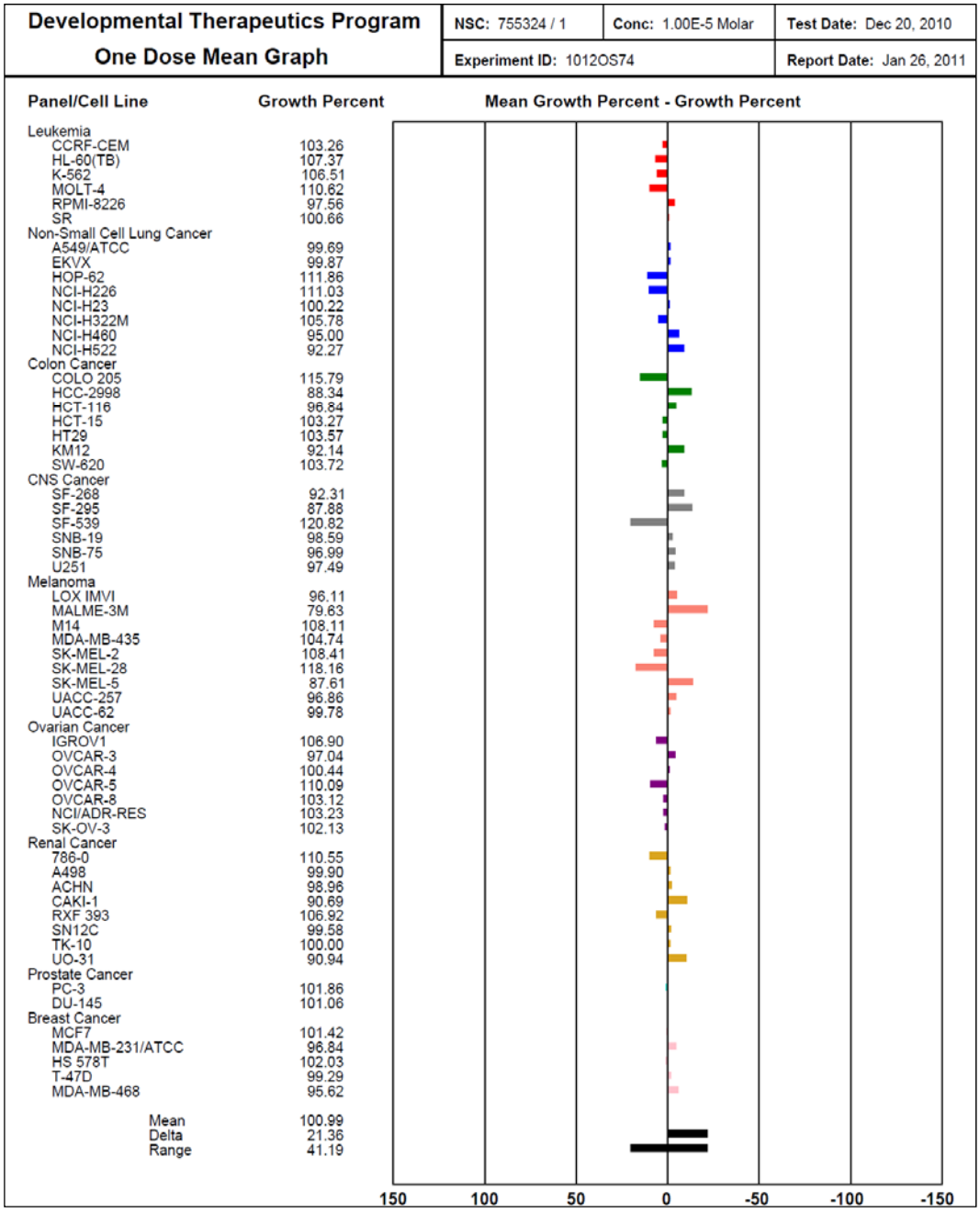

Developmental Therapeutics Program

One Dose Mean Graph

NSC: 755324 / 1	Conc: 1.00E-5 Molar	Test Date: Dec 20, 2010
Experiment ID: 1012OS74		Report Date: Jan 26, 2011

Panel/Cell Line	Growth Percent
Leukemia	
CCRF-CEM	103.26
HL-60(TB)	107.37
K-562	106.51
MOLT-4	110.62
RPMI-8226	97.56
SR	100.66
Non-Small Cell Lung Cancer	
A549/ATCC	99.69
EKVX	99.87
HOP-62	111.86
NCI-H226	111.03
NCI-H23	100.22
NCI-H322M	105.78
NCI-H460	95.00
NCI-H522	92.27
Colon Cancer	
COLO 205	115.79
HCC-2998	88.34
HCT-116	96.84
HCT-15	103.27
HT29	103.57
KM12	92.14
SW-620	103.72
CNS Cancer	
SF-268	92.31
SF-295	87.88
SF-539	120.82
SNB-19	98.59
SNB-75	96.99
U251	97.49
Melanoma	
LOX IMVI	96.11
MALME-3M	79.63
M14	108.11
MDA-MB-435	104.74
SK-MEL-2	108.41
SK-MEL-28	118.16
SK-MEL-5	87.61
UACC-257	96.86
UACC-62	99.78
Ovarian Cancer	
IGROV1	106.90
OVCAR-3	97.04
OVCAR-4	100.44
OVCAR-5	110.09
OVCAR-8	103.12
NCI/ADR-RES	103.23
SK-OV-3	102.13
Renal Cancer	
786-0	110.55
A498	99.90
ACHN	98.96
CAKI-1	90.69
RXF 393	106.92
SN12C	99.58
TK-10	100.00
UO-31	90.94
Prostate Cancer	
PC-3	101.86
DU-145	101.06
Breast Cancer	
MCF7	101.42
MDA-MB-231/ATCC	96.84
HS 578T	102.03
T-47D	99.29
MDA-MB-468	95.62
Mean	100.99
Delta	21.36
Range	41.19

Mean Growth Percent - Growth Percent

150 100 50 0 -50 -100 -150

3,4,8,9,10,11-Hexahydro-1*H*-[1,4]oxazino[4,3-*a*]pyrido[1',2':1,2]imidazo[5,4-*f*]benzimidazol-6,13-dione (125)

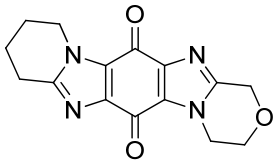

NSC 756997

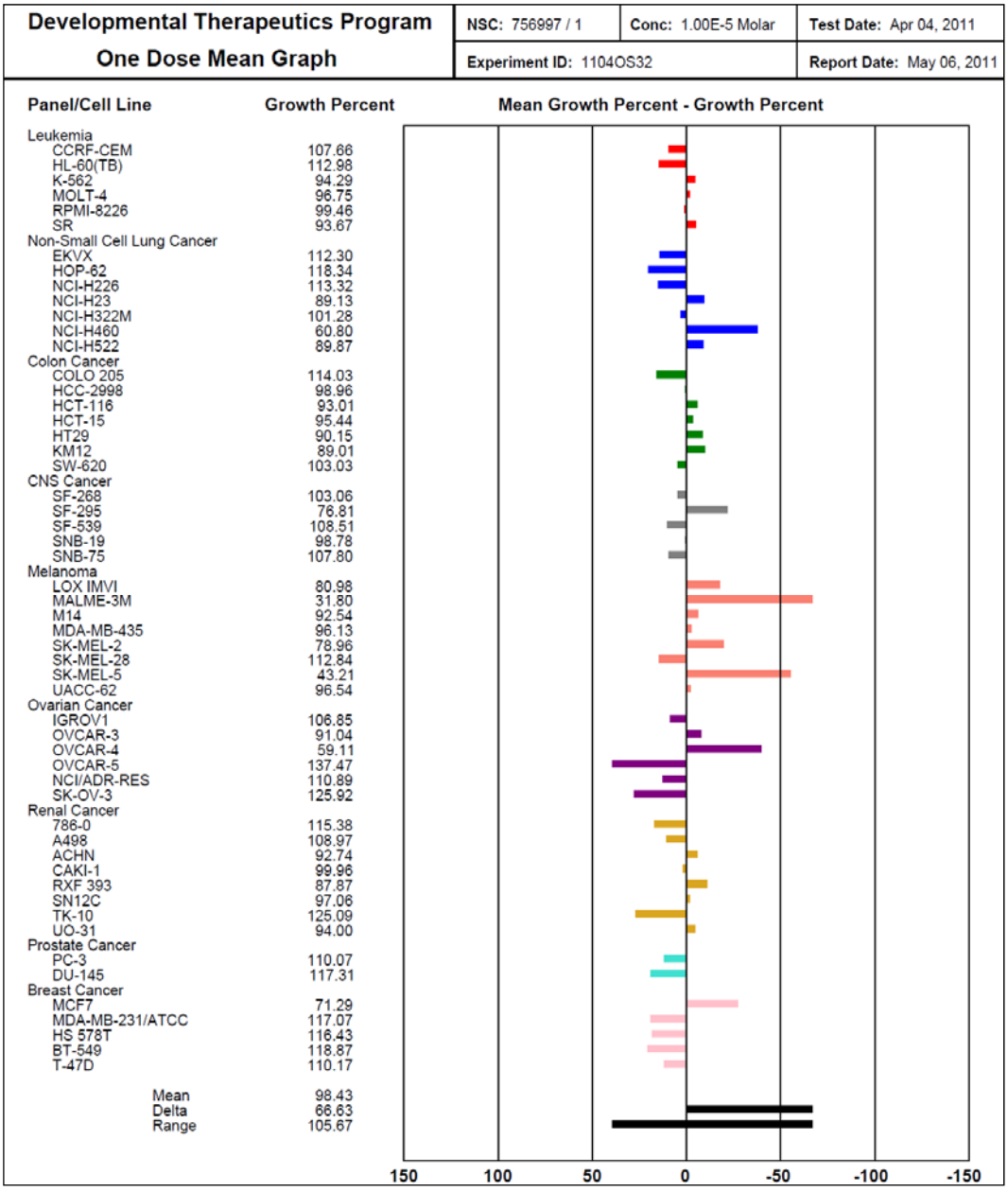

A.4 COMPARE analysis

3-Butyl-6,7,8,9-tetrahydroimidazo[5,4-*f*]pyrido[1,2-*a*]benzimidazol-4,11-dione (72)

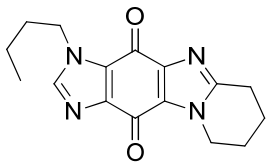

NSC 756996

Compound **72** (single dose) to Molecular Target **TP53**

----SEED----
NSC:S756996 Endpt:GIPRCNT ExpId:AVGDATA hiConc:1.0E-5
vectorId: 1713821 count expts: 1
—TARGET—
MolId:MT94 Genecard:TP53 TargetSet:MOLTID_MT_SERIES
vectorId: 1555166 count expts: 1

correlation: 0.585
compareResultId: 3947370

Compound **72** (single dose) to Molecular Target **MDM2**

----SEED----
NSC:S756996 Endpt:GIPRCNT ExpId:AVGDATA hiConc:1.0E-5
vectorId: 1713821 count expts: 1
—TARGET—
MolId:MT125 Genecard:MDM2 TargetSet:MOLTID_MT_SERIES
vectorId: 1542473 count expts: 1

correlation: 0.491
compareResultId: 3948180

6-Imino-1,2,3,4,8,9,10,11-octahydropyrido[1,2-*a*]pyrido[1′,2′:1,2]imidazo[5,4-*f*]benzimidazol-13-one (73b)

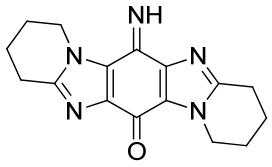

NSC 753790

Compound **73b** (single dose) to Molecular Target **NQO1**

----SEED----
NSC:S753790 Endpt:GIPRCNT ExpId:AVGDATA hiConc:1.0E-5
vectorId: 1684115 count expts: 1
—TARGET—
MolId:MT22 Genecard:NQO1 TargetSet:MOLTID_MT_SERIES
vectorId: 1548454 count expts: 1

correlation: 0.446
compareResultId: 3947796

Compound **73b** (five dose) to Molecular Target **NQO1**

----SEED----
MolId:MT22 Genecard:NQO1 TargetSet:MOLTID_MT_SERIES
vectorId: 1548454 count expts: 1
—TARGET—
NSC:S753790 Endpt:GI50 ExpId:AVGDATA hiConc:-4.0
vectorId: 1690716 count expts: 2

correlation: 0.512
compareResultId: 3920455

Compound **73b** (five dose) to Synthetic Compound **128**

----SEED----
NSC:S753790 Endpt:GI50 ExpId:AVGDATA hiConc:-4.0
vectorId: 1690716 count expts: 2
—TARGET—
NSC:S84167 Endpt:GI50 ExpId:AVGDATA hiConc:-4.0
vectorId: 34076 count expts: 2

correlation: 0.865
compareResultId: 3968431

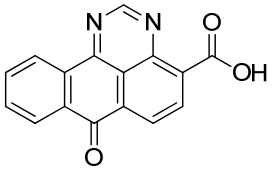

127
NSC: 84167

Compound **73b** (five dose) to Synthetic Compound **129**

----SEED----
NSC:S753790 Endpt:GI50 ExpId:AVGDATA hiConc:-4.0
vectorId: 1690716 count expts: 2
—TARGET—
NSC:S94945 Endpt:GI50 ExpId:AVGDATA hiConc:-4.0
vectorId: 257299 count expts: 2

correlation: 0.765
compareResultId: 3968432

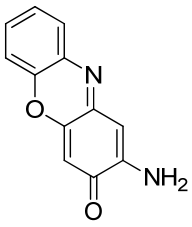

128
NSC: 94945

7-Imino-2,3,4,5,10,11,12,13-octahydro-1*H*,9*H*-azepino[1,2-*a*]azepino[1′,2′:1,2]imidazo[5,4-*f*]benzimidazol-15-one (73c)

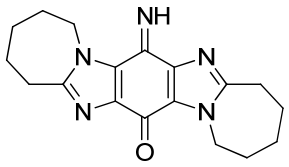

73c
NSC 756995

Compound **73c** to Molecular Target **TP53**

----SEED----
NSC:S756995 Endpt:GIPRCNT ExpId:AVGDATA hiConc:1.0E-5
vectorId: 1713819 count expts: 1
—TARGET—
MolId:MT94 Genecard:TP53 TargetSet:MOLTID_MT_SERIES
vectorId: 1555166 count expts: 1

correlation: 0.513
compareResultId: 3948072

Compound **73c** to Molecular Target **MDM2**

----SEED----
NSC:S756995 Endpt:GIPRCNT ExpId:AVGDATA hiConc:1.0E-5
vectorId: 1713819 count expts: 1
—TARGET—
MolId:MT125 Genecard:MDM2 TargetSet:MOLTID_MT_SERIES
vectorId: 1542473 count expts: 1

correlation: 0.422
compareResultId: 3948078

2,3,8,9-Tetrahydro-1*H*,7*H*-pyrrolo[1,2-*a*]pyrrolo[1′,2′:1,2]imidazo[5,4-*f*]benzimidazol-5,11-dione (74a)

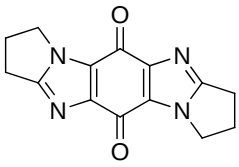

74a
NSC 755325

Compound **74a** to Molecular Target **TP53**

----SEED----
NSC:S755325 Endpt:GIPRCNT ExpId:AVGDATA hiConc:1.0E-5
vectorId: 1702917 count expts: 1
—TARGET—
MolId:MT94 Genecard:TP53 TargetSet:MOLTID_MT_SERIES
vectorId: 1555166 count expts: 1

correlation: 0.47
compareResultId: 3947980

3,4,8,9,10,11-Hexahydro-1*H*-[1,4]oxazino[4,3-*a*]pyrido[1',2':1,2]imidazo[5,4-*f*]benzimidazol-6,13-dione (125)

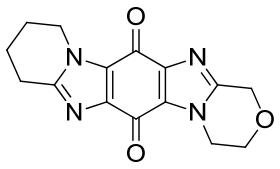

125
NSC 756997

Compound **125** to Molecular Target **TP53**

----SEED----
NSC:S756997 Endpt:GIPRCNT ExpId:AVGDATA hiConc:1.0E-5
vectorId: 1713823 count expts: 1
—TARGET—
MolId:MT94 Genecard:TP53 TargetSet:MOLTID_MT_SERIES
vectorId: 1555166 count expts: 1

correlation: 0.542
compareResultId: 3947472

Compound **125** to Molecular Target **MDM2**

----SEED----
NSC:S756997 Endpt:GIPRCNT ExpId:AVGDATA hiConc:1.0E-5
vectorId: 1713823 count expts: 1
—TARGET—
MolId:MT125 Genecard:MDM2 TargetSet:MOLTID_MT_SERIES
vectorId: 1542473 count expts: 1

correlation: 0.461
compareResultId: 3948298

COMPARE correlations of NQO1 to other synthetic compounds

Highest correlation to NQO1 of all synthetic compounds

----SEED----
MolId:MT22 Genecard:NQO1 TargetSet:MOLTID_MT_SE
vectorId: 1548454 count expts: 1
—TARGET—
NSC:S409304 Endpt:GI50 ExpId:AVGDATA hiConc:-4
vectorId: 387380 count expts: 1

correlation: 0.674
compareResultId: 3920444

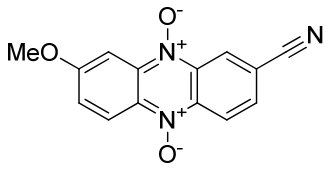

129
NSC: 409304

Second highest correlation to NQO1 of all synthetic compounds

----SEED----
MolId:MT22 Genecard:NQO1 TargetSet:MOLTID_MT_SE
vectorId: 1548454 count expts: 1
—TARGET—
NSC:S84167 Endpt:GI50 ExpId:AVGDATA hiConc:-4
vectorId: 34076 count expts: 2

correlation: 0.64
compareResultId: 3920445

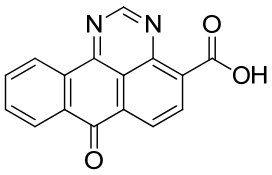

127
NSC: 84167

Compound **128** to NQO1

----SEED----
NSC:S94945 Endpt:GI50 ExpId:AVGDATA hiConc:-4
vectorId: 257299 count expts: 2
—TARGET—
MolId:MT22 Genecard:NQO1 TargetSet:MOLTID_MT_SE
vectorId: 1548454 count expts: 1

correlation: 0.469
compareResultId: 3948671

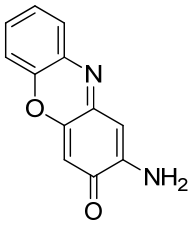

128
NSC: 94945

MMC to NQO1

----SEED----
MolId:MT22 Genecard:NQO1 TargetSet:MOLTID_MT_SI
vectorId: 1548454 count expts: 1
—TARGET—
NSC:S26980 Endpt:GI50 ExpId:AVGDATA hiConc:-4
vectorId: 24911 count expts: 76

correlation: 0.425
compareResultId: 3920393

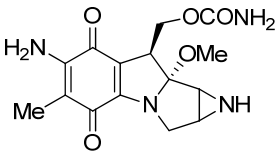

MMC
NSC: 26980

Conference proceedings

"One-pot double intramolecular homolytic aromatic substitution routes to dialicyclic ring fused imidazobenzimidazolequinones and preliminary analysis of anticancer activity,"
Vincent Fagan, Sarah Bonham, Michael P. Carty and Fawaz Aldabbagh; Annual College of Science research Day, NUI Galway, April 2010. Book of Abstracts; **Poster 5**

"One-pot double intramolecular homolytic aromatic substitution routes to dialicyclic ring fused imidazobenzimidazolequinones and preliminary analysis of anticancer activity,"
Vincent Fagan, Sarah Bonham, Michael P. Carty and Fawaz Aldabbagh; Institute of Chemistry of Ireland Annual Congress 2010: High Performance Computing at the Chemistry/Biochemistry Interface, NUI Galway, May 2010. Book of Abstracts; **Poster 7**

"One-pot double intramolecular homolytic aromatic substitution routes to dialicyclic ring fused imidazobenzimidazolequinones and preliminary analysis of anticancer activity,"
Vincent Fagan, Sarah Bonham, Michael P. Carty and Fawaz Aldabbagh; The 12th RSC-SCI Joint Meeting on Heterocyclic Chemistry, Brighton, UK, June 2010. Book of Abstracts; **P5**.

Peer-reviewed publications

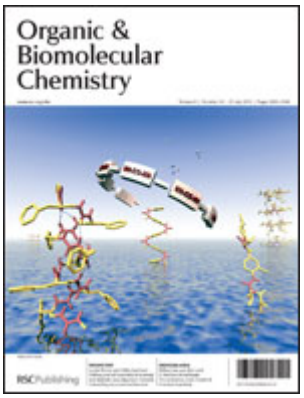

One-pot double intramolecular homolytic aromatic substitution routes to dialicyclic ring fused imidazobenzimidazolequinones and preliminary analysis of anticancer activity

Vincent Fagan, Sarah Bonham, Michael P. Carty and Fawaz Aldabbagh*, *Organic and Biomolecular Chemistry*, **2010**, *8*, 3149-3156 (RSC Prospect)